Exploring SARM1 as a target to delay programmed axon degeneration

Stacey Anne Gould

Wolfson College

September 2020

This thesis is submitted for the degree of Doctor of Philosophy

Declaration

This thesis is the result of my own work and includes nothing which is the outcome of work done in collaboration except as declared in the preface and specified in the text. It is not substantially the same as any work that has already been submitted before for any degree or other qualification except as declared in the preface and specified in the text. It does not exceed the prescribed word limit for the Clinical Medicine and Clinical Veterinary Medicine Degree Committee.

Stacey Anne Gould. Exploring SARM1 as a target to delay programmed axon degeneration.

Abstract:

Programmed axon degeneration (Wallerian degeneration) can occur after physical injury, inhibition of axon transport, exposure to neurotoxic compounds, and in diseases involving mitochondrial or metabolic dysfunction. There is increasing evidence that this pathway can be activated in human painful neuropathies and preclinical evidence suggests it is also active in neurodegenerative conditions, such as Parkinson's disease and Amyotrophic Lateral Sclerosis. Programmed axon degeneration is a potentially druggable pathway with preclinical studies showing that increasing levels of pro-survival factor NMNAT2, and removal of MYCBP2 involved in protein ubiquitination and turnover, or prodegenerative protein SARM1 can delay programmed axon degeneration. Preclinical studies indicate that complete genetic removal of *Sarm1* leads to the strongest protection *in vivo* after physical transection injury and also prevents perinatal lethality in mice lacking NMNAT2. This makes SARM1 an attractive protein to explore in the context of delaying programmed axon degeneration for therapeutic effect. However, until this thesis, the extent to which SARM1 activity needs to be decreased has been unclear.

This thesis explores the possibility of targeting the SARM1 protein for therapeutic effect. Firstly, since decreasing protein levels or activity is more achievable than completely eliminating them, the effect of *Sarm1* hemizygosity in mice was assessed. Data presented here show that the rate of programmed axon degeneration can be slowed by the absence of one allele after *in vivo* transection injury, and axon outgrowth deficits in a developmental system where the pathway is active can be partially restored. Degeneration can also be slowed after a range of *in vitro* triggers of programmed axon degeneration showing clearly that decreasing (and not just removing) SARM1 can be beneficial. Secondly, targeting SARM1 through antisense oligonucleotides shows that SARM1 protein levels can be decreased *in vitro* to a similar extent as *Sarm1* hemizygosity using exogenously-applied nucleotides. This decrease in protein levels confers a delay in programmed axon degeneration in a range of *in vitro* models suggesting that targeting SARM1 is a viable therapeutic approach. Finally, use of a non-transgenic dietary model of sporadic Alzheimer's disease (sAD) was used to explore links between sAD and programmed axon degeneration but no differences in axon transport or signs of programmed axon degeneration were detected in this model. Nevertheless, this thesis demonstrates that targeting SARM1 pharmacologically is feasible and can delay degeneration after diverse triggers. Thus, further research into the relevant *in vivo* disease models could advance this strategy towards clinical application.

Acknowledgements

I would like to thank my supervisor Professor Michael Coleman for recognising my potential and offering me this position in the first instance. Thank you for the academic opportunities you have provided me, the lessons you have taught me, and the space for personal growth you have afforded me.

A colossal thank you goes to Dr. Jonathan Gilley, Dr. Robert Adalbert, and Dr. Andrea Loreto for exercising the patience of saints in training me on techniques needed for this work, and for our many conversations discussing axon degeneration and life in the lab. Thank you also to members of the Coleman lab past and present whose work and conversation have informed, inspired, and will continue on from that which I present in this thesis.

A few thanks also go out for technical assistance: Antisense oligonucleotides used in Chapter 4 were kindly provided by Ionis Pharmaceuticals. Slice cultures used in Chapter 5 were provided by Dr. Claire Durrant and Olivia Sheppard. Graphs showing results from Takeda (Cambridge) presented in the introduction of Chapter 5 were provided by Dr. Wayne Chadwick. I am grateful also to the original funders of this project; the Biotechnology and Biological Sciences Research Council and Industrial Collaborators Takeda (Cambridge), and to Funds for Graduate Women, the Lundgren Fund, and Wolfson College Hardship Fund for recognising my academic potential and providing financial assistance in the final year of my time as a PhD student, despite the challenging circumstances.

In particular, I would like to express my gratitude to the Crane's Charity, and Amy O., Claire C., Charlotte S., and Chris T., for their support through the darkest most intense non-academic challenges I have ever experienced. This thank you extends also to my incredible life-long friends who have demonstrated their immeasurable support and joined me in making some of the most precious Cambridge memories that I will treasure forever.

Thank you also to my parents for the lessons in resilience and persistence that prepared me to complete this degree, and for encouraging my pursuit of knowledge. Also, to my sister Sarah, her husband James, and their dog Pippa for an endless supply of hugs and always having space for me and a cup of tea in their cosy home.

Finally, to Kathleen Fraser: Thank you for instilling a sense of curiosity, creativity, and adventure in me. Even though you are no longer present in this life, I think of you daily and hope that over time I can become as kind, wise, and gracious as you were.

Table of Contents

Chapter 1: Introduction

Nervous systems control essential functions ranging from breathing, digestion and heart rate, to movement and sensing our environment, through to more complex traits of human behaviour, like cognition, memory, and personality. Correct functioning of the nervous system is thus crucial to most life-forms, and when nervous system function goes awry this can have devastating effects depending on the neurones affected. One of the main cell types in the nervous system are neurones: highly polarised cells which grow processes from the soma (cell body). Action potentials are passed along dendrites to the soma and then along a single extended projection (the axon) which actively transmits signals to the next neurone or target tissue. Directionality of information flow through the neurone is essential for transmission of signals, thus correct functioning of neuronal circuitry. This directionality is achieved through intrinsic and extrinsic signalling which ensure neurones remain highly polarised with differential patterns of protein expression, direction of microtubule cytoskeletal structures, and the presence of distinct lipid tags to spatially anchor or restrict signalling complexes to distinct regions of the neurone [1]. Being up to one metre long in humans, the proportional length of a single axon has been described as ~20 miles (~30 km) long if a Volkswagen beetle sprouted a tail [2]. This comparable length of axons to the soma makes them vulnerable structures. Since axon terminals are comparatively far away from the soma, where nuclear-encoded proteins are synthesised, axons are highly-dependent on intracellular trafficking (axonal transport) of proteins, RNA, and organelles in order to survive and maintain healthy synapses. When axonal transport is interrupted, this puts strain on axons – particularly their terminals – making them either vulnerable to injury or activating an axon-intrinsic programmed death pathway (Wallerian degeneration).

1.1 Wallerian degeneration: Augustus Waller's observations

Wallerian degeneration is named after Augustus Waller, whose experiments in the early 19th century describe a form of axon-specific degeneration where fragmentation of axons occurred distal to the site of a transection injury in frog papillary nerve [3], shown in his original drawings in Figure 1.1. Since Waller's original injury-induced observations, much has been done to elucidate the underlying molecular mechanisms of this pathway and its disease-related activation in non-transection injuries.

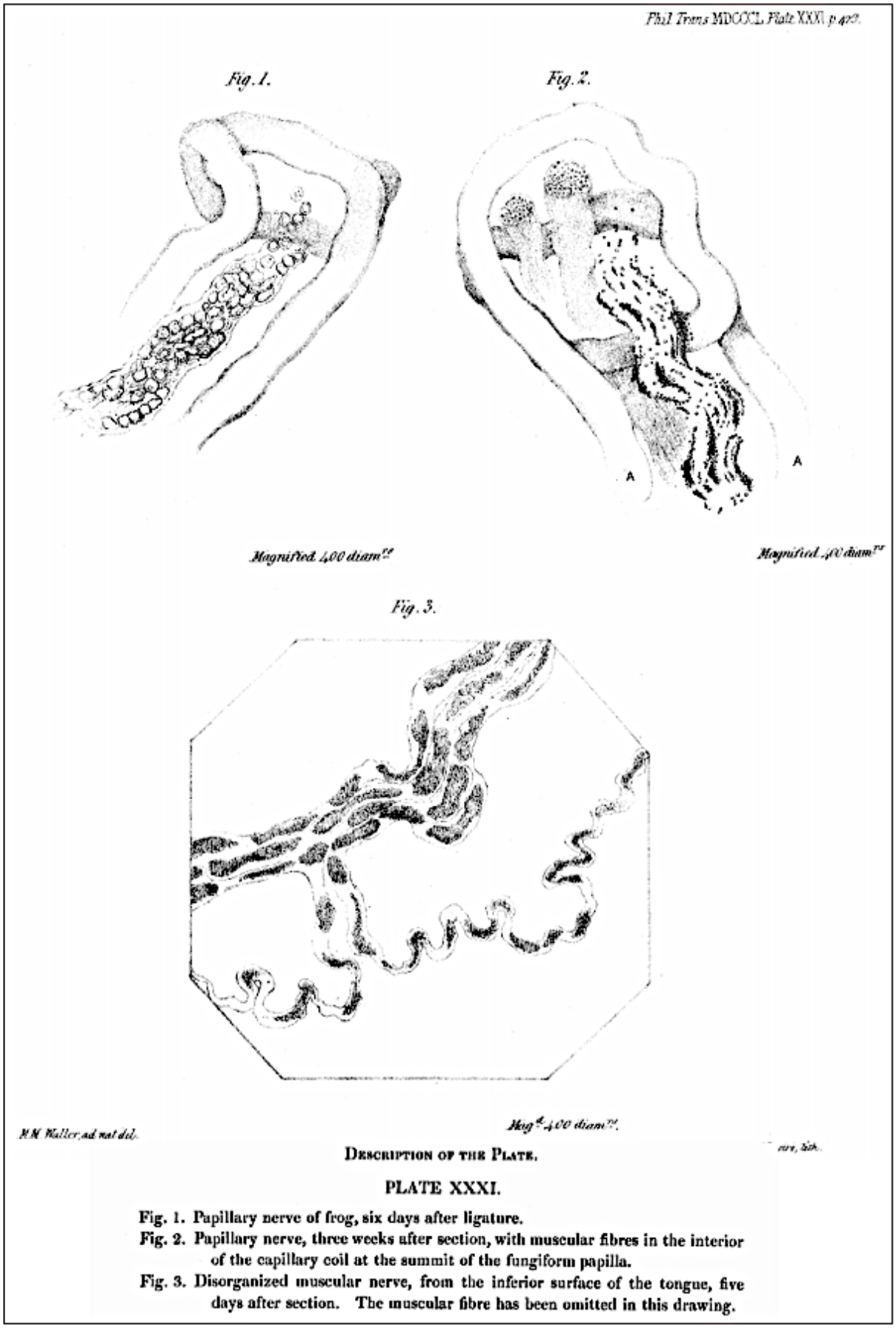

Figure 1.1: Augustus Waller's hand drawn observations of Wallerian degeneration over time in frog papillary nerve after transection

When the Wallerian degeneration pathway (hereafter referred to as programmed axon degeneration) is activated, it causes fragmentation of axons independently from the neuronal soma. Activation of programmed axon degeneration in disease precedes loss of the soma and frequently occurs in a retrograde pattern beginning at the distal ends of the axon proceeding towards the soma. This is known as 'dying back' degeneration [4] which is recognised as an early feature of neurodegenerative diseases [2,5–7].

1.1.1 Three morphologically distinct phases of programmed axon degeneration

The immediate phase of programmed axon degeneration is known as acute axon degeneration (AAD) which occurs within minutes of injury affecting both the proximal and distal stumps [8–10]. Within 5-60 minutes of injury, several hundred micrometres of rapid degeneration occurs in sites both proximal and distal to injury [8]. This is followed by formation of bulbar structures comprising accumulated axonal organelles from continued antero- and retrograde transport [11,12].

Next is a latent phase where the distal axon remains intact, electrically excitable [13,14], and with continued bi-directional axonal transport within the distal stump [15]. The proximal stump begins sprouting towards the lesion within a few hours [8]. The latent phase occurs over a variable timeframe before degeneration of the distal axon ensues; for 25 h in rat phrenic nerve [16], 35 h in mouse sciatic nerve, 24-48 h in explanted mouse nerves [17] and up to several days in primates, including humans [18,19]. Programmed axon degeneration is seen also *in vitro* in mouse neurites, though occurs over a shorter time-frame (within 8-24 h of transection) [20–25].

Finally, the latent phase is followed by rapid axon disintegration; the fragmentation and degeneration of distal axons. Though this was initially thought to occur simultaneously along an injured portion of a nerve, it has now been shown to occur over a 1-2 h timeframe [12,26,27] with the latency being longer in thicker fibres than in thinner ones [16]. Degeneration spreads anterogradely in wild-type mouse nerve after cut, but retrogradely after crush [27] with calcium-dependent proteases (calpains) degrading the axonal cytoskeleton [11,28,29]. Morphologically, before fragmentation, axonal swellings appear in the axons of the CNS followed by the appearance of myelin ovoids [30].

Extrinsic to the axon, during or shortly after this final phase in the peripheral nervous system (PNS), Schwann cells proliferate and act in concert with bone-marrow-derived macrophages to mediate clearance of axonal debris, along with formation of Bands of Bünger and sprouting

of new axons into the distal stump [24,31–34]. Delaying the early degeneration phases also delays these regenerative ones [35–38]. In the central nervous system, oligodendrocytes and microglia remove axonal fragments and this occurs over a longer timeframe than in the PNS [32,39–41].

1.1.2 Programmed axon degeneration differs from other programmed cell death mechanisms

The mechanism of programmed axon degeneration is independent from other mechanisms of programmed cell death, such as apoptosis or necroptosis, with different mechanisms of degeneration occurring in the neurone soma than in the axon [5,42,43]. Moreover, the soma of different neuronal subpopulations can respond in different ways to injury or toxic insults [5,44,45]. WLD^S (a protein which delays programmed axon degeneration that is described in more detail below) does not protect against apoptosis in the neuronal soma *in vitro* [42,43] and fails to delay somatic degeneration in a rat model of glaucoma [46], despite delaying axon degeneration. Furthermore, both the presence of WLD^S and removal of pro-degenerative protein SARM1 (also described in more detail below) delays retinal ganglion cell axon degeneration after optic nerve injury without affecting the somal death pathways [47].

Whilst some hallmarks of apoptosis are shared, such as distal cut axons staining positive for Annexin V and loss of mitochondrial membrane potential during the early stage of axon degeneration [25], others are not. Removal or inhibition of caspases [48–50], overexpression of members of the BCL-2 protein family [49,51] or removal or BAX and BAK do not prevent programmed axon degeneration [52], despite playing roles in apoptosis [53].

In a model of retinal degeneration, removal of SARM1 has been shown to protect against rod and cone soma death induced by lack of rhodopsin [54]. However, neither the presence of WLD^S or absence of SARM1 protect against retinal ganglion cell death in models of glaucoma or optic nerve crush[22,55], despite preventing axon degeneration [46,47]. Activation of SARM1 has been seen downstream of neuroinflammatory and necroptotic signalling [56]. However, necroptotic signalling leads to a decrease in axonal survival factors NMNAT2 and SCG10 which have previously been shown to activate or accelerate programmed axon degeneration [22,55].

There is some evidence supporting a role of SARM1 in somal death, but this comes from overexpression of artificially active SARM1 constructs which promote death in the neuronal soma and non-neuronal cells [57,58]. Removal of SARM1 also protects neuronal somas against rotenone and CCCP toxicity [59] and the presence of WLD^S prevents STZ-induced painful

diabetic neuropathy independently from its axonal actions by preventing death of pancreatic islet cells [60]. Whilst SARM1 can induce cell death in non-neuronal cells, its regulation by NMNAT2, which is predominantly expressed in axons, is what makes the role of SARM1 in axon degeneration unique to other cell death mechanisms.

1.1.3 Molecular mechanisms of programmed axon degeneration

Over the past few decades there have been huge developments in elucidating the precise molecular mechanisms driving programmed axon degeneration, which are summarised in Figure 1.2. These mechanisms will be discussed in detail below, but briefly, they include: Identification of a slow Wallerian degeneration phenotype in spontaneous mutant *Wld*^{S} mice. The need for nicotinamide mononucleotide adenylyltransferase (NMNAT) enzyme activity of WLD^S for its neuroprotective effect. Identification of the endogenous labile axonal survival factor (NMNAT2) whose injury-induced loss WLD^S substitutes for. Identification of a strong prodegenerative protein SARM1 whose activation state is altered by the balance of nucleotides NMN and NAD^+, controlled by NMNAT activity. Roles of the ubiquitin proteasome system, particularly MYCBP2 (PHR1), in regulating axon survival factor turn over and subsequent activation of SARM1, as well as less influential modifiers of the pathway, such as activation of the MAPKs cascade, altered calcium homeostasis, and calpain activation. Two critical processes to note in the programmed axon degeneration pathway are (i) NMNAT2 is a pro-survival factor which (along with other overexpressed NMNATs) limits accumulation of NMN by covalently binding NMN to the ADP moiety of ATP producing NAD^+, and (ii) SARM1 is a prodegenerative protein containing NADase activity which is activated by NMN and inhibited by NAD^+. Therefore, either overexpression of NMNAT or removal of SARM1 activity prevents activation of the programmed axon degeneration pathway, whereas loss of NMNAT activity or activation of SARM1 leads to activation of programmed axon degeneration.

1.2 Delaying programmed axon degeneration in preclinical disease models

It has been proposed that programmed axon degeneration may play a role in neurodegenerative disease, where axons begin to undergo degeneration whilst still connected to the soma [2,3,61]. Both removal of SARM1 and aberrant axonal expression of NMNAT activity (in the form of WLD^S or cytoplasmic NMNAT1) confer potent neuroprotective effects in a range of preclinical disease models. The neuroprotective effects of WLD^S were first demonstrated in models of physical injury [58,62–66], which led to the thinking that presence of WLD^S or absence of SARM1 may confer protection against disease-related axon degeneration. If the mechanism by which these modifications protect is active in non-transection injuries, this could open up opportunities to target the pathway therapeutically. Indeed, aside

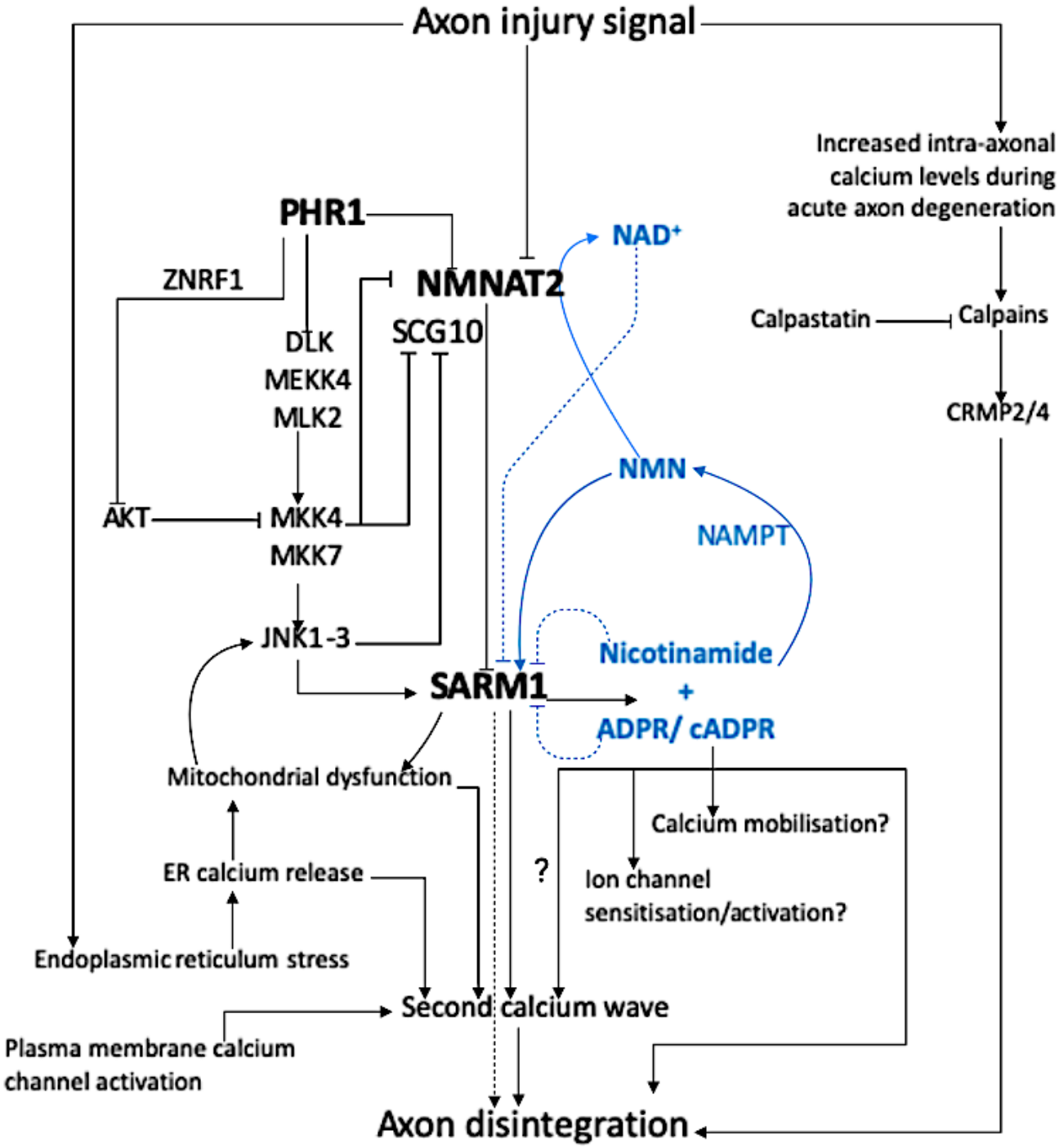

Figure1.2: Key proteins and modifiers of programmed axon degeneration. Overexpression of NMNATs, removal of SARM1 or PHR1, and depletion of NMN have the strongest protective phenotypes. Black text indicates proteins and cellular events leading to axon disintegration. Blue text indicates key nucleotides whose levels are altered in the lead up to axon disintegration. Dotted blue lines indicate weak inhibitory effects of nucleotides on SARM1 and dotted black lines or question marks indicate unknown steps in the pathway. Pointed arrows indicate activating effects. Flat arrow heads indicate inhibitory effects.

from neuroprotective effects in transection and crush injuries, the protective effects have since been demonstrated across a wide range of *in vitro* and *in vivo* disease models. The first non-injury delay in programmed axon degeneration was demonstrated after application of chemotherapeutic agents vincristine and paclitaxel [67,68], then in a progressive motor neuropathy (pmn) model of motor neurone disease [69], peripheral neuropathy associated with myelin disorders [70], and gracile axonal dystrophy [71].

Cultured *Sarm1*$^{-/-}$ or *Wld*^{S} neurones show delayed axon degeneration after a range of *in vitro* triggers of degeneration; for example, up to 6 h post-NGF-withdrawal [72]; 24 h to 4 days post-vincristine application [58,67,73]; and up to 72 h post mitochondrial stressors rotenone or CCCP [59,74,75]. Both *Sarm1*$^{-/-}$ or *Wld*^{S} protect against programmed axon degeneration and developmental defects induced by NMNAT2 depletion [76–78].

In the peripheral nervous system *in vivo*, *Sarm1*$^{-/-}$ mice are protected against painful chemotherapy-induced peripheral neuropathies (CIPN) [79–81], as well as high-fat diet-induced neuropathy [79]. Similarly, WLD^{S} protects against painful CIPN [68,82–84], injury-induced chronic neuropathic pain [85–87], and models of CMT types 1A and 1B [70,88], but not CMT type 2D [89].

In the central nervous system, axon damage is attenuated in models of traumatic brain injury both in the presence of WLD^{S} [90] and absence of SARM1 [91]. WLD^{S} is neuroprotective in models global cerebral ischaemia [92] and models of glaucoma, raised intra-occular pressure, and optic nerve and retinal injuries [46,93–96]. SARM1 is upregulated after excitotoxic retinal ganglion cell (RGC) injury [97] and its removal prevents axon degeneration in RCGs [47] and promotes photoreceptor survival in a model of retinal degeneration [54]. Furthermore, WLD^{S} delays degeneration caused by mitochondrial stress in rodent models of Parkinson's disease [66,98–100] and removal of Drosophila dSARM decreases rotenone-induced dopaminergic neurone degeneration [101].

Neither *Sarm1*$^{-/-}$ nor *Wld*^{S} are neuroprotective in SOD1 mutant mouse models of ALS [102–104]. However, *Sarm1*$^{-/-}$ does protect against axon degeneration and dendritic spine loss in a novel *Tardbp* overexpressing mutant mouse model of ALS/FTD [105] and WLD^{S} delays degeneration in the experimental autoimmune encephalomyelitis (EAE) model of MS [106–108].

In the abovementioned models, the term Wallerian-like degeneration is often used. This describes axon degeneration occurring in the absence of physical axotomy or crush injury which shares morphological features similar to programmed axon degeneration [109]. The abovementioned studies provide experimental evidence supporting the theory that a common mechanism of programmed axon degeneration is involved in disease pathophysiology. Therefore, disease course could be modified with anti-SARM1 therapies.

In addition to these disease models, there are some instances where programmed axon degeneration clearly initiates or exacerbates disease, as *in vitro* and *in vivo* studies have shown. When *Nmnat2* levels are decreased by around 70%, mice show axon loss as they age, decreased temperature sensitivity, and in culture, neurites are more vulnerable to axonal stresses showing a lower activation threshold and accelerated rate of degeneration [110]. When NMNAT2 is removed from mature axons, they degenerate in the absence of other injuries [76] and mice lacking NMNAT2 during development die at birth exhibiting absent or truncated axons in the peripheral and central nervous system, with *in vitro* outgrowth stalling at around 1 mm [77]. These studies highlight NMNAT2 as a crucial axonal survival factor. Importantly, they can reversed with the removal of SARM1 [78,111]. Therefore, human equivalent diseases could respond to anti-SARM1 therapies most effectively. So, how relevant is this pathway to human disease?

1.3 Relevance of programmed axon degeneration to human disease

Altered NMNAT2 activity in a rare human disorder leads to neuropathic pain in sisters possessing homozygous loss of function (LoF) mutations in *NMNAT2* [112] and a complete lack of functional NMNAT2 resulting from biallelic complete LoF mutations leads to stillbirths in humans [113]. Phenotypes in these stillborn foetuses resemble, but appear more extreme than, developmental defects in muscle and nervous system of mice lacking functional NMNAT2 which also die peri-natally [77,78,114]. In mice, this extreme phenotype can be completely prevented with removal of *Sarm1*, where *Nmnat2:Sarm1* double homozygous null mice living full apparently healthy lifespans [78,111]. Another rare *NMNAT2* mutation was found in a patient who presented with progressive brainstem atrophy [115]. However, the patient was also heterozygous for 11 other mutations so the functional effects of these need to be further explored.

In a far more common neurodegenerative disease, Alzheimer's disease (AD), human post-mortem brains show lowered *NMNAT2* mRNA levels in patients with AD relative to nondemented controls [116]. This study also found that, lower *NMNAT2* mRNA correlates with worse cognitive abilities in the general population. However, since axons require NMNAT2 to survive and they are the main endogenous source of NMNAT2, neurones without axons have a decreased need to produce NMNAT2. This leads us to the age-old conundrum of cause vs consequence; do decreased levels of NMNAT2 in AD cause axon degeneration, or are detectable NMNAT2 levels lower in AD as a result of axon degeneration? Nonetheless, mouse

studies have shown that axonal transport of NMNAT2 does decline with age [117] and that low expression of *Nmnat2* in mice leads to axon vulnerability and accelerated programmed axon degeneration in response to physical and neurotoxic injuries [110]. Relevant to Chapter 5 of this thesis, are proposed links between NMNAT2 and pathology in mouse models of AD. Specifically, decreased NMNAT2 protein levels are seen in AD models of amyloid pathology and tau hyperphosphorylation and misfolding: Aside from the well-established role of NMNAT2 in NAD synthesis, it has been proposed that NMNAT2 could act to prevent accumulation of hyperphosphorylated tau through chaperone activity [116] and via PP2A activation [118]. Moreover, pTau has been shown to lower *Nmnat2* gene expression via decreased pCREB occupancy at the two CRE sites in the *Nmnat2* promotor in cortex and hippocampus of rTg410 mice, which model fronto-temporal degeneration (FTD)-tauopathy [119].

Finally, two genome-wide association studies (GWAS), associate variation in the chromosomal locus which encompasses SARM1 with ALS [120,121]. The first GWAS noted this association in a cohort of 6,100 cases and 7,125 controls ($p=3.21 \times 10^{-7}$; odds ratio = 0.845) [120], which was replicated in a second study in a cohort of 12,577 cases and 23,475 controls ($p=8.96 \times 10^{-11}$; odds ratio 0.9) [121]. Although the second study did note *SARM1* variation in ALS patients, authors also noted variation in Polymerase delta-interacting protein 2 (*POLDIP2*) which they suggest is more likely to be the causative gene [121]. Whilst the size of the GWAS cohorts and possible influence of other genes in the chromosomal region highlighted in these studies make the precise role of SARM1 in ALS unclear, there are some other suggestions that SARM1 can play a role in ALS pathophysiology which warrant further investigation. For example, there are a number of *SARM1* variants seen only in ALS patients compared to controls in the Project MinE database and unpublished work from the Coleman lab demonstrates existence of other *SARM1* loss and gain of function alleles in the human population, which affect the rate of axon degeneration. Furthermore, other experimental data support a role of programmed axon degeneration in ALS [122–124] which will be discussed in more detail in Chapter 3 of the thesis.

Together, these data begin to link human neurological disease or vulnerability to disease with key proteins in a conserved pathway of programmed axon degeneration. This could indicate a contributory role of programmed axon degeneration in axon loss in common human diseases through a lowered activation threshold leading to aberrant activation, in addition to disease caused by *NMNAT2* LoF. Of course, more research is needed to separate cause and effect, confirm these links to disease susceptibility, and to identify potential vulnerable human populations.

Human neurodegenerative diseases are difficult to model in the preclinical setting; mice often do not display axon degeneration and white matter loss that humans develop in late stages of neurodegeneration, and there are huge differences in the environments between species. Even though direct evidence for a role of programmed axon degeneration in AD is lacking, these questions are difficult to resolve in mouse models which do not fully represent human AD pathology. Furthermore, many mouse models of AD rely on overexpression of genes involved in familial AD (fAD), whereas most patient cases are sporadic (sAD) in nature. In order to improve translation of therapeutic interventions from preclinical studies into the clinic, use of non-genetic sAD models is needed to explore commonalities in the mechanism causing fAD and sAD, and therefore whether different treatment options are needed. One such model is the D-Galactose dietary-induced model of sAD, where rodents display signs of accelerated ageing and AD-like phenotypes which have been extensively reviewed by Shwe et al., (2018) [125]. Chapter 5 will go into more depth, but briefly, D-Galactose administration leads to a plethora of pathological changes which are associated with human AD. These include; changes to Aβ and Tau favouring isoforms seen in AD brains, markers of oxidative stress, inflammation, and alterations in synaptic structure and function. The industrial partners to this project, Takeda (Cambridge), have observed these alterations which occur centrally only in the nervous system and not systemically in other organs. These results, together with significant changes in cognitive function, which occur over a relatively short time-frame (starting at 4 weeks), potentially make the D-Galactose model a time- and cost-effective non-genetic model of AD. Chapter 5 of this thesis explores the use of a D-Galactose-induced model of sAD to study links between programmed axon degeneration and sAD including proposed roles of NMNAT2 in chaperone activity and tau homeostasis [116,118,119], and whether axon transport of mitochondria or NMNAT2 are impaired.

The indications that SARM1 and NMNAT2 may be involved in human disease, at least in rare human disease, along with the similarity in preclinical protective phenotypes of *Sarm1*$^{-/-}$ and *Wld*^{S} highlight the importance of studying programmed axon degeneration and the protective mechanism(s) by which modulation of the pathway (such as removal of *Sarm1*) act. Since there are many molecules now linked to programmed axon degeneration and much is understood about their positions in the pathway and influence over axon health, this provides a plethora of options for therapeutic intervention. Each target brings varying levels of potential protection as well as their own problems to overcome in terms of developing a therapy. Involvement of each of these and possibilities to intervene therapeutically will be discussed in more detail below, starting with SARM1, whose removal leads to one of the strongest axon-protective phenotypes of all modifications to the programmed axon degeneration pathway.

1.4 SARM1: a prodegenerative protein

A large-scale genetic screen in *Drosophila melanogaster* identified prodegenerative protein Sterile α and TIR motif–containing protein (dSARM), whose orthologue is known as SARM1 in mammals [62]. Removal of this protein strongly delays injury-induced programmed axon degeneration in *Drosophila* and mammalian systems [58,62]. SARM1 was originally classed as a protein in the Toll-like receptor adaptor family, due to sharing sequence similarity to other proteins (such as MyD-88) which are typically involved in innate immune responses. Indeed, early studies exploring SARM1 confirmed a role in cytokine release and responses to viral infection [126–132]. However, a recent study demonstrates that passenger mutations in chemokine ligand genes close to the *Sarm1* locus are more likely to underlie some of these previously reported roles for SARM1 in immunity, though increased susceptibility to West Nile Virus remains newly generated *Sarm1*$^{-/-}$ mice [133]. Despite uncertainty over the proposed role of SARM1 in immunity, the role of SARM1 in promoting programmed axon degeneration remains undisputed [133] with *Sarm1* removal repeatedly, robustly and reliably protecting against programmed axon degeneration in the central and peripheral nervous systems of mice and *Drosophila* [47,58,62,79–81,91,101,133].

1.4.1 Distinct SARM1 protein domains have distinct functions

The SARM1 protein comprises a mitochondrial localisation sequence (MLS; also referred to as the mitochondrial targeting sequence), an Armadillo (ARM) domain, two tandem sterile alpha motif (SAM) domains, and a Toll-interleukin receptor 1 homology (TIR) domain, as shown in Figure 1.3. Each of these regions has a distinct function which recent mutagenesis, structural, and functional studies have begun to disentangle.

Mitochondrial localisation sequences tend to be short N-terminal sequences that direct a protein for translocation into the mitochondrion from the cell cytoplasm [134–136]. The MLS is dispensable for axon degeneration since its complete removal does not prevent the injury-induced prodegenerative activity of SARM1 [58]. However, this region (particularly Arginine 14) is crucial for SARM1 to associate with mitochondria and induce apoptosis in HEK cells [137].

ARM domains typically mediate protein-protein interactions via a sequence of seven highly conserved hydrophobic residues. However, despite being present in over 240 proteins, no common function has been observed between proteins that possess these domains. In SARM1, the ARM domain is thought to be responsible for autoinhibition of SARM1 activity since its removal leads to constitutively active SARM1 [58]. Recently, the structure of a near full

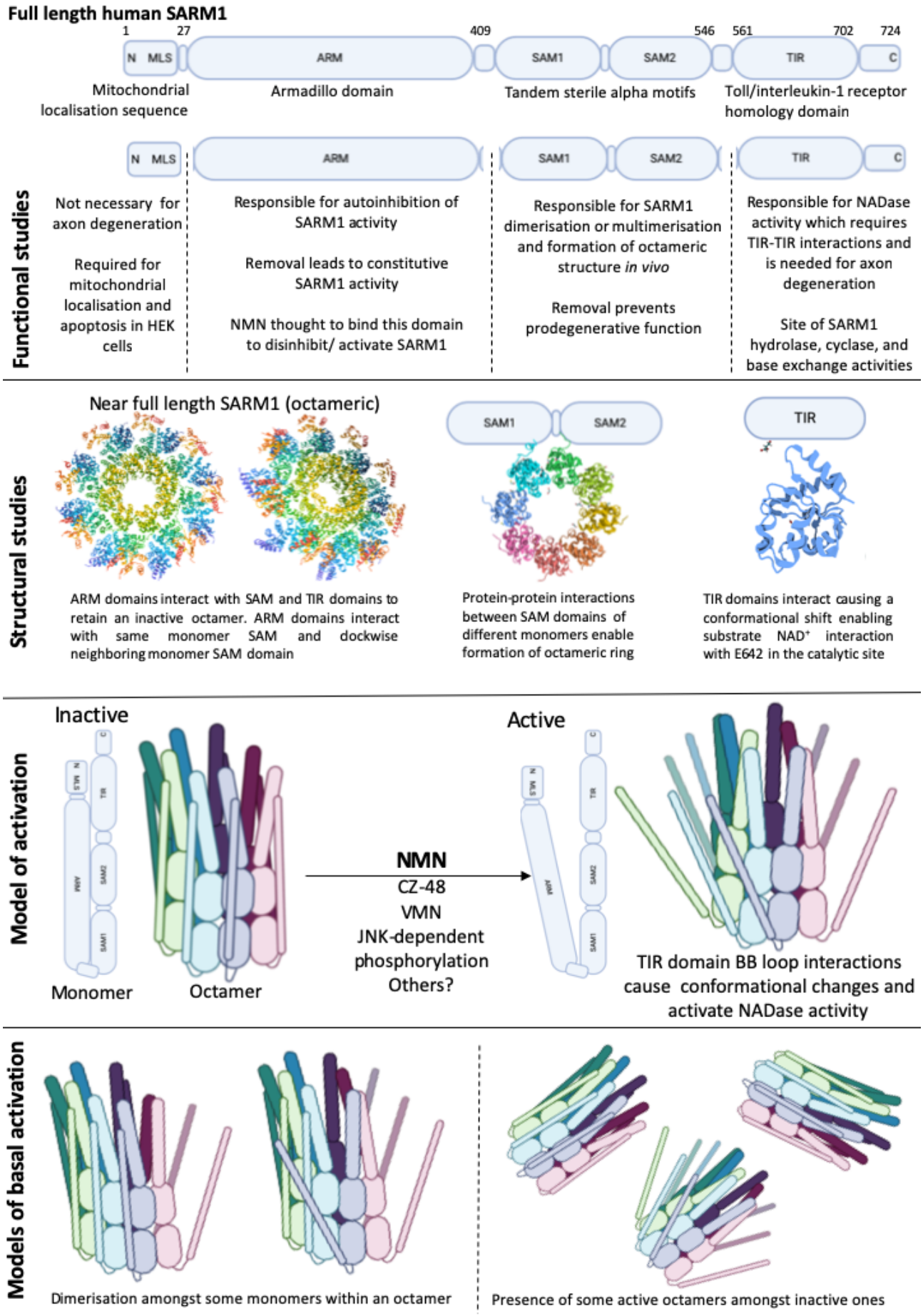

Figure 1.3: A summary of information known about SARM1. Functional studies demonstrated which regions of the SARM1 protein are involved in its prodegenerative function. Structural studies aided in understanding how SARM1 exists in its active and inactive forms. Working models of SARM1 activation and basal activation are derived from combining information from the structure and function studies.

length SARM1 construct has been reported, and the cryoEM study demonstrates that the ARM domain of inactive SARM1 physically interacts with TIR domains to keep them in an inactive conformation [138] via several non-covalent interactions with both a same-chain SAM domain and a clockwise neighbouring SAM domain [139].

SAM domains are present in a diverse range of proteins and often enable the formation of homo- and heterodimers [140,141]. SARM1 SAM domains show high structural similarity to previously reported SAM domains and are also thought to mediate protein-protein interactions. Full-length SARM1 has been reported to self-associate [57] and disruption of the tandem SAM domains abolishes SARM1 function [58]. The crystal structure of SARM1 SAM domains confirm they form an octameric ring [142,143] and near full-length active and inactive SARM1 cryoEM structures demonstrate a stable octameric core is established via SAM domain interactions [138]. In near full-length SARM1, the ARM domain interacts with both SAM domains [138] and prevents the dimerisation of TIR domains required for NADase activity [139]. Taken together, this evidence suggests that SARM1 is constitutively oligomeric in both injury and non-injury conditions and this multimerisation is driven by interactions between SAM domains of adjacent SARM1 monomers.

TIR domains are usually present in multi-domain proteins involved in innate immune signalling, such as membrane bound Toll-like receptors (TLRs; on the cytoplasmic side) and their downstream cytosolic adaptor proteins [144,145]. TIR domain-containing proteins are ubiquitously expressed across all cellular life forms; from bacteria, to plants, to higher organisms and humans. These domains usually enable protein-protein interactions and form a nucleated assembly to amplify and spatially propagate a signal [146–152]. Chemically-induced forced self-association of isolated SARM1-TIR domains induces axon degeneration in the absence of injury [57,58,153]. TIR domains are usually not catalytic [147] and so it was initially thought that aside from axon degeneration, SARM1 played a role in innate immunity with its TIR domains facilitating protein-protein interactions [127,128,154,155]. However, SARM1 TIR domains have recently been shown to possess NADase activity [143,156,157] and this activity is required for its prodegenerative phenotype. Interestingly, forced dimerisation of TIR domains from other proteins TLR4 or MYD88 does not induce NADase activity [57] indicating possible differences in TIR domain function between different proteins.

Combining information from the structural and functional studies mentioned above, SARM1 appears to have three separate domains which enable protein-protein interactions as well as intrinsic enzyme activity capable of degrading NAD^+.

1.4.2 Activators and products of SARM1 activation

Activation of SARM1 occurs with the first 4 hours of injury [57] and is associated with rapid or accelerated NAD^+ depletion in nerves post-injury [57,158]. Therefore, SARM1 seems a likely candidate for accelerating axotomy-induced loss of NAD^+ which overexpressed NMNATs (WLD^S or axonal cytoplasmic-NMNAT1) protect against.

Increased levels of endogenous nucleotide nicotinamide mononucleotide (NMN), which is also a substrate for NAD^+ anabolism, activates SARM1 [159,160]. Indeed, CZ-48, which is a cell-permeable synthetic NMN mimetic structurally similar to NMN activates the enzymatic functions of SARM1 [160]. During the course of this thesis our group found that VMN, a metabolite arising from vacor – a rodenticide and structural analogue of nicotinamide, activates SARM1 enzyme activity [161]. Finally, phosphorylation of SARM1 at Ser548 by stress-response kinase c-Jun n-terminal kinase (JNK) activates SARM1 to inhibit mitochondrial respiration in a model of oxidative stress [162].

All of the aforementioned activators of SARM1 induce NADase activity. As NAD^+ substrate levels are depleted, products nicotinamide (Nam), adenosine diphosphate ribose (ADPR), and cyclic-ADPR (cADPR) are generated, depending on the micro-environment surrounding active SARM1 (illustrated in Figure 1.4). A SAM-TIR construct has been shown to cleave NAD^+ and NADP into nicotinamide and ADPR or ADPRP (respectively), though it lacks the ability to cleave nucleotides NMN, NaAD, or flavin adenine dinucleotide (FAD) [143].

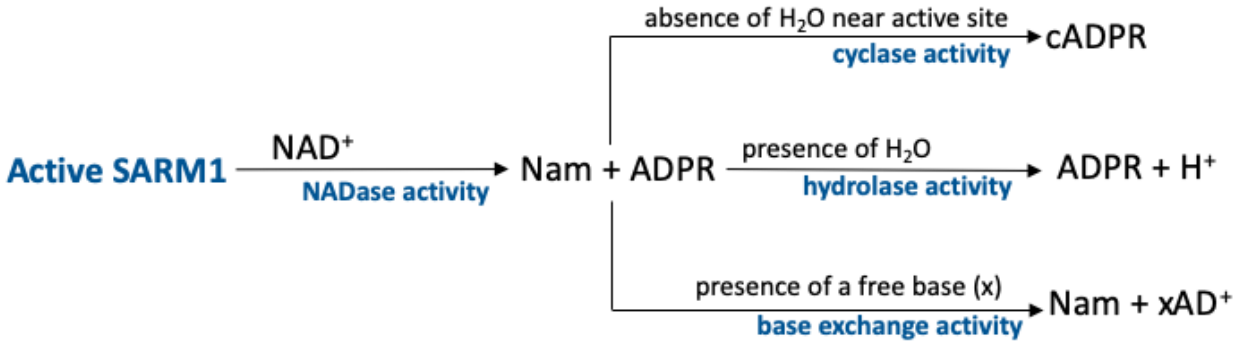

Figure 1.4: A summary of known SARM1 enzyme activities and product formation. Cyclase activity is predominantly active under basal conditions.

In addition to NADase activity, SARM1 also has base-exchange activity, shown in Figure 1.4. The first step of this process is dependent on NADase activity to cleave the Nam and ATP-derived moieties of NAD^+ apart. When this cleavage occurs in the presence of free nucleotide bases, Nam, ADPR or cADPR are not produced. Rather, the free base is switched for a base in NAD^+ in the active site of SARM1 [160]. Whilst this base exchange activity has been demonstrated biochemically, the biological relevance (if any) remains to be determined.

cADPR has been identified as the major detectable product of SARM1 activity produced under basal circumstances in healthy neurones and is the first product to rise after injury before morphological degeneration occurs, making it a potential biomarker of disease pre-degeneration [163]. Moreover, neurofilament light chain (NfL) also appears in blood serum prior to morphologically identifiable sciatic nerve degeneration and this is prevented by removal of *Sarm1* in a gene-dose dependent manner [163]. However, no direct ability of SARM1 to cleave NfL has been reported, so the appearance of NfL may be indicative of the early stages of axon disintegration caused by an indirect effect of SARM1 activation. Exogenous enzymes engineered to modulate intraneuronal cADPR levels without SARM1 activation do not alter the rate of degeneration in cultured DRGs [163], suggesting that this particular product of SARM1 NADase activity is not alone responsible for axon disintegration. Activation of SARM1 and increased levels of its products ADPR and cADPR have been demonstrated in the absence of degeneration after low-dose application of mitochondrial toxin CCCP [163]. This raises the possibility that active SARM1 could be involved in pre-degenerative pathologies of nervous system disease.

1.4.3 A working model of SARM1 activation

Putting together information from the crystal structure, cryoEM, and mutagenesis studies described above, and summarised in Figure 1.3 (lower two panels), this section will outline a working model of SARM1 activation. This is important to understand in the context of targeting SARM1 as a therapeutic approach to delay or prevent programmed axon degeneration in disease, since it could aid with rational design of small molecule inhibitors. However, it is important to note that this model is based on information from artificial constructs, SARM1 overexpression, and crystal or cryoEM structures of distinct protein domains and near full-length SARM1.

SAM domains of inactive SARM1 monomers interact with SAM domains of neighbouring molecules to form an octameric ring under non-injury conditions [142]. Activity of SARM1 is inhibited by the ARM domain which prevents interactions between TIR domains that are needed for NADase activity to occur. ARM domain autoinhibition can be inferred since removal of the ARM domain leads to constitutively active SARM1 [58]. When SARM1 is inactive, amino acid residue K597 of the TIR domain auto-interacts with residue E642 in the catalytic site to prevent NAD^+ substrate binding [143]. NAD^+ binds full-length human SARM1 allosterically (at a site distinct from its catalytic NADase core) to stabilise the inactive octamer [139]. Additionally, high concentrations of ATP inhibit SARM1 activity without altering the structure of SARM1, suggesting ATP may be a competitive inhibitor binding the TIR domain catalytic site [139].

In the presence of a signal after injury or when the intracellular micro-environment around SARM1 octamers alters to favour activation, ARM domain autoinhibition is released. This signal could be an increase in NMN [159] or altered phosphorylation of SARM1 under stress conditions [162]. It is likely that NMN interacts directly with the ARM domain of SARM1 and the isolated TIR domain does not cleave it [143].

During activation, TIR domains interact and there is a conformational change in their BB loops relating to a shift of residue K597 out of the catalytic site [143]. This enables substrate NAD^+ to interact with the E642 residue in the catalytic site [143]. Functional studies showed that the E642 residue is indispensable for SARM1 NADase activity and prodegenerative function [157], as well as the cyclase, hydrolase, and base exchange activities of SARM1 [160]. In this model, the BB loop is thought to act as a gatekeeper preventing NAD^+ substrate interaction with the active site through interacting with the E642 residue until there is a signal for SARM1 activation. Once NAD^+ (or NADP) binds the SARM1 TIR domain, it is cleaved into nicotinamide and ADRPR (or ADPRP) as has been demonstrated in SAM-TIR constructs [143] in the presence of water. In the absence of water, cyclic-ADPR (cADPR) is generated and in the presence of a free base, base exchange activity can occur, as demonstrated by Zhao et al. (2019)[160].

Since biological systems are in constant flux with ever changing cell environments and microenvironments, stabilisation of protein conformations or localisation is needed for a strong or lasting effect. For example, localised increases in calcium for neurotransmitter release or tethering of ion channels to a specific subcellular region. If an axon is committed to degenerate, stabilisation of the prodegenerative forces will ensure this outcome. In the context of SARM1, the octameric multimerisation of SARM1 monomers are further stabilised by additional interactions between BB loops (mediated by residues D594, E5 programmed96, and G601), and αA helix and EE loop (L579 and H685, respectively) as mutant versions of

these residues possess decreased NADase activity [143]. Conversely, autoinbitory actions of the ARM domain, lower levels of NMN, and allosteric inhibition by NAD^+ confer greater stability of the inactive SARM1 conformation. The next few sections will explore how healthy axons maintain the SARM1 inhibitory balance of NMN:NAD^+.

1.5 NMNAT2 generates the endogenous axonal source of SARM1 substrate NAD^+

NMNATs catalyse the conversion of nicotinamide mononucleotide (NMN) to nicotinamide adenine dinucleotide (NAD^+), an oxidative cofactor which is crucial for cell survival. NAD^+ (or NADH, the reduced form) provides electrons for redox reactions involved in energy production (glycolysis, the citric acid cycle and oxidative phosphorylation) and is essential for activity of many enzymes, as well as posttranslational protein modification, cellular signal transduction, gene silencing via deacetylation of histones and the release of calcium from intracellular stores [164]. There are three known endogenous mammalian NMNAT isoforms (NMNAT 1-3).

In 2010, NMNAT2 was found to be the predominant endogenous NMNAT enzyme in axons [22]. Depletion of NMNAT2 *in vitro* via small interfering ribonucleic acids (siRNAs) was shown to cause spontaneous programmed axon degeneration in the absence of any physical injury[22]. In contrast to the deleterious effects of NMNAT2 depletion, NMNAT2 overexpression is neuroprotective *in vitro* in mouse primary cultures [76,165], *in vivo* in mouse sciatic nerve [166,167], *Drosophila* wing axons [168], and in zebrafish [169] after injury. Due to rapid turnover of NMNAT2, overexpression of NMNAT2 has a modest effect unless expression levels are very high [166] and this may explain the lack of protection by NMNAT2 expression in *Drosophila* 5 days after olfactory neurone axotomy [170].

Another labile survival factor, Stathmin2 (SCG10), is also rapidly depleted in axons post-axotomy [55] across a similar timespan as pro-survival factor NMNAT2 [76]. Knocking down SCG10 accelerates axon degeneration [55], similar to how lowered levels of NMNAT2 accelerate degeneration in response to *in vitro* axotomy or vincristine [110]. However, down regulation of SCG10 is not sufficient to induce programmed axon degeneration in the absence of injury like depletion of NMNAT2 [76]. There is a clear relationship between NADase SARM1 and NAD-synthesising enzyme NMNAT2, where removal of SARM1 protects against degeneration caused by loss of NMNAT2 and prevents peri-natal lethality in mice lacking NMNAT2 [78]. However, the relationship between SCG10, a microtubule regulator, and NMNAT2 or SARM1 is less well-defined.

NMNAT2 undergoes fast axonal transport from the soma to the axon, co-migrating with markers of trans-Golgi and synaptic vesicles in an interaction mediated by cysteine-linked palmitoylation of C164/165 residues encoded by exon 6 [171]. Palmitoylation at these residues is required for initial association with vesicle membranes (membrane anchoring), though the association is maintained after de-palmitoylation [167], probably via the central isoform-specific targeting and interaction domain (ISTID) which is also required for NMNAT2 vesicle targeting [166].

It has been proposed that NMNAT2 palmitoylation state determines its subcellular localisation [167] and that de-palmitoylation causes NMNAT2 to detach from vesicles and assume a diffuse, cytosolic location [171] in order to carry out its function in regulating axoplasmic NMN and NAD^+. Evidence that NMNAT2 is required in the cytosol to confer its neuroprotective function comes from disruption of vesicular targeting in cytosolic NMNAT2 mutants possessing increased capacity for neurite protection *in vitro* [171] and *in vivo* [166]. These mutants do not co-migrate with membrane-bound NMNAT2. Furthermore, abolition of the ISTID removes NMNAT2 vesicle binding capacity and increases protein stability *in vivo* in peripheral mouse axons after sciatic nerve transection and in *Drosophila* after olfactory neurone injury [166]. NMNAT2 half-life can be extended in cytosolic deletion mutants beyond the usual 40 minutes, without disrupting enzyme activity [171]. This is associated with decreased ubiquitination and significantly increased axon protection and suggests that NMNAT2 must dissociate from vesicles into the cytoplasm to promote axon survival optimally.

Palmitate cycling of NMNAT2 is regulated by zinc Finger DHHC-Type palmitoyltransferases (zDHHCs) and de-palmitoylation thioesterases APT1 and APT2 [167]. Interestingly, there there is significant overlap in zDHHC enzymes that promote palmitoylation of NMNAT2 (2, 7, 15, 16, 17, and 21) [167] and SCG10 (zDHHC2, 3, 7, 15, 17, and -1) . Given that levels of NMNAT2 and SCG10 are important for axon survival and determining latency of programmed axon degeneration, regulation of these survival factors by a similar group of zDHHC palmitoyltransferases could be functionally important. The evidence relating to NMNAT2 above suggests that decreasing palmitoylation of NMNAT2 could be protective. However, it has recently been demonstrated that knockdown of zDHHC17, responsible for NMNAT2 palmitoylation and resulting dissociation from vesicles, actually induces distal programmed axon degeneration *in vitro* and *in vivo* in optic nerve despite decreasing levels of palmitoylated NMNAT2 [173]. At first this appears to contradict the finding that NMNAT2 has a stronger protective effect in its de-palmitoylated state. However, palmitoylation is required for the initial association of NMNAT2 with vesicles [167]. Therefore, removal of zDHHC17 palmitoyltransferase activity may prevent this initial palmitoylation and association with

vesicles thereby decreasing levels of NMNAT2 at the distal ends of axons triggering activation of SARM1. Whilst disruption of NMNAT2 vesicular targeting was shown to increase NMNAT2 capacity for neuroprotection [166,171], NMNAT2 mutants were overexpressed in these mice alongside endogenous NMNAT2 which may have allowed some transport of NMNAT2 to the distal axons. Indeed, overexpression of NMNAT2 and other NMNATs confers protection against programmed axon degeneration, and is the topic of the next section.

1.5.1 Overexpression of NMNATs delays programmed axon degeneration

The fortuitous discovery of a spontaneous mutation in mice resulting in slowed nerve degeneration after injury [174] changed long-held views that axon degeneration was a passive process occurring as a consequence of lack of neuronal soma support. Originally referred to as C57BL/6/Ola mice, these mice later became known as Wallerian degeneration slow (*Wld*^{S}) mice. The *Wld*^{S} gene is a chimeric gene comprising the nucleotide sequence encoding a 70 amino acid N-terminal fragment of ubiquitination factor E4B (Ube4b) fused to the complete nicotinamide mononucleotide adenylyltransferase (Nmnat) gene [175]. The resulting WLD^S protein is a UBE4B-NMNAT1 fusion protein which possesses NMNAT enzyme activity [175]. This knowledge greatly improved understanding of the role of NMNATs in axon health and degeneration. A short sequence that forms part of the NMNAT1 5' untranslated region (UTR) links together the two domains of the WLD^S protein [2,70,176].

Presence of the WLD^s protein protects the structure and function of injured axons in both the central and peripheral nervous system against degeneration for to 2-3 weeks *in vivo* compared to the 2-3 days in wild-type axons [17,64,82,177–179] WLD^S also delays degeneration after *in vitro* axotomy where axons remain intact for at least 72 hours in comparison to 6-16 hours in wild-type cells [23,62,180,181].

The structure and function of synaptic terminals is also preserved after injury in both the central and peripheral nervous systems of *Wld*^{S} mice and rats [66,182–185]. However, synapse withdrawal from motor nerve endplates does eventually occur and precedes degeneration of axon trunks [182]. The level of WLD^S-conferred synaptic protection depends on synapse maturity [182], the length of the nerve distal to injury [185], and is stronger in rats than mice [186]. The rate of synaptic withdrawal is increased in mice that exercise *ad libitum* pre-lesion [187] and accelerated in older mice [185], though age has a less pronounced effect in *Wld*^{S} rats [185,186]. WLD^S can prevent neurite outgrowth deficits in mice lacking functional NMNAT2 who then survive into adulthood, though develop motor deficits around 3 months of age [77].

Neuronal plasticity is decreased in *Wld*^{S} mice after injury in sciatic nerve, phrenic nerve, and spinal cord [35–38], though it has been shown to increase in striatal neurones shortly after cortical lesion [184]. The mechanism causing axon degeneration and WLD^S-dependent slowed degeneration is intrinsic to the axon [23,63,188] with the role of monocytes and glial cells proposed to be limited to clearance of axonal debris after fragmentation, and regeneration of the proximal stump [2]. However, it is possible that glial cells modulate the rate of degeneration since DRGs co-cultured with Schwann cells exhibit accelerated degeneration after *in vitro* axotomy than DRGs alone [189] and a recently published paper highlights a role of axon-glial metabolic coupling and glycolytic upregulation in Schwann cells post injury which promotes survival of injured axons [190]. Aside from slowed programmed axon degeneration, presenting with altered plasticity and slowed nerve regeneration after injury, *Wld*^{S} mice appear otherwise healthy.

Since NAD^+ levels were unchanged in *Wld*^{S} mice despite a four-fold increase in NMNAT activity compared to wild-type brain [175,181,191], it was also proposed that the mechanism of WLD^S protection was mediated by altered ubiquitination or pyridine nucleotide metabolism [82,192,193]. However, since only 6% of the *Ube4b* sequence is present and its catalytic U-box sequence is absent (in comparison to the entire *Nmnat1* sequence), WLD^S is unlikely to possess ubiquitin ligase activity [2,61]. Furthermore, the enzyme activity of WLD^S was later demonstrated as essential for protection against axotomy-induced axon degeneration, since enzyme dead WLD^S possessing the normal UBE4B containing N-terminal domain does not protect against axotomy [181,194,195]. Additional studies with mutations in the *Nmnat1* portion of *Wld*^{S}, vital for NAD^+ synthesis, demonstrate a lack of WLD^S protection after *in vitro* and *in vivo* injury [195,196].

The fact that transgenic expression of WLD^S is protective in mice, rats, *Drosophila*, zebrafish, *C. elegans*, and in primary human neuronal cultures [82,177,186,197–199], indicates strong evolutionary conservation of the axon degeneration pathway it modulates. This makes the *Wld*^{S} mouse an important tool for studying a mechanism of axon degeneration and how this may be modulated.

1.5.2 Axonal localisation of NMNATs needed for an axon-protective phenotype

WLD^S was originally thought to confer its protection by actions in the nucleus, where it is most highly expressed [70,82,180,194,200]. However, it was later shown that WLD^S acts in extranuclear regions of neurones and when targeted to the axon, its protective capacity increases [201–203]. Moreover, destabilizing WLD^S specifically in axons abolishes its protective ability [84,204].

Along with the capacity to synthesise NAD^+, it was established that WLD^S binds valosin-containing protein (VCP) via its UBE4B domain and this is required for WLD^S protection in both mouse [181] and *Drosophila* [170]. VCP is a multifunctional AAA-ATPase protein present in the nucleus and cytoplasm which plays a role in protein homeostasis and mobility via ubiquitination [205] as well as protein degradation, autophagy and mitochondrial quality control [206–211]. The UBE4B domain of WLD^S may therefore be required for localisation, stability, or binding interactions in order for axon protection to occur.

Localisation of increased NMNAT activity is crucial for neuroprotections since overexpression of endogenous *Nmnat1* does not protect as strongly as the presence of WLD^S , unless targeted to axons and synapses [202,203]. Decreasing levels of NMNAT1 (which is mostly expressed in the nucleus) does not alter the rate of injury-induced axon degeneration [212]. In studies reporting a protective effect of NMNAT1 overexpression, lentivirus-based transduction lead to increased NMNAT1 in the axon [84,213]. In addition, overexpression of mitochondrial NMNAT3 is also detected in cytoplasm and confers robust protection against programmed axon degeneration [170,196]. Finally, when endogenous axonally expressed NMNAT2 half-life is extended beyond the usual 40 minutes, without disrupting enzyme activity [171], this significantly increases axon protection which surpasses that conferred by the presence of WLD^S.

Combined, this evidence implies that increased NMNAT activity is required locally in the axoplasm for axon protection to occur after injury. Molecules aimed at improving endogenous NMNAT2 stability or increasing NMNAT2 expression levels could therefore enhance its neuroprotective effect. However, targeting increased NMNAT activity specifically to axons in a therapeutic setting could prove challenging.

1.6 SARM1 and NMNAT2 are regulators of axonal nucleotides

1.6.1 Nucleotide synthesis pathways relevant to programmed axon degeneration

There are several nucleotides and their synthesis/degradation pathways which are important for maintaining axon health and whose disequilibrium is seen in axon degeneration. As already mentioned, NMNAT2 produces NAD^+, the substrate for SARM1, and products of SARM1 activity can be recycled back into NMN or NAD^+. These pathways are summarised in Figure 1.5. Briefly, NMN is synthesised from nicotinamide (Nam) by enzyme nicotinamide phosphoribosyltransferase (NAMPT), the rate limiting enzyme for NMN synthesis. NMN is then covalently bound to the ADP moiety of ATP by NMNAT2 in the axon (or NMNAT1 or NMNAT3 elsewhere) to generate NAD^+. In the endogenous mammalian system, NMN can

also be synthesised from nicotinamide riboside (NR) by nicotinamide riboside kinase (NRK) and depleted by conversion to NR via enzyme CD73. Mammals also have the capacity to synthesise NMN *de novo* from tryptophan via a multi-enzyme process that leads to the formation of NaMN which can be converted to NMN via the salvage pathway or converted into NaAD then nicotinic acid (NA), then NAD^+ via enzymes NMNAT, NamPRT, and NADs, respectively. Extracellular NMN is converted to NR for transportation into the cell via the equilibrative nucleoside transporter (ENT) where it can then be converted back to NMN via NRK. An NMN transporter (Scl12a8) has also been identified as a means of direct NMN transport into the cell [214]. When aberrantly expressed in mammalian cells, bacterial enzyme NMN deamidase can convert NMN into NaMN, thus deplete NMN levels whilst allowing the neurone to synthesise NAD^+ via an alternative pathway (in the presence of NMNAT2). These nucleotide synthesis, degradation, and recycling pathways have been exploited in various studies to modulate NAD^+ and NMN levels and test the effects on programmed axon degeneration.

It is interesting to note that products of SARM1 NADase activity (Nam, ADPR, and cADPR) appear to have the capacity to inhibit SARM1 [138,139,157,215], which could indicate an intrinsic cell mechanism for feedback on SARM1 activity to inhibit serendipitous or aberrant activation in an otherwise healthy axon (via product inhibition). However, concentrations of SARM1 products need to reach or exceed 500 µM for these effects to occur, and these effects were studied on TIR domain alone [215], so the biological relevance of SARM1 inhibition by its products needs to be explored further. Alternatively, SARM1 products can also be recycled into SARM1 activator NMN and act as a positive regulator of SARM1 activation in the context of an injured axon, or be converted into allosteric inhibitor NAD^+ in the presence of NMNAT2. Indeed, it has been suggested that Nam binds weakly to SARM1, likely because it is sequestered or metabolised [215]. To elaborate, Nam is covalently attached to PRPP to form NMN in the presence of NAMPT. Under healthy physiological circumstances, in the presence of axonal NMNAT2, NMN is then covalently bound to ATP to form NAD^+ (which would then favour axon survival by boosting NAD^+ and depleting NMN). However, in the absence of NMNAT2, such as occurs after axotomy, protein translation inhibition, and mitochondrial toxins which initiate programmed axon degeneration, NMN synthesised from SARM1-produced Nam could accumulate and act as a positive reinforcer of SARM1 activity.

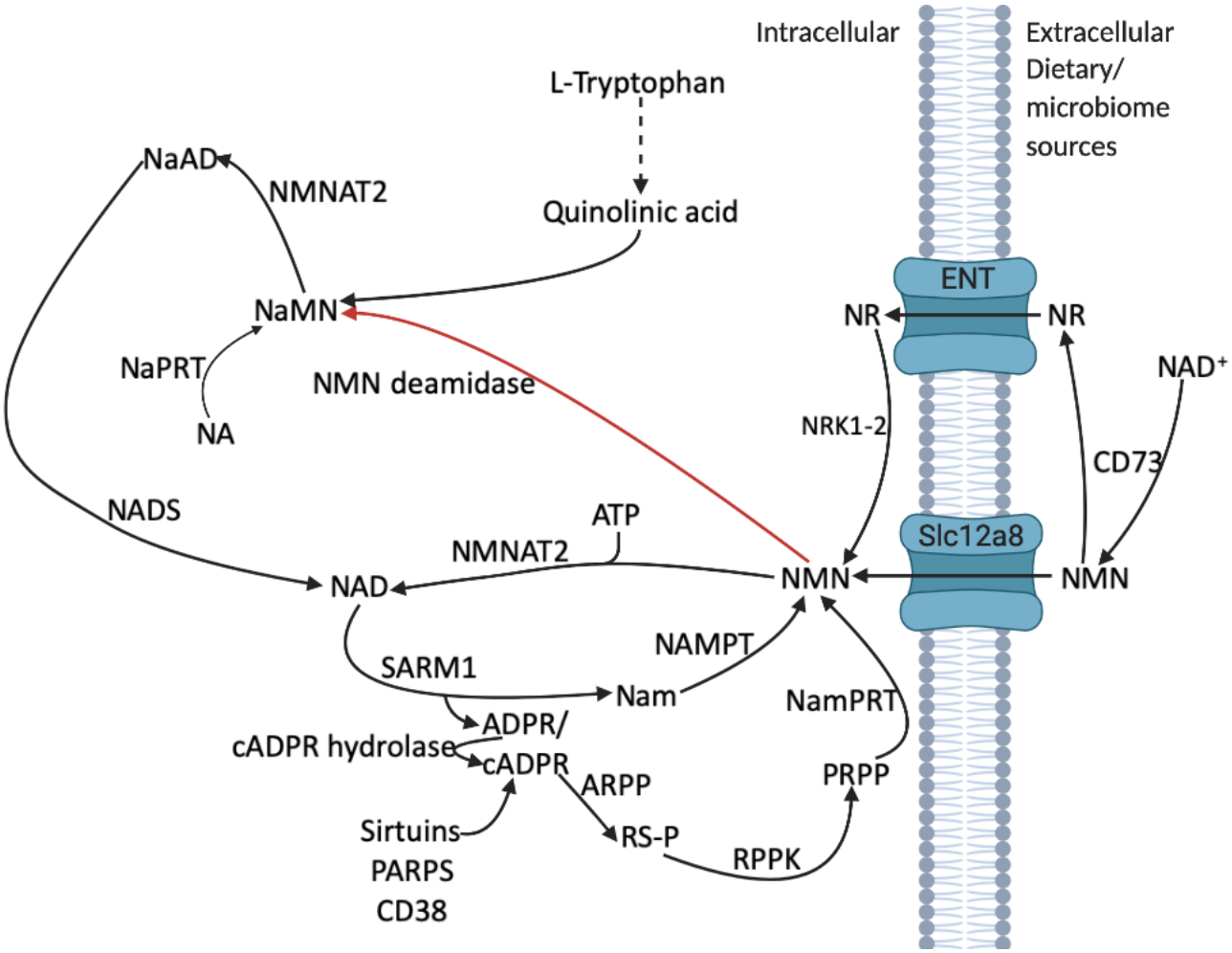

Figure 1.5: Nucleotide synthesis and recycling mechanisms important in the role of programmed axon degeneration. The orange arrow indicates a pathway not usually present in the mammalian system, but aberrantly expressed in experimental models showing protection against axon degeneration.

1.6.2 NMN accumulation versus NAD^+ depletion hypotheses of programmed axon degeneration

How the activity of NMNAT2, an NAD^+ synthesising enzyme, and SARM1, an NAD^+ consuming one, relates to one another and nucleotide levels (particularly those of NAD^+ and its precursor NMN) was a source of controversy in this field. Conflicting evidence supported conflicting hypotheses; one in which accumulation of NMN causes SARM1 activation and degeneration [159,216,216]; the other in which depletion of NAD^+ leading to metabolic catastrophe causes degeneration [57].

Recently, NMN has been shown to activate near full-length SARM1, as resolved by cryoEM [138] and both NMN and NMN mimetic CZ-48 activate SARM1 NADase activity [160]. After injury, the WLD^S protective effect is phenocopied by aberrant expression of bacterial enzyme NMN deamidase (which converts NMN into NaMN thereby depleting NMN levels) in axons of zebrafish and mouse *in vitro* and *in vivo* systems [159,216]. NMN deamidase also prevents perinatal lethality in mice lacking NMNAT2, similar to Wld^S and $Sarm1^{-/-}$ [77,78,216]. Furthermore, pharmacologically decreasing NMN using FK866 (an inhibitor of NAMPT, thus inhibitor of NMN production) delays degeneration for 24h after *in vitro* axotomy [191,216] despite causing a concurrent decline in NAD^+ levels.

WLD^S (and NMNATs) also deplete NMN by covalently binding it to ADP to produce NAD^+. Since protection conferred by NMNAT1 overexpression requires NMNAT enzyme activity [195,196,202], but NAD^+ levels are not increased [82,181,202], combined with the evolving evidence for NMN activation of SARM1, it seems that NMNAT-dependent depletion of NMN likely underlies WLD^S protection. Moreover, high levels of NAD^+ in $Parp^{-/-};Cd38^{-/-}$ mice are not sufficient to prevent or delay programmed axon degeneration after *in vivo* axotomy and cytoplasmic NMNAT1 still delays axon degeneration after NAD^+ depletion by siRNA knockdown of *Nampt*, which encodes the enzyme producing NMN for use in NAD^+ synthesis [202].

In contrast to the NMN hypothesis, NAD^+ depletion resulting in metabolic catastrophe has been proposed as the cause of degeneration since SARM1 activation induces rapid depletion of NAD^+ [57]. This, together with NMNAT2 loss (and its function in NAD^+ synthesis), could explain the depletion of axonal NAD^+ after injury [180]. Furthermore, SARM1 NADase activity is needed for its prodegenerative function and it was suggested that WLD^S/NMNATs preserve axons by rapidly resynthesizing NAD^+ to counteracting SARM1-dependent toxic NAD^+ depletion [57]. In support of this, pre-treatment with NAD^+ for at least 24 hours increased the number of in-tact axons present 72 h post-transection [194] and increased levels of NMN do not

cause spontaneous axon degeneration [158]. Genetic and pharmacological manipulation of the NAD^+ biosynthetic pathway in DRG cultures which result in a rise of NMN levels, actually delays degeneration in injured axons [158]. However, in these experiments, axon preservation in the presence of raised NMN levels also occurred in the context of raised NAD^+ levels due to the presence and activity of NMNAT2 prior to injury. Therefore, whilst NMN levels are increased, the ratio between NMN and NAD^+ is likely unchanged meaning SARM1 inhibition is likely favoured. This could suggest that accumulating NMN levels need to occur in the context of declining NAD^+ levels in order to be pro-degenerative.

1.6.3 Towards resolving the NMN vs NAD^+ hypotheses: the NMN:NAD ratio

Indeed, the recent demonstrations of SARM1 substrate inhibition by NAD^+ [139], activation by NMN [138], and NMN-induced NADase activity of SARM1 [160] provide a possible explanation for the conflicting evidence of the roles of NAD^+ and NMN in programmed axon degeneration. Together, these key pieces of evidence suggest that maintenance of a ratio of high NAD^+ (SARM1 inhibition) to low NMN (SARM1 activation) is necessary for preventing activation of SARM1. If circumstances alter the levels of either nucleotide enough, this can favour SARM1 activation.

With this knowledge in mind, combined therapeutic strategies to boost NAD^+ levels and decrease NMN levels may prove beneficial. Indeed, therapies countering NAD^+ loss through supplementation with NAD^+ precursors NR or NMN are being explored as neuroprotective agents [217] showing positive effects in models of injury and disease [218–223].

However, caution should be taken with using these therapies in injuries that deplete NMNAT2: since NMNAT2 under healthy conditions depletes NMN and produces NAD^+, disease related depletion of NMNAT2 could lead to increased NMN levels and decreased NAD^+ levels if therapies involve supplementation with NAD^+ precursors. This would likely lead to a favouring of SARM1 activation/disinhibition which is precisely what therapies against programmed axon degeneration aim to avoid. Even supplementing with NAD^+ directly would not avoid this problem since there is no known NAD^+ transporter meaning that exogenous or extracellular sources need to be converted to NR or NMN to enter cells where NMNAT2 then converts them back to NAD^+. Furthermore, if NAD^+ loss is the ultimate cause of axon fragmentation, the rapidity of its degradation after SARM1 activation makes increasing NAD^+ production after injury an unlikely possibility for therapeutic intervention, especially where long-lasting protection is required.

1.7 A mitogen-activated protein kinase cascade in programmed axon degeneration

Aside from key roles of NMNAT2 and SARM1, other proteins and pathways have been reported as modulators of axon degeneration. This section will cover the mitogen-activated protein kinase (MAPK) cascade, which comprises a family of signal amplification and transduction proteins that regulate a huge range of cell responses. Activation (or sometimes inhibition) of this cascade usually occurs via phosphorylation of a specific residue of a kinase which triggers a cascade of subsequent phosphorylation events in subsequent proteins. Activation of the pathway begins with a stimulus which activates a MAPK kinase kinase kinase (MAP4K) or a GTPase (like a cell membrane receptor), which then activates a (usually cytosolic) MAPK kinase kinase (MAP3K), which activates a MAPK kinase (MAP2K), then a MAPK which activates a target, usually a transcription factor to elicit an appropriate cell response [224], as outlined in Figure 1.6.

Proteins in this cascade have long been known to play a role in apoptosis and other cell death mechanisms and programmed axon degeneration is no exception. Dual leucine zipper-bearing kinase (DLK), a MAP3K involved in synaptic development [225,226], was first to be linked to programmed axon degeneration [227]. Removal of DLK in transgenic mice confers a 52 h *in vivo* delay in degeneration post-sciatic nerve transection, as well as *in vitro* delays in degeneration after axotomy and vincristine for 48 h [227]. Supporting this, removal of the *Drosophila* DLK orthologue Wallenda (Wnd) has comparable protective capacity [227]. In addition, heat shock protein 90 (HSP90, and its *Drosophila* orthologue Hsp83) play a chaperone role in stabilising DLK (Wnd) and Hsp83 is required for Wnd protein stabilisation and injury-induced JNK signalling in *Drosophila* larvae [228]. Two other mammalian MAP3Ks, MEKK4 and MLK2, also affect the rate of axon degeneration, since knocking down each modestly delays degeneration after *in vitro* axotomy [229]. It seems there is functional redundancy between the three identified MAP3Ks in their role in axon degeneration since removal of all three together increases the strength of protection post-optic nerve injury to 6 days compared with the weaker delays afforded by removal each individual protein [229].

DLK is thought to act via MAP2K proteins MKK4 and MKK7 [230] and then MAPK JNK [227]. Decreased MKK4 or MKK7 expression protects neurites up to 24 h after *in vitro* axotomy via slowing the rate of NMNAT2 turnover [230]. Combined removal or downregulation of both MKK4 and MKK7 significantly prolongs protection compared to knockdown of the individual kinases [229]. JNK inhibition delays axon degeneration after *in vitro* axotomy for 12-48 h [55,227] and also slows the rate of SCG10 depletion [55]. Later the roles of JNK2 and 3 in optic nerve degeneration and JNK1, 2, and 3 in cortical neurone degeneration were confirmed [229]. Finally, Death

Receptor 6 (DR6), has also been linked to programmed axon degeneration with 38% axons remain intact 14 days post-transection compared to 100% in *Sarm1*$^{-/-}$ and 80% in *Wld*^{S} mice [72]. However, it appears that DR6 does not play a role in axon degeneration after optic nerve crush [47].

Combining the evidence above, it seems that activation of a MAPK signalling cascade plays a role axon degeneration, as illustrated in Figure 1.6. However, there is debate over where the MAPK cascade acts and whether it regulates programmed axon degeneration or is regulated by it. For example, *Sarm1*$^{-/-}$ prevents MKK4 activation [229], but not JNK activation [47] in a model of optic nerve crush. NMNAT2 turnover is accelerated by MAPK activation [230] and the presence of cytoplasmic-NMNAT1 blocks MAPK activation [229], but MKK4/7 knockdown does not prevent axon degeneration initiated by loss of NMNAT2 or constitutively active SARM1 [230]. In addition to the unclear involvement of MAPK signalling in programmed axon degeneration, none of the reported modifications to the cascade show protection as strong as that afforded by addition of WLD^{S} or removal of SARM1, even when multiple targets are removed.

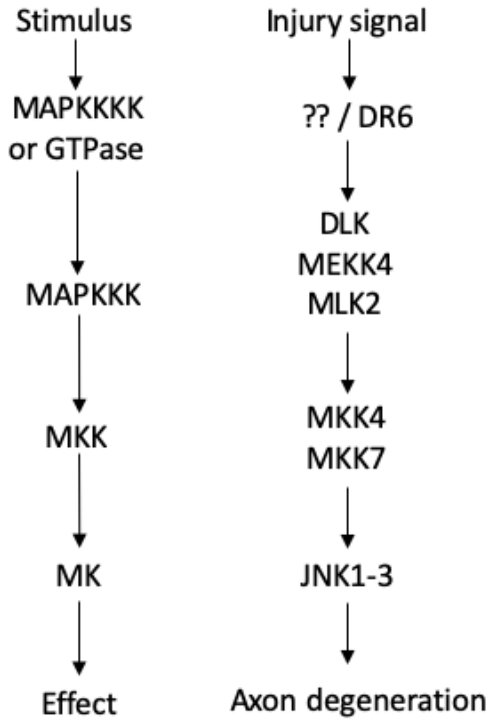

Figure 1.6: Accepted central dogma of the mitogen-activated protein kinase (MAPK) cascade and the corresponding proteins identified as weak modulators of programmed axon degeneration.

1.8 The role of the ubiquitin proteasome system in programmed axon degeneration

The ubiquitin proteasome system (UPS) is an ATP-dependent intracellular protein degradation system whereby proteins are targeted for degradation by attachment of ubiquitin proteins. This is activated through a series of enzymes starting with activating ubiquitin enzymes (E1), then ubiquitin conjugase enzymes (E2), and finally ubiquitin ligase enzymes (E3) which bind a ubiquitin tag to lysine residues in the target protein [231,232].

Chemical inhibition of the proteasome or genetic removal of proteins key to its function delay axon degeneration after injury [24,55,153,153,233–239]. MYCBP2/PHR1 (Highwire) deletion confers protection against axon degeneration approaching the efficacy conferred by WLD^S. This protection is likely due to decreased turnover of axon survival factors, since increased levels of NMNAT2 [73,167] and SCG10 [55] are present after proteasome inhibition. Depletion of axon survival factors can induce axon degeneration or accelerate degeneration after injury whereas increased levels can delay degeneration [22,55,166].

NMNAT2 ubiquitination occurs at lysine residues positioned outside the region important for targeting NMNAT2 to transport vesicles [167] and lower levels of NMNAT2 ubiquitination lead to expression of more stable variants with stronger neuroprotective phenotypes [171], suggesting a role of the ubiquitin-proteasome system in NMNAT2 turnover. Indeed, NMNAT2 has been reported to bind the substrate recognition domain of the PHR1 ubiquitin ligase complex (FBXO45, SKIP1, and PAM) [240]. When the proteasome is inhibited by MG132, both NMNAT2 and dNMNAT accumulate, adding further evidence that NMNAT2 levels are regulated via the ubiquitin proteasome system [73] and that overactivity of the proteasome can deplete axon survival factor NMNAT2.

DLK (Wnd) is also a target of MYCBP2 (Highwire) and interestingly, protein levels of pro-degenerative DLK (Wnd) are increased in mice lacking PHR-1 and *Drosophila* lacking Highwire, respectively [239,241]. However, axon degeneration is still strongly delayed in mutants lacking the protein [239,241], placing the signal to activate the MAPK pathway upstream of the proteasome. Activation of MKK4 and MKK7 also promotes the turnover of axon survival factors NMNAT2 and SCG10 [230]. This process which appears to be regulated by an endogenous inhibitor, AKT, which prevents downstream activation of JNK [229]. AKT levels are decreased after injury and E3 ubiquitin ligase ZNRF1 is responsible for targeting AKT to the proteasome for degradation [229]. This likely leads to activation of the MAPKs cascade. Deletion of ZNRF1 confers modest protection against programmed axon degeneration [153,234].

1.9 The role of calcium in programmed axon degeneration

It has long been known that intracellular calcium levels increase during programmed axon degeneration [11,242–244]. Early studies placed this increase as a late event in the axon degeneration pathway [11,61,245–247], though more recent studies place it early [59,248]. In fact, axotomy injury triggers two distinct rises in intra-axonal calcium levels:

> One occurs in the axon stump during the acute axon degeneration (AAD) phase immediately after axotomy [8,12]. This is likely not essential for committal of the axon to degenerate since this wave also occurs in the presence of WLD^S or NMN deamidase, absence of SARM1, or after application of FK866 despite these modifications all significantly delaying axon degeneration [59,246,249,250].
>
> The other calcium wave occurs hours after axotomy spreading along the entire length of the distal axon stump [246]. The presence of WLD^S does suppress this second wave, and exogenous addition of calcium is sufficient to abolish this protection [246,249]. Indeed, a recent report notes that the late intra-axonal calcium rise is dependent on the presence of SARM1 and its activation by NMN [250].

Loreto et al, (2015)[250] distinguish between the two waves of increased calcium levels placing the SARM1-independent wave seen by Summers et al., (2014)[59] in the AAD phase which occurs near the site of injury. They show that it is the second NMN- SARM1-dependent calcium wave is crucial for execution of axon degeneration. Indeed, axon degeneration rapidly ensues after the second wave of extracellular calcium influx in zebrafish after axotomy [250], placing late increased calcium levels as a key signal for axon fragmentation. Indeed, since products of SARM1 activation ADPR and cADPR [143,157] are involved in calcium mobilisation and homeostasis [251] they could contribute to the second calcium wave, though this remains to be determined.

1.9.1 Calpain activation

The early wave of calcium influx is likely important for activation of calpains, calcium-dependent cysteine proteases which are responsible for axon cytoskeleton disintegration, since their activation occurs within hours of *in vivo* axotomy [11,29,252]. Calpains have been demonstrated to cleave all three light, medium, and heavy neurofilament chains (NfL, NfM, and NfH), as well as microtubules [29,253–256]. Prevention of calpain activation and axon

degeneration in cultured DRGs by can be achieved through application of leupeptin analogues and cysteine protease inhibitor aloxistatin [11]. In addition, calpains cleave collapsin response mediate protein-2 (CRMP2) to cause AAD [257]. Modulating calpain activation and subsequent cleavage of CRMPs can modestly delay injury-induced degeneration. Inhibition of calpains via the endogenous inhibitor, calpastatin, or exogenous application of calpain inhibitors can delay degeneration for up to 16 h after *in vitro* axotomy [247] and 24 h after *in vivo* optic nerve crush [29,258]. Calpastatin overexpression has been shown to protect against optic nerve transection, leaving around 90% of axons in-tact 2 days post-transection [29] and 55% axons in-tact after 3 days [247]. Removal of CRPM4 delays *in vivo* degeneration for 36 h post-sciatic nerve transection [259].

1.9.2 Calcium channels

Calcium chelation using EGTA in culture medium delays axotomy-induced degeneration for 24 h [59] up to 4 days post-cut [11]. Extracellular calcium influx is required for degeneration since axons remain intact when the calcium concentration in culture medium is less than 200 µM [11]. Axon degeneration delayed by calcium chelation is stronger than that achieved by exogenous calpain inhibitor [24,59] or calcium channel inhibitor nifedipine [245,260], which both modestly delay axon degeneration for 15-18 hours post-axotomy.

Calcium levels in cells are regulated by the presence of calcium permeable plasma membrane channels and transporters, as well as intracellular stores such as the mitochondria and endoplasmic reticulum (ER). Inhibition of plasma membrane channels, such as L-type calcium channels by dihydropyridines and voltage- and receptor-gated slow calcium channels by bepridil [11] and verapamil [260] all modestly delay axon degeneration *in vitro*. *In vitro* inhibition of the Na^+/Ca^{2+} exchanger by KB-R7943 also delays degeneration [250], but inhibition of sodium and potassium channels by tetrodotoxin or conotoxin, which allow some non-selective calcium entry, does not [11].

1.9.3 Intracellular calcium buffering

As well as plasma membrane calcium channels, organelles such as mitochondria and the ER, play an important role in modulating intracellular calcium levels. Mitochondria are also responsible for producing ATP and reactive oxygen species (ROS), and releasing pro-apoptotic and other cell death signals [261,262]. The ER, which extends from the neuronal soma along axons also plays crucial roles in lipid and protein synthesis, post-translational modifications, and glucose metabolism [263]. As such, mitochondrial and ER dysfunction have both been linked to pathogenesis in various neurodegenerative disorders [263–267]. Interestingly,

multiple contact points between axonal ER and mitochondria have been observed [268] along with mitochondrial localisation at sites of calcium accumulation [250].

Changes to intra-axonal calcium homeostasis after injury stimulates an axonal ER stress response [269], as well as loss of mitochondrial membrane potential, ATP depletion, and decreased mitochondrial transport [25,180,229,237,248,270]. Increased intracellular calcium levels regulate mitochondrial movement by arresting both antero- and retrograde mitochondrial transport [271,272], possibly to allow the axon to utilise the calcium buffering capacity mitochondria possess [273]. Morphologically, axonal mitochondria display signs of damage after transection injury [274,275], and calcium release from the ER has been shown to contribute to injury-induced mitochondrial swelling [268].

Calcium-releasing channels in the ER are inositol 1,4,5-triphosphate receptors (IP_3R) and ryanodine receptors (RyR) [28,276]. Preventing calcium release from the ER (via inhibition of RyR or IP3R or siRNA knockdown of RyR1-3 or IP3R) or inhibiting the mitochondrial calcium uniporter delays mitochondrial swelling and axon degeneration in *ex vivo* nerves 3 days post-axotomy, as well as delaying axon degeneration for 12 h *in vitro* post-axotomy [268]. Another study shows that pharmacological inhibition of the RyR, and increased mitochondrial calcium buffering can delay axon fragmentation for up to 15 h post-axotomy, where blockage of extracellular calcium influx can protect for 18 h [250], suggesting a combined role of extracellular calcium influx as well as release from intracellular stores in the second calcium rise.

The role of mitochondria in programmed axon degeneration is thought to occur through the mitochondrial permeability transition pore (mPTP) [237,268]. High calcium levels induce mitochondrial permeability transition (mPT) [277,278] and when open, the mPTP can enhance ROS production [279]. ROS accumulation has been observed in programmed axon degeneration and can be prevented in the presence of WLD^S . Mitochondrial impairment by CCCP depletes levels of NMNAT2 and activates programmed axon degeneration which the presence of WLD^S or absence of SARM1 protects against [75]. Some co-localisation of WLD^S with mitochondria has been noted [196,201,203], though mitochondria are unlikely to be the site at which WLD^S elicits its protective capacity since it has been shown that NMNAT2 (which WLD^S substitutes for) loses its efficacy when targeted to the mitochondria [171]. Whilst removal of mitochondria does modestly delay axon degeneration in *Drosophila*, mitochondria are dispensable for programmed axon degeneration since WLD^S-conferred protection persists even in axons lacking mitochondria [197].

Compared to other proteins involved in programmed axon degeneration, targeting ion channels and calcium release stores to decrease the second intracellular rise in calcium levels affords very modest delay in axon fragmentation. Indeed, since fragmentations occurs rapidly after the second calcium wave, this indicates a late process in the committal of the axon to degenerate. Therefore, therapies targeting this part of the pathway are unlikely to be beneficial for long-term prevention of programmed axon degeneration.

1.10 Therapeutic opportunities to intervene with programmed axon degeneration

It seems there are many opportunities to intervene with the programmed axon degeneration pathway which confer varying levels of protection against programmed axon degeneration, as summarised in Figure 1.7. Particularly strongly axon protection can be conferred by increasing levels of axonal NMNAT, preventing NMN accumulation and SARM1 activation, or by inhibiting the proteasome.

Depletion of *Sarm1*, viral transduction of *Nmnat1* into axons, and application of FK866 within the first 4 hours of transection injury confers strong protection against degeneration [57,159,213] and JNK inhibitors can be applied 3 hours after axotomy and still be effective [227]. Taken together, it appears that there is a 4-hour period of reversibility in programmed axon degeneration where treatment may be effective at preventing degeneration after injury. In disease, this pre-committal to degeneration phase could be longer.

Despite early activation of calpains and the MAPK cascade after injury [29,227,229,252] making these protein a potential target in early stages of degeneration, genetic or pharmacological interference with these pathways is far weaker than removal of SARM1 or the presence of WLD^S or cytoplasmic-NMNAT1 [29,72,227,229,257–259]. Roles of extracellular calcium influx and intracellular calcium release which are crucial for committal of axons to degenerate are late events in the pathway and their modulation has even weaker protective effects than those of calpains and the MAPK cascade. Furthermore, additional roles of proteins and organelles involved in these processes outside of programmed axon degeneration mean there could be negative side effects occurring via off-target actions if therapies aim to modulate their activity.

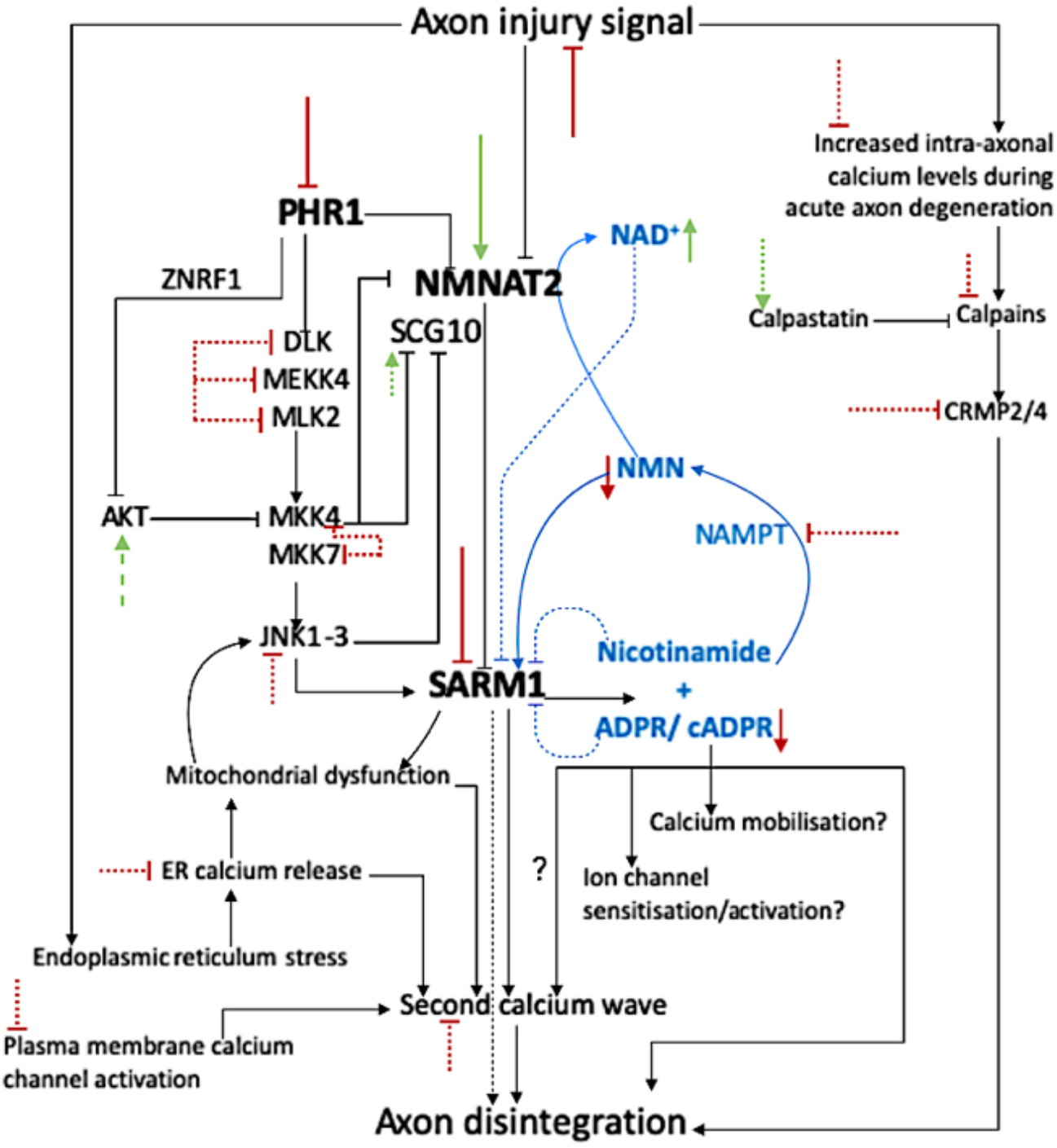

Figure 1.7: Potential targets to modulate programmed axon degeneration. Black text and arrows indicate the endogenous mammalian drivers and modulators of programmed axon degeneration. Blue text indicates key nucleotides whose levels are altered in the lead up to axon disintegration. Red indicates that a decrease in activity or levels could protective. Green indicates an increase in activity or levels could protective. Dotted coloured lines indicate relatively weak modifiers/effects and dotted black lines or question marks indicate unknown steps in the pathway.

Mostly, the protection afforded by removal of *Sarm1* is comparable to that achieved by overexpressing WLD^S and cytoplasmic-NMNAT1. However, the effects of *Sarm1*$^{-/-}$ appear to supersede those of WLD^S in a developmental model where mice lacking functional NMNAT2: reversal of deficits in these mice are retained into old-age in the absence of *Sarm1* unlike those of WLD^S where mice develop motor deficits at three months of age [111]. In addition, 100% of *Sarm1*$^{-/-}$ axons remain intact after sciatic nerve transection injury, with 80% remaining intact neuroprotection if targeting SARM1. The strength of protection after SARM1 removal, its apparent specificity to programmed axon degeneration, and the unexpected discovery that SARM1 possesses intrinsic enzyme activity make it an attractive therapeutic target. Importantly, mice lacking SARM1 are healthy for their lifespan without demonstrating obvious abnormalities, implying a low risk of negative side effects if therapies remove its function. Indeed, the evidence presented above raises the possibility that decreased SARM1 levels (which is more therapeutically achievable than complete removal) may afford greater protection against axon fragmentation compared to other modulators of the pathway. For these reasons, exploring the validity of SARM1 as a therapeutic target will form the basis of this thesis.

1.11 Approaches for anti-SARM1 therapies

1.11.1 Small molecule inhibition of TIR domain NADase activity

Small molecule inhibitors are required to bind perfectly and tightly to small cavities in the three-dimensional structure of a protein to prevent the associated disease-related protein activity. Recently SARM1-TIR domain NADase enzyme activity has been demonstrated [157,280] and structural studies have identified the NAD^+ binding pocket (SARM1 NADase active site) [143], as well as distinct allosteric sites on the ARM domain where SARM1 can be activated by NMN [138] and inhibited by NAD^+ [139]. Nicotinamide, a product of SARM1 NADase activity, inhibits hydrolase activity of isolated TIR domains [157] and inhibits SARM1 at a site close to the E642 residue [138] which is required for interaction with NAD^+ when activated or residue K597 when inactive [143]. Furthermore, ATP inhibits SARM1 activation in a dose-dependent manner without affecting protein conformation [139] making it a potential competitive inhibitor at the TIR NAD^+ binding site.

Each of these binding pockets are in theory amenable to small molecule inhibition. Disruption of TIR domain interactions via small molecule inhibition has been demonstrated on Toll-like receptor 2 (TLR2) TIR domain thereby preventing TLR2 interactions with MyD88 and subsequent inflammatory signalling [281]. In addition, a high-throughput screen has recently identified several small molecules that are capable of non-competitively binding and inhibiting

the NADase activity of isolated SARM1 TIR domains [282]. However, the capacity of these molecules to bind full length SARM1 and whether they confer any neuroprotective effects have not yet been shown. Given that SARM1 forms an octameric structure and there are many ionic interactions maintaining its inactive form [139], there could be stochiometric issues around small molecules accessing TIR domain binding sites. Inhibition of the putative NMN-binding site on the ARM domain may therefore be an alternative, more easily accessible site at which to prevent SARM1 activation.

1.11.2 Small molecule inhibition of protein-protein interactions in the SARM1 octamer

Small molecules are also capable of interfering with protein-protein interactions by binding the large flat planes which proteins use to interact with one another [283]. Knowledge that SARM1 SAM domains interact with other SAM domains in neighbouring molecules [142,143] raises the possibility that disrupting these protein-protein interactions could be beneficial. However, this is challenging since small molecules usually bind small deep cavities of a protein's tertiary structure which are mostly absent on flat planes. Protein-protein interactions are driven by hydrophobic regions of these flat planes which have higher proportions of charged and polar residues. These residues enable hydrogen bonds and ionic and electrostatic interactions [284,285] to form between the interacting proteins. It is possible during formation of these interactions, which have been described as multistep process requiring multiple random collisions between interacting proteins until they orientate such that weak ionic/electrostatic/hydrogen interactions can occur (Schreiber, Haran, and Zhou 2009). During the process of forming these interactions (i.e., SAM-SAM interactions for the formation of SARM1 octamers) there is an opportunity for small molecule inhibitors to bind a 'hotspot' on the flat plane competing with the usual protein binding partner thus preventing the usual protein-protein interactions [283]. Even after formation of the protein-protein interactions, allosteric binding of small molecule can cause a conformational change some distance from the binding interface thus decreasing the propensity for non-covalent binding interactions [283]. Targeting protein-protein interactions to weaken SAM-SAM or TIR-TIR interactions could destabilise the octameric structure SARM1 required for its pro-degenerative role.

Since small molecules are required to bind perfectly and tightly to small cavities in a protein, when such a cavity is not identifiable (e.g., there is no known enzyme function or protein-protein interactions identified as a driver of disease) or there are technical difficulties in designing small molecule inhibitors, alternative approaches are needed. Instead of targets the protein monomers or octamers with small molecules, there are also therapeutic methods available that act upstream. One such method is gene therapy.

1.11.3 Gene therapy

Gene therapy involves introducing a gene or other construct into cells where the endogenous encoded protein causes disease through its absence or aberrant activity. There are various vectors which can be used to deliver genes, such as retro-, lenti-, adeno-, and adeno-associated viral (AAV) vectors, which are derived from viral genomes [286,287]. Indeed, feasibility of AAV-mediated genes delivery has been demonstrated preclinically in the treatment of a range of neurological diseases (REF). Early clinical studies utilising AAV vectors to mediate gene delivery in patients with neurological disorders were for Canavan disease [288], Parkinson's disease [289], and late infantile neuronal ceroid lipofuscinosis [290]. These studies showed that it was possible to use this approach to modify CNS diseases, though some adverse effects were observed, including; high levels of AAV-neutralising antibodies [288] and transient humoural responses after injection into the CNS [290]. Whilst many participants experienced adverse effects in these Phase I clinical trials, investigators considered most to be unlikely caused by administration of therapy. Since these initial studies, robust efficacy without reporting of adverse events has been demonstrated in 15 patients with spinal muscular atrophy type 1 (SMA1) in a Phase II clinical trial [291]. First reports of the Phase III trial (NCT03306277) indicate similar efficacy, with some adverse events and 91% of children (20/22) survive at 14 months with 59% (13/22) achieving the primary outcome of being able to sit independently. This offers hope that gene therapy may be utilised as a therapeutic approach, at least in spinal and peripheral nerve diseases where AAV uptake is more easily achieved than in brain where expression is confined to areas close to the injection sites [286,289,292]. Indeed, a recent trial involving AAV-mediated delivery of nerve growth factor (NGF) to patients with Alzheimer's disease showed no efficacy since the vector did not reach cholinergic neurone targets [292].

1.11.4 Antisense oligonucleotide therapies

Antisense oligonucleotide therapies have passed Phase 3 trials for SMA where infants receiving antisense oligonucleotides showed decreased mortality and improved motor phenotypes [293]. This is the first FDA-approved treatment for SMA and is now in regular use. Antisense oligonucleotides have also been used in a rare polyneuropathy caused by hereditary transthyretin-mediated amyloidosis where patients reported improved quality of life [294]. In terms of neurodegeneration, an antisense oligonucleotide therapy targeting mutant Huntingtin (mHTT) in HD has passed safety clinical trials showing a dose-dependent decrease in mHTT and several Phase II clinical trials are currently active [295]. Theoretically, genetic targeting of *SARM1* may be more effective than small molecule inhibition given that a strong

decrease in SARM1 levels or activity is needed for prolonged protection. Therefore, inhibiting expression of a gene could yield greater results than targeting the corresponding protein. Practically, there are greater challenges to ensuring bioavailability of gene-based therapies and their *in vivo* ability to modify the target that are not present with small molecule inhibition (such as the capacity to easily enter cells and act on cytoplasmic targets). A common barrier to all therapies targeting the nervous system is ensuring efficient delivery to the correct cell types without causing off-target effects in others. Chapter 4 will go into more depth about the mechanism by which antisense oligonucleotides act since the aim of that chapter is to explore the use of antisense oligonucleotides as an anti-SARM1 therapy.

1.12 Aims of this thesis

There are three data chapters in this thesis which will each address a question relating to the potential for therapies targeting SARM1 in disease. These questions are:

1) If SARM1 is to be targeted pharmacologically, how much do levels need to be decreased in order to have a protective effect?

    a) This question will initially be addressed through generating *Sarm1* hemizygous mice to genetically decrease SARM1 protein levels and observe the rate of programmed axon degeneration *in vitro* after physical transection injury and diverse chemical triggers of programmed axon degeneration.

    b) If there is a slowed rate of degeneration in primary cultures from *Sarm1* hemizygous mice, the relevance *in vivo* will be assessed by sciatic nerve transection and the ability for removal of one *Sarm1* allele in preventing neurite outgrowth deficits in mice lacking functional NMNAT2.

2) Is it possible to decrease SARM1 levels with exogenous application of antisense oligonucleotides and if so, does this translate to a protective effect on axon health after injury?

   a) This question will be addressed by *in vitro* application of *Sarm1* anti-sense oligonucleotides and measuring whether this causes a decrease in SARM1 protein levels.

   b) If SARM1 protein levels are decreased, the impact on the rate of programmed axon degeneration will be assessed *in vitro*

   c) During the course of this thesis, the Coleman group started work on determining the phenotypic effects of *SARM1* predicted loss of function mutants present in the human population. Therefore, effects of combining antisense oligonucleotides to *Sarm1* hemizygous cultures will be assessed.

3) Is programmed axon degeneration active in a model of sporadic Alzheimer's disease, and if so, can SARM1 be targeted to alleviate pathology?

   a) Links between Alzheimer's disease and programmed axon degeneration will be explored in the context of axon transport of mitochondria and axon survival factor NMNAT2 in a D-Galactose model of sporadic Alzheimer's disease.

   b) If there is a link between programmed axon degeneration, the next goal would be to determine whether this model and the associated pathology respond to anti-SARM1 therapies.

Chapter 2: Materials and Methods

2.1 Animals

All animal work was approved by the Babraham Institute and University of Cambridge Animal Welfare and Ethical Review Bodies and performed in accordance with the Animals (Scientific Procedures) Act (ASPA), 1986 and Home Office regulations under project licence numbers 70/7620 and P98A03BF9. All animals were kept on a 12:12 hour light:dark cycle at a constant temperature of 19 °C in a pathogen-free environment with *ad libitum* access to drinking water and standard rodent chow (unless otherwise stated).

2.1.1 *Sarm1* mice

Sarm1 hemizygous mice were generated by crossing the Babraham C57BL/6Babr wild-type line with *Sarm1*$^{-/-}$ (*MyD88-5*) mice generated by Kim et al., (2007)[132]. The F1 progeny from these matings were then crossed together to generate mixed litters containing *Sarm1*$^{+/+}$, *Sarm1*$^{+/-}$, and *Sarm1*$^{-/-}$ mice, as shown in Figure 2.1. Littermates were used for all *in vivo* and *in vitro* experiments assessing the protective effect of *Sarm1* hemizygosity. The *in vitro* studies assessing the effects of antisense oligonucleotides in *Sarm1* hemizygous cultures were done on mice generated from either the Babraham C57BL/6Babr wild-type line, the *Sarm1*$^{-/-}$ line[132], or crosses between the two lines. This generated complete litters of *Sarm1*$^{+/+}$, *Sarm1*$^{+/-}$, and *Sarm1*$^{-/-}$ mice, respectively. Mice aged P0-P2 from the *Sarm1*$^{+/+}$ or *Sarm1*$^{-/-}$ crosses were used as a reference point to already well-defined rates of degeneration to compare the rate of degeneration in the *Sarm1*$^{+/-}$ cultures which received antisense oligonucleotides.

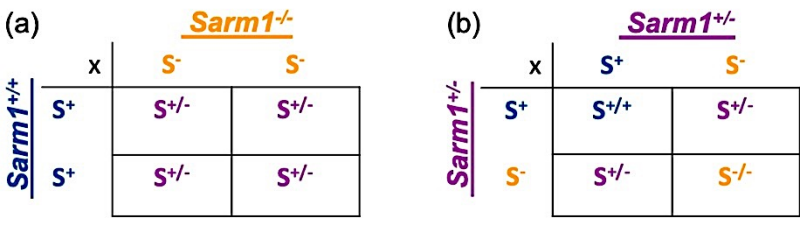

Figure 2.1. Generation of *Sarm1*$^{+/-}$ mice from *Sarm1*$^{+/+(C57BL/6Babr)}$ and *Sarm1*$^{-/-}$ mice (a). Resulting F1 progeny were crossed to generate mixed genotype littermates needed for cell culture and *in vivo* sciatic nerve transection studies.

2.1.2 Mice lacking NMNAT2

Mice lacking NMNAT2, hereafter referred to as *Nmnat2*$^{gtE/gtE}$ mice, were previously generated[77] These mice exhibit perinatal lethality with severely truncated axons present in the peripheral and central nervous system which can be prevented by the presence of WLD^{S} or removal of SARM1[77,78,111]. Experiments in this thesis explore the effects of *Sarm1* hemizygosity on these mice. Mice for the *in vitro* outgrowth data (described in more detail below) were generated from two separate timed-matings, with wild-type controls (*Nmnat2*$^{+/+}$*;Sarm1*$^{+/+}$) and mice lacking NMNAT2 wild-type for *Sarm1* (*Nmnat2*$^{gtE/gtE}$*;Sarm1*$^{+/+}$) being obtained from a cross between two mice *Nmnat2*$^{+/gtE}$*;Sarm1*$^{+/+}$, as illustrated in Figure 2.2.a. Mice lacking NMNAT2 hemizygous for *Sarm1* (*Nmnat2*$^{gtE/gtE}$*;Sarm1*$^{+/-}$) were obtained from a cross between *Nmnat2*$^{+/gtE}$*;Sarm1*$^{+/+}$ and *Nmnat2*$^{gtE/gtE}$*;Sarm1*$^{-/-}$, as illustrated in Figure 2.2.b. For the *in vivo* study, double hemizygous mice were generated from a cross between *Nmnat2*$^{+/gtE}$*;Sarm1*$^{+/+}$ and *Nmnat2*$^{gtE/gtE}$*;Sarm1*$^{-/-}$ mice (Figure 2.3.a). The resulting F1 progeny that were double hemizygous (*Nmnat2*$^{+/gtE}$*;Sarm1*$^{+/-}$) were then crossed together to generate littermate mice for the *in vivo* study (Figure 2.3.b) where neurite outgrowth was assessed in *Nmnat2*$^{gtE/gtE}$ mice with wild-type, hemizygous, or homozygous null *Sarm1* status.

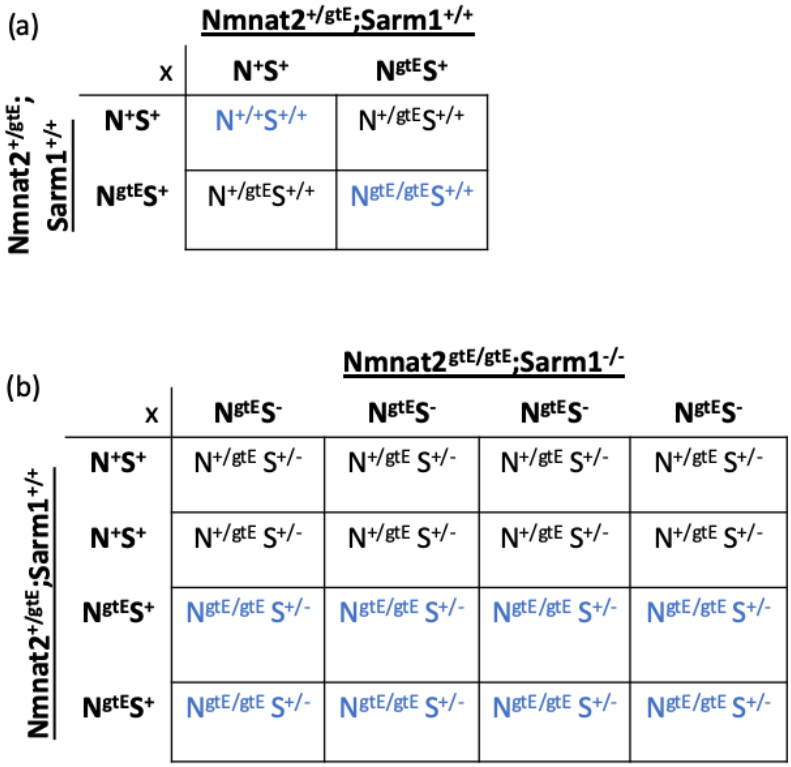

Figure 2.2. Generation of E13.5 mice needed for testing the effects of *Sarm1* hemizygosity on neurite outgrowth in DRGs lacking NMNAT2. These were generated from two coinciding timed-matings; one (a) from a cross between two *Nmnat2*$^{+/gtE}$*;Sarm1*$^{+/+}$ mice to generate *Nmnat2*$^{+/+}$*;Sarm1*$^{+/+}$ (wild-type) and *Nmnat2*$^{gtE/gtE}$*;Sarm1*$^{+/+}$ mice and the other (b) to generated *Nmnat2*$^{gtE/gtE}$*;Sarm1*$^{+/-}$. This was the most reliable way to ensure all genotypes were present for the *in vitro* outgrowth assay. Genotypes indicated in blue were used for the experiment.

(a) ***Nmnat2*$^{+/gtE}$*; Sarm1*$^{+/+}$**

Rows: ***Nmnat2*$^{gtE/gtE}$*;Sarm1*$^{+/-}$**

x	N^+S^+	$N^{gtE}S^+$	N^+S^+	$N^{gtE}S^+$
$N^{gtE}S^-$	$N^{gtE/gtE}\ S^{+/-}$	$N^{+/gtE}\ S^{+/-}$	$N^{+/gtE}\ S^{+/-}$	$N^{gtE/gtE}\ S^{+/-}$
$N^{gtE}S^-$	$N^{gtE/gtE}\ S^{+/-}$	$N^{+/gtE}\ S^{+/-}$	$N^{+/gtE}\ S^{+/-}$	$N^{gtE/gtE}\ S^{+/-}$
$N^{gtE}S^-$	$N^{gtE/gtE}\ S^{+/-}$	$N^{+/gtE}\ S^{+/-}$	$N^{+/gtE}\ S^{+/-}$	$N^{gtE/gtE}\ S^{+/-}$
$N^{gtE}S^-$	$N^{gtE/gtE}\ S^{+/-}$	$N^{+/gtE}\ S^{+/-}$	$N^{+/gtE}\ S^{+/-}$	$N^{gtE/gtE}\ S^{+/-}$

(b) ***Nmnat2*$^{+/gtE}$*;Sarm1*$^{+/-}$**

Rows: ***Nmnat2*$^{+/gtE}$*;Sarm1*$^{+/-}$**

x	N^+S^+	N^+S^-	$N^{gtE}S^+$	$N^{gtE}S^-$
N^+S^+	$N^{+/+}S^{+/+}$	$N^{+/+}S^{+/-}$	$N^{+/gtE}S^{+/+}$	$N^{+/gtE}S^{+/-}$
N^+S^-	$N^{+/+}S^{+/-}$	$N^{+/+}S^{-/-}$	$N^{+/gtE}S^{+/-}$	$N^{+/gtE}S^{-/-}$
$N^{gtE}S^+$	$N^{+/gtE}S^{+/+}$	$N^{+/gtE}S^{+/-}$	$N^{gtE/gtE}S^{+/+}$	$N^{gtE/gtE}S^{+/-}$
$N^{gtE}S^-$	$N^{+/gtE}S^{+/-}$	$N^{+/gtE}S^{-/-}$	$N^{gtE/gtE}S^{+/-}$	$N^{gtE/gtE}S^{-/-}$

Figure 2.3. Generation of E18.5 mice needed for testing the effects of *Sarm1* hemizygosity on neurite outgrowth *in vivo*. These were generated from two breeding steps. First, double homozygous null mice *Nmnat2*$^{gtE/gtE}$*;Sarm1*$^{+/-}$ were crossed with *Nmnat2*$^{+/gtE}$*;Sarm1*$^{+/}$ $^{+}$mice to generate double hemizygous (*Nmnat2*$^{+/gtE}$*;Sarm1*$^{+/-}$) progeny, indicated in green (a). These double hemizygotes were then crossed to generate mixed litters of the desired genotypes, indicated in blue (b) *Nmnat2*$^{gtE/gtE}$*;Sarm1*$^{+/+}$, *Nmnat2*$^{gtE/gtE}$*;Sarm1*$^{+/}$, *Nmnat2*$^{gtE/gtE}$*;Sarm1*$^{-/-}$, and *Nmnat2*$^{+/+}$*;Sarm1*$^{+/+}$.

2.1.3 Fluorescently labelled transgenic mice

Finally, for the D-Galactose work (described in sections 2.5 and 2.6), several transgenic mice expressing fluorescent proteins were used to image axon transport. Transgenic mice expressing cyan fluorescent protein (CFP)-labelled mitochondria (mitoCFP)[296] or yellow fluorescent protein (YFP)-labelled NMNAT2 (*Nmnat2*-venus)[166] under control of the neurone-specific *Thy1.2* promotor were maintained as separate hemizygous lines. Transgenic mice homozygous for YFP under the *Thy1.2* promotor (YFP-H mice)[297,298] obtained from The Jackson Laboratory (stock # 003782) were crossed with the Babraham C57BL/6Babr wild-type line to generate hemizygous offspring. Three-month old male mice hemizygous for either

mitoCFP, Nmnat2-venus, or YFP-H were used for the D-Galactose studies, described in sections 2.5 and 2.6.

2.1.4 Mouse genotyping

DNA was extracted from embryonic or P0-P2 mouse nose/tail (to determine *Nmnat2* and/or *Sarm1* status for cell culture experiments). Ear biopsies were taken from 10-day old mice (from MitoP and *Nmnat2*-venus mice) using QuickExtract™DNA Extraction Solution (epicentre; QE09050) according to manufacturer's instructions. Briefly, 35 μl QuickExtract was added to biopsies. Samples were vortexed for 15 seconds then placed on a heat block at 65 °C for 15 minutes. Samples were then vortexed for 15 seconds and placed on a heat block at 98 °C for 2 minutes before being vortexed for 15 seconds again. Then, 1 μl extracted DNA was mixed with 19 μl master mix, comprising; PCR water, Taq Polymerase, 100 mM KCl, 3 mM $MgCl_2$, 0.002 % gelatin, 0.4 mM dNTP mix (dATP, dCTP, dGTP, TTP), and 20 mM Tris-HCl at pH 8.3 (in the form of REDTaq® ReadyMix™ PCR Reaction Mix from Sigma-Aldrich; R2523) and 1 μl of mixed forward and reverse primers specific to the gene in question (see Table 2.1) from a 100 μM stock concentration to make a final PCR reaction volume of 20 μl. Alternatively, GoTaqGreen (Promega) was used in place of RedTaq. Samples were then mixed and placed in a BioRad T100 PCR machine using the appropriate protocol (see Table 2.1) to amplify the gene of interest before being loaded into a 2% agarose gel with ethidium bromide and run in an electrophoresis tank (Apparatus GNA 200; Pharmacia) with Tris/Borate/EDTA (TBE) buffer for 30-60 minutes at 200V or until bands were clearly distinguishable when imaged with a UviTech UV reader.

2.2 *In vitro* studies

2.2.1 Superior cervical ganglia and dorsal root ganglia cultures

For the *in vitro* experiments, superior cervical ganglia (SCGs) were dissected from P0-P2 mice and dorsal root ganglia (DRGs) from E13.5 mouse embryos. Dissected ganglia were plated on 35 mm culture dishes precoated with poly-L-lysine (20 μg/ml overnight; Sigma) and laminin (20 μg/ml for 1–2 h; Sigma), as previously described[22]. Ganglia were plated in 635 μl culture medium (below) which was topped up with 1 ml the following day. Culture medium comprised Dulbecco's Modified Eagle's Medium (DMEM) (type 41966029; ThermoFisher Scientific) supplemented with 2% B27 supplement (type 17504-044; Gibco) and 1% penicillin-streptomycin (type P4333; Sigma). In addition, 4 μM aphidicolin (Merck) and 50 ng/ml 2.5S NGF (Invitrogen) were added fresh to the culture medium as it was replaced every 2-3 days.

Table 2.1 Details of genotyping transgenic mice used in this project; Tg (transgene); wt (wild-type)

Gene	Fragment size (base pairs)	Forward primer sequence/ Reverse primer sequence	PCR amplification protocol	Time under electrophoresis	Reason for being genotyped
Nmnat2 (Tg)	**552**	**GCTGGCCTAGGTGGTGATTTGC CAGTCAATCGGAGGACTGGCG**	**Step 1. 94 °C, 2:00; Step 2. 94 °C, 0:30; Step 3. 60 °C, 0:30; Step 4. 68 °C, 0:45; Repeat 2-4 34x; 72 °C 5:00; 4 °C, ∞**	**60**	To distinguish between mice heterozygous for the wild-type and Nmnat2 gtE gene and those null for the wild-type and homozygous for the Nmnat2 gtE gene. Both sets of primers added to the PCR reaction so when run on the gel there are two bands.
Nmnat2 (wt)	**491**	**GCTGGCCTAGGTGGTGATTTGC ACTGGGATGCACGAGACCCTGC**			
***Sarm1* (Tg)**	**496**	**GGTAGCCGGATCAAGCGTATGC CTCATCTCCGGGCCTTTCGACC**	**Step 1. 94 °C, 2:00; Step 2. 94 °C, 0:30; Step 3. 60 °C, 0:30; Step 4. 68 °C, 0:45; Repeat 2-4 32x; 72 °C 5:00; 4 °C, ∞**	**50-60**	To confirm that all offspring from a cross between a *Sarm1*$^{+/+}$ and *Sarm1*$^{-/-}$ were all *Sarm1*$^{+/-}$, as expected. Also, to identify appropriate genotypes from *Sarm1*$^{+/-}$ x *Sarm1*$^{+/-}$ cross for experiments. Both sets of primers added to the PCR reaction so when run on the gel there are two bands.
***Sarm1* (wt)**	**508**	**ACGCCTGGTTTCTTACTCTACG CCTTACCTCTTGCGGGTGATGC**			
mitoCFP		**CGCCAAGATCCATTCGTT/ GAACTTCAGGGTCAGCTTGC**	**Step 1. 93 °C, 5:00; Step 2. 93 °C, 0:30; Step 3. 57 °C, 0:30; Step 4. 68 °C, 0:30; Repeat 2-4 35x; 68 °C 2:00; 4 °C, ∞**	**30**	Line maintained as heterozygous so genotyped to identify carriers of the fluorescent gene.
Nmnat2-venus	**170 (Tg) 300 (wt)**	**ATGGAAGTGATTGTTGGGGAC/ CTGCTCTTGGTGGAGCTGAC**	**Step 1. 95 °C, 2:00; Step 2. 95 °C, 0:30; Step 3. 64 °C, 0:20; Step 4. 72 °C, 1:15; Repeat 2-4 39x; 72 °C 5:00; 4 °C, ∞**	**30**	Line maintained as heterozygous so genotyped to identify carriers of the fluorescent gene. Two separate genotyping protocols run to confirm the presence of the fluorescent gene.
Nmnat2-venus	**~1000 (Tg) <200 (wt)**	**CACCTGTCCTACCAGCTGGCTG/ GTGGCCGTTTACGTCGCCGTC**			

2.2.2 Antisense oligonucleotides

Antisense oligonucleotides were obtained from Ionis Pharmaceuticals at a stock concentration of 100 mg/ml. The control antisense oligonucleotide is referred to in text as cASO and the anti-*Sarm1* oligonucleotides are referred to in text as ASOa and ASOb. For all experiments, stocks were diluted 1:3000 in culture medium to a final concentration of 5 μM. Where antisense oligonucleotides were combined, the culture medium comprised a 50:50 mix of ASOa and ASOb, resulting in the final culture medium containing 7.5 μM of each *Sarm1* antisense oligonucleotide, referred to as ASOa+b in text. Medium containing antisense oligonucleotides was applied to cultures for the durations indicated in text.

2.2.3 Neurite outgrowth assay

Similar to previously described experiments[77,78], DRGs were dissected from E13.5 mouse embryos plated on precoated 35 mm tissue culture dishes, as described in section 2.2.1. Tissue was collected from the embryos for genotyping and the experimenter was blind to genotype until experiments were quantified. Radial neurite outgrowth was imaged in phase-contrast at low magnification (5x objective) using the 'Tile Scan' function of a DMi8 Leica moving stage inverted epifluorescence microscope using the Leica Application Suite X software. This was done at the same time on each specified day after plating. Neurite length on each day was determined by taking the average of two measurements of representative neurite outgrowth for each explant and generating an average for each dish (2-3 ganglia per dish). For the antisense oligonucleotide reversal of neurite outgrowth deficit in mice lacking NMNAT2, three DRGs from each embryo of the appropriate genotype *Nmnat2*$^{gtE/gtE}$/*Sarm1*$^{+/+}$ or *Nmnat2*$^{+/+}$/*Sarm1*$^{+/+}$ were plated in 5 separate 35 mm tissue culture dishes and treated with either normal culture medium, or medium containing cASO, *Sarm1* ASOa, *Sarm1* ASOb, or combined *Sarm1* ASOa+b. DRG cultures treated with Sarm1 ASOb or combined *Sarm1* ASOa+b consistently detached in both genotypes between 3 and 5DIV, and so were excluded from analysis.

2.2.4 *In vitro* assays of Wallerian and Wallerian-like degeneration

Aside from the *in vitro* transection injury (axotomy) which completely separates cultured neuronal somas from distal neurites [23], there are a number of other *in vitro* chemical triggers of programmed axon degeneration that overexpression of NMNATs or removal of SARM1 can protect against. Firstly, vincristine is a chemotherapeutic which stabilises microtubules and inhibits axon transport. It triggers programmed axon degeneration which can be prevented by

the presence of WLD^S or by the absence of SARM1[299,83,300,81]. Mitochondrial toxins carbonyl cyanide m-chlorophenyl hydrazone (CCCP) and rotenone both trigger programmed axon degeneration[301,101,260,75]: CCCP is a protonophore which dissipates the mitochondrial H^+ gradient thereby inhibiting ATP production and triggering axon degeneration which can be prevented by the presence of WLD^S or by the absence of SARM1[75]. Degeneration triggered by mitochondrial complex IV inhibitor rotenone can be prevented by the absence of SARM1[301]. Finally, protein translation inhibition can be modelled through cycloheximide (CHX) administration, which rapidly decreases levels of labile proteins such as axon survival factor NMNAT2 [76] and SCG10 [55,230]. The CHX-induced depletion of NMNAT2 initiates programmed axon degeneration which the presence of WLD^s prevents [76].

In all of the *in vitro* degeneration assays, the same field of neurites were imaged in phase contrast repeatedly at the timepoints indicated, using a DMi8 Leica moving stage inverted epifluorescence microscope and Leica Application Suite X software. In all assays using both DRGs and SCGs, neurites were allowed to extend from ganglia for 7DIV before the inducer of degeneration (described below) was applied along with a media immediately preceding timepoint 0h.

For axotomy, neurites were physically cut with a sterile scalpel (No.22 blade) several mm away from the ganglion[23]. Stocks (1000x) of vincristine and rotenone in DMSO were diluted 1:1000 in culture medium to final concentrations of 20 nM vincristine and 10 μM rotenone, previously shown to induce axon degeneration[299,301]. CCCP was applied at 25 μM or 50 μM concentrations, also shown to induce axon degeneration[75]. An aqueous stock solution of CHX in DMSO (Sigma) were diluted 1:1000 or 1:100 in culture media to give final 1 μg/ml and 10 μg/ml CHX concentrations, respectively, as previously described[76]. The extent to which distal neurites degenerated was quantified using the Degeneration Index plugin for ImageJ (FIJI) developed and described in detail by Sasaki et al., (2009)[202].

2.3 *In vivo* studies of axon degeneration

2.3.1 Sciatic nerve transection surgeries

A slightly modified version of a published method[62] was employed to surgically transect the right sciatic nerve of 2-3 month old male mice. Briefly, mice were anesthetized with isoflurane, and the skin on their right hind limb was shaved and cleaned with denatured ethanol. Sterile surgical technique was used to make an incision directly beneath the hip joint, and the gluteal muscles were separated carefully with a pair of forceps. The sciatic nerve was transected

immediately adjacent to the sciatic notch with a pair of sterile surgical scissors. The gluteal muscles were then placed back into their original anatomical position, and the overlying skin glued closed using Vetbond. Mice were monitored post-operatively and if wounds re-opened mice were re-anaesthetised and the wound re-closed.

2.3.2 Sciatic nerve dissections and embedding

At 2, 3, and 5 days post-lesion, mice were euthanized via cervical dislocation and nerve segments 4 mm distal to the lesion up to the point of nerve trifurcation at the level of the knee were collected from both the cut and uncut hindlimb nerves. Nerves were fixed in 4% paraformaldehyde and 2.5% glutaraldehyde in 0.1 M PBS, pH 7.4 for at least 72 h at 4 ºC. Fixed nerves were then washed in 0.1 M PBS, placed in 1% osmium tetroxide for 2 h, and dehydrated in increasing concentrations of ethanol from 50%, 70%, 80%, 90%, 95%, to 100%, and then 100% propylene oxide. Nerves were then embedded in Durcupan resin (Fluka Chemie) and polymerized for 48 h at 60 ºC.

2.3.3 Sciatic nerve imaging and quantification

Transverse semithin sections (100 µM) were cut on a Leica ultramicrotome, stained with Richardson's solution, and imaged on a light microscope at 100x magnification. Images were taken across the entire nerve section and automatically merged on Photoshop Elements 13 using the Photomerge® Panorama function. To quantify the number of intact and degenerated axons, a complete cross section of the tibial nerve was counted for each mouse. The criteria for categorizing intact axons were: the presence of myelin sheaths, uniform axoplasm, and intact mitochondria. The experimenter was blinded to mouse genotype for the surgeries, sectioning, imaging, and quantification.

2.4 *In vivo* studies on neurite outgrowth in mice lacking NMNAT2

2.4.1 DiI staining of intercostal nerves

E18.5 embryos were generated from a *Nmnat2*$^{+/gtE}$/*Sarm1*$^{+/-}$ x *Nmnat2*$^{+/gtE}$/*Sarm1*$^{+/-}$ cross. Embryos of the appropriate genotypes (*Nmnat2*$^{gtE/gtE}$/*Sarm1*$^{+/+}$, *Nmnat2*$^{gtE/gtE}$/*Sarm1*$^{+/-}$, and *Nmnat2*$^{gtE/gtE}$/*Sarm1*$^{-/-}$, as well as wild-type *Nmnat2*$^{+/+}$/*Sarm1*$^{+/+}$) were immersion fixed in 4% paraformaldehyde. After at least one week, intercostal nerves of the embryos were labelled using the lipophilic dye DiI (1,l"-dioctadecyll3,3,3",3"tetramethylindocarbo-cyanine perchlorate), as previously described[302]. DiI crystals were inserted into a rostrocaudal incision along the entire spinal cord, then kept at 37°C in 4% paraformaldehyde for 8 weeks, to allow diffusion of the dye through neuronal membranes thereby labelling nerves exiting the spinal

cord. After 8 weeks of labelling, ribcages were dissected and cleaned then immersed in an increasing glycerol:PBS series from 25%, 50%, 75%, up to 100% glycerol for optical clearing.

2.4.2 Diaphragm dissection and staining

Diaphragms were dissected at the same time as ribcages from the same E18.5 embryos stained with DiI. As described by DiStefano et al., (2017)[159], diaphragms were washed in PBS and incubated with 10 µg/ml tetramethylrhodamine (TRITC)-conjugated α-bungarotoxin (Invitrogen T1175) for 20 minutes at room temperature. Diaphragms were then permeabilized and blocked in PTX (PBS, 0.5% TritonX-100) with 2% BSA for 2 h at room temperature and incubated overnight at room temperature with a rabbit polyclonal anti-βIII-tubulin (TUJ1) antibody (Sigma, T2200) in blocking solution (1:500 dilution). After 3x washes in PTX, diaphragms were incubated with an AlexaFluor488-conjugated anti-rabbit antibody (1:200 dilution) in blocking solution for 5 h at RT. After another 3x washes in PTX, diaphragms were mounted in Vectashield on glass sides and imaged using an inverted DMi8 Leica fluorescence microscope using 5x and 10x objectives.

2.5 D-Galactose administration and live sciatic nerve collection

Three-month-old male mice received 4 g/kg D-Galactose in 0.01% sodium benzoate or 0.01% sodium benzoate (vehicle) in place of normal drinking water continuously for 8 weeks. On a weekly basis, mice were weighed and had their blood glucose levels measured using an Accu-Chek glucometer with a drop of blood collected via tail puncture.

2.6 *Ex vivo* studies using D-Galactose to model sporadic Alzheimer's disease

Mice were humanely sacrificed via cervical dislocation and confirmed dead via exsanguination after receiving D-Galactose or vehicle for 8 weeks. The head from *Nmnat2*-venus mice was placed immediately in pre-oxygenated Neurobasal A medium (Gibco) warmed to 37 °C. The right sciatic nerve was dissected from MitoP and *Nmnat2*-venus mice within 3 minutes and immersed immediately into oxygenated pre-warmed Neurobasal A medium. Brains from YFP-H and MitoP mice were harvested for biochemical analysis, as described in section 2.8.1.

2.6.1 Live imaging and quantification of axonal transport in Sciatic nerve explants

Live time-lapse images were captured with an Olympus CellR imaging system (IX81 microscope, Hamamatsu ORCA ER camera, using Immersol immersion oil from Zeiss) at a rate of 2 frames per second for 2 or 3 minutes when imaging *Nmnat2*-venus sciatic nerve and MitoP sciatic nerve, respectively. Five separate videos were created per explant, with fields of view of different axons within the nerve. Total time spent imaging the sciatic nerves did not exceed 45 minutes and explants were maintained in Neurobasal A medium at 37 °C in an environment chamber (Solent Scientific) for the duration of imaging. The first images of sciatic nerves were made no more than 10 minutes after the mouse was culled. An equal number of vehicle and D-galactose treated mice were imaged in each imaging session. Individual axons were straightened using the Straighten ImageJ plugin and axonal transport parameters defined using DifferenceTracker plugins, as previously described[303]. This enabled identification of moving particles in each frame which were normalised to axon length and presented as particle count per second per 100 µm axon length.

2.6.2 Organotypic Hippocampal Slice Cultures

Organotypic hippocampal slice cultures (OHSC) were generated by Claire Durrant who made 350 µm thick slices through the hippocampus and dentate gyrus of P6 C57BL/6Babr mouse brains. Two dishes each containing three slices were generated per mouse, according to her published protocol[304]. This generated eight mouse-matched conditions. OHSCs were cultured on membranes which provide two interfaces; one allowing tissues oxygenation and the other enabling movement of essential nutrients from culture media into the slices and waste from the slices into the media. OHSCs were cultured for 2 weeks before the addition of 55 mM D-Galactose dissolved in MEM or control media containing MEM by Olivia Sheppard who treated the cultures for 3 weeks with either D-Galactose or vehicle (MEM) and collected media after the first, second, and third week of treatment. I measured Aβ40 and Aβ42 levels through ELISA (Life Technologies: KMB3481 and KMB3441, respectively). After the third week of treatment, I harvested slice tissue for Western blot at the end of the experiment.

2.7 Immunoblotting

2.7.1 Enhanced chemiluminescence detection

DRGs and SCGs were collected in culture medium, centrifuged at 13,000 RPM, supernatant removed, washed with 1 ml room temperature (RT) phosphate-buffered saline (PBS) containing protease inhibitors (Roche, one tablet per 10 ml PBS), recentrifuged, supernatant removed and resuspended in Laemmli buffer containing 10% 2-mercaptoethanol (10 µl per SCG or DRG). Samples were then placed on a heat block at 100 °C for 90 s, vortexed, and placed back on the heat block for another 90 s before being frozen at -20 °C. Immediately before running the Western blot, samples were thawed and 10 µl loaded into 15 well 4-20% Mini-PROTEAN TGX Precast Protein Gels (Bio-Rad). Samples were run for 90 minutes at 150 V in 1x Tris/Glycine/SDS Electrophoresis Buffer (Bio-Rad) before being transferred onto methanol-activated Immobilon-P PDVF Membrane (MerckMillipore) for 60 minutes in transfer buffer (Tris/Glycine/20% methanol) at 100 V. Membranes were blocked at RT for 1 h in TBS containing 5% milk (Sigma). Primary antibodies used were: mouse SARM1 (1:2000-1:5000), mouse β-ACTIN (1:5000), and rabbit TUJ1 (1:2000) followed by the corresponding anti-mouse or rabbit IgG (H+L)-HRP Conjugate (Bio-Rad), more details are listed in Table 2.2. Antibodies were added to TBST containing 5% milk (Sigma); primary antibodies were applied overnight at 4°C and secondary antibodies were applied at RT for 2 h before the Pierce ECL Western Blotting Substrate (ThermoFisher) was added 5 minutes prior to chemiluminescence exposure using a UviTech Alliance chemiluminescence machine. Western blot band intensity was quantified using Fiji (ImageJ).

2.7.2 Infrared dual colour detection

OHSCs were scraped off the culture membrane into Laemmli buffer + 10 % 2-mercaptethanol (180 µl per 2 slices). Samples were prepared and run as described above for ECL, except they were transferred onto methanol-activated Immobilon-FL PDVF Membrane (MerckMillipore). Membranes were blocked at RT for 2 h in Odyssey TBS Blocking Buffer (LI-COR Biosciences). Antibodies were applied in TBS-T containing 5% Bovine Serum Albumin (Sigma-Aldrich); primary antibodies were applied overnight at 4°C and secondary corresponding anti-mouse or rabbit IgG (H+L) infrared (IRDye) antibodies were applied at RT for 2 h before being imaged using a LI-COR Odyssey detection system. Band intensity was quantified using ImageStudioLite software. Antibody details are listed in Table 2.2.

2.8 Biochemical assays

2.8.1 Collection of mouse brain regions for biochemical studies

Whole brain was extracted immediately from MitoP and YFP-H mice treated with D-galactose or vehicle once humanely culled, as described above. The brain hemispheres were separated longitudinally, then prefrontal cortex, remaining cortex, hippocampus, and cerebellum were separated using fine forceps and immediately placed in pre-chilled Eppendorf tubes and snap frozen in dry ice. Tissue from both hemispheres were collected from MitoP mice, but only a single hemisphere was taken from YFP mice (the other hemisphere was fixed for immunohistochemistry). The hemisphere collected alternated between right and left so as to avoid confounds of any potential single hemisphere effects. In total, 6 right and 6 left hemispheres were collected from YFP-H mice for both biochemical analysis and immunohistochemistry. Please note that ultimately immunohistochemistry and imaging were not performed on the YFP-H samples since no axonal transport impairment or AD-related biochemical differences were observed between vehicle- and D-Galactose-treated mice. Therefore, there was no drive to investigate morphological changes in YFP-H neurones since the absence of other AD-related phenotypes meant any potential differences in YFP-H mice could not be attributed to sporadic AD-like mechanisms in the D-Galactose model used.

2.8.2 Preparation of brain extracts

Samples previously frozen on dry ice and stored at -80 °C were thawed on ice and then placed at room temperature for 2 minutes. Homogenisation buffer comprising PBS containing protease inhibitors (Roche, one tablet per 10 ml PBS) was added to the samples along with a 5 mm steel ball (Qiagen). The amount of homogenisation buffer added varied on brain region: 50 μl was added to frontal cortex and hippocampus and 100 μl was added to cortex and cerebellum. Samples were then placed in an LT Tissue lyser (Qiagen) and homogenised at a rate of 20 oscillations per minute for 2 minutes. Homogenised samples were placed immediately on ice. Samples were transferred to a fresh Eppendorf (minus the steel ball) and a BCA Protein assay (Thermo Fisher Scientific: 23225) was employed to determine protein levels. Samples were then normalised to 5.5 mg/ml total protein using PBS containing 1% lauryl chloride, briefly vortexed and places on ice for 30 minutes. Samples were then centrifuged at 16000xg at 4 °C for 20 minutes and supernatants (known as the soluble fractions) were collected and stored in a 96 well plate at -20 °C. The pellets (insoluble fractions) were then solubilised Guanidine buffer (6M guanidine-HCl, 1% sarkosyl, 50 mM Tris pH8) overnight on a rotary at room temperature. They were then diluted 40x in PBS for use as the insoluble (guanidine) fraction and collected and stored in a 96 well plate at -20 °C.

Table 2.2: Details of antibodies used in this thesis

Primary/ Secondary	Antibody	Raised in	Mono- or Polyclonal	Dilution	Supplier	Cat. No.
Primary	APP	Mouse	Monoclonal	1:1000	Merck	MAB348
Primary	AT180	Mouse	Monoclonal	1:200	Thermo Fisher Scientific	MN1040
Primary	β-actin	Mouse	Monoclonal	1:5000	Sigma	A5316
Primary	β-III Tubulin	Rabbit	Polyclonal	1:2000	Sigma	T2200
Primary	Calbindin D-28K	Rabbit	Polyclonal	1:2000	Merck	AB1778
Primary	Cyclophilin B	Rabbit	Polyclonal	1:500	Abcam	AB16045
Primary	PSD95	Rabbit	Polyclonal	1:500	Abcam	AB18258
Primary	SARM1	Mouse	Monoclonal	1:3000	Provided by the Hsueh lab [154]	
Primary	Synaptophysin (SY38)	Mouse	Monoclonal	1:1000	Abcam	AB8049
Primary	Total Tau	Rabbit	Polyclonal	1:5000	Dako	A0024
Secondary	Mouse IgG(H+L)-HRP Conjugate	Goat	Polyclonal	1:3000	Bio-Rad	1721011
Secondary	Rabbit IgG(H+L)-HRP Conjugate	Goat	Polyclonal	1:3000	Bio-Rad	1721019
Secondary	Mouse IgG(H+L)-IRDye 800CW	Donkey	Polyclonal	1:10000	LI-COR Biosciences	926-40003
Secondary	Rabbit IgG(H+L)-IRDye 800CW	Donkey	Polyclonal	1:10000	LI-COR Biosciences	925-32213

2.8.3 Meso Scale Discovery assays

A Meso Scale Discovery assay was then used to measure total Tau and hyperphosphorylated Tau present in the insoluble fractions. These levels were quantified using a Phospho (Thr231)/Total Tau Kit (K15121D) assay, which was run according to manufacturer's instructions. Meso Scale Discovery assays were run by technicians in the Core Biochemical Assay Laboratory in Addenbrooke's Hospital who provided me with the raw data.

2.8.4 Immunoblotting

Soluble hippocampal fractions were diluted 1:1 in Laemmli buffer. A total of 30 μg protein (10 μl) was loaded to measure phosphotau levels with the AT180 antibody, according the same ECL protocol described earlier. Since loading control proteins saturate the gel at protein concentrations needed to detect phosphorylated tau, 2 μl of sample was then loaded on a separate gel to measure levels of Total Tau and β-actin.

2.9 Statistical analyses

Data values generated from Fiji (ImageJ), manual counting, or plate readers were compiled in Microsoft Excel. Statistical analyses were performed and graphs created using Prism 8 (GraphPad). Figures were created in Prism8, PowerPoint, and mechanistic schematics were created with the use of BioRender online. The precise method of statistical analysis performed for each experiment is noted in each Figure legend. However, in general, when an effect over time was measured for more than two groups, a two-way repeated measures ANOVA was employed. If significant, the two-way ANOVA was followed by post-hoc analysis (Dunnett when all experimental groups were compared to a control group or Bonferroni when experimental groups were compared to each other over time). When more than two groups were compared at a single time-point, a one-way ANOVA was employed to determine significance followed by an unpaired t-test where appropriate, as indicated in the text. A two-tailed unpaired t-test was used to determine whether there were differences between a control and experimental group at a single time-point in the D-Galactose imaging studies and paired t-tests were employed to assess whether there was a difference between vehicle- and D-Galactose-treated OHSCs. Data are presented as mean standard error of mean (SEM). Statistical significance is indicated as follows: ns = not significant; ****$p<0.0001$; ***$p<0.001$; **$p<0.01$; *$p<0.05$

Chapter 3: *Sarm1* hemizygosity delays programmed axon degeneration

3.1 Introduction

Two separate genome-wide association studies (GWAS) have associated the chromosomal locus encompassing *SARM1* to sporadic ALS [120,121]. These findings are supported by experimental data showing further links between ALS and Stathmin-2 (SCG10) [122–124], which negatively regulates programmed axon degeneration [55]. Promisingly, *Sarm1* deletion is protective in a model of ALS and FTD [105] and many animal models demonstrate in principle that removing *Sarm1* can prevent disease phenotypes [61,122].

3.1.1 Altered expression of genes involved in programmed axon degeneration

Altered gene expression is one mechanism which leads to the identification of genes linked to disease in genome wide association studies (GWAS) [305] and a growing body of evidence links altered NMNAT2 protein function (therefore programmed axon degeneration in which SARM1 plays a pro-degenerative role) in humans to susceptibility to disease [112,113,116]. There are also a number of predicted loss of function (*LoF*) *SARM1* alleles present in the human population [306] from which one predicts that a small percentage of the population would be hemizygous for *SARM1 LoF* alleles with some nullizygous and compound heterozygous humans possibly existing. It will be important to determine empirically what effect these GWAS hits and predicted *LoF* mutants have on axonal health and whether these effects extend to chronic disease (for *GoF* mutations) or protection (in *LoF* mutants). Since hemizygous *LoF* humans may possess a (partially) axon-protective phenotype, at least in non-transection injuries such as peripheral neuropathy or protein synthesis-aggregation disorders. Whereas those with *GoF* alleles may be at greater risk of developing neurodegenerative diseases. Unpublished findings by Coleman Laboratory members Jonathan Gilley and Mirlinda Ademi demonstrate that some of these predicted *LoF* and *GoF* variant alleles present in the human genome translate to altered SARM1 NADase activity and axon susceptibility *in vitro*.

Given that variant *SARM1* alleles may be associated with human disease and predicted *LoF* human alleles may be protective, there is hope that; (i) modulating SARM1 in disease states could be beneficial and; (ii) that *Sarm1 LoF* hemizygous humans may be less susceptible to neurodegenerative disease, or more responsive to therapies targeting SARM1.

Preventing expression or completely eliminating a specific protein or its activity pharmacologically or therapeutically is challenging. Therefore, if therapeutic strategies targeting SARM1 are to be effective, it is important to determine empirically whether *decreased*, rather than *complete* removal, of SARM1 levels or activity can elicit a protective

effect. Whilst one study showed that 70% or greater siRNA knockdown of *Sarm1* was needed to be protective *in vitro* [58], most published evidence suggests that complete removal of *Sarm1* from the murine system is required in order to significantly delay axon degeneration in the central and peripheral nervous systems: *Sarm1* hemizygosity does not detectably protect against oxygen-glucose deprivation in hippocampal cultures[132] or sciatic nerve transection at 14 days post-lesion[62] where full removal of *Sarm1* protects in both cases.

3.1.2 Capacity to delay programmed axon degeneration by removing other proteins

Other proteins, discussed in more detail in the thesis introduction, do modify the rate of programmed axon degeneration, but none have quite the level of protection as removal of SARM1. Briefly, overexpression of NMNAT activity, the ubiquitin proteasome system, mitogen-activated protein kinase (MAPK) cascade, and calpain activation can delay degeneration after injury to varying extents. Severed sciatic nerve axons are preserved for several weeks in the presence of WLD^S or cytoplasmic NMNAT1 [203], 5 days in mice lacking PHR1 (a protein involved in NMNAT2 turnover) [227,239,259], up to 52 h in mice lacking DLK (a kinase involved in the activation of MAP kinase pathway) [227], and 36 h in mice lacking CRPM4 (which is cleaved downstream of calpain activation leading to axon degeneration) [259]. Endogenous calpain inhibition can protect retinal ganglion cell axons for 24 h after optic nerve crush [29,258] and overexpression of endogenous calpain inhibitor, calpastatin, has been shown to protect against optic nerve transection for 2-3 days post transection [29,247]. Introduction of bacterial enzyme NMN deamidase into mice, which depletes SARM1 activator NMN, leads to strong delay of axon degeneration with 50% axons remaining intact 14 days post-sciatic nerve lesion [159]. However, removal of no gene matches the protective effects of *Sarm1* removal in which sciatic nerve axons are fully preserved *in vivo* even 14 days post-transection [58,62,72].

This chapter will explore whether decreased levels of SARM1 in *Sarm1* hemizygous mice confer any protection against programmed axon degeneration and how translatable any protection observed is to diverse triggers of programmed axon degeneration.

3.2 Results

3.2.1 *Sarm1* hemizygous mice express lower levels of SARM1 than *Sarm1* wild-type mice

Firstly, it was important to confirm that *Sarm1* hemizygosity leads to a decrease in SARM1 levels, as shown in the original paper characterising the mouse strain used [132]. This was demonstrated through Western blot of cultured SCG explants from *Sarm1*$^{+/+}$, *Sarm1*$^{+/-}$, and *Sarm1*$^{-/-}$ mice where, there is an approximately 60% decrease in Western blot band intensity in mice hemizygous for *Sarm1* compared to wild-type littermates (Figure 3.1.a). Serial dilution of a *Sarm1*$^{+/+}$ sample was done to test whether a 50%, 75%, or 87.5% decrease in SARM1 protein levels corresponded to the same decrease in Western blot band intensity (Figure 3.1.b). It appears that a 50% decrease in protein levels corresponds to a 60% decrease in Western blot band intensity. For added certainty, a *Sarm1*$^{+/+}$ sample was run alongside increasing, known amounts of purified SARM1 to determine whether the band intensity is within the linear range of the antibody sensitivity. The *Sarm1*$^{+/+}$ band intensity does lie within the linear range, albeit at the lower end, providing confidence that the decreases in Western blot band intensity correspond to a similar decrease in protein levels (Figure 3.1.c).

3.2.2 *Sarm1* hemizygosity delays programmed axon degeneration in *in vitro* assays

DRG explants were initially employed as a higher-throughput system to rapidly explore the ability of *Sarm1* hemizygosity to protect against a range of programmed axon degeneration initiators (Figure 3.2.a-b). This enabled tracking the rate of degeneration in the same cultures using time-lapse imaging. However, the rate of degeneration is slower and more variable in DRGs than in SCGs (compare Figures 3.2 and 3.3). Thus, a switch from DRGs to SCGs was made for the remaining experiments.

In vitro axotomy of SCG explants was then performed to explore whether the decrease in protein expression detected in Figure 3.1 corresponds to a delay in axon fragmentation after injury. Indeed, there was a notable delay in degeneration 8 h post-cut in the *Sarm1* hemizygous SCGs compared to littermate wild-types (Figure 3.2.a), though no protection was present at 24 h. *Sarm1* hemizygosity notably delayed degeneration up to 54 h post-vincristine, a chemotherapeutic which stabilises microtubules and blocks axonal transport causing degeneration of distal axons (Figure 3.3.b), with axons finally degenerating 72 h post-application.

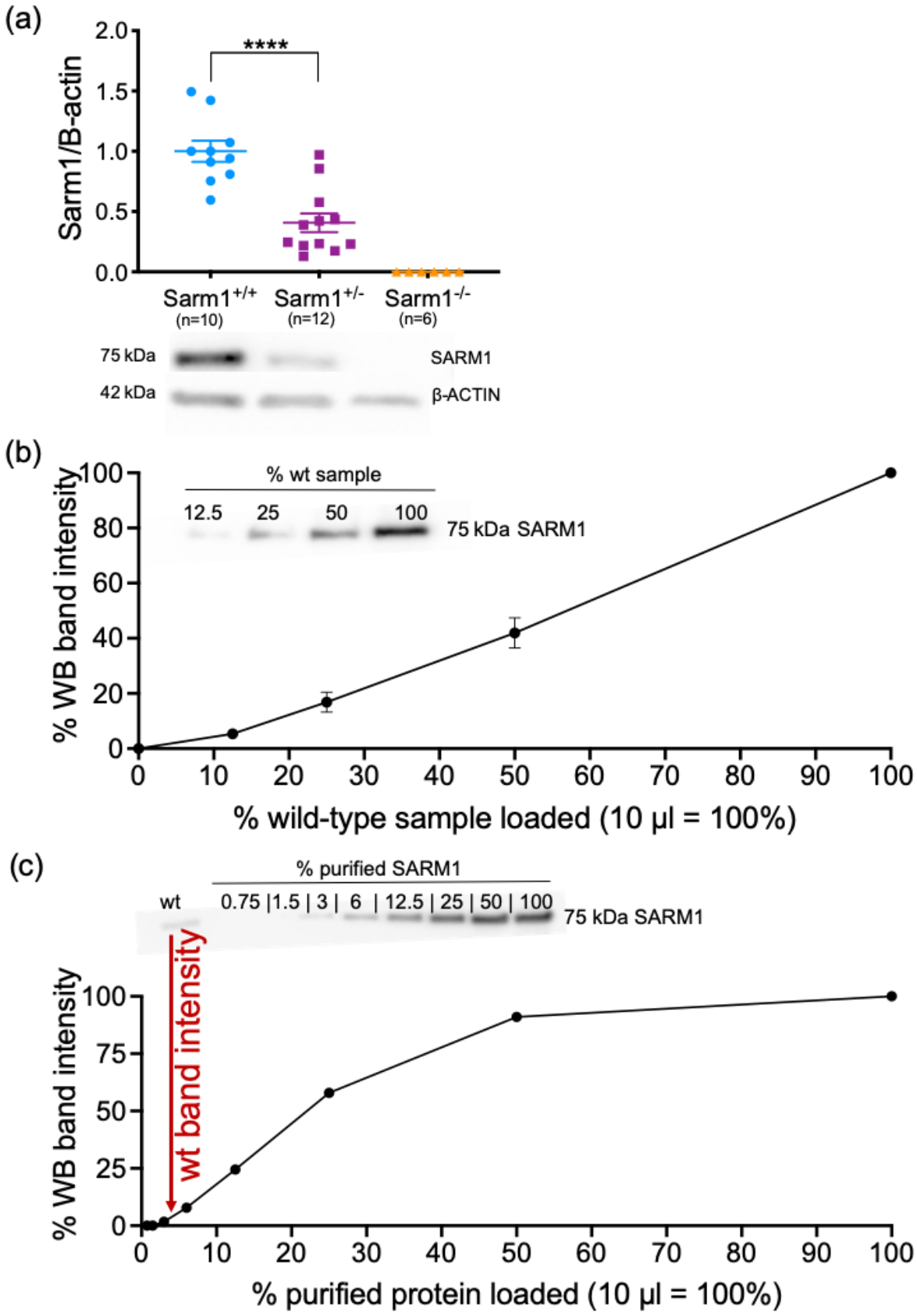

Figure 3.1: Western blot band intensity in SCGs cultured for 7 days *in vitro* from *Sarm1* hemizygous mice is 60% less intense than those from *Sarm1* homozygous wild-type mice (a). Each data point corresponds to an individual mouse where both SCGs were cultured in the same dish for 7 days and then collected. A 50% decrease in wild-type SCG sample leads to a 60% decrease in SARM1 band intensity (b) and wild-type band intensity is within the lower end of the linear range for the SARM1 antibody used (c). A one-way ANOVA was performed followed by an unpaired t-test to determine whether there was a significant difference between *Sarm1* hemizygous and *Sarm1* homozygous wild-type SCGs. ****p<0.0001.

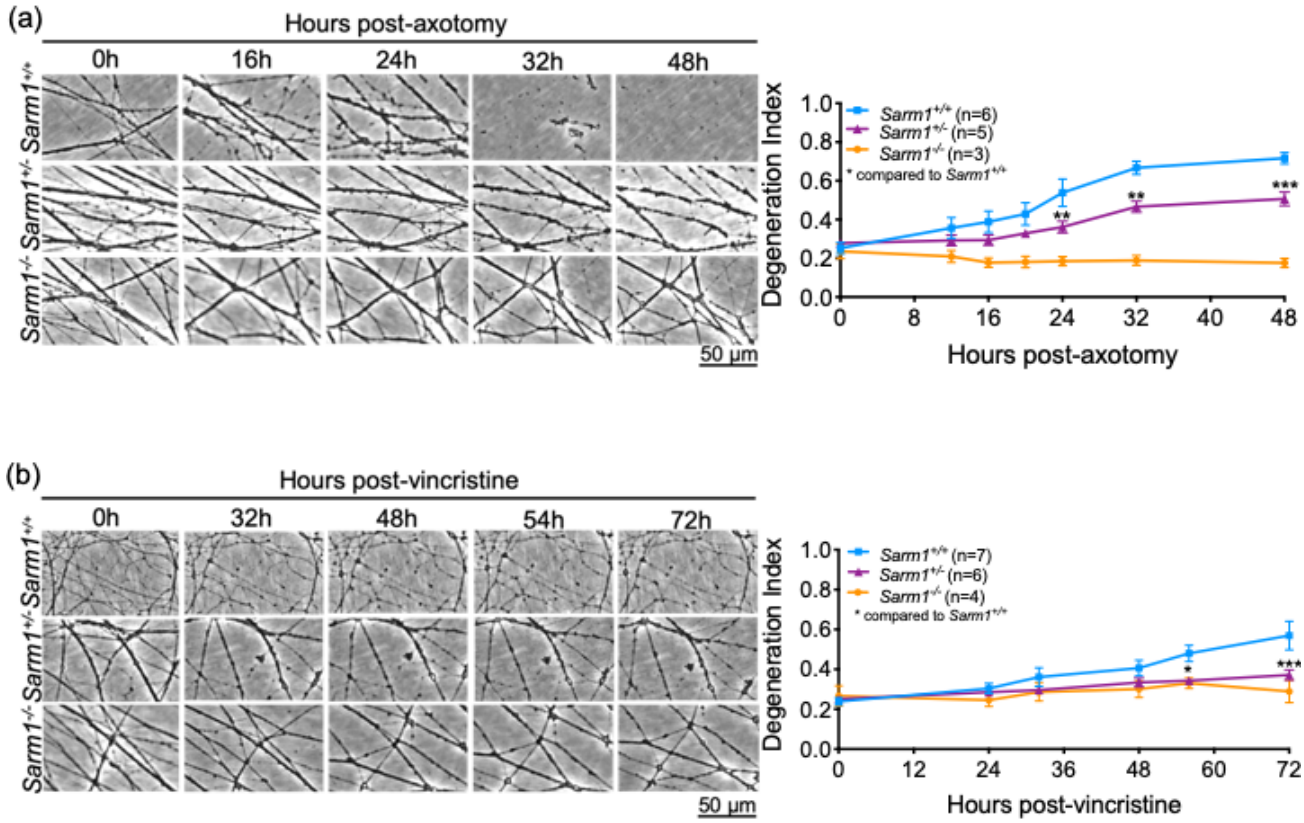

Figure 3.2: *Sarm1* hemizygosity delays the rate of programmed axon degeneration in DRGs after *in vitro* axotomy (a) and vincristine (b) compared to that of *Sarm1* homozygous wild-type DRGs. As previously shown, *Sarm1* homozygous null DRGs remain intact after injury. Rotenone did not induce degeneration up to 72 h post-application before detaching by 96 h. Representative micrographs for each genotype at each timepoint are shown next to quantification of axon degeneration. DRGs were cultured for 7DIV before injury. Each data point represents an average value from three fields of view from three individual DRGs cultured in the same dish. Data were obtained across three individual repetitions with mixed genotypes. A two-way repeated measures ANOVA was performed followed by Bonferroni post-hoc analysis to determine whether there was a difference between *Sarm1* hemizygous and *Sarm1* homozygous wild-type DRGs. *p<0.05; **p<0.01; ***p<0.001

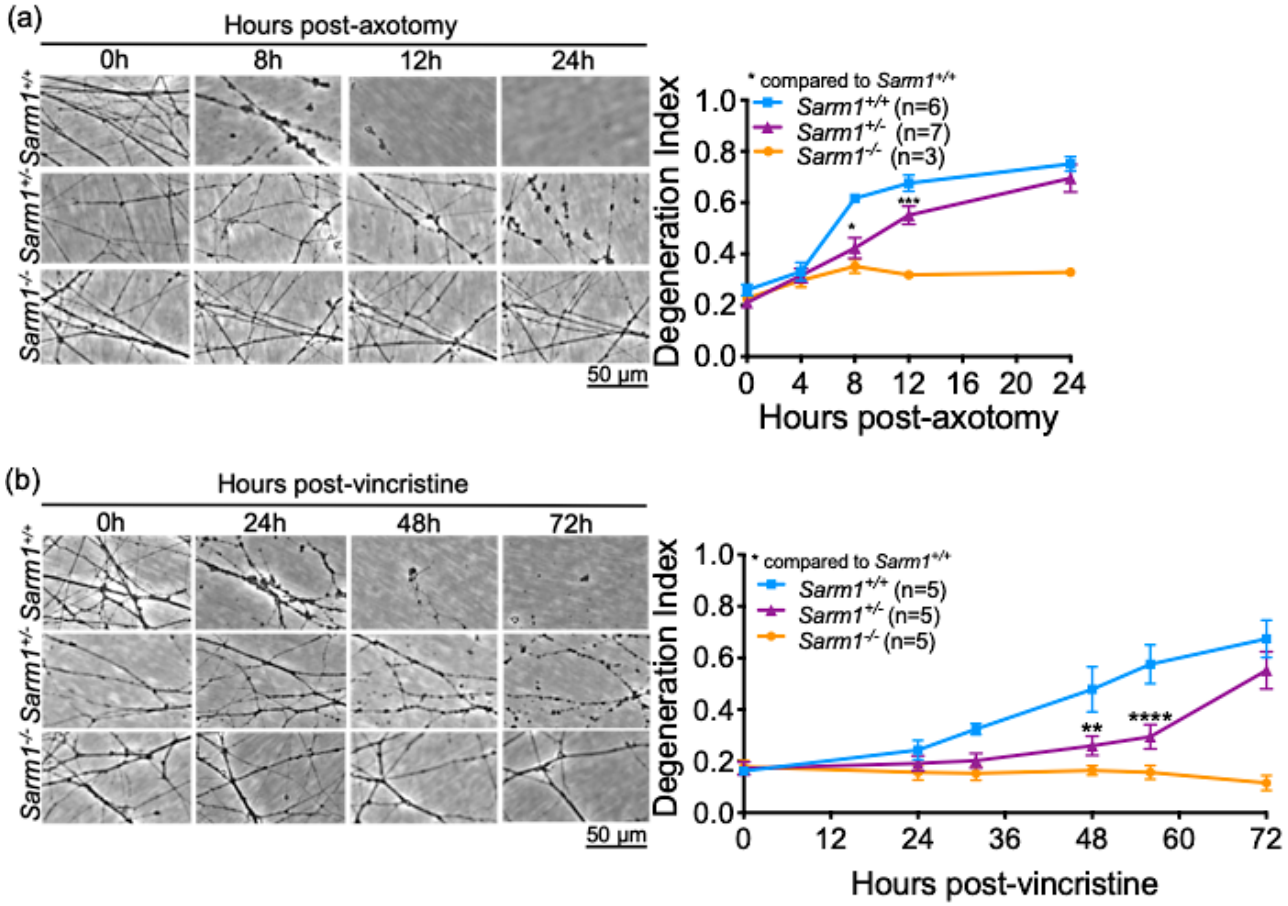

Figure 3.3: *Sarm1* hemizygosity delays the rate of programmed axon degeneration after physical axotomy injury (a) and neurotoxic vincristine application (b) compared to that of *Sarm1* homozygous wild-type SCGs. As previously shown, *Sarm1* homozygous null SCGs remain intact after injury. Representative micrographs for each genotype at each timepoint are shown next to quantification of axon degeneration. SCGs were cultured for 7DIV before injury. Each data point represents an average value from two fields of view from two individual SCGs cultured in the same dish. Data were obtained across three individual repetitions with mixed genotypes. A two-way repeated measures ANOVA was performed followed by Bonferroni post-hoc analysis to determine whether there was a difference between *Sarm1* hemizygous and *Sarm1* homozygous wild-type SCGs. *p<0.05; **p<0.01; ***p<0.001

Mitochondrial stressors rotenone (which inhibits mitochondrial complex IV and leads to ROS generation) and CCCP (a protonophore which dissipates the mitochondrial H^+ gradient thereby inhibiting ATP production) were then tested. Here, *Sarm1* hemizygosity confers dissimilar effects on the rate of degeneration; there was protection up to 48 h post-rotenone (Figure 3.4.a), but no delay in degeneration after CCCP (Figure 3.4.b-c). Finally, protein translation inhibition was modelled through cycloheximide (CHX) administration, which rapidly decreases levels of labile proteins such as axon survival factor NMNAT2 [76] and SCG10 [55,230]. The CHX-induced depletion of NMNAT2 initiates programmed axon degeneration that can be prevented by the presence of WLD^S [76]. Until the present study, it was unknown whether removal of SARM1 would protect against this and thus whether *Sarm1* hemizygosity would confer protection. At higher dose CHX, *Sarm1* hemizygosity significantly protects against degeneration up to 48 h post administration where neurites then detach before degeneration is clearly seen (Figure 3.5.a). *Sarm1*$^{-/-}$ protects for the duration of the experiment. With low dose CHX – which may better model chronic disorders of protein translation – *Sarm1* hemizygosity displays an equal protective capacity to complete removal of *Sarm1,* with neurites remaining intact for 96 h post-CHX application (Figure 3.5.b).

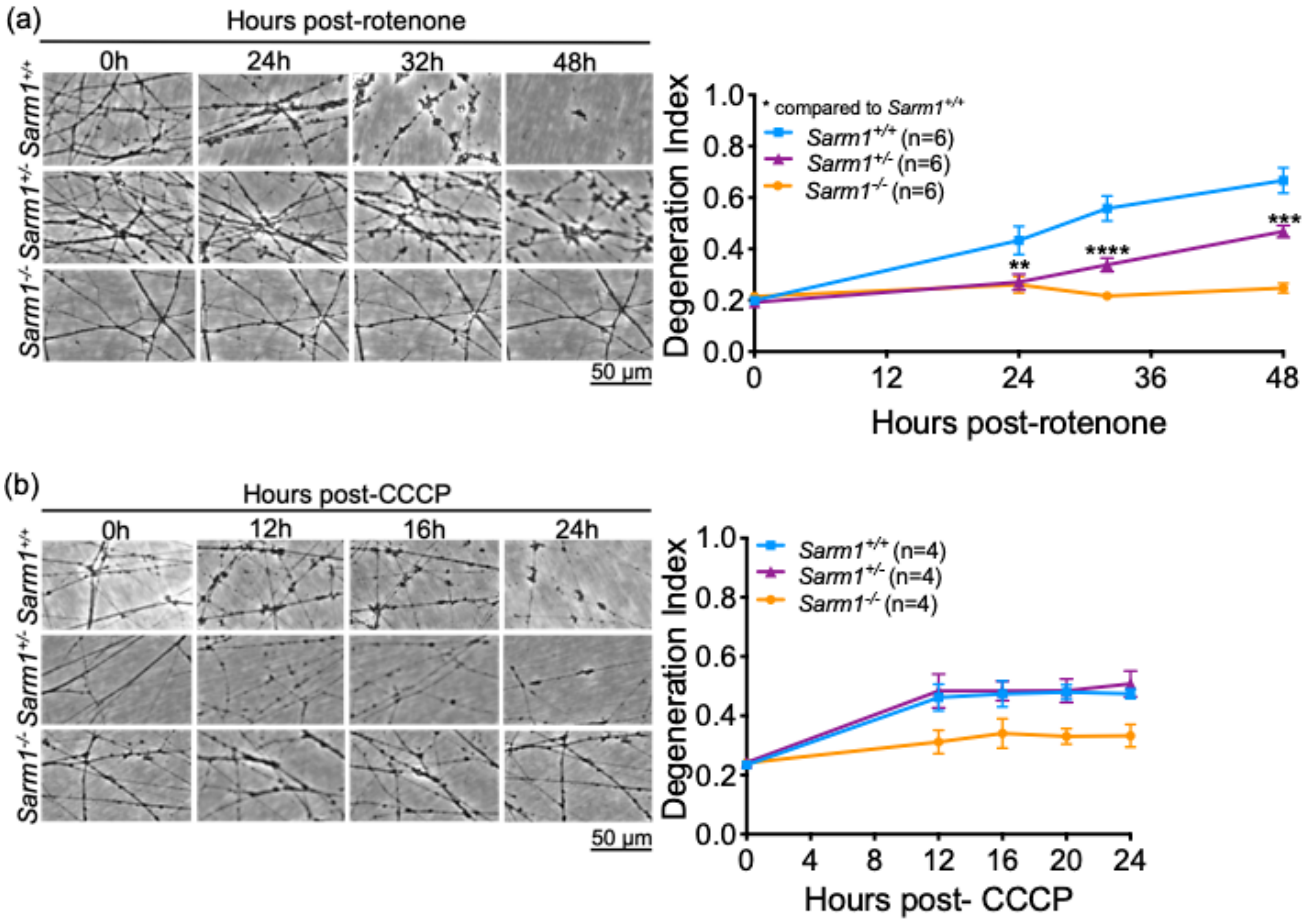

Figure 3.4: *Sarm1* hemizygosity delays the rate of programmed axon degeneration induced by rotenone-induced mitochondrial dysfunction (a), but not after 50 µM CCCP (b) or 25 µM CCCP (c). As previously shown, *Sarm1* homozygous null SCGs remain intact after administration of these mitochondrial toxins. Representative micrographs for each genotype at each timepoint are shown next to quantification of axon degeneration. SCGs were cultured for 7DIV before injury. Each data point represents an average value from two fields of view from two individual SCGs cultured in the same dish. Data were obtained across three individual repetitions with mixed genotypes. A two-way repeated measures ANOVA was performed followed by Bonferroni post-hoc analysis to determine whether there was a difference between *Sarm1* hemizygous and *Sarm1* homozygous wild-type SCGs. *p<0.05; **p<0.01; ***p<0.001

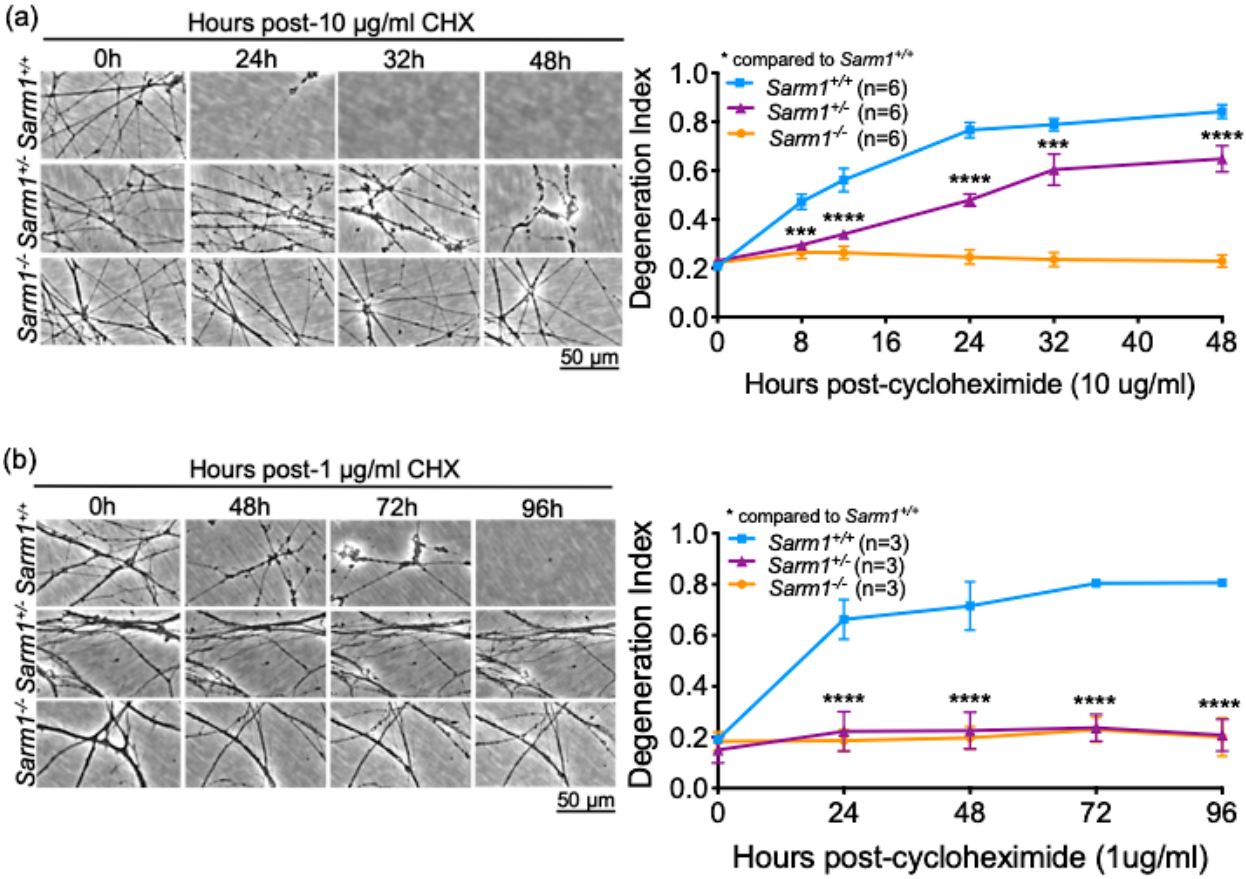

Figure 3.5: *Sarm1* hemizygosity delays the rate of programmed axon degeneration induced by protein translation inhibition after high-dose 10 µg/ml cycloheximide (a) low-dose 1 µg/ml cycloheximide. *Sarm1* homozygous null SCGs are also protected for the duration of the experiments when neurites detach before degeneration is observed. Representative micrographs for each genotype at each timepoint are shown next to quantification of axon degeneration. SCGs were cultured for 7DIV before injury. Each data point represents an average value from two fields of view from two individual SCGs cultured in the same dish. Data were obtained across three individual repetitions with mixed genotypes. A two-way repeated measures ANOVA was performed followed by Bonferroni post-hoc analysis to determine whether there was a difference between *Sarm1* hemizygous and *Sarm1* homozygous wild-type SCGs***p<0.001; ****p<0.0001

3.2.3 *Sarm1* hemizygosity delays programmed axon degeneration *in vivo*

After confirming there is an effect of *Sarm1* hemizygosity *in vitro*, which allows higher-throughput, is less expensive, and better for animal welfare, the relevance of these results was assessed *in vivo*. In order to test the biological relevance of *Sarm1* hemizygosity on the rate of programmed axon degeneration, *in vivo* sciatic nerve transections were performed. It was necessary to choose an initial timepoint immediately beyond that which wild-type axons fragment in anticipation of a subtle effect. It has been shown that 100% of axons in *Sarm1*$^{+/+}$ mice fragment 48 h post-lesion, with 80% of axons already fragmented at 42 h post-lesion [27]. By 14 days post-lesion there is no preservation of axons in *Sarm1*$^{+/-}$ mice [62]. Here, there is clear preservation of axons in the largest central fascicle of the sciatic nerve from *Sarm1*$^{+/-}$ mice compared to *Sarm1*$^{+/+}$ mice at 2- and 3- days post-lesion (Figure 3.6.a shows representative micrographs and 3.6.b shows quantification). There are still some axons preserved at 5 days post-lesion, but this number is not statistically significant compared to *Sarm1*$^{+/+}$ mice and unlikely to have biological relevance. This demonstrates for the first time that *Sarm1* hemizygosity is sufficient to significantly delay programmed axon degeneration after an extreme *in vivo* injury.

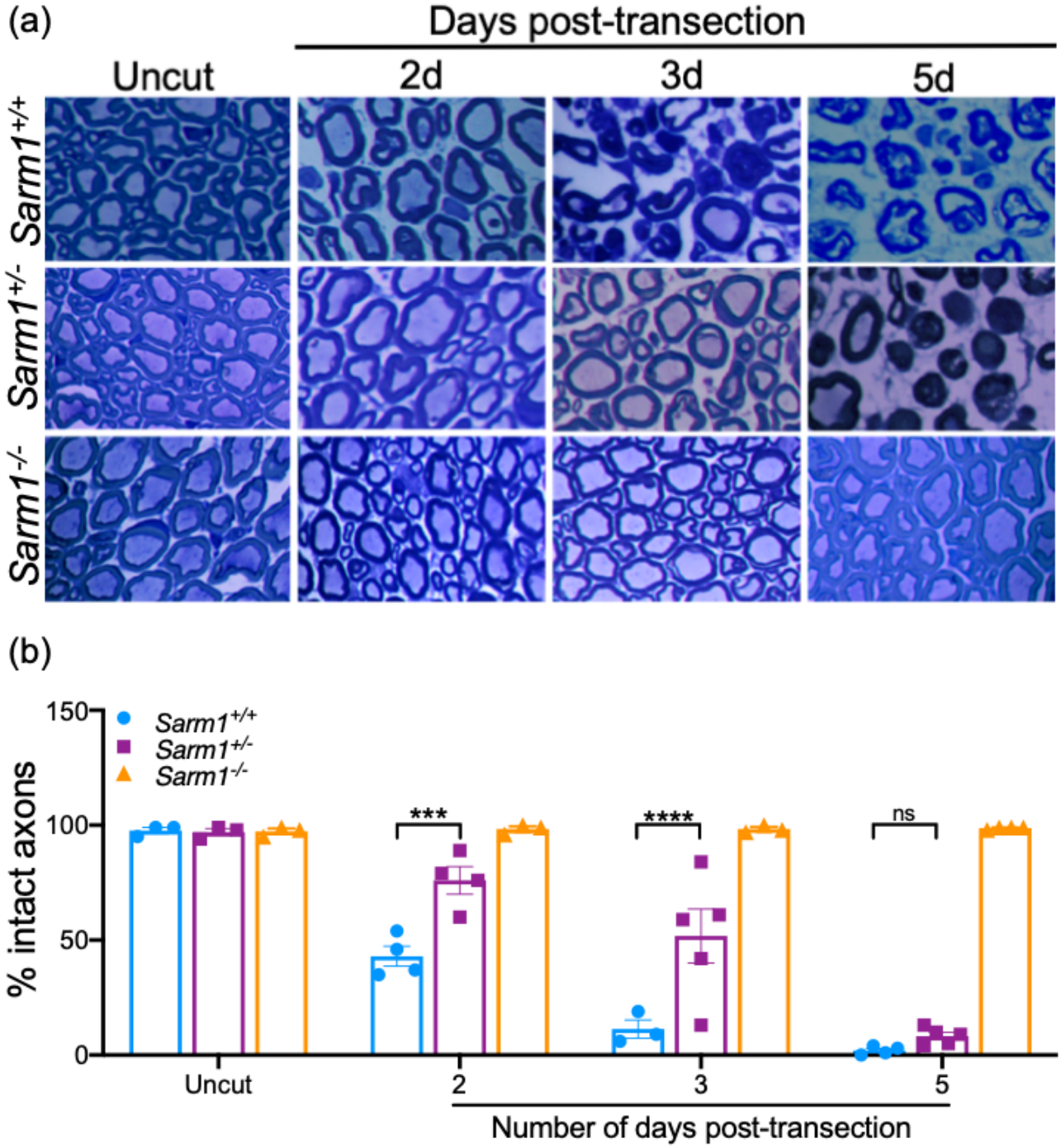

Figure 3.6: *Sarm1* hemizygosity delays the rate of programmed axon degeneration *in vivo* after sciatic nerve transection (a). *Sarm1* hemizygous mice have significantly more in-tact axons present 2- and 3 days post-transection and most axon are degenerated by 5 days post lesion, unlike *Sarm1* homozygous null axons which remain intact (b). Each data point corresponds to the quantification of an entire tibial nerve cross section from a single mouse. A two-way ANOVA was performed followed by Dunnett post-hoc analysis to determine whether there was a difference between *Sarm1* hemizygous and *Sarm1* homozygous wild-type mice. ***p<0.001; ****p<0.0001; n=3-5 per group.

3.2.4 *Sarm1* hemizygosity partially restores neurite outgrowth deficits in mice lacking NMNAT2

In addition to their roles in programmed axon degeneration, NMNAT2 and SARM1 have reported roles in nervous system development [77,114,154]. Mice lacking NMNAT2 die at birth exhibiting neurite outgrowth deficits which are rescued by complete removal of SARM1 where mice appear healthy throughout a normal mouse lifespan [111]. In this developmental model, mouse embryos lacking NMNAT2 hemizygous for *Sarm1* (hereafter referred to as *Nmnat2*$^{gtE/gtE}$;*Sarm1*$^{+/-}$ mice) exhibit peri-natal mortality with all 10 *Nmnat2*$^{gtE/gtE}$;*Sarm1*$^{+/-}$ pups born dying in a hunched posture similar to *Nmnat2*$^{gtE/gtE}$;*Sarm1*$^{+/+}$ mice [77]. Perinatal lethality of littermate *Nmnat2*$^{+/gtE}$;*Sarm1*$^{+/-}$ mice was low, with only 2 pups dying and the other 5 surviving. However, an *in vivo* rescue of intercostal nerve length in *Nmnat2*$^{gtE/gtE}$;*Sarm1*$^{+/-}$ E18 embryos was observed, where nerves grow longer than in littermate *Nmnat2*$^{gtE/gtE}$;*Sarm1*$^{+/+}$ intercostals – which barely extend beyond the spine. Intercostal nerve length in *Nmnat2*$^{gtE/gtE}$;*Sarm1*$^{+/-}$ embryos appear indistinguishable from wild-type (*Nmnat2*$^{+/+}$;*Sarm1*$^{+/-}$) or double homozygous null (*Nmnat2*$^{gtE/gtE}$;*Sarm1*$^{-/-}$) intercostals (Figure 3.7.a), appearing qualitatively like those of wild-type intercostals (Figure 3.7.b), though this observation is limited by the distance of DiI diffusion along nerves. An example of the whole-mount rib cage structure (Figure 3.7.c) indicates the point where intercostal nerves from *Nmnat2*$^{gtE/gtE}$;*Sarm1*$^{+/-}$ and *Nmnat2*$^{gtE/gtE}$;*Sarm1*$^{-/-}$ and wild-type embryos extend beyond. Interestingly, whilst the phrenic nerve of *Nmnat2*$^{gtE/gtE}$;*Sarm1*$^{+/-}$ mice appears to grow initially, it fails to innervate the whole diaphragm (Figure 3.7.d) suggesting an incomplete reversal of neurite outgrowth deficits in these mice. This reflects the partial rescue of outgrowth observed in cultured DRGs, and also explains why these mice die at birth. Due to the technical limitations in quantifying nerve outgrowth *in vivo*, DRGs were cultured from mixed litters to determine a quantifiable effect on neurite outgrowth. The reversal of neurite outgrowth is significant, but partial with mice *Nmnat2*$^{gtE/gtE}$ mice hemizygous for *Sarm1* showing intermediate outgrowth compared those on a wild-type *Sarm1* background and those that are wild-type for both genes (Figure 3.7.e).

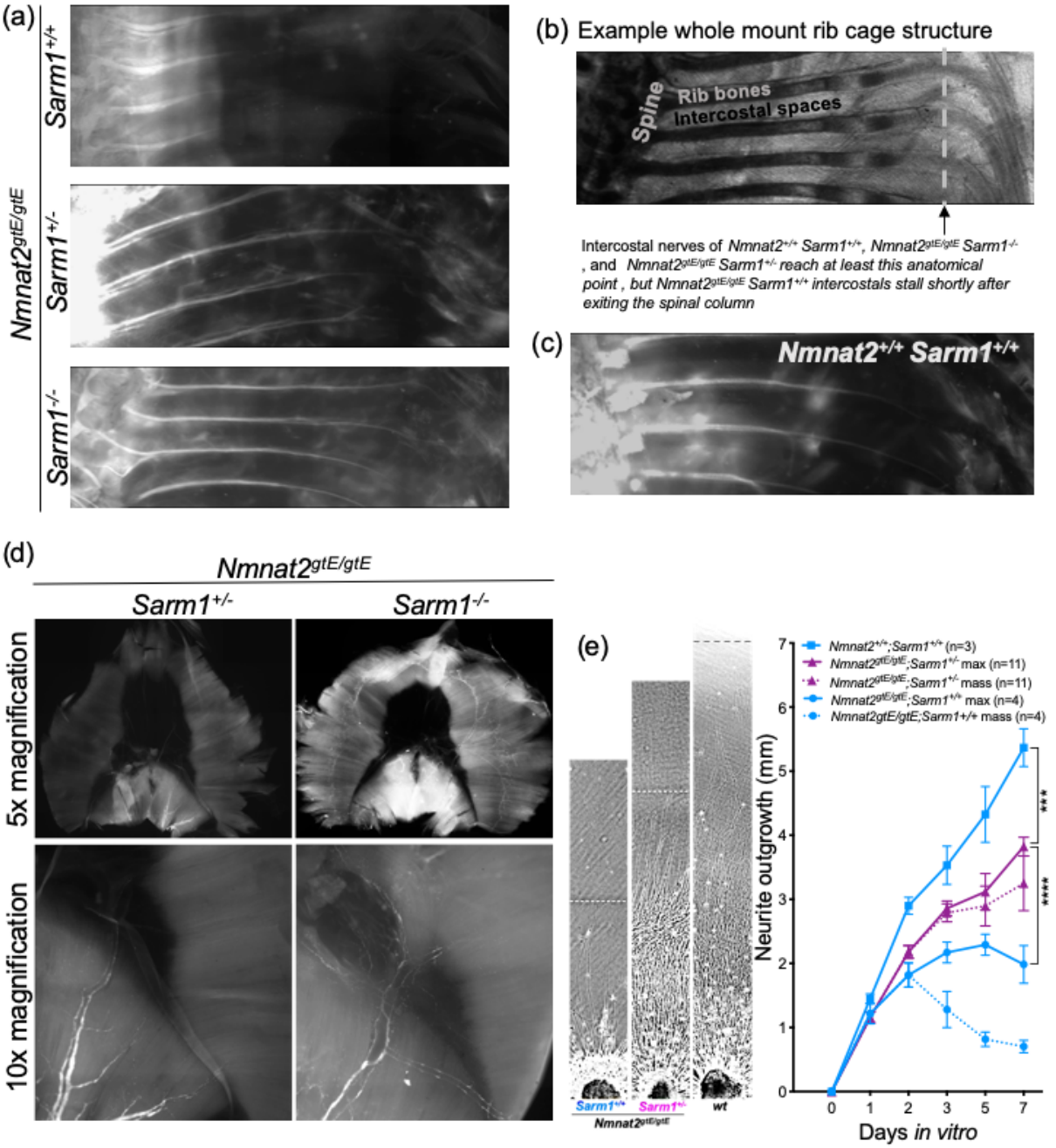

Figure 3.7: *Sarm1* hemizygosity partially restores neurite outgrowth deficits in mice lacking NMNAT2. DiI labelled intercostal nerves from E18.5 embryos in *Nmnat2*$^{gtE/gtE}$*;Sarm1*$^{+/+}$ barely extend from the spinal cord, whereas those of *Nmnat2*$^{gtE/gtE}$*;Sarm1*$^{+/-}$ and *Nmnat2*$^{gtE/gtE}$*;Sarm1*$^{-/-}$ extend much longer (a), appearing qualitatively like those of wild-type intercostals (b). An example of the whole-mount rib cage structure (c) indicates the point where intercostal nerves from *Nmnat2*$^{gtE/gtE}$*;Sarm1*$^{+/-}$ and *Nmnat2*$^{gtE/gtE}$*;Sarm1*$^{-/-}$ and wild-type embryos extend beyond (grey line and black arrow). It was previously shown that phrenic nerve outgrowth is non-existent in *Nmnat2*$^{gtE/gtE}$*;Sarm1*$^{+/+}$ embryos. In *Nmnat2*$^{gtE/gtE}$*;Sarm1*$^{+/-}$ E18.5 embryos, the phrenic nerve grows initially, but axons are truncated and most fail to cross from the crural muscle (crus) to the costal muscles, unlike in *Nmnat2*$^{gtE/gtE}$*;Sarm1*$^{-/-}$ nerves (d). Grey boxes indicate the area of diaphragm selected for 10x magnification. Neurite outgrowth was quantified in DRGs (e) where *Sarm1* hemizygous DRGs lacking NMNAT2 grew longer than *Sarm1* homozygous wild-type DRGs lacking NMNAT2, though remained shorter than wild-type neurites. Each data point represents average neurite length from three fields of view from three DRGs cultured together from one embryo. A two-way repeated measures ANOVA was performed followed by Tukey post-hoc analysis to determine whether there was a difference between *Sarm1* hemizygous and *Sarm1* homozygous wild-type DRGs lacking NMNAT2 or DRGs wild-type for both genes. ****p<0.0001. E18.5 embryos for the *in vivo* studies were obtained from multiple *Nmnat2*$^{+/gtE}$*;Sarm1*$^{+/-}$ x *Nmnat2*$^{+/gtE}$*;Sarm1*$^{+/-}$ crosses which also yielded many embryos of non-desired genotype. Therefore, E13.5 embryos for the *in vitro* outgrowth were obtained from a mixture of *Nmnat2*$^{+/gtE}$*;Sarm1*$^{+/+}$ x *Nmnat2*$^{+/gtE}$*;Sarm1*$^{+/+}$ and *Nmnat2*$^{gtE/gtE}$*;Sarm1*$^{-/-}$ x *Nmnat2*$^{gtE/gtE}$*;Sarm1*$^{-/-}$ to ensure all genotypes needed were present in litters at the time of plating.

3.3 Discussion

3.3.1 Discussion of results

Altered gene expression is one mechanism which leads to the identification of genes linked to disease in genome wide association studies (GWAS) [305] and may explain why *Sarm1* was highlighted as a GWAS hit in sporadic ALS. Since the association was made in to a non-coding intronic region of *SARM1* this could indicate altered expression, though this needs to be explored empirically. If aberrant activation of programmed axon degeneration can contribute to disease progression, it is feasible that decreased SARM1 activity through *LoF* alleles can protect against it. With unpublished evidence in the Coleman Lab that *LoF Sarm1* alleles can alter the rate of axon degeneration after *in vitro* injury, and since there is growing interest in targeting SARM1 therapeutically [122,307–310], it is important to determine whether decreased SARM1 levels or activity can be protective since small molecule inhibition may not supress SARM1 activity completely.

Results from this chapter have demonstrated that removing one *Sarm1* allele leading to a 50% decrease in SARM1 protein levels is sufficient to delay programmed axon degeneration in contrast to what was previously thought [62,132]. This applies to highly damaging *in vivo* models of sciatic nerve transection and NMNAT2-related developmental defects, as well as in a range of *in vitro* non-transection injuries. The strongest effect of *Sarm1* hemizygosity occurs after low-dose cycloheximide (CHX) where the effects are as strong as complete *Sarm1* removal. Delayed degeneration was also seen after chemotherapeutic vincristine and rotenone-induced mitochondrial dysfunction. Of the models tested, only degeneration associated with CCCP-induced mitochondrial was unresponsive to *Sarm1* hemizygosity.

The level of protection observed in *Sarm1* hemizygous mice after sciatic nerve transection, where 75% axons remain in-tact at 2 days and 50% at 3 days post-transection, exceeds that of complete removal of either CRMP4 or DLK [227,259], and is comparable to calpastatin overexpression in optic nerve at 3 days post-lesion [247]. However, *Sarm1* hemizygosity confers less robust protection than complete removal of MYCBP2 (PHR1) at 5 days post-lesion [239], or aberrant expression of bacterial enzyme NMN deamidase at 7 days post-transection [159], or WLD^S up to 3 weeks post-transection[64,82,177–179,311]. Since partial removal of protein activity is more achievable clinically than complete removal, or introduction of an exogenous gene/protein, the strength of protection seen with partial lowering of SARM1 levels in comparison to complete removal of other proteins makes it an attractive target.

In the extreme developmental model, where mice lacking NMNAT2 die at birth [77,114] but survive and live normal healthy lifespans when *Sarm1* is removed [78,111], *in vivo* intercostal and phrenic nerves grew longer in *Sarm1* hemizygous mice than *Sarm1* wild-type. However, axons of the phrenic nerve were still truncated in comparison to mice with wild-type NMNAT2 which explains why peri-natal lethality in these mice is not prevented by *Sarm1* hemizygosity. Neurite outgrowth *in vitro* demonstrated that the rescue of outgrowth deficits is partial, confirming that *Sarm1* hemizygosity can modulate axon health in response to NMNAT2 depletion. This also adds to the growing evidence that modifications which protect against axon degeneration show comparable levels of rescue in this developmental model: the presence of WLD^S, absence of SARM1, and introduction of NMN deamidase all reverse or partly reverse the outgrowth deficits [77,78,159] as well as delaying programmed axon degeneration.

By using a range of *in vitro* assays, this increases confidence that *Sarm1* hemizygosity is able to delay programmed axon degeneration with diverse triggering events and widens the scope for potential human conditions where anti-SARM1 therapies may be useful. Despite the use of diverse triggers, each of the *in vitro* assays employed leads to depletion of NMNAT2 which occurs before 4 h post-transection injury [76], 12-24 h post-vincristine [81], 4 h post-cycloheximide [76,230], and 2 h post-CCCP [75]. Loss of NMNAT2 leads to increased NMN levels which activate SARM1. The rate at which NMNAT2 is depleted in these models varies and coincides with the time course of degeneration, with vincristine being slowest at depleting NMNAT2 and inducing programmed axon degeneration in wild-type neurites.

CCCP depolarises mitochondria within 10 minutes of application and within 2 h, ATP is rapidly depleted in wild-type DRGs and SCGs, as well as DRGs lacking SARM1 which remain protected after CCCP administration [59,75]. In the same time-frame, CCCP leads to a depletion of NMNAT2 levels in wild-type SCG neurites [75] and there is a significant increase in NMN and NMN:NAD ratio in neurites measured 8-12 h post-CCCP in SCG neurites completely lacking SARM1 [75]. Thus, it is possible in the CCCP model that there are multiple triggers of SARM1 activation which activate the remaining pools of SARM1 quicker than in the other models explored.

Sarm1 hemizygous protection against axon degeneration in response to protein translation inhibition by low-dose cycloheximide is as efficient as complete removal of *Sarm1*. Since low dose protein translation inhibition is more representative of slow chronic disease mechanisms than transection injury, this data suggests that partial removal of SARM1 may be sufficient to confer robust neuroprotection in disease even though it is only partially protective after transection injury. Of course, these findings need to be confirmed in *in vivo* disease models,

but the translatability of protection between *in vitro* axotomy with *in vivo* transection, as well as *in vitro* and *in vivo* neurite outgrowth deficits in mice lacking NMNAT2, suggests that lowering rather than removing SARM1 could be neuroprotective.

3.3.2 Is targeting SARM1 a valid therapeutic strategy?

Excluding removal of *Sarm1*, the strongest delayers of programmed axon degeneration in mouse are removal of *Phr1*, overexpression of NMNATs, or introduction of bacterial NMN deamidase [62,159,177,203,239]. However, complete *Phr1* removal leads to peri-natal lethality where respiratory failure occurs due to lack of phrenic nerve development[312] since the corresponding protein is required for axonal outgrowth[313,314]. MYCBP2 (PHR1) is involved in the turnover of many proteins so does not present a safe and specific target. Whilst introduction of bacterial enzyme NMN deamidase to mice strongly delays axon degeneration *in vivo* [159], introducing a non-mammalian gene (or protein) into a human disease patient is more challenging than removing or decreasing an endogenous disease-related protein. Pharmacologically decreasing NMN levels through NAMPT inhibition delays degeneration for 24 h after *in vitro* axotomy[159,191]. However, chronic inhibition of NAMPT leads to depletion of NAD^+ since there NAMPT produces NAD^+ precursor NMN. Although FK866 has been shown to modestly delay degeneration in larval zebrafish after laser axotomy [159] its protective capacity has yet to be explored in an *in vivo* mammalian system.

In vitro data demonstrate that modifications to the MAPK cascade can delay degeneration for up to 48 h in DRGs lacking DLK or after JNK inhibition [227], and up to 24 h post-axotomy when both MKK4 and 7 levels are decreased [230]. JNK activity can both increase the rate of NMNAT2 turnover [227] and activate SARM1 via phosphorylation in response to mitochondrial stress [162], presenting the possibility of modulating SARM1 at two separate points in the programmed axon degeneration pathway. However, JNK inhibition and decreased MKK4/7 levels remain unexplored in the context of programmed axon degeneration *in vivo* and given the ubiquitous nature of MAPK signalling and JNK activity across cell types and signalling mechanisms, it is likely there will be many non-axonal effects of targeting this pathway. Complete removal of DLK, the initiating kinase in this MAP kinase cascade, only protects axons up to 52 h post-sciatic nerve transection [227] and removal DLK along with other MAP3Ks MEK4 and MLK2 is needed for axon preservation to reach 6 days post-transection [229]. Furthermore, the ubiquitous function of MAPK cascade signalling across cell types and cell responses means targeting this pathway will likely induce off-target negative side effects. Taken together, aiming to achieve axon protection through modulating the MAPK cascade is less robust and less specific than targeting SARM1.

Further down the pathway to axon degeneration is calpain activation, which occurs within hours of *in vivo* axotomy [29,252], and is thought to cleave collapsin response mediate protein-2 (CRMP2) to cause acute axon degeneration [257]. Modulating calpain activation and subsequent cleavage of collapsin response mediate proteins can modestly delay injury-induced degeneration. Inhibition of calpains via the endogenous inhibitor calpastatin or exogenous application of calpain inhibitors can delay degeneration for up to 16 h after *in vitro* axotomy [247] and 24 h after optic nerve crush [29,258] and removal of CRPM4 has been shown to delay *in vivo* degeneration for 36 h post-sciatic nerve transection [259]. Furthermore, calpastatin overexpression delays optic nerve degeneration with 90% of axons remaining in-tact 2 days post-transection [29] and 55% axons in-tact after 3 days [247]. However, calpains and collapsins are not specific to programmed axon degeneration, but also play a role in non-neuronal cell death (required for cell turnover/possible protective death mechanisms). DRG neurites lacking CRPM4 have defects in neurite outgrowth and show only weak and short-lasting delay against degeneration after *in vitro* axotomy [259].

Whilst the aforementioned modifications and *Sarm1* hemizygosity significantly delay degeneration to varying extents, complete removal of *Sarm1* still confers the strongest protection and the data presented here demonstrate that even low levels of SARM1 enable degeneration to occur. It has been shown though that complete removal of endogenous SARM1 can be bypassed by expressing a dominant negative mutant version of *Sarm1* which over-rides wild-type SARM1 pro-degenerative function [80]. However, with 50% axons remaining preserved at 10 days post-lesion, this is still not as strong as protection seen in mice lacking *Sarm1,* supporting the suggestion that long-term protection from degeneration requires full removal or inhibition of SARM1. With this in mind, therapies targeting SARM1 will likely need to involve a multi-targeted approach. This could be, for example, a therapy which combines decreasing *Sarm1* expression levels with small molecule inhibition of its NADase enzyme activity or NMN activation.

In contrast to the risks or lack of robust protection of the above-mentioned proteins involved in programmed axon degeneration, removal of SARM1 appears mostly innocuous. Mice lacking SARM1 appear to be healthy and live normal lifespans, neurite outgrowth is unaffected [111], and SARM1 activity appears to be more specific to neuronal death than ubiquitously expressed proteins in the MAPK and proteasome pathways. *Sarm1* expression has been observed at low levels the lymph nodes and blood cells [132] and there is some literature which suggests that SARM1 plays a role in immunity and susceptibility to viral infection [130,131,162,315,316]. However, the extent to which SARM1 is responsible for these changes has been questioned with the recent identification of passenger mutations in chemokine ligand

(*Ccl*) genes of commonly used *Sarm1* homozygous null mice [133]. Newly generated *Sarm1* CRISPR knockout mice do not possess *Ccl* gene expression changes reported in original knockout strains, but retain their robust axo-protective phenotype after sciatic nerve transection [133]. Furthermore, systemic removal of SARM1 does not affect macrophage recruitment to an injured nerve and protects Schwann cells against chemotoxic insults that cause axon degeneration [317].

This is promising in the context of targeting SARM1 therapeutically since one would predict there to be no significant immune consequences to SARM1 removal and less chance of inducing side effects through actions in non-neuronal cells requiring SARM1 activity. It remains unknown whether the SNP mutations identified in commonly used *Sarm1*$^{-/-}$ mice have a functional effect and whether they are responsible for immune system-related phenotypes reported in these mice. These are important details to be determined before taking SARM1 therapies into the clinic.

Results from this chapter show that degeneration in *Sarm1* hemizygotes is delayed, the next chapter will explore whether a similar decrease in SARM1 levels and delay in programmed axon degeneration can be achieved through application of exogenous antisense nucleotides. However, even though the rate of degeneration is slowed, it does still occur, clearly demonstrating that hemizygotes possess sufficient SARM1 to cause axon destruction. Therefore, the next chapter will also explore whether SARM1 levels can be further decreased in order to further delay axon fragmentation, *in vitro*.

Chapter 4: *Sarm1* antisense oligonucleotides delay programmed axon degeneration

4.1 Introduction:

The previous chapter demonstrated that decreased levels of SARM1 lead to delayed degeneration both *in vivo* and *in vitro* in response to diverse triggers of programmed axon degeneration. If *Sarm1* hemizygosity can lower SARM1 levels sufficiently enough to confer delayed degeneration or partial axon protection, it follows that partial removal of the protein could have therapeutic use. Decreasing protein expression or partially decreasing its activity is more achievable clinically than complete elimination. Since the strength of protection seen in *Sarm1* hemizygotes with partial lowering of SARM1 levels is comparable to or exceeds that of other modulators of degeneration discussed in the previous chapter, this makes SARM1 an attractive target to modulate axon degeneration therapeutically, as has been suggested in recent reviews [122,307–310].

4.1.1 SARM1: no longer an undruggable target

Druggability has been defined as the likelihood of being able to modulate a target with a small-molecule drug to cause a disease-modifying effect [318]. However, the definition of druggable targets evolves with advances in scientific methodologies. Over the past two decades, the definition of druggability has evolved from identification of; (i) genes involved in disease, (ii) proteins that theoretically have a disease-modifying effect, (iii) the presence of small pockets in the tertiary structure of a disease-related protein, and more recently (iv) to the presence of 'hotspots' on the protein which are capable of binding a small molecule for therapeutic effect [319]. However, by these terms, only 10% of the human genome represents druggable targets [318] and most proteins in the human proteome are non-enzymatic (or have no known enzyme function) playing roles in signalling pathways and complexes, structural integrity, and other functions requiring protein-protein interactions [320]. Therefore, there is need to extend views of druggability beyond the use of small molecule enzyme inhibitors to incorporate other therapeutic strategies that can cause a disease-modifying effect. As such, the term druggability can now refer to therapeutic strategies which disrupt protein-protein interactions, or utilise peptide- or nucleic acid-based approaches to modify disease states [321], extending the definition beyond small molecule inhibition of enzyme activity.

Initially, due to the lack of structural and functional information about SARM1 it was considered an unlikely drug target. However, the recent finding that SARM1 does in fact possess intrinsic enzyme activity [143,157,280] and advances in understanding its constitutive and injury-induced active structures [138,139,142,143], are crucial to understanding how its prodegenerative function can be inhibited. These studies, along with earlier functional studies [57,58] have elucidated

regions of the protein that are involved in autoinhibition, multimerisation, crucial residues required for SARM1 NADase activity, and putative binding pockets for small molecule binding, as well as its proposed octameric structure in both injured and uninjured cells. This knowledge has greatly improved understanding of how the protein functions; therefore, how it can be inhibited. Hypothetically, there are now many ways in which SARM1 could be targeted to prevent its pro-degenerative function, including;

- preventing NADase activity via small molecule inhibition [282]
- promoting the allosteric substrate inhibition by NAD^+ [139]
- preventing NMN-dependent activation of SARM1 through developing a competitive antagonist or allosteric inhibitor of NMN-binding, or by sequestering NMN [160,216]
- preventing octamerisation of monomers via disrupting SAM-SAM interactions [142,143]
- preventing TIR domain association via disrupting TIR-TIR or SAM-SAM interactions[57,58]
- gene therapy overriding endogenous SARM1 activity by introducing a dominant negative gene, as recently demonstrated in a preclinical study showing efficacy [80]
- downregulating *Sarm1* or increasing turnover of SARM1 (results from this and the previous chapter)
- simultaneously targeting or combining more than one of the above approaches

There are various approaches that could be taken to achieve the above goals, such as design of small molecule inhibitors, gene therapy, and nucleic acid-based interventions. Recently, a high-throughput screen has identified several small molecules that are capable of non-competitively binding and inhibiting the NADase activity of isolated SARM1 TIR domains [282]. However, the capacity of these molecules to bind full length SARM1 and whether they confer any neuroprotective effects have not yet been shown. Given that SARM1 forms an octameric structure and there are many ionic interactions maintaining its inactive form [139], there could be stochiometric issues around small molecules accessing TIR domain binding sites. However, small molecule inhibitors could still bind if present upon SARM1 activation before TIR-NAD^+ interactions. Inhibition of the putative NMN-binding site on the ARM domain may therefore be an alternative, more easily accessible site at which to prevent SARM1 activation. Notably, introduction of a dominant negative version of *Sarm1* utilising an AAV-mediated delivery has recently been shown to preserve axons 5 days post-transection with 50% of axons remaining 10 days post-lesion [80]. This gene encodes a mutant version of SARM1 comprising K193R, H194A, and H685A mutations which decreases NADase activity and disrupts the

prodegenerative function of endogenous SARM1 [80], through a mechanism that remains to be determined.

Theoretically, genetic targeting of *SARM1* may be more effective than small molecule inhibition given that a strong decrease in SARM1 levels or activity is needed for prolonged protection. Therefore, inhibiting expression of a gene could yield greater results than targeting the corresponding protein. However, practically, there are greater challenges to ensuring bioavailability of gene-based therapies and their *in vivo* ability to modify the target that are not present with small molecule inhibition (such as the capacity to easily enter cells and act on cytoplasmic targets). A common barrier to all therapies targeting the nervous system is ensuring efficient delivery to the correct cell types without causing off-target effects in others.

The focus of this chapter is on exploring antisense oligonucleotides as a method to decrease SARM1 expression levels. By targeting the mRNA of a protein, it is possible to effectively eliminate the prodegenerative protein from axons after a period of time during which octamers already present in the axon are naturally turned over. Removing (or significantly decreasing levels of the protein) avoids the need to inhibit many SARM1 monomers/octamers, introduce an exogenous gene, or interfere with highly regulated DNA.

4.1.2 Antisense oligonucleotide therapies

> In addition to the cited references, the information presented below is based on a presentation by Rob MacLeod, PhD who is Vice President of Oncology Research and Development, and Franchise Head at Ionis Pharmaceuticals. Ionis Pharmaceuticals provided the antisense oligonucleotides for the work in this chapter. MacLeod's talk entitled *Ionis Drug Discovery: From Ideas to Patients* and subsequent answers to audience questions was available online at the time of writing here: https://www.oligotherapeutics.org/antisense-oligonucleotides-mechanisms-of-action-and-rational-design/

As mentioned in the main introduction, antisense oligonucleotide therapy is routinely used in infants with SMA and there are therapies for a rare polyneuropathy, with clinical trials for use in Huntington's disease also underway[293]. Antisense oligonucleotides are small nucleotide sequence copies of an antisense region of the target RNA. However, natural nucleic acids with phosphodiester backbones have poor drug-like qualities; they are labile to nuclease cleavage in blood and tissue; they are large molecules with poor cell uptake that do not diffuse through the plasma membrane; and they accumulate in the liver and are rapidly cleared by the kidneys. Nonetheless, these highly labile antisense oligonucleotide molecules can be transformed into highly stable ones with a few chemical modifications. The addition of a phosphorothioate backbone improves stability and protein binding capacity, a heterocyclic

base improves target RNA recognition, and a 2'-Methoxyethyl (MOE) side chain improves potency and safety. The MOE side chain confers four main improvements to unmodified antisense oligonucleotides [322] which are: (i) increased RNA affinity, (ii) increased stability through hindering attack by nucleases (iii) increased cellular uptake, and (iv) decreased class toxicity caused by off-target effects via hindering non-specific interactions. 2'MOE modifications also decrease phosphorothioate backbone toxicity in the CNS [323].

There are different types of antisense oligonucleotides and mechanisms by which they act. The antisense oligonucleotides provided by Ionis Pharmaceuticals are 5-10-5 MOE 'gapmer' molecules with a mixed backbone. In these improved molecules, the nucleotide sequence is flanked at either end with a 2'-Methoxyethyl (MOE) side chain. This results in a 'gapmer' where the flanking MOE side chains improve binding affinity, are nuclease resistant, and direct RNase H-mediated hydrolysis of the target mRNA to the central region [295,324,325].

RNase H enzymes are a group of endonuclease proteins involved in maintaining genome stability which hydrolyse RNA residues in double-stranded nucleic acids [326]. RNase H1 has been reported as the major effector molecule through which ASO-targeted RNA destruction occurs [327] in both the cytoplasm and nucleus [328]. When antisense oligonucleotides hybridise with their target mRNA, they form DNA:RNA duplexes which becomes a substrate for RNase H1[326]. This enzyme then cleaves the endogenous mRNA strand resulting in posttranscriptional downregulation of the target gene, with efficiency reported up to 95% [326,329].

The precise mechanisms of antisense oligonucleotide uptake into cells and delivery to the nucleus remain somewhat elusive. There are several mechanisms whereby antisense oligonucleotides could be internalised, which have been recently reviewed [330–332]. Briefly, antisense oligonucleotides can trigger receptor-mediated or fluid-phase endocytic pathways [330,332], as well as clathrin- and caveolin-independent endosomal internalisation [333]. The Asialoglycoprotein Receptor (ASGR) has been shown to mediate phosphorothioate antisense oligonucleotide uptake [334] and other studies have implicated integrins, stabilins, receptor tyrosine kinases, as well as GTPase, Toll-like, and scavenger receptors in receptor-mediated uptake [330–333,335,336]. Indeed, cellular uptake of antisense oligonucleotides can be increased by conjugating antisense oligonucleotides to cell-surface receptor ligands, which targets them to receptors for receptor-mediated uptake [330,333,334,337,338].

Once internalised, gapmer antisense oligonucleotides form distinct punctae and localise in perinuclear structures and 58K Golgi protein-associated cytoplasmic vesicles, as well as undergoing endosomal processing [332]. The chemical stability of these antisense

oligonucleotides allows them to survive this processing through early, mid, and late endosomes, but they need to be released from these membrane-bound organelles in order to reach their target in the nucleus or cytoplasm [330–332]. In endosomal uptake, many antisense oligonucleotide molecules accumulate in late endosomes and lysosomes and thus are unable to perform their therapeutic function [332]. However, microinjection studies performed with earlier less potent antisense oligonucleotides suggest that only a few molecules are needed to elicit a strong effect on the target RNA and thereby levels of its corresponding protein. Therefore, the few antisense oligonucleotide molecules that enter the cytoplasm between the late endosome and lysosome through an unknown mechanism appear to be sufficient to elicit a therapeutic effect. It is thought that the reason so few antisense oligonucleotide molecules are actually required is because a single molecule can be re-used in the cell once RNase H1 has degraded the target mRNA.

Once in the cytoplasm, it is again unclear how the antisense oligonucleotides enter the nucleus and this process is difficult to image since most studies utilise fluorescently labelled antisense oligonucleotides in cells [332] and many of them remain trapped in endosomes. However, antisense oligonucleotides can bind multiple proteins in the cytoplasmic and nuclear compartments [332]. Hydrophilic MOE-modified nucleotides, such as those present in the 5-10-5 gapmers, tend to bind to fewer proteins than earlier antisense oligonucleotides [332,339,340]. Many of these interactions occur with proteins that have nucleic-acid-binding domains or act as chaperones and most proteins found to bind antisense oligonucleotides do not affect their activity [341–343]. However, those that do influence antisense oligonucleotide activity, tend to influence their subcellular localisation [341–343]. Indeed, it has been hypothesized that phosphorothioate antisense oligonucleotides bind to unidentified cellular molecules that are shuttled between the cytoplasm and nucleus via a small GTPase RAN-mediated pathway since they are shuttled continuously between the nucleus and cytoplasm in a saturable carrier-mediated manner [332,344].

This chapter will explore whether or not SARM1 levels can be decreased through application of exogenous antisense oligonucleotides and delay degeneration to a comparable or greater extent than removal of one *Sarm1* allele. For this purpose, antisense oligonucleotides optimised for *in vitro* use that can later be modified for use *in vivo* were utilised.

4.2 Results

4.2.1 SARM1 levels can be decreased by exogenous application of antisense oligonucleotides

SCGs treated with *Sarm1* antisense oligonucleotides for 3 days showed a trend towards lowered SARM1 protein levels, though this was not statistically significant for ASOa (Figure 4.1.a). However, treatment with *Sarm1* antisense oligonucleotides for 6 days leads to significantly decreased levels of SARM1 expression, with a 60-90% lowering of expression depending on the oligonucleotide used compared to control cells (Figure 4.1.b). When DRGs were treated with the *Sarm1* antisense oligonucleotides, there was almost complete suppression of SARM1 protein levels with ASOa (Figure 4.1.c). It was not possible to ascertain the effects of ASOb or combined ASOa+b since DRG explant neurites consistently detached after 3-5 days of treatment (data not shown). Whilst the antisense oligonucleotides are bioinformatically specific to *Sarm1* mRNA, their specificity was not empirically determined in the present study. Therefore, there could be off-target effects which impact on neurite adhesion or outgrowth. Alternatively, antisense oligonucleotides could initiate toxic effects at the level of endosomes/lysosomes under these culture conditions in DRGs.

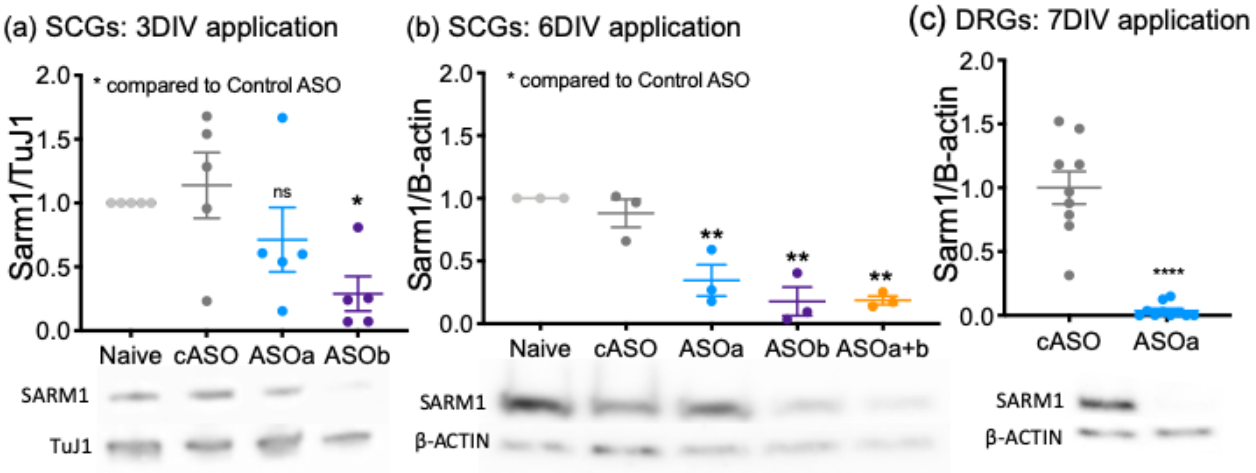

Figure 4.1: Western blot band intensity in *Sarm1* antisense oligonucleotide-treated SCGs (a-b) and DRGs (c) cultured for 7 days *in vitro* from *Sarm1* homozygous wild-type mice. ASOa application to SCGs for 3DIV showed a trend towards decrease SARM1 levels with ASOb application causing a significant decrease in SARM1 levels (a). Application of ASOs to SGCs for 6DIV significantly lowers SARM1 levels (b) as well as in DRGs for when applied for 7DIV (c). DRGs treated with ASOb or combined ASOa+b consistently detached so it was not possible to assess their effects. Representative Western blot band intensities are shown below each quantification. Each data point corresponds to an individual mouse where both SCGs were cultured for 7 days in the presence of ASOs for the indicated time. All comparisons were made between the cASO using a one-way ANOVA followed by Dunnett post-hoc analysis for (a) and (b) and a two-tailed unpaired t-test for (c). ns = no significant difference; *p<0.05; **p<0.01; ****p<0.0001

4.2.2 *Sarm1* antisense oligonucleotide reverse neurite outgrowth deficit in DRGs lacking NMNAT2

DRG neurites lacking NMNAT2 stall around 1-2 mm [77] and removal of *Sarm1* reverses this [78]. The previous chapter showed that *Sarm1* hemizygosity partially restores the outgrowth deficit. Here, application of *Sarm1* ASOa to *Nmnat2*$^{gtE/gtE}$ DRG explants on the day of plating completely reversed their outgrowth deficit with no difference being seen between *Nmnat2* wild-type DRG neurites treated with or without the same antisense oligonucleotide (Figure 4.2.a-b). Even the most distal ends of the neurites, which in *Nmnat2*$^{gtE/gtE}$ explants show signs of degeneration, were indistinguishable from *Nmnat2*$^{+/+}$ neurites after ASOa treatment (Figure 4.1.a; left panel). Delayed degeneration up to 72h post *in vitro* axotomy and protection for up to 120h post-vincristine is also seen in DRG neurites treated with ASOa (Figure 4.3.a-b).

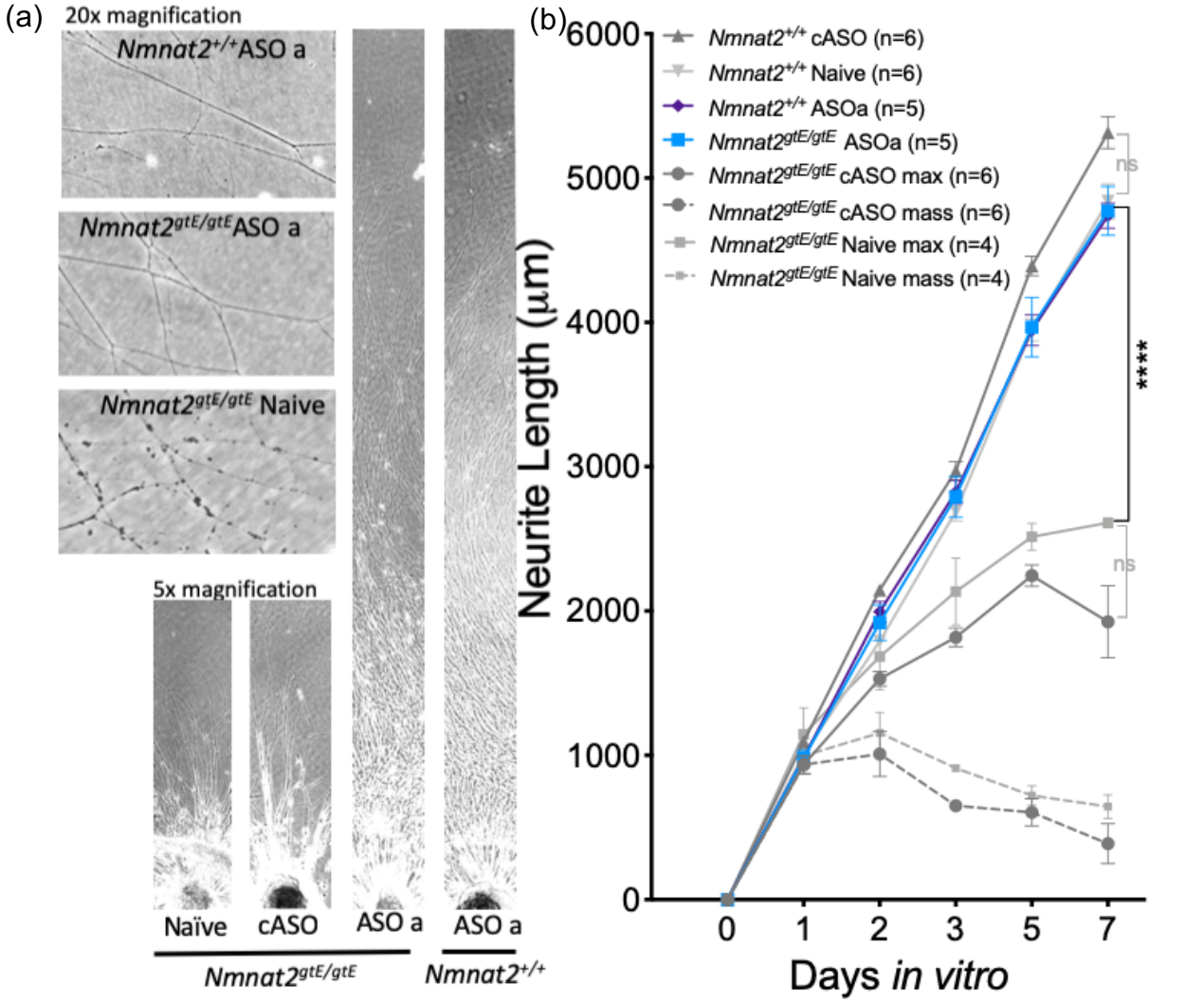

Figure 4.2: *Sarm1* antisense oligonucleotide restores neurite outgrowth mice lacking NMNAT2 and delays programmed axon degeneration. Neurite outgrowth of DRGs lacking NMNAT2 treated with ASOa are indistinguishable from wild-type DRGs treated with the same ASO even at the distal ends (a) and neurite outgrowth is significantly longer than cASO-treated DRGs lacking NMNAT2 as quantified in (b). Each data point represents an average neurite length from three fields of view from three DRGs cultured together from one embryo. A two-way repeated measures ANOVA was performed followed by Dunnett post-hoc analysis to determine whether there was a difference between *Nmnat2*$^{gtE/gtE}$ cASO and *Nmnat2*$^{gtE/gtE}$ 918 or *Nmnat2*$^{gtE/gtE}$ Naive, and between *Nmnat2*$^{gtE/gtE}$ ASOa and *Nmnat2*$^{+/+}$ ASOa. ns = not significant; ****p<0.0001; ***p<0.001; **p<0.01

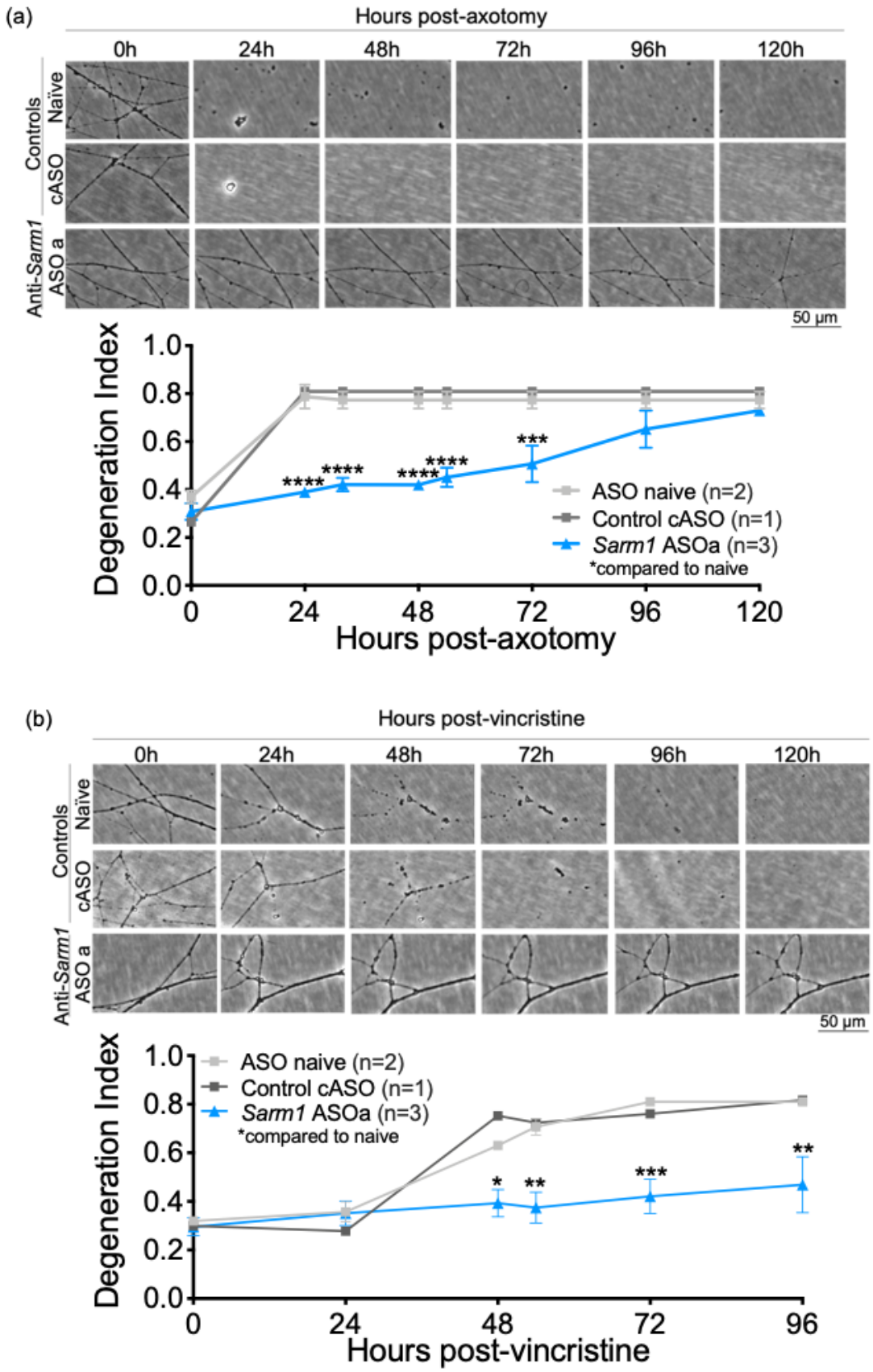

Figure 4.3: ASOa treatment delays programmed axon degeneration after axotomy (a) and vincristine (b). Each data point represents an average value from three fields of view from three individual DRGs cultured in the same dish. A two-way repeated measures ANOVA was performed followed by Dunnett post-hoc analysis to determine whether there was a difference between the *Sarm1* homozygous wild-type naive DRGs and ASOa-treated ones (c-d). ns = not significant; ****p<0.0001; ***p<0.001; **p<0.01; *p<0.05

4.2.3 Antisense oligonucleotides do not affect SCG outgrowth *in vitro*

After demonstrating reversal of the neurite outgrowth deficit and delayed programmed axon degeneration in DRGs, the next step was to study the efficacy of *Sarm1* antisense oligonucleotides in SCG models of degeneration that were used to assess the effects of *Sarm1* hemizygosity. Firstly, since application of antisense oligonucleotide to DRGs caused detachment, the rate of outgrowth in SCGs was assessed during 6-day application to ensure neurites remained healthy (Figure 4.4) and did not detach.

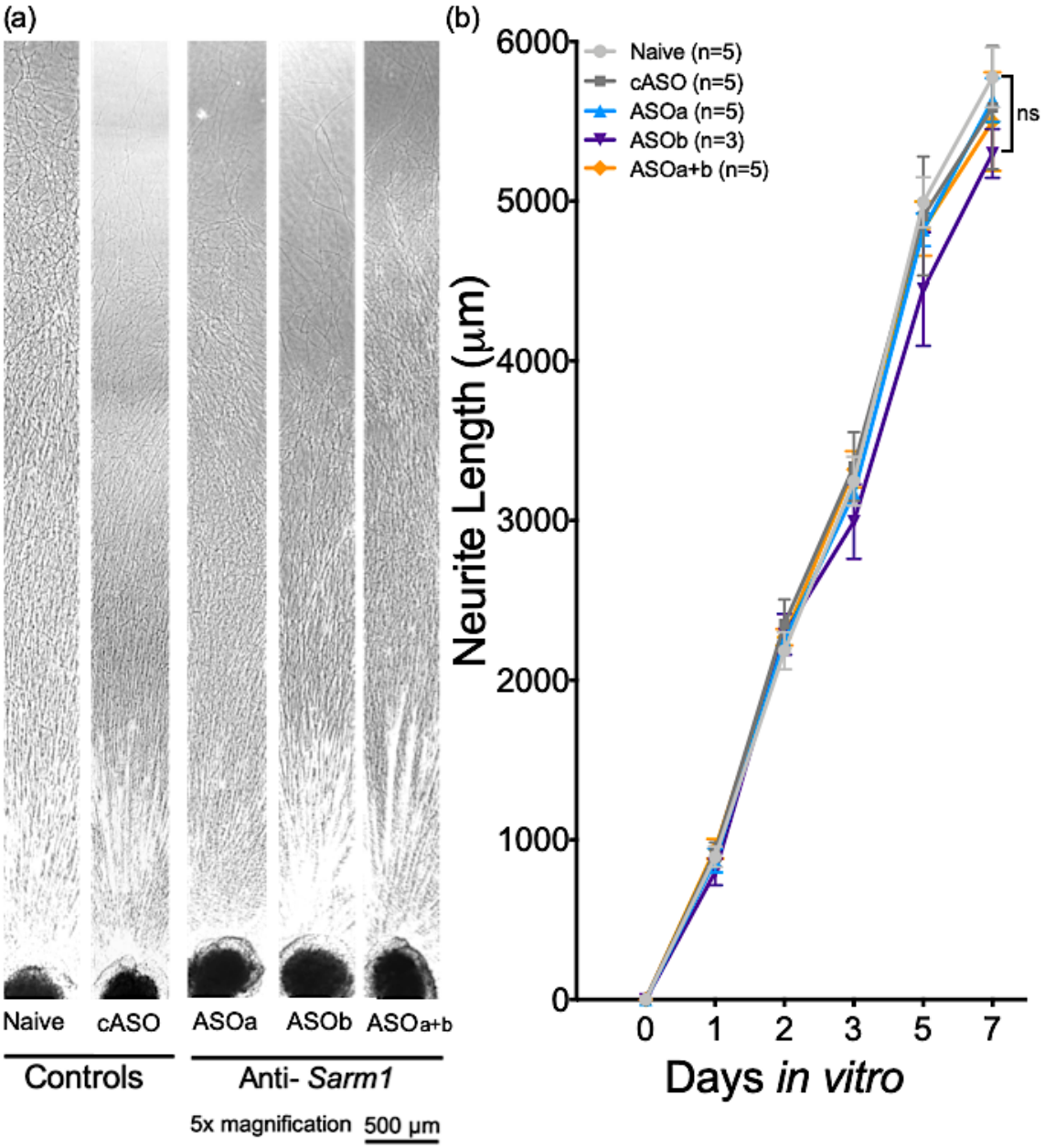

Figure 4.4: *Sarm1* antisense oligonucleotides do not impair neurite outgrowth when applied to wild-type SCGs. Each data point represents average neurite length from three fields of view from two SCGs cultured together from one mouse. A two-way repeated measures ANOVA was performed to determine whether there was an effect. ns = not significant

4.2.4 Decreased SARM1 levels confer protection against programmed axon degeneration *in vitro*.

After confirming the SCGs appeared healthy, the effects of decreased SARM1 expression after 3- and 6-day antisense oligonucleotide application were assessed. After 3-day application, axons remained intact for 8 h after *in vitro* axotomy (Figure 4.5.a). As expected, based on the higher level of knockdown (Figure4.1), greater delay in degeneration was achieved after 6-day application of antisense oligonucleotides where axons remained intact at 8 h post-axotomy and degeneration was delayed for up to 32 h with ASOb (Figure 4.5.b).

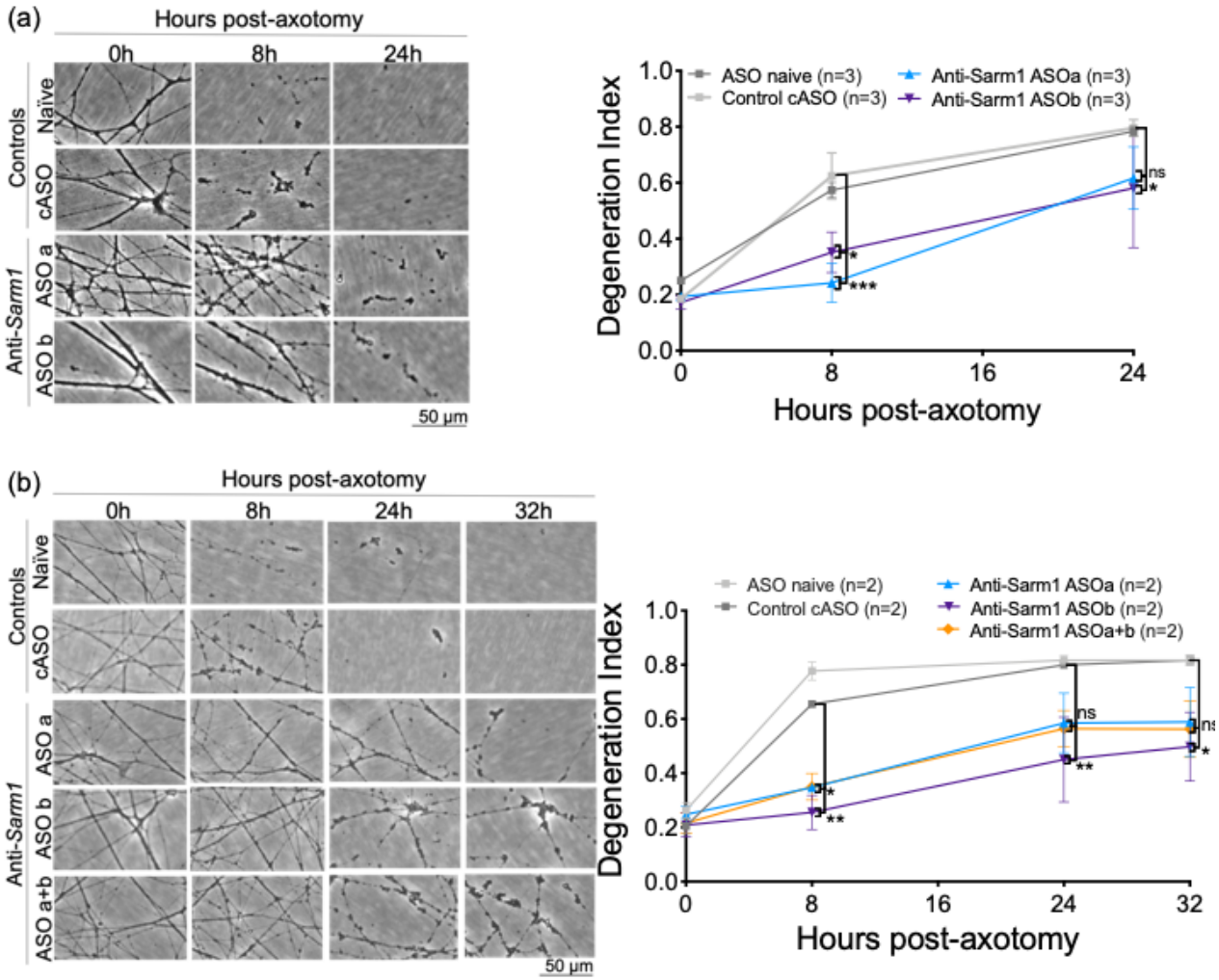

Figure 4.5: *Sarm1* antisense oligonucleotides delay programmed axon degeneration after axotomy. ASOs applied 3DIV prior to axotomy (a) and delay axon fragmentation for even longer when applied 6DIV prior to cut (b). Each data point represents an average value from two fields of view from two individual SCGs cultured in the same dish. A two-way repeated measures ANOVA was performed followed by Dunnett post-hoc analysis to determine whether there were any differences compared to cASO. ***p<0.001; **p<0.01; *p<0.05

For the remaining experiments, antisense oligonucleotides were applied for 6DIV before the chemical inducers of programmed axon degeneration were applied. As expected, decreased SARM1 expression induced by *Sarm1* antisense oligonucleotide application confers delayed degeneration against vincristine for up to 72 hours (Figure 4.6) and both low and high-dose CHX (Figure 4.7.a-b).

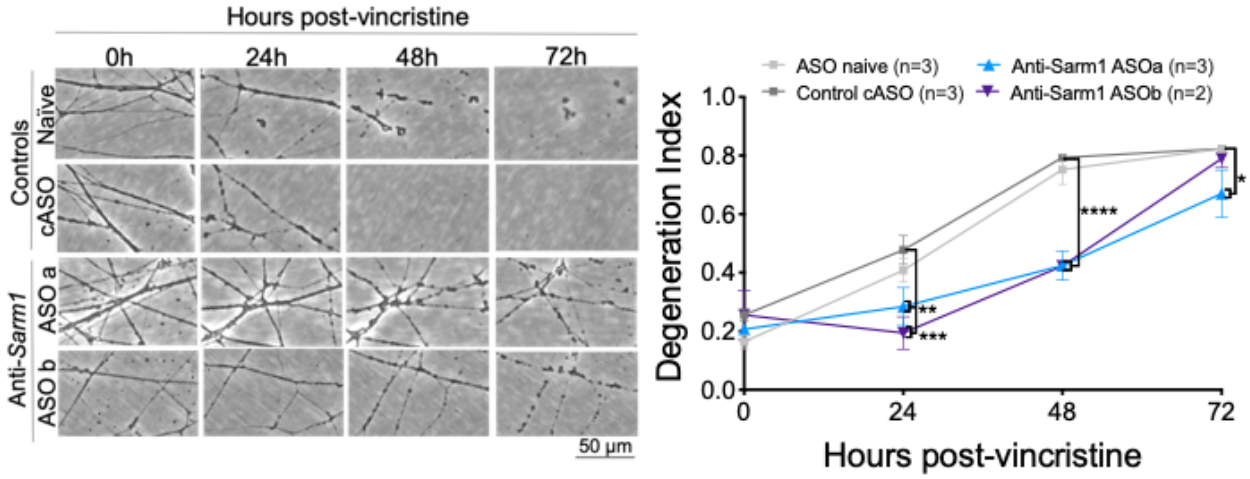

Figure 4.6: *Sarm1* antisense oligonucleotides delay programmed axon degeneration after vincristine. Each data point represents an average value from two fields of view from two individual SCGs cultured in the same dish. A two-way repeated measures ANOVA was performed followed by Dunnett post-hoc analysis to determine whether there were any differences compared to cASO. Data are presented as mean±SEM; ****p<0.0001; ***p<0.001; **p<0.01; *p<0.05

After high-dose CHX (Figure 4.7.a), each of the antisense oligonucleotides conferred stronger protection against degeneration than seen in the *Sarm1* hemizygous experiments (Figure 3.5.a), where hemizygous neurites were degenerated by 48 h post- high-dose CHX. Neurites of all, antisense oligonucleotide-treated cells remained intact at 48 h and those of ASOb-treated cells remaining intact even at 72 h post- high-dose CHX application (Figure 4.7.a). The strength of protection afforded by *Sarm1* antisense oligonucleotides post- low-dose CHX (Figure 4.7.b) is comparable to that which occurs in *Sarm1* hemizygous neurites (Figure 3.5.b) with all neurites remaining intact up to 96 h.

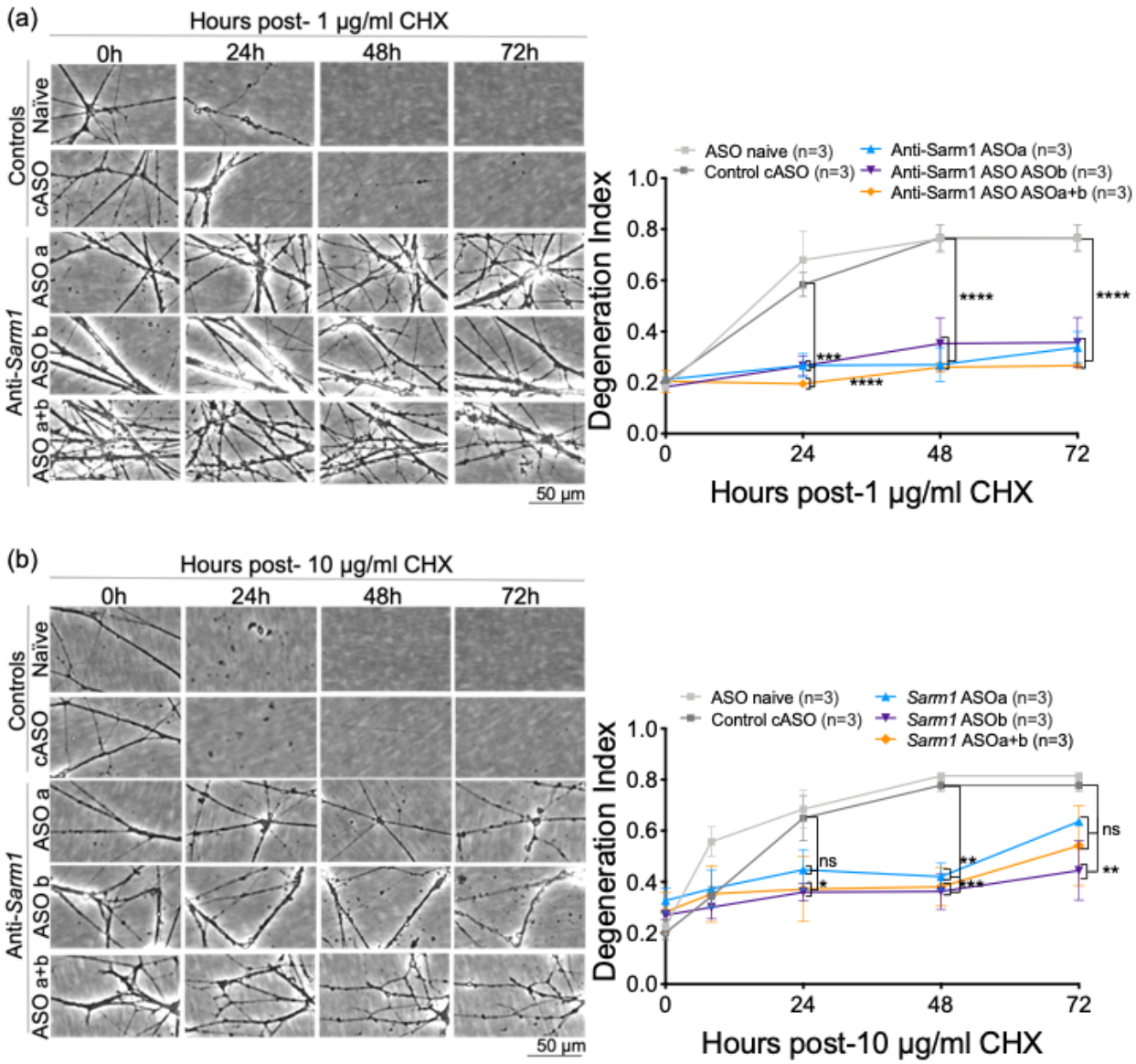

Figure 4.7: *Sarm1* antisense oligonucleotides delay programmed axon degeneration after protein translation inhibition with high-dose cycloheximide (a) and low-dose cycloheximide (b). Each data point represents an average value from two fields of view from two individual SCGs cultured in the same dish. A two-way repeated measures ANOVA was performed followed by Dunnett post-hoc analysis to determine whether there were any differences compared to cASO. ****p<0.0001; ***p<0.001; **p<0.01; *p<0.05

4.2.5 SCGs remain healthy upon prolonged exposure to antisense oligonucleotides

Cultures for these experiments using chemical inducers of degeneration were continuously supplied with ASOs for the duration of the experiment. Therefore, it was then confirmed that SARM1 levels were not further decreased upon continued application up 12DIV – the longest duration of the *in vitro* assays used – and that SCG neurites remained intact and healthy in the presence of ASOs for up to 12DIV (Figure 4.8.a-c).

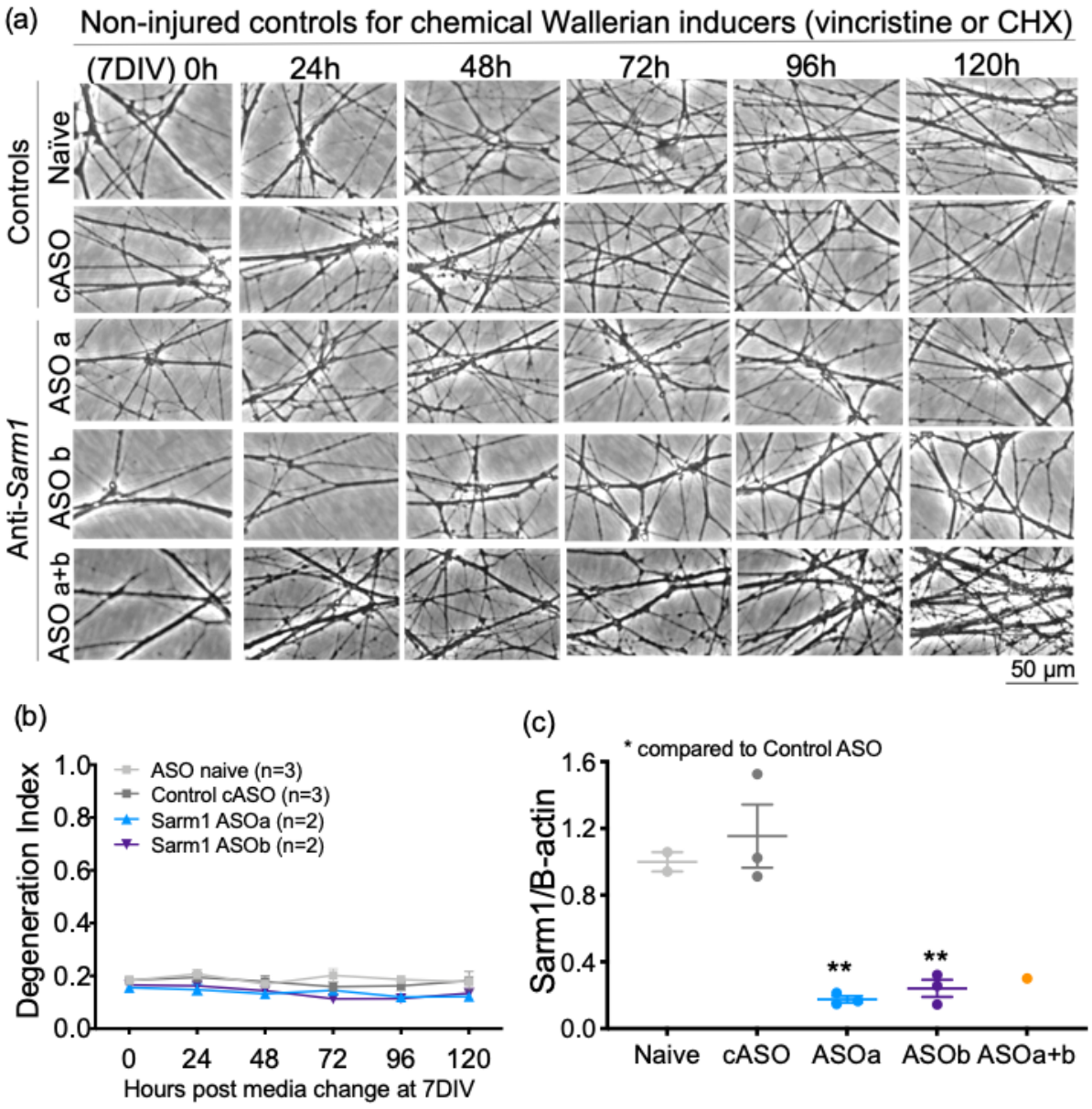

Figure 4.8: Prolonged exposure to antisense oligonucleotides does not cause spontaneous axon degeneration (a-b) or further decrease SARM1 Western blot band intensity (c). Each data point represents an average value from two fields of view from two individual SCGs cultured in the same dish (a-b) or an individual mouse where both SCGs were cultured for 7 days in the presence of ASOs for 12DIV (c). A two-way repeated measures ANOVA was performed followed by Dunnett post-hoc analysis to determine whether there were any differences compared to cASO. **p<0.01; *p<0.05

4.2.6 Programmed axon degeneration is further delayed by applying *Sarm1* antisense oligonucleotides to *Sarm1* hemizygous SCGs

Combining *Sarm1* hemizygosity with antisense oligonucleotides further decreases SARM1 levels and prolongs protection against axotomy and vincristine-induced degeneration *in vitro*. There likely exists humans that are heterozygous for *Sarm1 LoF* alleles [306]; the human equivalent to *Sarm1* hemizygous mice. Therefore, antisense oligonucleotides were applied to *Sarm1* hemizygous SCGs to determine whether it was possible to further decrease SARM1 levels and confer greater protection. This could have relevance to human disease if aberrant activation of programmed axon degeneration can cause or contribute to disease, as suggested in the previous chapter, and patients already have lowered SARM1 levels.

SARM1 levels are significantly further decreased in *Sarm1* hemizygous SCGs after ASOa application (Figure 4.9.a). There is also a trend towards decreased expression after ASOb application or combined ASOa+b application. However, these decreases are not significant, likely because there is a very narrow window between $Sarm1^{+/-}$ and $Sarm1^{-/-}$ signal intensity. Nevertheless, the further decrease in SARM1 levels is biologically relevant since the rate of programmed axon degeneration is further delayed after *in vitro* axotomy and vincristine (Figure 4.9.b-c). The rate of degeneration after vincristine is delayed up to 96 h in *Sarm1* hemizygous SCGs treated with *Sarm1* antisense oligonucleotides in comparison to the control antisense oligonucleotide-treated *Sarm1* hemizygous SCGs which are completely degenerated at 72 h.

It seems degeneration is further delayed post-vincristine when comparing the combined *Sarm1* hemizygous + antisense oligonucleotide-treated SCGs (Figure 4.9.c) with either *Sarm1* hemizygous SCGs (Figure 3.3.b) or wild-type antisense oligonucleotide-treated SGCs (Figure 4.6). *Sarm1* hemizygous SCGs (Figure 3.3.b) and most wild-type antisense oligonucleotide-treated SGCs (Figure 4.6) are degenerated by 72 h post-vincristine, whereas when combined, protection is seen up to 96 h post-vincristine (Figure 4.9.c). A side-by-side comparison with wild-type antisense oligonucleotide-treated SCGs and *Sarm1* hemizygous antisense oligonucleotide-treated SCGs run in a separate experiment would be needed to confirm the extent of additional protection. The situation after axotomy is less clear, likely due to variability in the sample sizes as well as the rate of degeneration between replicates. More replicates need to be performed to determine the effects of further decreasing SARM1 levels on the rate of degeneration after extreme injury.

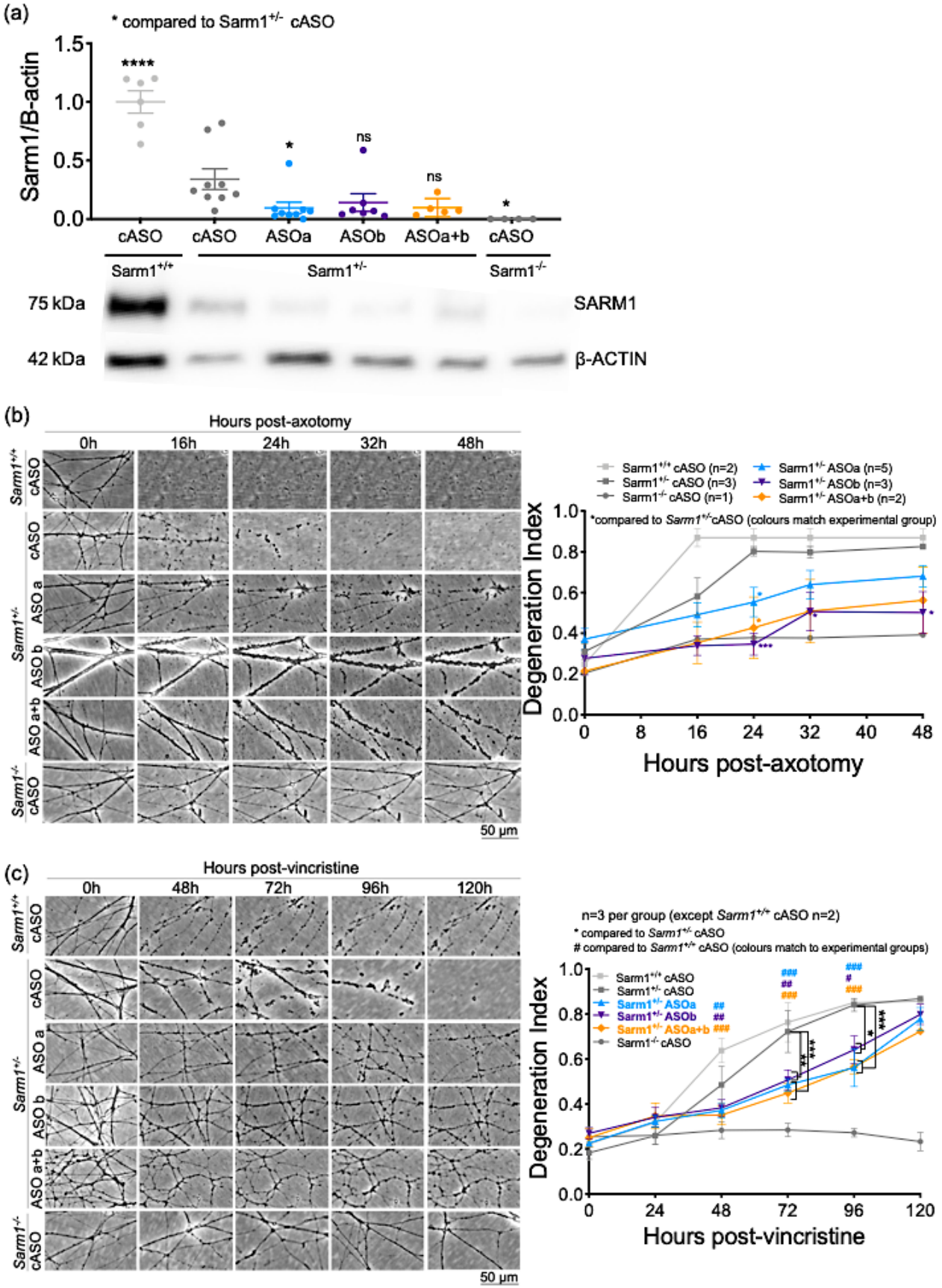

Figure 4.9: SARM1 levels can be further decreased by applying antisense oligonucleotides to *Sarm1* hemizygous SCGs (a) and this corresponds to a further delay in programmed axon degeneration after axotomy (b) and vincristine (c) compared to the rate in either *Sarm1* hemizygous SCGs or *Sarm1* antisense oligonucleotide-treated wild-type SCGs. Each data point represents an individual mouse where both SCGs were cultured for 7 days in the presence of ASOs (a) or an average value from two fields of view from two individual SCGs cultured in the same dish (b-c). A two-way repeated measures ANOVA was performed followed by Dunnett post-hoc analysis to determine whether there were any differences compared to cASO. ***p<0.001; **p<0.01; *p<0.05

4.3 Discussion:

4.3.1 Discussion of results

In vitro, a similar or greater level of SARM1 knockdown is achieved with application of antisense oligonucleotides as observed in *Sarm1* hemizygous mice. This knockdown confers a delay in axon fragmentation after axotomy, vincristine, or protein translation inhibition, and a reversal of neurite outgrowth deficits in neurites lacking NMNAT2. This demonstrates that it is possible to modulate SARM1 levels via exogenous application of an agent with potential for therapeutic use, and that this delays axon degeneration caused by diverse triggering events.

The most striking effect noted with application of the antisense oligonucleotides was seen in neurite outgrowth of DRGs lacking NMNAT2. Unlike in the *Sarm1* hemizygous DRGs, where an intermediate rescue was observed, knockdown with antisense oligonucleotides led to a complete reversal with even the most distal ends of axons qualitatively looking as healthy as those with wild-type NMNAT2. The strength of this rescue is likely due to more efficient knockdown of *Sarm1* where protein levels are virtually undetectable compared to around an 80% decrease achieved in SCGs. The greater knockdown in DRGs is likely due to the timing of antisense oligonucleotide application (at time of plating in DRGs vs 1DIV after plating in SCGs) where the antisense oligonucleotides are likely able to target *Sarm1* mRNA before SARM1 protein levels become established in neurites. In any case, this result, along with prolonged delay against axotomy- and vincristine-induced degeneration in DRGs (Figure 4.3) compared to that seen in SCGs (Figures 4.5 and 4.6) demonstrates that SARM1 levels need to be undetectable in order to elicit a strong protective effect after strong triggers of programmed axon degeneration.

The extent to which axon fragmentation is delayed after high-dose cycloheximide is greater after antisense oligonucleotide application than that which is afforded by *Sarm1* hemizygosity, likely due to greater knockdown of SARM1 levels in DRGs after antisense oligonucleotide application. After low-dose cycloheximide, degeneration is prevented for up to 96 h after antisense oligonucleotide application equalling the protective effects of complete removal of *Sarm1*. Cycloheximide was administered to model chronic protein translation inhibition and depletion of proteins to mimic protein aggregation/translation disorders. Protein aggregation occurs in neurodegenerative disorders such as prion diseases and tauopathies. This aggregation triggers an unfolded protein response, which supresses translation of new proteins as a survival mechanism to enable the ER time to clear the backlog of unfolded proteins. Suppression of the initiation and elongation phases of translation (mediated by eukaryotic initiation or elongation factors eIFs and eEFs, respectively) is seen in

neurodegenerative diseases [345,346]. This suppression occurs via phosphorylation of eIF2α by ER membrane-bound receptor PERK or eEF2 by eEF2 kinase (eEF2K) leading to sustained attenuation of protein translation [346]. This results in chronic depletion of proteins which are required for creating and maintaining healthy axons and synapses. Indeed, inhibition of phosphorylated eIF2α-mediated protein translation suppression alleviates readouts of neurodegeneration in prion-infected mice and an FTD model of tauopathy [347]. Both the presence of WLD^S (or overexpressed NMNAT) or removal of SARM1 show promise in preventing disease progression in models of FTD [105,119,348,349] and the results presented here suggest that targeting SARM1 when protein translation is inhibited could be beneficial. However, neither the presence of WLD^S nor removal of SARM1 have yet to show efficacy in protecting against neurodegeneration in prion-infected mice [350,351]. This indicates that deciding which protein aggregation disorders to target with anti-SARM1 therapies would likely require careful assessment of the role of other pathophysiological elements of disease before deciding on therapeutic intervention. It could be that in prion (or other neurodegenerative) diseases, neuronal soma death pathways are initially triggered rather than axon-intrinsic ones, or that loss of physiological roles of the aggregated proteins can trigger multiple disease mechanisms. Therefore, further study is required in *in vivo* disease models to confirm the extent to which antisense oligonucleotide-mediated knockdown of SARM1 is possible and how this corresponds to altered disease progression.

Finally, the capacity to decrease SARM1 levels even further in *Sarm1* hemizygous SCGs by applying antisense oligonucleotides was explored. Unsurprisingly this was possible, though a narrow window between *Sarm1*$^{+/-}$ and *Sarm1*$^{-/-}$ mice meant that statistical significance was only seen after application of ASOa. Nevertheless, the trend towards decreased SARM1 expression with ASOb or ASOa+b is biologically relevant since this led to a further delay in the rate of degeneration in both the axotomy and vincristine *in vitro* models compared with either *Sarm1* hemizygosity or antisense oligonucleotide application alone.

Despite similar rates of degeneration after axotomy in *Sarm1* hemizygous SCGs treated with ASOb or combined ASOa+b, there are differences in the statistical significance of these conditions. This is likely due to the variability in sample sizes caused by detachment of some neurites and variability of the rate of degeneration between different experimental replicates. Some neurites remained intact up to the 48 h timepoint in one replicate, but were degenerated or detached by 48 h in other replicates, despite being in the same experimental group. In the axotomy model, distal neurites are physically separated from soma and repeatedly imaged under the microscope which leaves them vulnerable to detachment. Variation in the rate of degeneration could be due to differences in antisense oligonucleotide uptake, or perhaps level

of SARM1 knockdown achieved. Indeed, Western blot analysis showed there are a few samples where SARM1 knockdown in the *Sarm1* hemizygous antisense oligonucleotide-treated SCGs was less efficient. Alternatively, a technical limitation of the axotomy model is the possibility that some uncut axons are included in the fields of view selected for analysis. This is unlikely since care was taken to select fields at 0 h where neurites were traced back towards the cut site to ensure they were cut. However, it is difficult to trace individual neurites in the explant culture system used so it is possible that some uncut neurites grew around the cut site into the field of view being imaged. Nevertheless, in the vincristine model where the chemical neurotoxic injury affects all neurites, a clear delay in the rate of degeneration was observed after antisense oligonucleotide application.

These results showing that applying antisense oligonucleotides to neurites already possessing lowered levels of SARM1 could indicate that if it is possible to identify *Sarm1 LoF* allele heterozygotes in the human population, they may be more likely to respond to treatments targeting SARM1. Alternatively, if variation in NMNAT2 or SARM1 levels or function is linked to human disease, such as in the case of human neuropathies [112] or as could be the case in ALS, identifying these diseases and patients for anti-SARM1 therapies could normalise the vulnerability of affected axons and prevent or delay the onset or progression of disease.

4.3.2 Comparing therapeutic strategies to target SARM1

The data presented in this chapter show that programmed axon degeneration can be delayed by antisense oligonucleotides and protection was strongest in models where NMNAT2 or protein translation inhibition triggered the pathway. Therefore, disorders involving dysfunction of NMNAT2 and protein translation may respond better to *Sarm1* antisense oligonucleotide-based therapies. However, it remains to be determined whether the similarities in *in vitro* protection between *Sarm1* hemizygous SCGs and SCGs treated with antisense oligonucleotides correspond to a similar delay after *in vivo* transection, and whether *Sarm1* hemizygosity or antisense oligonucleotides are protective in models of disease. If using anti-SARM1 therapies in human disease, the therapeutic strategy used requires careful planning to develop a technique that patients will accept, respond to, and comply with over a potentially prolonged period of time. This means the therapy needs to be minimally invasive, maximally effective, and with the lowest potential for inducing negative side effects.

Small molecule inhibition and gene therapy have both recently been reported as potential strategies to target SARM1, and the *in vitro* data presented in this chapter support a role of antisense oligonucleotide therapy. Antisense oligonucleotides have combined characteristics

of large and small molecules, they decrease levels of disease-related protein at the level of mRNA pre-translation, they are specific to the target mRNA, and are considered low risk in terms of their capacity to induce an immune response [352]. These features make antisense oligonucleotides a promising therapeutic strategy.

The inhibitory effects of recently identified small molecules inhibiting isolated SARM1 TIR domains are moderate and have not been assessed on full-length SARM1 or the ability to delay programmed axon degeneration [282]. However, other work has demonstrated in principle that small molecule SARM1 inhibition can preserve axons in primary mouse cultures after *in vitro* axotomy, vincristine, and rotenone application and human iPSC-derived motor neurones after axotomy [353]. Furthermore, FK866 is a small molecule inhibitor of NAMPT which delays programmed axon degeneration [216] likely due to depletion of SARM1 activator NMN. These data suggest small molecule inhibitors can modulate programmed axon degeneration. However, small molecule inhibition is temporary and reversible and potentially requires high concentrations (many molecules) to effectively inhibit its target, particularly when only weak inhibition can be achieved *in vitro* or biochemically. Since small molecules are administered systemically and have the capacity to bind many types of protein, they have the potential to engage in widespread non-specific actions and off-target binding both within and outside of the axon. This increases the likelihood of side effects occurring as a result of the therapy.

Aside from directly targeting NADase activity or upstream activation of SARM1, small molecule inhibitors could interrupt SARM1 octamer formation via preventing protein-protein interactions. However, in this case small molecule inhibition would alter the structure-function of SARM1 in ways that are unpredictable and potentially damaging. For example, small molecules could alter protein stability, increase the likelihood of other negative protein interactions, or cause aggregation of inhibited SARM1 monomers. In turn, this could trigger neuronal stress responses, which is exactly what the therapy is designed to avoid. It is often difficult to predict what will happen to on- and off-target biological pathways in response to inhibition of protein-protein interactions [320]. One could argue that trapping of antisense oligonucleotides in the endosomal pathway and their chemical resistance to degradation may result in a similar aggregation toxicity [330], especially since some antisense oligonucleotides have been shown to bind proteins and aggregate [340]. However, release of antisense oligonucleotides from endosomes into the cytoplasm can be overcome by adding an endosomal release sequence which has been shown to decrease endosomal trapping and increase the biological effectiveness of antisense oligonucleotides [354]. Furthermore, newer 2'-O-Methylinosine (2'OMe) modifications decrease off-target binding and associated toxic effects [340].

Antisense oligonucleotides persist in tissues thus they mediate their effects for a long time after a single dose, in contrast to small molecule inhibition which requires frequent dosing. However, antisense oligonucleotide-mediated therapies are not permanent [355], unlike AAV-mediated gene delivery which clinical trials demonstrate can result in long-term or permanent transgene expression after a single administration [233,289,292,356].

AAV-mediated gene delivery is less immunogenic than use of other viral vectors and is largely considered safe for use in humans [286]. Positive results using gene therapy in SMA patients offer hope that this type of therapy can induce biologically significant long-term effects [291]. However, the number of gene therapy clinical trials with encouraging results in neurological disorders remains relatively small [286,287]. Some studies note patients with high levels of AAV-neutralising antibodies as well as systemic signs of inflammation and transient humoural responses [288,290], though others report none [289,292]. Whilst some studies have not noted adverse immune events, immune-related responses were not considered as an outcome measure [233,356]. Since most people have already been exposed to AAVs and therefore already have neutralising antibodies, the pre-existing adaptive immune response has potential to decrease the clinical efficacy of the therapy [357]. Indeed, studies in non-human primates demonstrated that exposure to natural AAVs decreases efficacy of AAV-mediated gene delivery due to the presence of neutralising antibodies [358]. Like gene therapy using viral vectors, antisense oligonucleotides have the potential to induce immune responses and some antibodies have been noted in humans after antisense oligonucleotide treatment. However, these antibodies are neither neutralising nor high titre[359], unlike those which are associated with gene therapy.

In addition to potential immune effects, questions remain over whether AAV-delivered genes integrate into host DNA and what effects this could have. AAV-insertion into host DNA was noted in human hepatocellular carcinomas [360] (Nault et al. 2015) and later confirmed to occur in mice at the Rian locus [361]. High levels of integration have been observed across mouse brain at CRISPR-induced double stranded DNA breaks [362] with reported preference for active genes in mouse [363]. However, other studies have shown a lack of AAV-induced toxicity in rodents [364] and AAVs have been reported as having low levels of insertional mutagenesis and immunogenicity in comparison to other vectors [286,365]. Antisense oligonucleotides alter gene expression without risk of integrating into host DNA and can decrease levels of the endogenous protein without overexpressing an additional modified gene and its corresponding protein.

Authors acknowledge that AAV-mediated delivery of compound dominant-negative SARM1 is not as strong as complete removal of *Sarm1* [80], and there is another potential caveat to using this strategy. Two of the mutations in this construct are present in the ARM domain and one in the TIR domain; the TIR domain mutation alone does not abolish SARM1 prodegenerative capacity, though it does cause a significant delay in degeneration caused by *in vitro* axotomy. Another dominant negative mutation (K597E) present in full-length SARM1 overrides wild-type SARM1 activity, but presence of the same mutation in SAM-TIR domain (in a construct lacking the ARM domain) reinstates SARM1 pro-degenerative function [366]. The effects of removing ARM domain and its autoinhibition was not reported in the compound dominant-negative construct. If ARM domain removal elicits a similar effect to that in the K597E dominant negative mutant, this could indicate that disease-related events leading to strong enough disruption of ARM domain autoinhibition could restore SARM1 prodegenerative activity thereby contributing to the disease pathology it was designed to prevent. This potential, along with other negative effects relating to immunity could make this type of gene therapy potentially dangerous if used in certain circumstances.

Finally, a general barrier to targeting neurodegenerative disorders is being able to deliver therapies into the CNS which is highly impenetrable due to the presence of the blood brain barrier (BBB). Delivery in patients is usually achieved by lumbar puncture which introduces therapeutics into the cerebrospinal fluid (CSF), or by direct stereotaxic injection into brain regions. This type of delivery is usually considered inconvenient, but the inability of therapeutics to pass the BBB could be positive in the context of decreasing potential systemic toxicity. However, further study is required into the effects of antisense oligonucleotides on neuronal health at subcellular levels to ensure a lack of toxicity.

The experiments presented in this thesis thus far, along with results from the AAV-mediated therapy indicate that low levels of functional SARM1 can still elicit a prodegenerative effect. This points to therapies needing to remove wild-type prodegenerative SARM1 from axons in order elicit strong prolonged protection (at least in transection or other extreme activators of programmed axon degeneration). It is theoretically best to target SARM1 at a point where there are minimal molecules to inhibit with minimal invasiveness to elicit the strongest effect. Therefore, targeting the protein with small molecule inhibitors when it is fully formed or present in octamers, or overriding endogenous SARM1 protein with a dominant-negative gene construct, may not be as effective as preventing presence of the protein in the first instance. However, completely eliminating a protein requires complete suppression of its expression and allowing endogenous protein turnover mechanisms to degrade any monomers and octamers already established prior to the point of therapeutic intervention.

The results from this chapter demonstrated that decreased protein levels can be achieved through targeting mRNA. Since one mRNA molecule can give rise to many protein molecules, inhibiting SARM1 translation can effectively remove multiple protein monomers from the system using only one therapeutic molecule. However, if small molecule inhibitors have greater bioavailability and are taken up into axons more effectively than methods to inhibit translation, this could make using them a potentially more effective approach. On the other hand, modifications to improve delivery efficiency and decrease toxicity of antisense oligonucleotides could overcome issues pertaining to the promiscuity and transience of small molecule inhibition whilst preventing translation of endogenous SARM1. Studies have demonstrated the possibility of using an endosomal release sequence [354] and targeting antisense oligonucleotides to specific receptors for more efficient uptake into cells [330,333,334,337,338] as well as varying the 2' modifications to decrease toxicity and improve efficacy [340]. Continued development in this direction has potential to yield a useful therapy against SARM1 in disease involving programmed axon degeneration.

Chapter 5: The role of programmed axon degeneration in Alzheimer's disease

5.1 Alzheimer's disease

Alzheimer's disease (AD) is the third leading cause of adult death in the developed world and it comes with huge personal, social, and economic costs. As expected lifespan of the human population increases, so too does the incidence of AD. Most AD cases are sporadic in aetiology (sAD), meaning that any genetic causes are not inherited in a Mendelian pattern, and effects of the environment are unclear; only 1-6% of patients with AD develop it due familial causes (fAD)[367]. Clinically, there are seven stages observed in a patient with Alzheimer's disease outlined in detail in Figure 5.1.a. Briefly, patients start with no clinically observable symptoms and progress to complete loss of personality, basic bodily functions and eventually death. At the level of gross anatomy, the post-mortem brain of an AD patient exhibits enlarged ventricles and atrophy of the cerebral cortex and hippocampus in comparison to a (healthy) non-AD post-mortem brain (Figure 5.1.b).

5.1.1 Molecular hallmarks of Alzheimer's disease: Plaques and tangles

The two most well-known molecular markers of AD in brain are extraneuronal plaques comprising fibrillar amyloid beta (Aβ) oligomers and intraneuronal cytoplasmic neurofibrillary tangles comprising hyperphosphorylated tau; commonly referred to as plaques and tangles, shown in Figure 5.2.a,c. As the clinical AD symptoms progress in time, so does the severity of these molecular markers of disease, as shown in Figure 5.2.b,d. Early studies of AD suggested that the progressive accumulation of aggregated Aβ and hyperphosphorylated Tau were drivers of disease and that plaques and tangles were the toxic species. However, there is evidence to suggest that non-aggregated Aβ oligomers are the cause of neuronal stress [368] and their presence precedes tauopathy in human AD cortex [369].

As AD progresses, there is gross symmetrical loss of white brain matter which can be detected in later stages of disease using magnetic resonance imaging (MRI), as well as in post-mortem brain, and positron emission tomography (PET) imaging can be used to visualise specific proteins, such as Aβ. Cellular correlates of gross white matter loss include demyelination, axonal death and dystrophies, synaptic loss, mitochondrial hypometabolism, and defects in axonal transport mechanisms. Affected neurones also exhibit signs of cellular stress, such as; increased levels of reactive oxygen species (ROS), oxidative stress, and altered protein expression. Brain macrophage and astrocytic glial cell responses and altered inflammatory cytokine profiles are also seen, with debate over whether these inflammatory responses cause or contribute to disease progression or whether they fight it. With loss of axons and neuronal connectivity comes loss of cognitive functions and this makes the prevention of early axon loss an important therapeutic goal across most neurodegenerative diseases.

(a)

Stage 1: Patient is cognitively normal (no symptoms of Alzheimer's disease)

Stage 2: Patient has slight subjective memory loss which cannot be observed clinically and is generally not distinguishable from normal memory; e.g., recalls losing items.

Stage 3: Patient has mild cognitive impairment (MCI) which includes getting lost or having difficulty finding correct vocabulary; a decline in work may be noticed by co-workers.

Stage 4: Patient has mild-moderate dementia which includes poor short term memory, forgetting some personal history, reduced concentration and deficits in knowledge of current affairs. However, they can still recognize familiar people.

Stage 5: Patient has moderate-severe decline and requires help with day-to-day life as they suffer with confusion and cannot recall personal details like their phone number. They may have difficulties dressing and eating at this stage as well as being disoriented to time or place.

Stage 6: Patient has severe dementia requiring constant supervision and care. They fail to recognize family and friends and can be found wandering. The have major personality changes such as delusions and paranoia. They forget their spouse's name and are largely unaware of recent life events. Knowledge of old events begin to fade.

Stage 7: Patient is in the final stages nearing death. They are generally incontinent and need help with feeding, they have lost the ability to communicate and have motor symptoms. Developmental reflexes appear suggesting severe levels of neurodegeneration in the brain.

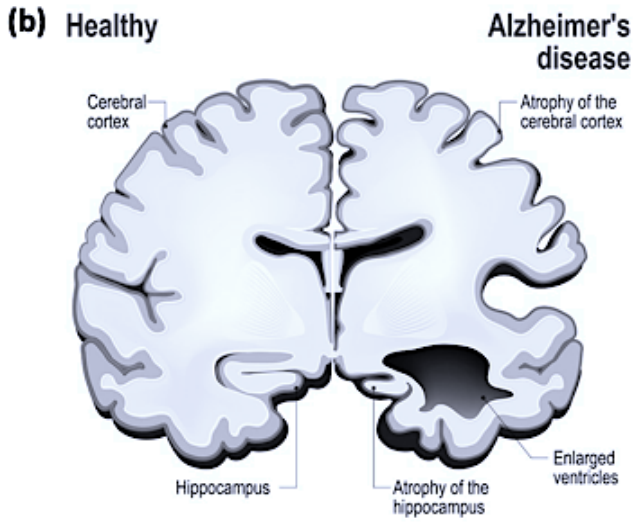

Figure 5.1: The seven clinical stages of Alzheimer's disease (a) and a representation of the gross brain differences between an aged healthy brain and one with late-stage Alzheimer's disease (b).

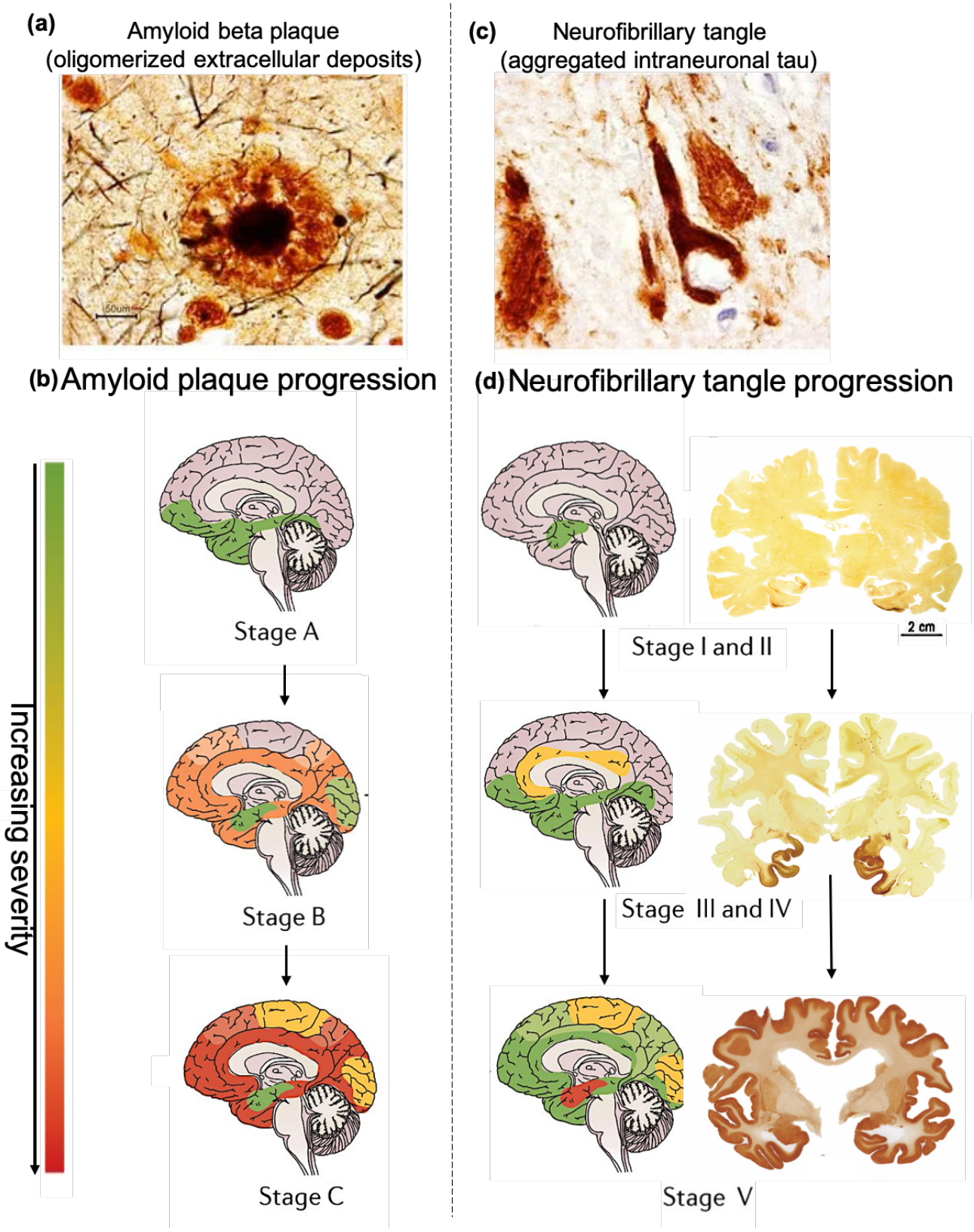

Figure 5.2: Progressive development of extracellular Aβ plaques (a-b) and intraneuronal neurofibrillary hyperphosphorylated Tau tangles (c-d).

5.1.2 Genetic causes and risk factors for AD

Mutations in amyloid precursor protein (APP), as well as presenilin 1 (PSEN1), and presenilin 2 (PSEN2), involved in processing APP to Aβ isoforms are all known to directly lead to the development of AD. Whilst mutations in *MAPT* (the gene encoding Tau, a microtubule associated protein) have been linked to development of frontotemporal dementia (FTD) and other tauopathies, they have not been linked to fAD. Some may argue that the pathological processes contributing to FTD are activated downstream of amyloid, making FTD a form of AD that can occur in the absence of amyloid pathology. Pathogenic mutations in *MAPT* can alter the relative expression of different Tau isoforms and its propensity to form aggregates or alter microtubule assembly and stability.

There are many genes associated with increased risk of developing AD. In September 2020, ALZFORUM had 695 genes listed that were associated with increased risk of developing AD and genome-wide association studies (GWAS) identified more than 21 risk loci for sAD[370]. Some of these risk genes relate to protein and organelle recycling (e.g., *BIN1* and *PICALM*), lipid homeostasis, inflammation (e.g., *TREM2* and *CR1*), and clearance pathways (e.g., *ABCA7* and *CLU*). The most well-researched risk allele for late-onset AD (LOAD) is the *ε4* polymorphism of apolipoprotein E (*APOE-ε4*), where possession of one or more *APOE-ε4* alleles increases risk of developing AD[371]. Conversely, possession of one or more *APOE-ε2* alleles decreases risk of AD in comparison to homozygous *APOE-ε3*. APOE disrupts Aβ clearance by reducing the ability of Aβ to bind low density lipoprotein related protein (LRP1) in mouse brain[372]. Another well-known risk factor allele conferring susceptibility for LOAD is *SORL1*, encoding protein sortilin-related receptor (SORLA), which is involved in directing intracellular APP trafficking to recycling pathways [373,374]. Whilst there are no known genetic mutations in axon transport proteins related to AD, axonal transport deficits have been observed in models of AD thus may underlie some pathologies in neurodegenerative diseases[375].

5.2 Axon Transport in AD

Axon transport is an ATP-dependent bidirectional phenomenon that involves movement of vesicle-bound proteins and organelles along intraneuronal microtubule tracts to support neuronal maintenance and survival. Axon transport occurs when motor proteins bind adapter molecules and vesicles to transport them along microtubule tracts in an anterograde or retrograde manner. Anterograde transport, away from the soma such as that of APP, is mainly mediated by kinesins[376]. Anterograde transport provides essential proteins, mRNA, and

organelles produced in the soma to other regions of the neurone, including the distal ends (e.g., for synapse formation and neurotransmitter release). Retrograde transport occurs in the opposite direction; towards the soma and is mainly mediated by dyneins[377] enabling the cell to receive signals (e.g., from trophic factors) and destroy and recycle dysfunctional proteins and organelles. Fast axonal transport involves transporting membrane bound particles[378] which can contain combinations of proteins, metabolites, and or organelles which may belong to a pathway or are needed for organelle survival during transit. Indeed, it has been suggested that APP and its processing enzymes (BACE1, PSEN1 and PSEN2) undergo fast axonal transport in vesicles together[378]. However, this has been disputed [379] and a recent study demonstrated *in vitro* that punctate vesicles containing APP, BACE1, and mitochondria are transported independently from one another[380]. Neither NMNAT2 nor SARM1 are known to be co-transported APP, its processing enzymes, or mitochondria [380].

Tau is a microtubule-associated protein[381–384] which stabilises microtubule tracts. Hyperphosphorylation of Tau, which occurs in AD, increases the propensity of Tau to dissociate from microtubules, thereby leaving neuronal transport tracts vulnerable to destabilisation[376,385–387]. Both monomeric and oligomeric Aβ species can inhibit fast axonal transport via different mechanisms depending on the isoform and whether it is intra- or extracellular [378,388–394]. This effect of Aβ on axonal transport may occur via Tau [7], since decreases in Tau levels prevented Aβ-induced deficits in axonal transport *in vitro* [395]. Furthermore, when CRND8 mice were crossed with mutant Tau MAPT^{P301L} mice, there was no impact on the prevalence of Aβ plaques or how they associated with dystrophic axons; however, anterograde mitochondrial transport was decreased [396]. Mitochondrial mobility can be slowed by decreased GSK3β activity in a Tau-dependent manner [397] accumulation of Aβ oligomers within mitochondria decreases anterograde mitochondrial transport, as well as altering mitochondrial energy production and life cycle [390]. More evidence supporting a role of Tau in AD-related axonal transport defects comes from mice deficient in PSEN1 and PSEN2, also overexpressing human Tau. These mice exhibit early Tau pathology and defective learning alongside deficits in axon transport[398]. Clearly there is a relationship between Aβ and Tau, and both of these species are considered neurotoxic in AD. However, how they related to one another and AD onset and progression is a controversial topic of discussion which has been debated since their discovery in human AD brain.

5.3 The amyloid cascade hypothesis: evidence to support and dispute

The amyloid cascade hypothesis (ACH) postulates that incorrect processing of APP leads to accumulation of Aβ protein into plaques which are the neurotoxic causative agent in AD; Aβ plaques subsequently lead to the formation of neurofibrillary Tau tangles, cell loss, vascular damage, and dementia [399]. Whilst there is evidence to support this hypothesis, there is also plenty that disputes it.

Amyloid isolated from AD patient brain was sequenced in 1984 and identified as the primary component in neuritic plaques a year later [400–403]. Shortly after these observations, the first mutations were identified in *APP* and linked to the development of fAD [404]. A few years later, mutations in genes which encode subunits of the γ-secretase enzyme, *PSEN1* [405] and *PSEN2* [406,407] were also linked to the development of fAD. However, there are no known causative AD mutations in *ADAM10* or *BACE1*, which encode the other APP processing enzymes α-secretase and β-secretase, respectively [408]. Therefore, the only genes known to *cause* AD, rather than *contribute* towards a person's *increased risk*, are involved in APP processing (*APP* itself, as well as *PSEN1* and *PSEN2*). These mutations increase the production of longer amyloid peptide isoforms (Aβ) in competition with healthy processing which leads production of a shorter (p3) product. This increases the ratio of long Aβ:short Aβ ($A\beta_{1\text{-}42}$:$A\beta_{1\text{-}40}$), though it remains unclear how these isoforms lead to pathology in AD [409–413].

Further genetic evidence supporting the ACH comes from people with Down Syndrome (DS), the majority of whom develop AD by the age of 65 [414–416], with some presenting with symptoms as early as 40. These individuals possess a third copy of chromosome 21 where APP is situated [417]. Similarly, families possessing rare duplication of the *APP* gene on chromosome 21 (known as Dup-APP) also develop EOAD [418–422]. In contrast, another rare *APP* mutation (A673T) leads to lower amyloidogenic Aβ production and is associated with decreased levels of cognitive decline in the elderly who do not develop AD [423,424]. In addition, those rare DS individuals that do not go on to develop AD actually do not possess the third APP allele [425].

The above-mentioned findings demonstrate a clear role of APP mutations leading to fAD. However, there is poor correlation between mutations in *APP*, as well as *PSEN* or *BACE1* genes with sAD [426–428]. Some weak associations between sAD in patients with both mutant *BACE1* and the APOE-ε4 allele have been noted [429–431], with one study suggesting that epistasis between *BACE1*, *APOE-ε4*, and other risk factor genes is a crucial factor in the aetiology of sAD [432]. In addition, *MAPT* variation and known pathogenic heterozygous variants of *PSEN1* and *PSEN2* have been identified in a small cohort of sAD patients [433], though larger

cohorts are required to confirm this finding. Furthermore, the *APOE-ε4* allele confers the strongest known genetic risk for sAD and this gene encodes a protein involved in Aβ clearance [371,434]. However, no association has been demonstrated between sAD and mutations in *LPR1,* which encodes the receptor APOE interacts with during Aβ clearance[435–437].

In preclinical studies, Aβ is toxic to cultured neurones causing axonal and dendritic retraction [438]. Overexpression of *APP* or *PSEN* mutants in mice produces plaques and memory deficits [439–441], and age-dependent neurodegeneration in *Drosophila* [442]. However, mouse studies show that mutations leading to increased Aβ production are not sufficient to induce AD [443]. Furthermore, overexpression of mutant APP does not lead to neurone loss [444,445], development of neurofibrillary tangles or AD-like dementia [408]. Similarly, no *PSEN* mutants develop plaques, tangles, or neurodegeneration [408] and removal of *PSEN2* does not affect APP processing in mice [446].

Two major arguments against the ACH are that individuals with substantial amyloid plaque burden can be cognitively normal [447–449], and there are a lack of anti-amyloid therapies showing efficacy against AD in the clinic [450–452]. Amyloid plaque burden can be significantly decreased in humans, but this does not correspond to improved cognition [450,453]. It has recently been suggested that a reason for this lack of translation could be due to the presence of synaptic Aβ oligomers in AD patient brain which precede and lead to raised levels of hyperphosphorylated Tau in early AD [369]. Therefore, anti-amyloid therapies are ineffective once Tau-related pathologies have been initiated since they do not reverse the Tau-related changes. In fact, neurofibrillary Tau tangles correlate better with neurodegeneration than amyloid plaques do [454–456] and the presence of pathological Tau has been shown to precede the appearance of amyloid plaques in cases of sAD [457]. These clinical data show that the presence of amyloid plaques is not sufficient to cause AD and its removal does not improve AD symptoms. Furthermore, inhibition of γ-secretase can worsen AD symptoms [458,459] despite decreasing amyloid production and epidemiology studies suggest that some non-steroidal anti-inflammatory drugs (NSAIDs) decrease AD risk by half [460], placing a role of inflammation as a potential causative factor.

5.4 Proposed causes and pathophysiology of sporadic Alzheimer's disease

Clearly there are more processes involved in AD initiation and progression than altered Aβ isoforms. Aside from the ACH there are many other hypotheses of what triggers AD pathology [461,462]. These include; inflammation[463], age-related mitochondrial dysfunction [464,465]; re-entry of mature neurones into the cell-cycle caused by age-related accumulation in DNA damage [466,467]; decreased and disorganised brain neurovascular and capillary networks [468–470]; metabolic disruption involving glucose hypometabolism and impaired insulin signalling [471–474]; and Tau propagation [475]. A dual hypothesis where an unknown trigger or triggers act upstream of both Aβ and Tau pathology which then converge causing AD, so treatments such as amyloid clearance therapies are insufficient to overcome the triggering signal of pathology [476]. Selective cholinergic neurone degeneration [477], and synapse dysfunction [478] also occur in AD.

A family history of sAD can increase risk of future generations developing it [479], suggesting a role in yet-to-be identified risk factor genes. However, in addition to genetic risk factors, there are many environmental factors that can promote the development of AD. In fact, it is often postulated that a combination of risk alleles and environmental stresses accumulate to precipitate AD pathology and worsen symptoms. Environmental stresses include lifestyles choices such as a lack of exercise [480] and diets causing midlife obesity [481] or hypertension [482]. Indeed a recent randomised controlled trial in patients with subjective cognitive decline (SCD) or mild cognitive impairment (MCI) suggests that following a Mediterranean diet and being physically active can slow cognitive decline [483]. Other environmental factors include; the composition of the gut microbiome [484], toxicity caused by exposure to metal ions or aluminium [487], and insomnia [488].

Physiological disturbances in lipid metabolism [489], calcium homeostasis [490], inflammation [463,491], oxidative stress [474,492], dysfunctional autophagy [493–495], and dysfunctional organelle turnover [7] are also thought to contribute to AD pathology. Clearly there are many contributors to AD and it is important to determine which of these alterations are a cause, consequence, coincidence, or correlation of AD. With AD incidence increasing, it is important for the scientific community understand disease onset and progression and work towards an effective therapy to alleviate symptoms and the associated distress to patients and their families.

5.5 Inefficient translation of drug efficacy in preclinical models to clinical patients and clinical pathophysiology into preclinical models.

The poor translation of anti-dementia drugs from preclinical models to human patients is common; most drugs put forward for clinical trials do not demonstrate efficacy in human patients. Only 5 out of 251 therapies that reached clinical trials have been approved for use in human patients (as published on ALZFORUM September 2020). Of these therapies, none cure or halt disease progression; they slow it down. There are many reasons for this lack of efficacy observed in humans despite positive outcomes in preclinical studies, which are discussed below.

Knowledge from early-onset AD (EOAD), or fAD, was used to generate early transgenic mouse models of AD; by introducing human mutations into mice, scientists aimed to understand the molecular mechanisms of AD precipitation and progression. Whilst providing important information for mechanisms in EOAD, these models may not be so useful for LOAD, where the majority of cases are sporadic in nature. These limitations associated with heavy reliance on overexpression of human genes has been recognised in the field by attempts at generating mouse models where *risk* alleles, such as *APOE-ε4*, were introduced, rather than the *causative* ones. However, whilst mice possessing the *APOE-ε4* alleles develop some pathophysiological phenotypes, including defective cholesterol trafficking, defective Aβ clearance and blood-brain barrier integrity, they do not develop an AD phenotype [370]. Furthermore, TREM2 haploinsufficiency in APP/PS1 overexpressing mice leads to altered microglial responses without affecting plaque burden[496] , prevention of blood-derived myeloid cell brain infiltration associated with ameliorated plaque burden[497], and augmentation of amyloid accumulation as a result of dysfunctional microglial responses . However, these findings are still in the context of APP and PSEN1 overexpressing mice.

Since introduction of known human risk alleles into mice is not sufficient to model AD, additional genetic or environmental factors are required to precipitate disease in preclinical models [370]. Incorporating factors that are more reflective sAD into new preclinical models of AD will involve a shift from studies in rodents with human causative disease-related genes, which tend to be young, male, housed in highly controlled unnatural environments with specific diets, and who are otherwise healthy. Instead, there is a strong case that models should attempt to mimic or incorporate factors thought to contribute to sporadic human cases where patients come from varied backgrounds, with varied lifestyles, and whom often present with other co-morbidities. Such models could include natural ageing, dietary alterations, metabolic disorders, and combinations of these elements with *risk* genes.

Another important consideration for preclinical studies involves the experimental comparisons being made and endpoints measured in the lab and whether they are relevant to the clinical situation. For example, a small rise in Aβ or hyperphosphorylated Tau may occur in sAD and be relevant to the disease state, but small changes are often not considered statistically significant and overlooked in preclinical studies. Assessment of comorbidities, like anxiety, depression, and loss of smell or vision could also be included in rodent models, along with non-cognitive behaviours (like locomotion) to rule out motor phenotypes confounding results of cognitive assays. Onos et al. (2016)[370] also suggest use of multiple mouse strains or genetically diverse strains, such as those which are available through Diversity Outbred or Collaborative Cross, to help filter out strain-specific responses and increase the predictive ability to detect efficacy in preclinical models. There are challenges and disadvantages to incorporating the elements mentioned above; by introducing more than one risk factor, this introduces more variables that could impact on reproducibility of results. However, since over-reliance on human fAD models contributes to lack of clinical efficacy, these changes to models could be what is needed to improve translation of therapies.

5.6 Movement of the field towards using sporadic models: a focus on the D-Galactose model of dietary-induced sporadic Alzheimer's disease

Despite challenges to modelling sAD the field of neurodegeneration understands the limitations of using fAD models in advancing understanding of sAD and there are now many attempt to improve AD models by including risk aspects of sAD [370,408,461]. One such model is the D-Galactose model of dietary-induced sAD. In this model, D-Galactose is administered to rodents who show accelerates signs of ageing and AD-like phenotypes which have been extensively reviewed by Shwe et al., (2018)[125]. Takeda (Cambridge) developed a version of this model which involves feeding wild-type mice a diet high in D-Galactose, a sugar which is naturally present in a wide range of foods [499]. D-Galactose is taken up into brain via glucose transporter 1 (GLUT1) and when consumed in excess can lead to oxidative neuronal stress, inflammation, and apoptosis [125].

D-Galactose is normally metabolised to glucose via the Leloir pathway by an enzyme and cofactor present in mammalian liver and yeast extract [500], later identified as galactokinase, and uridyl transferase (Figure 5.3). The glucose yielded from this pathway can then enter the citric acid cycle and provide NADH for mitochondrial-dependent oxidative phosphorylation

which yields energy in the form of ATP. When the Leloir pathway becomes overrun; for example, when there is an abundance of D-Galactose present, D-Galactose is catabolised by alternative pathways to form galactitol and galactonate products. Elevated levels of galactose alter the cellular redox state through altering activity of enzymes such as aldose reductase (thus depleting NADPH) and glutathione reductase activity (which usually reduces reactive oxygen species like H_2O_2), therefore increasing oxidative damage and elevating advanced glycan end products (AGEs).

5.7 Takeda (Cambridge) demonstrate AD-like pathology in mice after D-Galactose

Work by Dr. Wayne Chadwick at Takeda (Cambridge), as summarised in Table 5.1, shows there are many significant biochemical alterations after D-Galactose administration in the frontal cortex, cortex, hippocampus and cerebellum mouse brain regions. These changes include; increases in oxidative stress, reactive oxygen species, BACE1 protein levels and activity, soluble and insoluble hyperphosphorylated Tau, insoluble Aβ40 and Aβ42 levels and pro-inflammatory cytokines. Interestingly, these altered profiles were specific to the nervous system without any systemic changes being noted; D-Galactose administration did not alter lean or fat body mass percentage, blood LDL or HDL levels, food intake, glucose levels, insulin, WBC count, serum KC GRO, or levels of IL1β or KC GRO in the lung, liver or kidney (data not shown). With the knowledge that similar biochemical disruptions occur in human brain in AD, including increased ROS and accelerated appearance of AGEs (despite some appearance being normal with age), it seems that the mechanisms of D-Galactose metabolism induce similar cellular changes as those which occur in early stages of neurodegeneration.

These biochemical changes were associated with impaired memory as assessed by novel object and novel object location tests (Figure 5.4.a) without any potential confounding impacts caused by locomotion (Figure 5.4.b). These cognitive deficits remain after cessation of D-Galactose administration for up to 1 month (Figure 5.4.c) and can be reversed with three drugs used to ameliorate symptoms of AD clinically – memantinine, donepezil, and levetaracitam (Figure 5.4.d). Together, these data suggest that the D-Galactose model would be a useful preclinical model to better predict efficacy in human patients. The validity of this assay could be further improved by testing drugs which failed to produce a meaningful effect in clinical trials despite showing promising effects preclinically to determine whether this model has better predictive ability than those currently used.

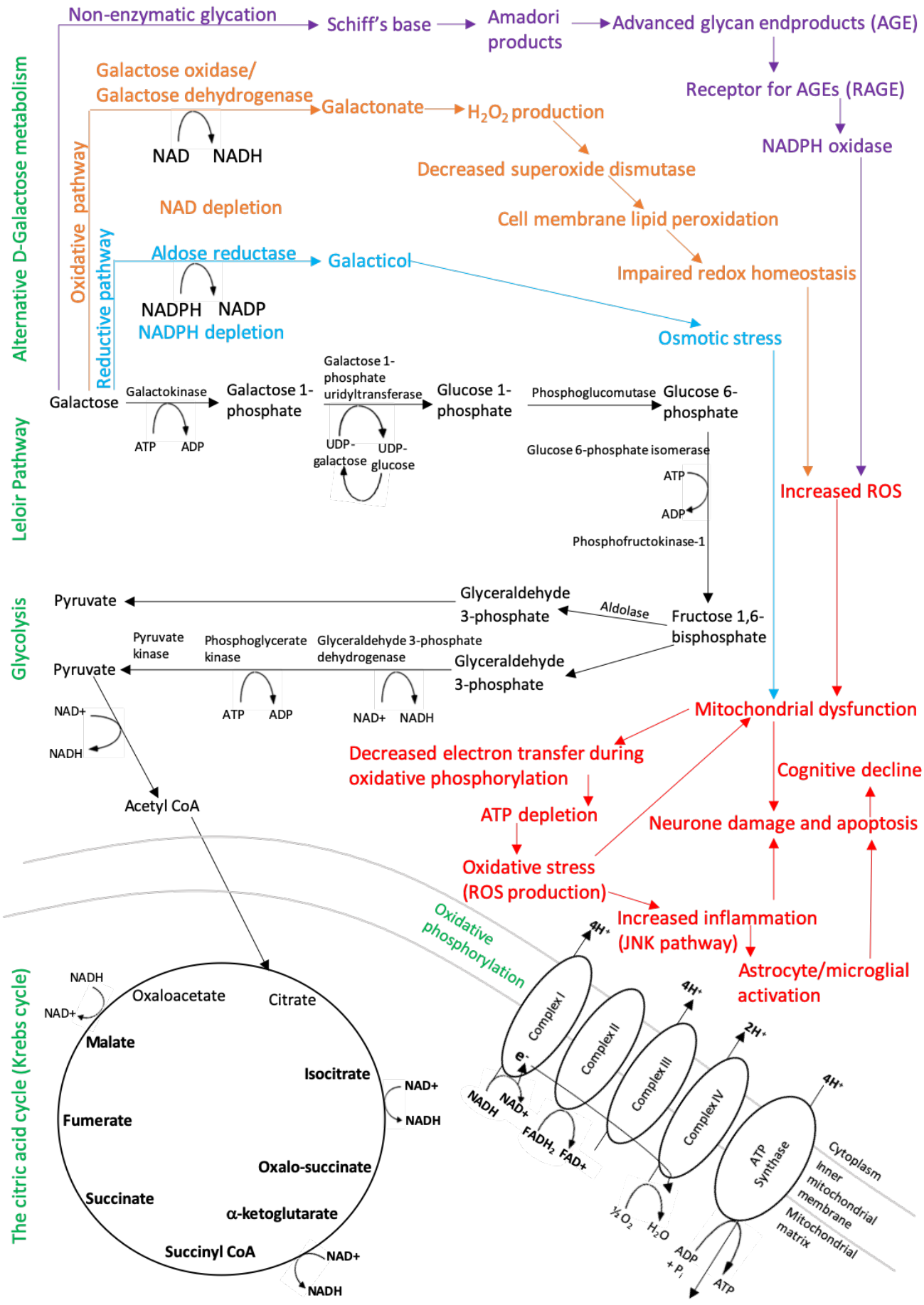

Figure 5.3: D-Galactose metabolism pathways and how activation of alternative metabolism pathways leads to cell stress and neuronal death associated with cognitive decline. The pathways in black are the main galactose metabolism pathway, but when this becomes saturated, alternative pathways (in blue, orange, and purple) become active leading to pathological changes (in red). Compiled with information from Shwe et al., (2018) and Bo-Htay et al., (2018)

Table 5.1: Summary of D-Galactose-induced biochemical alterations observed at (Takeda Cambridge)

Molecular measures	Difference between vehicle and D-Galactose-treated mice in: Cortex	Frontal Cortex	Hippocampus	Cerebellum
Soluble Aβ40	↑ (*)	–	–	–
Soluble Aβ42	↑ (*)	–	↑ (*)	–
Insoluble Aβ40	↑ (*)	↑ (**)	↑ (**)	↑ (**)
Insoluble Aβ42	↑ (*)	↑ (**)	↑ (**)	↑ (**)
Soluble pTau	↑ (ns)	↑ (*)	↑ (*)	–
Insoluble pTau	↑ (*)	↑ (*)	↑ (**)	↑ (**)
Oxidative stress (protein carbonyls)	↑ (*)	↑ (*)	↑ (**)	–
Soluble advance glycan end products (AGE)	↑ (**)	↑ (*)	–	↑ (**)
Insoluble advance glycan end products (AGE)	↑ (p=0.6)	–	↑ (**)	–
BACE1 activity	↑ (**)	↑ (*)	↑ (*)	–
BACE1 protein levels	–	↑ (*)	↑ (*)	–
TNFα	↑ (**)	↑ (*)	–	–
IL6	↑ (**)	↑ (**)	–	–
IFNγ	↑ (**)	↑ (*)	–	–
IL10	↑ (**)	–	–	–
IL12p70	↑ (**)	↑ (*)	–	–
IL1β	↑ (**)	↑ (**)	–	–
KC GRO	↑ (**)	↑ (*)	–	–
ATP	–	–	↓(*)	↓(*)
Complex I activity	↑ (**)	–	↑ (**)	↑ (**)
Complex IV activity	–	↓(*)	↓(*)	↓(**)

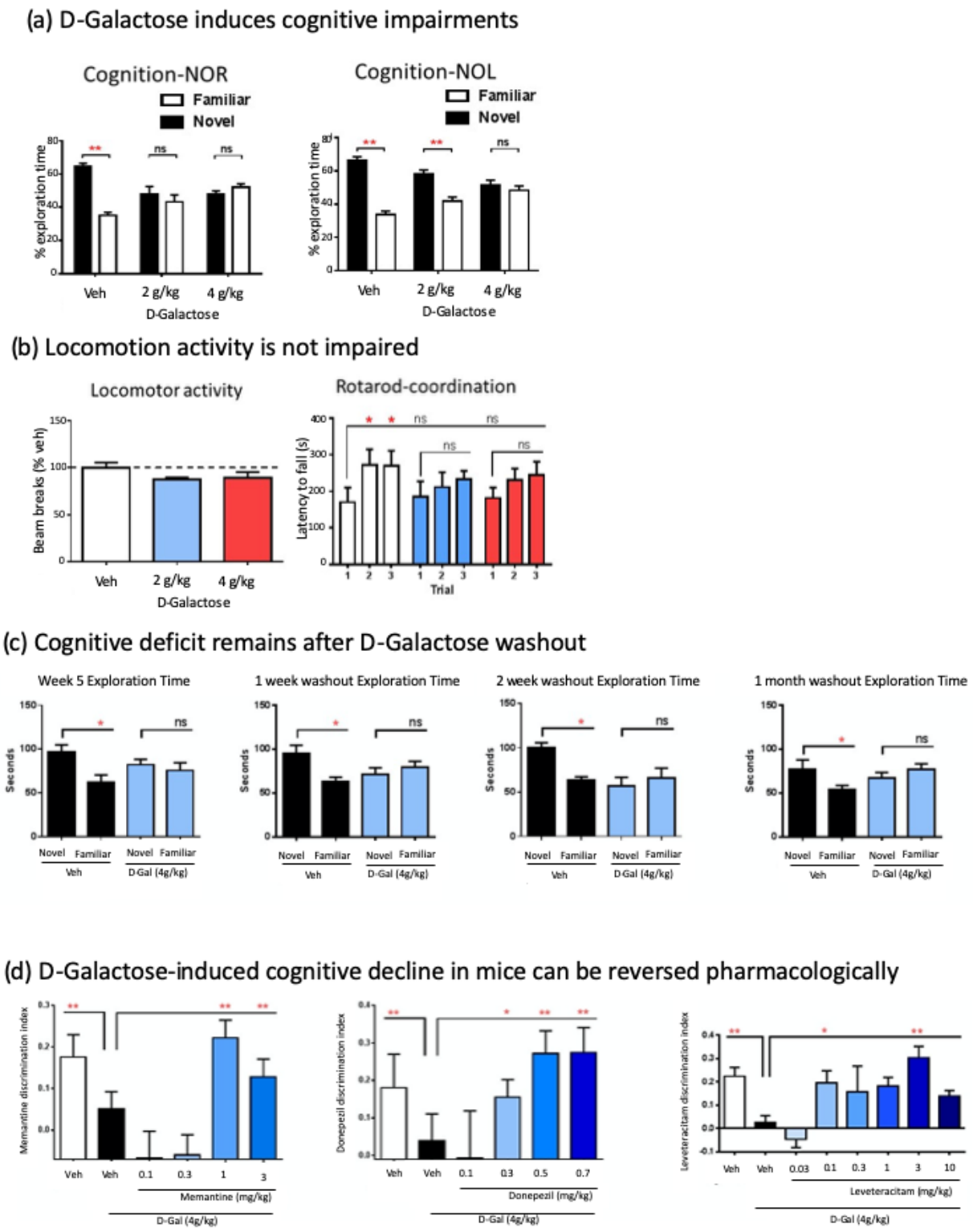

Figure 5.4: Data from Takeda (Cambridge) showing that in mice treated with 4 g/kg D-Galactose, there was no difference spent exploring novel objects/novel object location in contrast to vehicle-treated mice who spent significantly more time spent exploring novel objects/location indicating a memory deficit (a). There were no confounding effects of D-Galactose on motor abilities as there was no impairment in locomotor activity or Rotarod assays (b). These cognitive deficits are long-lasting and persist even after D-Galactose washout when up to 4 weeks after removal of D-Galactose from drinking water (c). However, the deficits were reversed pharmacologically by administration of memantinine, donepezil, and levetaracitan (d).

5.8 Programmed axon degeneration in Alzheimer's disease

Previously, the Coleman group searched for phenotypic evidence that programmed axon degeneration is involved in fAD pathology using the CRND8 mouse model. However, axons of layer V pyramidal neurones remained intact and connected to viable somas despite looking severely dystrophic [396]. There was no neurodegenerative phenotype, as is the case with many mouse models of neurodegeneration. Nevertheless, CRND8 axons displayed axonal swellings and impaired transport of mitochondria[396]. Furthermore, layer V pyramidal neurones of CRND8 mice overexpressing mutant APP show accumulation of mitochondria, APP, and synaptophysin in axonal swellings [396], which occur prior to hallmarks of neurodegeneration[501] (Stokin et al., 2005). Axons post-swelling containing accumulated particles remain intact, but there is synaptic disruption of varying degrees ranging from decreased numbers of synaptic vesicles through to electron dense regions of swollen organelles with no visible synaptic vesicles[396]. This could implicate axonal transport impairments in disease mechanism. Indeed, blocking axonal transport would theoretically lead to depletion of mitochondria, peroxisomes, synaptic vesicle precursors, and other proteins important in axon and synapse maintenance and function. This would likely decrease energy production, increase oxidative stress, lead to dysfunctional synapses, and accumulation of materials at the cell body destined for the axon or synapse [378].

Transgenic models of fAD have also suggested a role of axonal survival factor NMNAT2 in AD pathology. *Nmnat2* mRNA levels are downregulated in forebrain of the rTg4510 mouse model of FTD-related tauopathy[119] and cerebral cortex and hippocampus of APP overexpressing mice [118]. Decreased levels of NMNAT2 are associated with increased levels of hyperphosphorylated Tau species (pT205, pT231, and pS262) and protein phosphatase 2 (PP2A) in its phosphorylated inactive form (pY307-PP2A) [118]. PP2A in its dephosphorylated active state is required for Tau dephosphorylation and homeostasis [502].

AAV-mediated overexpression of NMNAT2 decreases levels of hyperphosphorylated Tau in the hippocampi of rTg4510 mice[119]. Conversely, *Nmnat2 siRNA* knockdown in HEK293/tau cultures increases pY307-PP2A, thereby decreasing PP2A activity which leads to increased levels of hyperphosphorylated Tau[118]. Moreover, a reciprocal effect has also been demonstrated whereby hyperphosphorylated Tau can lower *Nmnat2* gene expression via decreased pCREB occupancy at the two CRE sites in the *Nmnat2* promotor in cortex and hippocampus of rTg410 mice[119]. Furthermore, a role of NMNAT2 as a chaperone protein involved in decreasing levels of misfolded hyperphosphorylated Tau has also been proposed.

NMNAT2 has been shown to form a complex with HSP90 in rTg4510 mouse in aged hippocampus and cortex and this NMNAT2:HSP90 complexes with hyperphosphorylated Tau in insoluble cortex fraction[116]. The NAD-synthesis activity of NMNAT2 is separate from its chaperone foldase activity, the latter being indispensable for decreasing hyperphosphorylated Tau levels. Foldase activity is required for the formation of the NMNAT2:HSP90 complex, and NMNAT2 ATPase activity becomes active upon formation of the complex.

Furthermore, axon transport of NMNAT2 declines with age [503], which likely decreases levels of NMNAT2 in distal axons. Decreased levels of NMNAT2 leave axons vulnerable to age- and neurotoxic stresses [110], and depletion triggers programmed axon degeneration [76]. Therefore, a combination of natural decline in NMNAT2 transport with age and disease-related impeded axon transport could contribute to development or progression of sAD, particularly in humans with *LoF NMNAT2* mutations or lower-than-average expression levels.

Decreased axon transport would theoretically also lead to depletion of mitochondria, peroxisomes, synaptic vesicle precursors, and other proteins important in axon and synapse maintenance and function. This would decrease energy production, increase oxidative stress, lead to dysfunctional synapses, and accumulation of materials in the soma destined for the axon or synapse [378]. Whether impaired axonal transport is a cause, facilitating factor, or consequence of disease is still debated[378], since environmental stresses like oxidative or osmotic stress, can impede axonal transport so it is possible that increased ROS seen in AD patients can cause or worsen axonal transport mechanisms, rather than axon transport decreasing supply of factors to maintain healthy synapses.

The speculative pathways through which NMNAT2-dependent mechanisms may influence Tau phosphorylation levels are combined and shown in Figure 5.5. Taken together, these findings suggest that NMNAT2 could decrease hyperphosphorylated Tau levels via modulating activity of PP2A, as well as by acting in concert with HSP90 as a chaperone protein to refold hyperphosphorylated Tau thereby promoting healthy Tau species and reducing risk of neurodegenerative diseases involving tauopathies. If levels of hyperphosphorylated Tau become favoured over other Tau species, decreased occupancy of pCREB on the promotor of *Nmnat2* could have multiple impacts on neuronal health by removing the proposed mechanisms to keep pTau<Tau, as well as decreasing the NAD^+ synthesis capacity via NMNAT2 action in the axon. Furthermore, axon transport of mitochondria and NMNAT2 decline with age, thereby increasing neuronal susceptibility to degeneration through multiple channels.

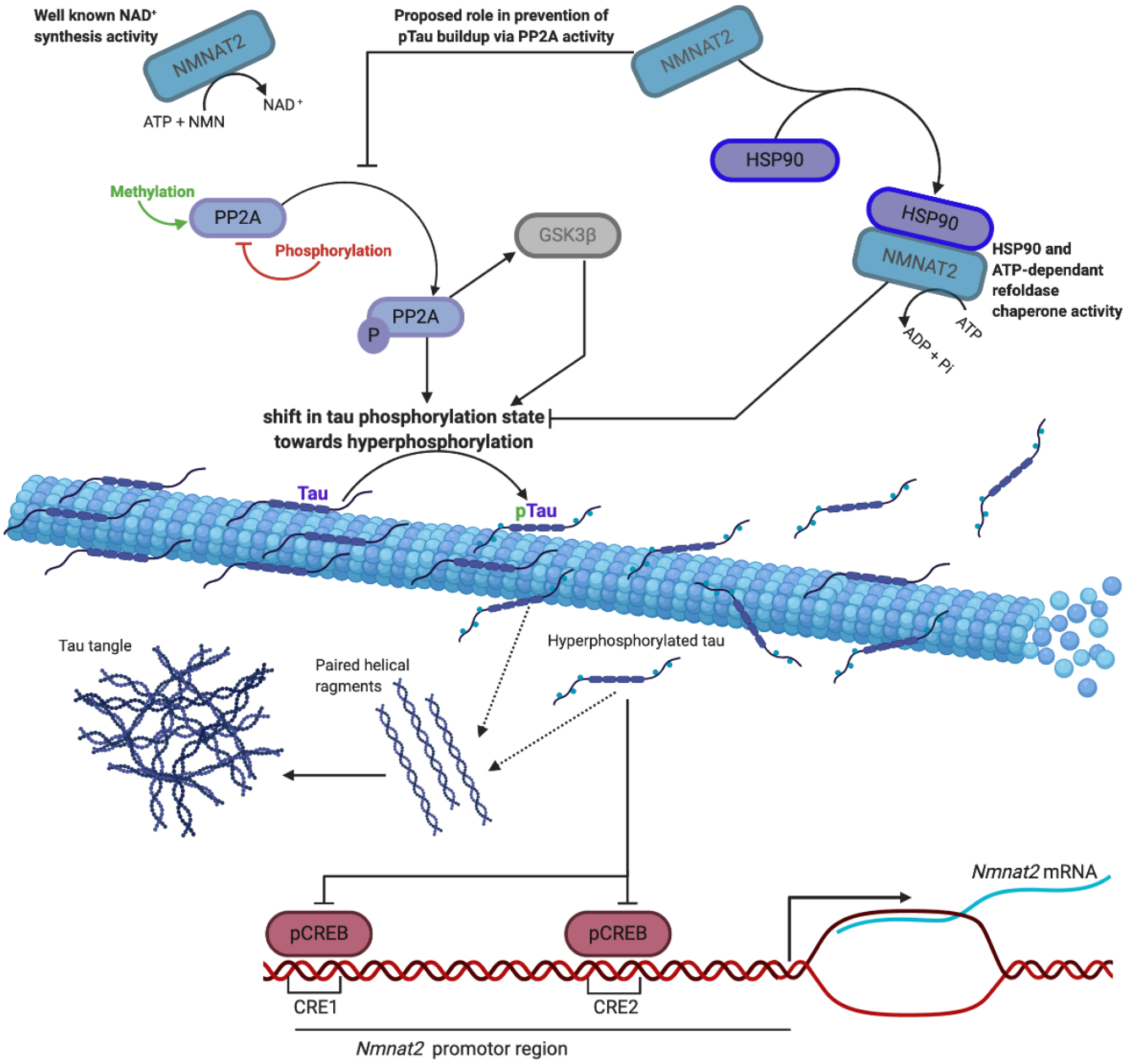

Figure 5.5: Proposed mechanisms by which NMNAT2 prevents hyperphosphorylated Tau accumulation and how hyperphosphorylated Tau decreases NMNAT2 levels in models of fAD. Compiled from studies by Ali et al., (2010), Ljungberg et al (2012), and Cheng et al., (2013). pTau indicates hyperphosphorylated Tau.

However, since fAD only represents up to 6% of human AD cases and there are questions regarding the cross over between disease mechanisms in fAD and sAD, these speculations need to be explored in models with relevance to sAD. If *APP* or *PSEN* mutations do not drive Aβ accumulation or trigger AD pathology in sporadic cases, there remains a question over what does. With this in mind, it is still possible that programmed axon degeneration is involved in sporadic cases, meaning it is important to test in the context of sporadic models.

The aim of this chapter is to determine whether axon transport of NMNAT2 and/or mitochondria is impaired in the D-Galactose dietary-induced model of sAD and whether there is axon degeneration in the cortex of this model. This would be relevant to whether impaired transport could explain a link between the biochemical and behavioural changes observed by Takeda (Cambridge) at the cellular level.

5.9 Results

5.9.1 Blood glucose levels and body weight are unaffected by D-Galactose

Takeda (Cambridge) noted that all changes in D-Galactose-treated mice were in the nervous system, with no changes in inflammatory markers seen. This includes no abnormal weight gain or increase in blood glucose levels for the duration of the study. It was confirmed during this experiment, that neither the weight nor the blood glucose levels of D-Galactose-treated mice were different from the sodium benzoate (vehicle)-treated ones (Figure 5.6.a-b).

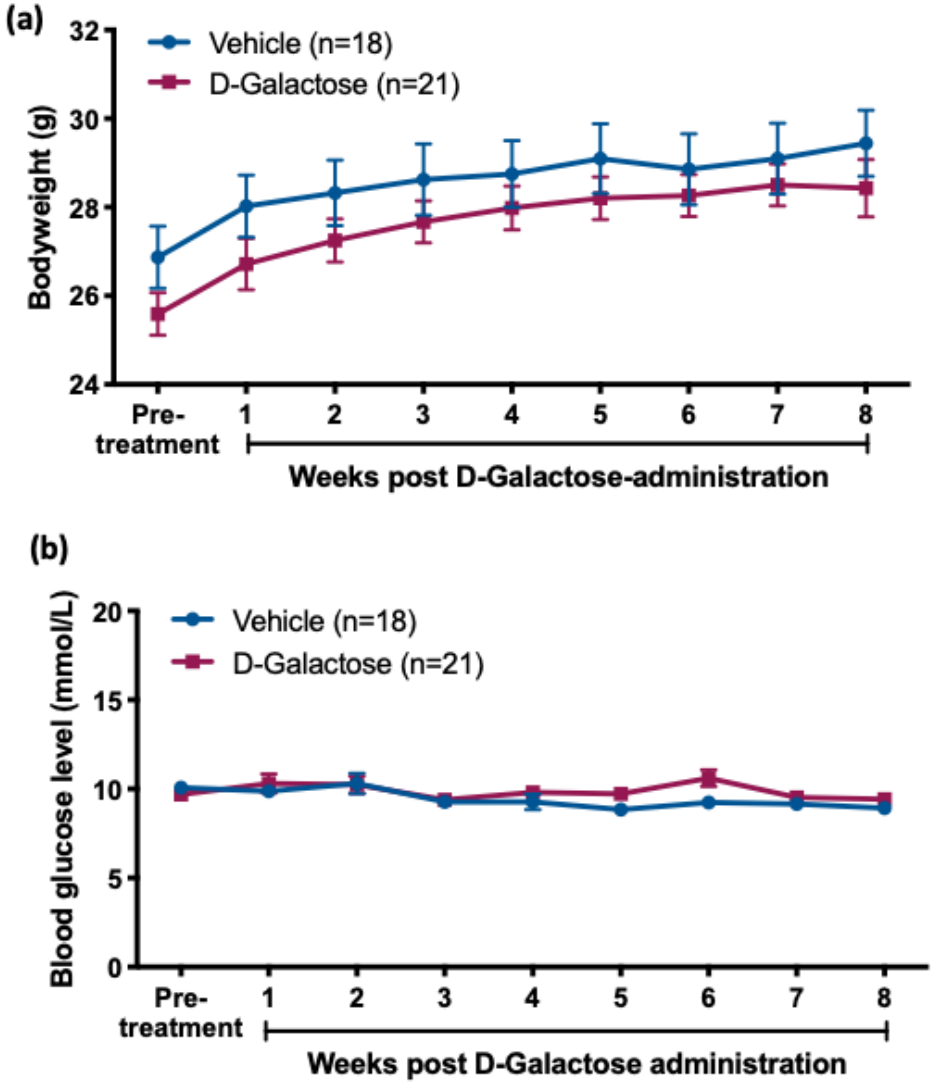

Figure 5.6: Neither blood glucose levels (a) nor bodyweight (b) are affected by administration of D-Galactose compared to sodium benzoate (vehicle) administration across the 8-week timeframe. Each data point was collected from an individual mouse across the duration of the experiment. A two-way repeated measures ANOVA was employed to determine significance. Data are presented as mean±SEM

5.9.2 Axon transport of CFP-labelled mitochondria is unaffected by D-Galactose

When comparing vehicle-treated and D-Galactose-treated mice, there was also no difference in the number of CFP-labelled mitochondria being transported anterogradely (Figure 5.7.a) or retrogradely (Figure 5.7.b) in the sciatic nerve. Furthermore, D-Galactose treatment did not alter the average or maximum particle velocity in either the anterograde (Figure 5.7.c) or retrograde (Figure 5.7.d) direction. It seems that, despite axonal transport of mitochondria being altered as mice age [503], treatment with D-Galactose (thought to accelerate ageing processes) does not alter axonal transport of mitochondria in the mouse sciatic nerve.

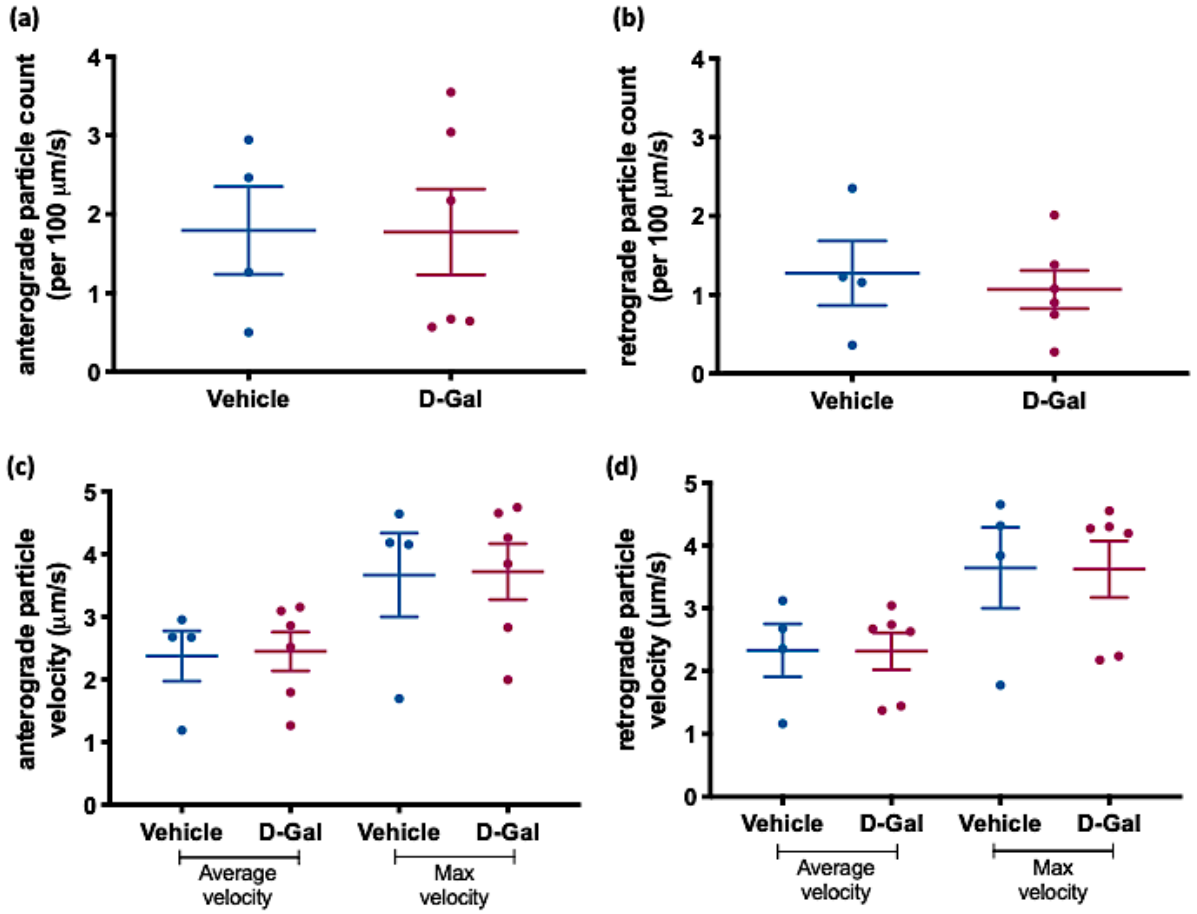

Figure 5.7: Axonal transport of CFP-labelled mitochondria in sciatic nerves is not altered after mice receive D-Galactose drink for 8 weeks. Compared to vehicle-treated animals, the anterograde (a) and retrograde (b) particle counts and velocity of anterograde (c) and retrograde (d) mitochondrial transport is not affected by D-Galactose treatment. Each data point represents the average transport in all axons across 5 fields of view for an individual mouse sciatic nerve. A two-tailed unpaired t-test was performed to determine whether there was a difference between vehicle- and D-Galactose-treated mice. Data are presented as mean±SEM

5.9.3 Axon transport of YFP-labelled NMNAT2 is unaffected by D-Galactose

Similarly, there were no differences in axonal transport of YFP-labelled NMNAT2 when anterograde and retrograde particle count (Figure 5.8.a-b) or average and maximum velocity (Figure 5.8.c-d) were assessed, despite declines in axonal transport of NMNAT2 being reported in aged mice [503]. Observations thus far were made in the peripheral nervous system. However, it is the central nervous system that is of interest and relevance to the Alzheimer's-like pathologies noted by Takeda (Cambridge). Thus, transport of NMNAT2 vesicles in the fimbria was also assessed (Figure 5.9).As in the peripheral axons, D-Galactose treatment did not alter YFP-labelled particle count (Figure 5.9.a) or particle movement (Figure 5.9.b).

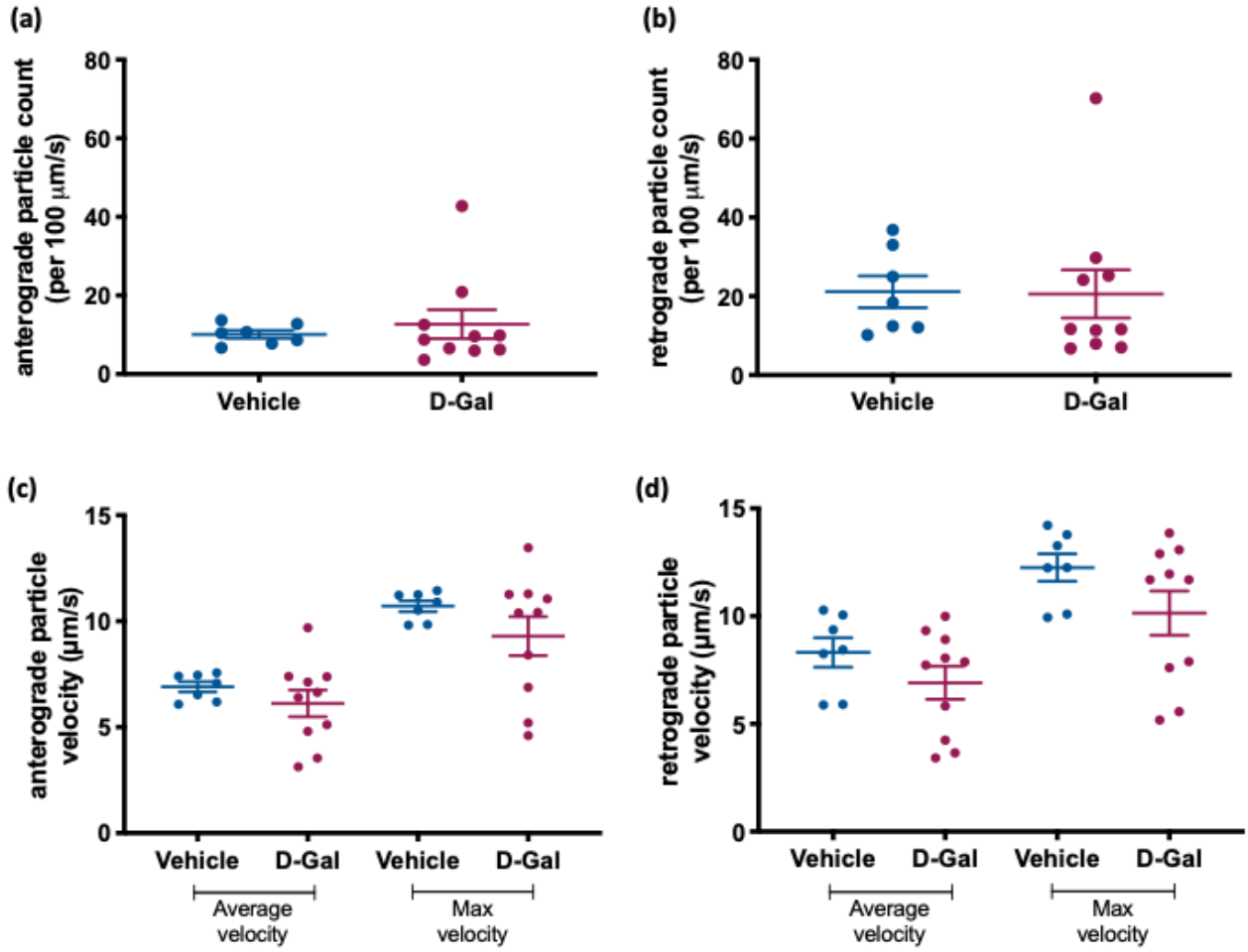

Figure 5.8: Axonal transport of YFP-labelled NMNAT2 vesicles in sciatic nerves is not altered after mice receive D-Galactose drink for 8 weeks. Compared to vehicle-treated animals, the anterograde (a) and retrograde (b) particle counts and velocity of anterograde (c) and retrograde (d) transport of NMNAT2 vesicles is not affected by D-Galactose treatment. Each data point represents the average transport in all axons across 5 fields of view for an individual mouse sciatic nerve. A two-tailed unpaired t-test was performed to determine whether there was a difference between vehicle- and D-Galactose-treated mice. Data are presented as mean±SEM

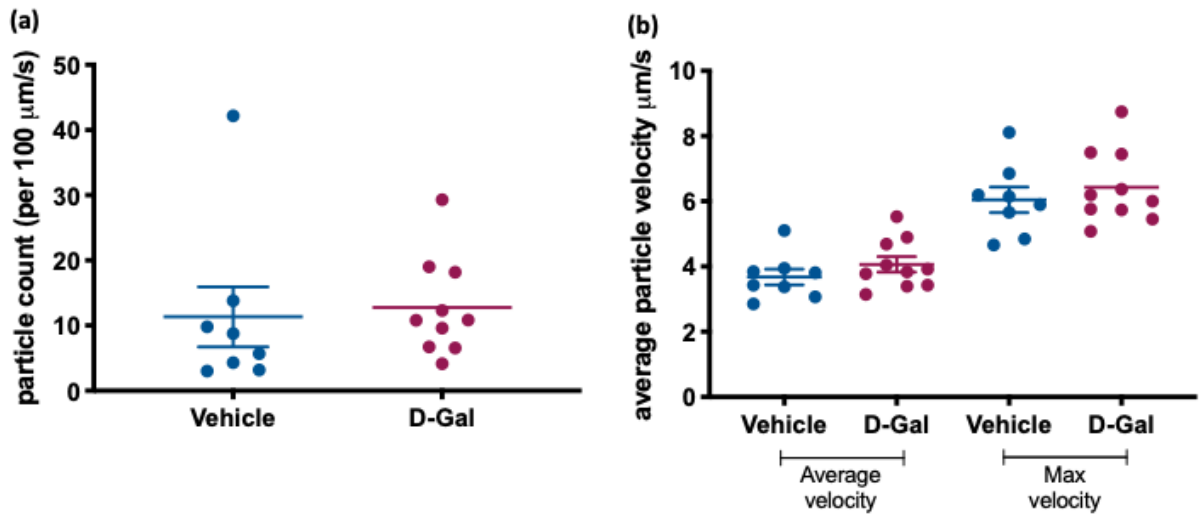

Figure 5.9: Axonal transport of YFP-labelled NMNAT2 vesicles in fimbria is not altered after mice receive D-Galactose drink for 8 weeks. Compared to vehicle-treated animals, the average anterograde + retrograde particle count (a) and anterograde + retrograde velocity (b) of NMNAT2 vesicle transport is not affected by D-Galactose treatment. It is not possible to distinguish between anterograde and retrograde transport in the fimbria due to the variety of neurone orientations present; therefore, combined particle counts and vesicle velocity were used. Each data point represents the average transport in all axons across 5 fields of view for an individual mouse fimbria. A two-tailed unpaired t-test was performed to determine whether there was a difference between vehicle- and D-Galactose-treated mice. Data are presented as mean±SEM

5.9.4 D-Galactose does not increase hyperphosphorylated Tau in any brain region

Before concluding that D-Galactose-treatment does not induce changes in axonal transport, it was important to confirm that the biochemical changes seen by Takeda (Cambridge) occurred in the brains of mice used in the present study. Therefore, a Meso-Scale Discovery (MSD) assay was used to check for levels of insoluble hyperphosphorylated Tau (Figure 5.10.a) and Western blot for levels soluble hyperphosphorylated Tau in the hippocampus (Figure 5.10b), in order to confirm that the percentage change observed by Takeda (Cambridge) (Figure 5.10.c) was also apparent in the present cohort of mice whose nerves and fimbria were taken for *ex vivo* axonal transport imaging. However, there were no significant increases in insoluble or soluble hyperphosphorylated Tau observed in the present cohort of mice. Hippocampus was selected for Western Blot analysis since that is the brain region where the most significant change was expected based on the data provided by Takeda (Cambridge).

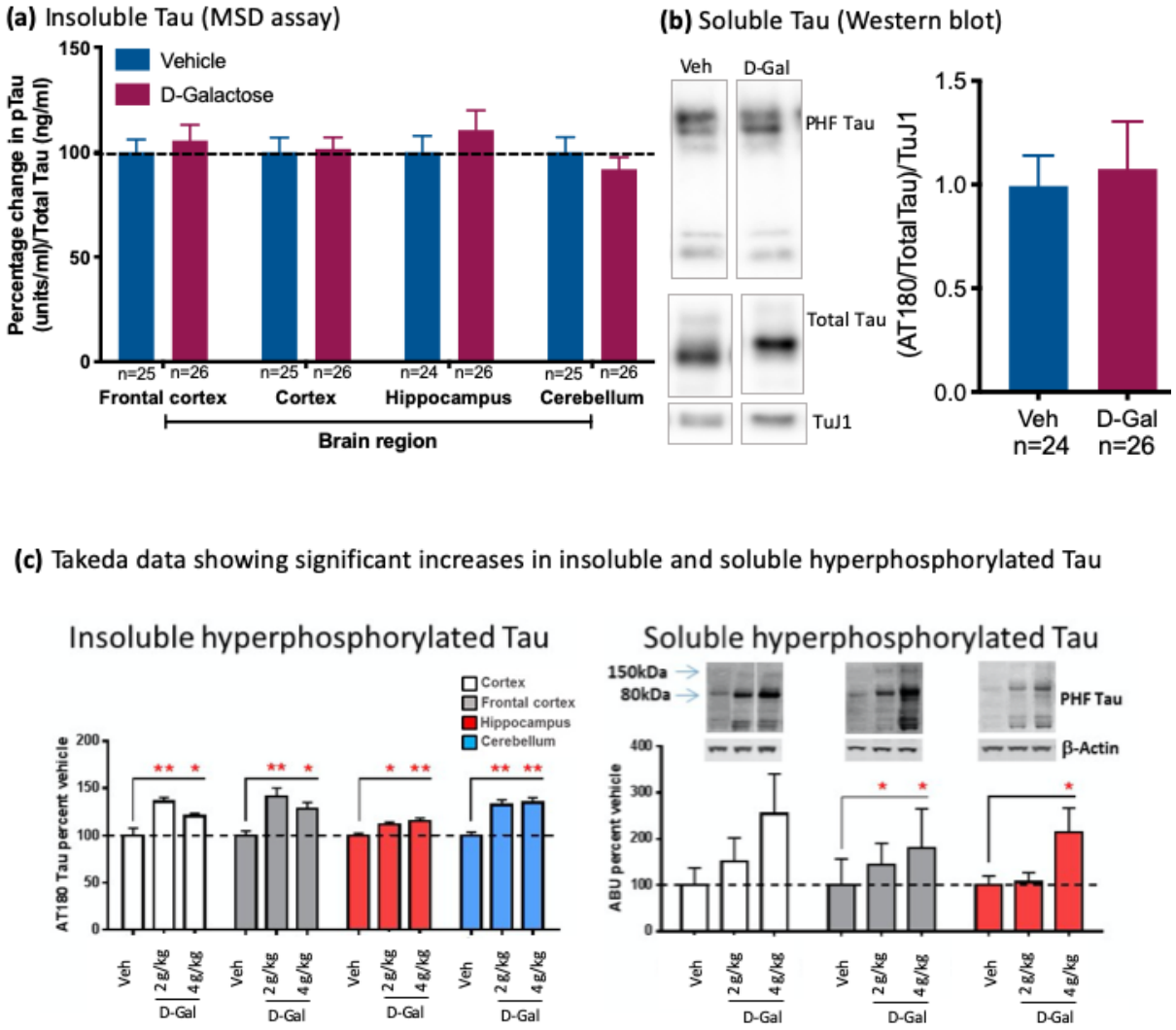

Figure 5.10: D-Galactose administration for 8 weeks does not significantly increase hyperphosphorylated Tau in any brain region compared to sodium benzoate (vehicle) administration when measure via Meso Scale Discovery ELISA (a) or Western blot (b). This is in contrast to a significant increase seen in all four brain regions noted after both 2 g/kg and 4 g/kg D-Galactose administered at an Industrial Partner site, Takeda (Cambridge) (c-d). Each data point represents values from an individual mouse (for MSD values, three technical replicates were made per mouse, per brain region and an average value used). A two-way ANOVA (a) or unpaired t-test (b) was performed to determine whether there were significant differences. Data are presented as mean±SEM

Taken together, the data presented in Figures 5.6-5.10 indicate that 4 g/kg D-Galactose administered through drinking water does not induce any significant changes in axonal transport of mitochondria or NMNAT2 in the central or peripheral nervous system and that the pathomolecular changes noted in our industrial partner's C57BL/6 mice were not translatable to our cohorts of MitoP and *Nmnat2*-venus mice, which express CFP-labelled mitochondria and YFP-labelled NMNAT2, respectively.

5.9.5 Aβ42:Aβ40 ratio is decreased in OHSCs after D-Galactose administration

Aside from the *in vivo* studies that show molecular and behavioural changes induced by D-Galactose, *in vitro* administration can induce senescence in cultured cortical astrocytes [504]. Putting together this and the positive inflammatory profile observed by Takeda (Cambridge), the direct effects of D-Galactose on organotypic hippocampal slice cultures (OHSCs) were assessed. Claire Durrant provided mouse organotypic hippocampal slice cultures which Olivia Sheppard administered 55 μM D-Galactose or vehicle (MEM) to so I could collect samples and run analysis to see if there were any changes observed in this system. Application of 55 μM D-Galactose in culture medium decreased release of Aβ40 and Aβ42 from slices into the culture medium (Figure 5.11.a-b) after 1, 2, and 3 weeks of D-Galactose application. The ratio of Aβ42:Aβ40 is also decreased in D-Galactose-treated slices after 1, 2, and 3 weeks of application (Figure 5.11.c).

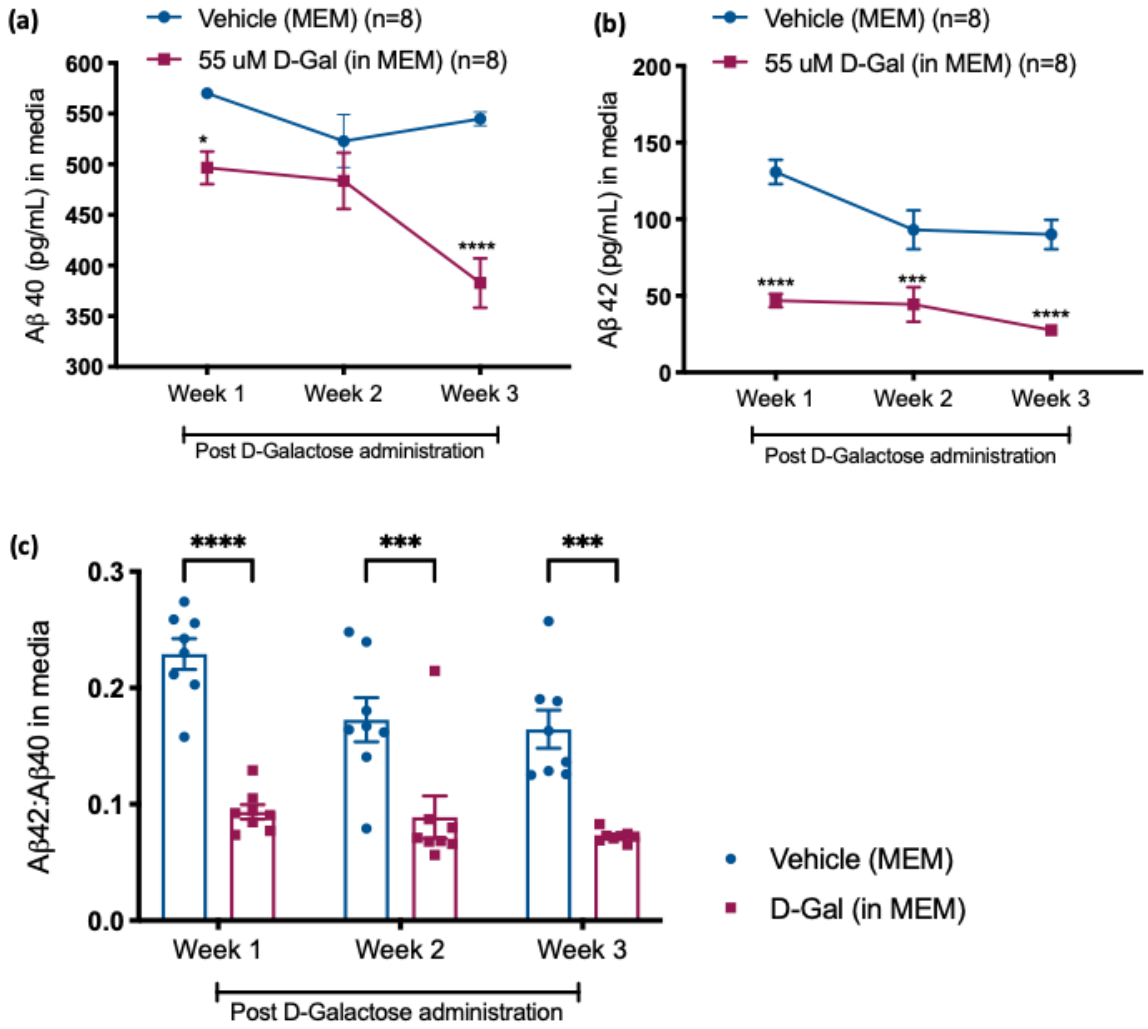

Figure 5.11: ELISA measurements showed a significant decrease in levels of both Aβ40 (a) and Aβ42 (b) secreted into the media after the first, second and third week of D-Galactose administration in comparison to that secreted by pup-matched vehicle-treated slices. The ratio of Aβ42:Aβ40 is decreased (d) at all timepoints in the D-Galactose-treated slices. Week 1 of treatment corresponds to week 3 of culture; week2 to week 4, and week 3 to week 5. Each data point represents values from three co-cultures slices from an individual mouse. A two-way repeated measures ANOVA followed by Bonferroni post-hoc analysis was performed to determine whether there was a significant difference. Data are presented as mean±SEM

5.9.6 No synaptic deficits were detected in OHSCs after D-Galactose administration

To explore whether the decrease of Aβ40 and Aβ42 into the media was associated with an increase in Aβ accumulation in the slices or synaptic deficits, immunohistochemistry (data not shown) and Western blots were performed. One problem with using non-transgenic models of Alzheimer's disease is the low expression level of Aβ peptides. This makes it unlikely to be able to visualise Aβ in wild-type tissue and even if this was possible, it is not yet possible to distinguish between the different isoforms. Therefore, it wasn't possible to detect any difference in Aβ accumulation through immunohistochemistry (data not shown). Currently, there is not a reliable antibody to detect changes in Aβ40/Aβ42 levels through Western blot, so it wasn't possible to check Aβ levels using this method either. However, there is a highly specific antibody against APP, the precursor to Aβ peptides. Therefore, if there was an increase in expression of Aβ proteins, this would likely be caused by an increase in expression of APP. However, there are no detectable differences in protein levels of amyloid precursor protein (APP) observed by Western blot (Figure 5.12.a-b), nor are there changes in presynaptic protein synaptophysin (Figure 5.12.c), or postsynaptic protein PSD95 (5.12.d) after D-Galactose application compared to vehicle-treated slices from the same mouse. Decreases in housekeeper genes were consistently seen in D-Galactose-treated slices compared to mouse-matched vehicle-treated ones (Figure 5.12.e-g). The possibility that application of D-Galactose was killing cells in the slices was then considered as an explanation for the significantly decreased levels of Aβ40 and Aβ42 being secreted into the media of slices treated with D-Galactose, in contrast to the hypothesis that D-galactose was causing Aβ to accumulate in the slices. Due to the abundance of negative data, this line of enquiry was not pursued.

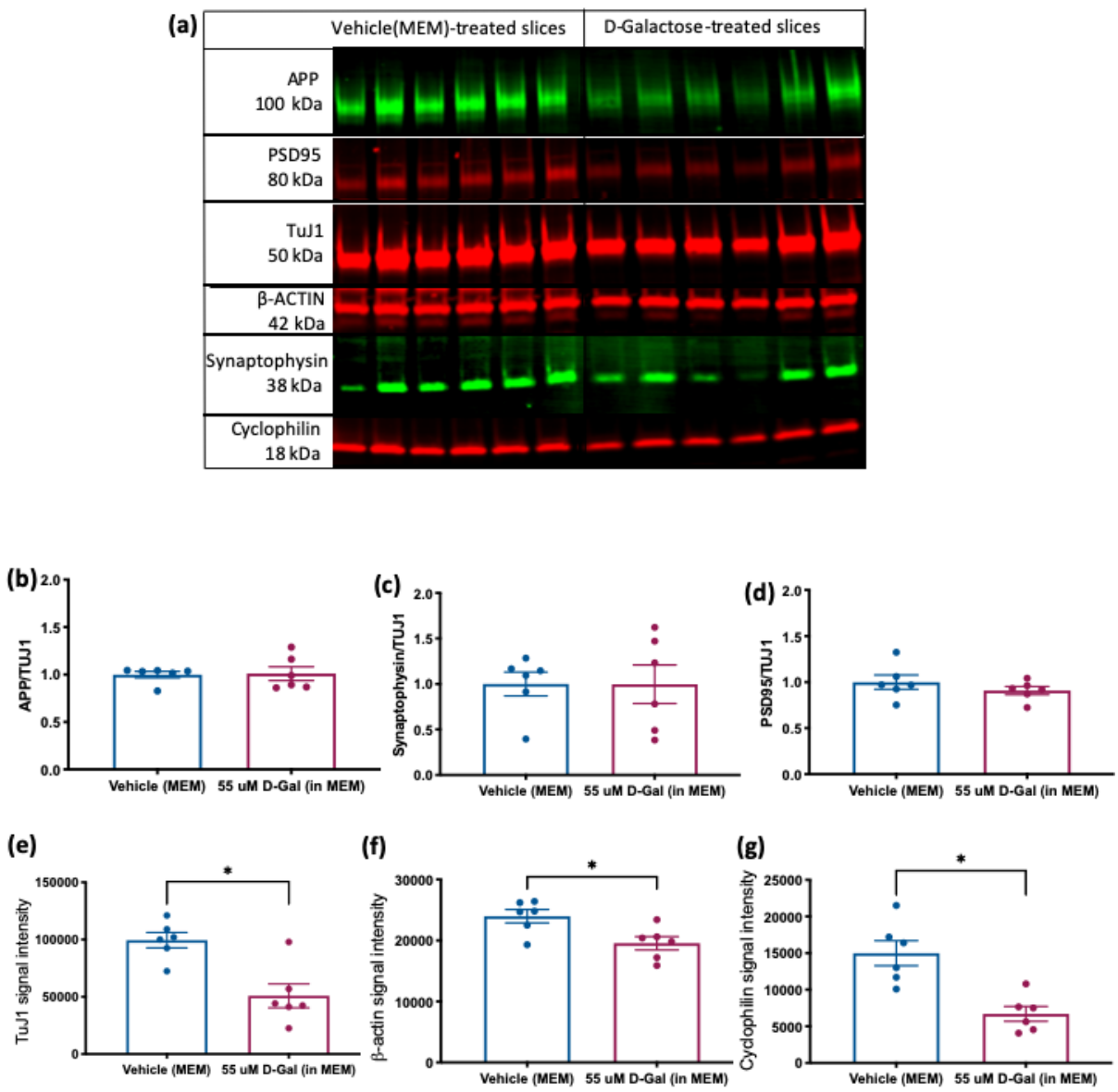

Figure 5.12: Western blot analysis (a) show that there is no difference in APP (b), PSD95 (c) or Synaptophysin (d) protein levels after 3-week D-Galactose treatment in comparison to pup-matched vehicle-treated slices. All housekeeper proteins (e-g) were consistently significantly downregulated after D-Galactose treatment in comparison to mouse-matched vehicle-treated slices. Each data point represents values from three co-cultures slices from an individual mouse. Paired t-tests were employed to assess whether there was a difference between vehicle- and D-Galactose-treated mice. Data are presented as mean±SEM

5.10 Discussion

5.10.1 The *in vivo* D-Galactose model

The results from this chapter show that administering D-Galactose in drinking water does not induce any significant changes in mouse bodyweight, blood glucose levels, axonal transport of mitochondria in sciatic nerve, or axonal transport of NMNAT2 in sciatic nerve or fimbria. Furthermore, there were no increases in insoluble hyperphosphorylated Tau in any brain region nor soluble phosphorylated Tau in hippocampus in contrast to results seen by the Industrial Collaborators to this project. Whilst application of 55 μM D-Galactose to OHSCs caused a decrease in secretion of Aβ40 and Aβ42, as well as ratio of Aβ42:Aβ40 into the media, this was not related to any increase in APP in slice tissue or a decrease in pre- or post-synaptic proteins Synaptophysin or PSD-95, respectively. Thus, these changes in slice cultures likely reflect D-Galactose-induced death of cultures, rather than a useful *in vitro* model of sAD.

Based on this study, D-Galactose administered in drinking water is not a reliable model of dietary-induced Alzheimer's disease. Indeed, meta-analysis showed heterogeneity in reported effects of the D-Galactose model[505]. Whilst the Industrial Collaborators saw clear differences in molecular hallmarks of early AD pathogenesis after D-Galactose administration, this was not reproducible in the present study, suggesting this model may not be suitable – or needs to be optimised further if it holds any promise – for use in finding clinically useful anti-dementing drugs. Since none of the cohorts of mice used in the present study developed any signs of AD, the complete lack of axonal transport changes in NMNAT2 or mitochondria does not provide any insight into whether these axonal transport cargoes are affected in sAD. There are many reasons why the inconsistencies between results from Takeda (Cambridge) and those presented here may exist, and these will be discussed below.

The mice used in the present study were different strains with slight differences in background to those used by Takeda (Cambridge) for the initial experiments. It is possible – no matter how unlikely – that the Takeda (Cambridge) C57BL/6 line has mutations in genes affecting risk/susceptibility to developing sAD or that the insertion of fluorescent proteins into the mice used in this study can decrease susceptibility to environmental risk factors of sAD development. Indeed, the YFP-tagged NMNAT2 transgenic mice used here to assess axonal transport of NMNAT2 show robust protection after *in vivo* transection of the sciatic nerve[171], demonstrating a clear protective effect against programmed axon degeneration in these mice. This is likely due to the overexpression and stabilisation of NMNAT2, thus having a similar protective effect as introducing the WLD^S protein. Whilst the specific effects of CFP-tagged

mitochondria on the rate of programmed axon degeneration haven't been demonstrated, it cannot be ruled out that a similar phenotype may be seen in these mice. If the rate of programmed axon degeneration after *in vivo* nerve transection is delayed in these mice, it could suggest that, whilst these mice are useful in seeing real-time transport of NMNAT2 and mitochondria, their effectiveness in studying links between programmed axon degeneration in disease models could be confounded. In hindsight, it would have been useful to include a non-transgenic C57BL/6 mouse strain to first confirm that the Takeda (Cambridge) model was translatable to the environment and mice used at the Babraham Institute in the present study. This was considered at the beginning of experiment; however, with regulations surrounding minimal use of animals in UK research, this additional group was ultimately not included. In contrast to neuroprotection in the *Nmnat2*-venus mice, there are accelerated axonal deficits in homozygous YFP-H labelled neurones[506], suggesting that high levels of fluorescent markers can have deleterious effects on axon health. Given that axons show accelerated ageing in YFP-H mice, perhaps the presence of fluorescent markers increase basal levels of inflammatory markers which are not further increased by feeding mice D-Galactose. Since there is increased susceptibility of axonal damage in YFP-H mice[506], but there were no AD-related biochemical changes, it is likely that there are other explanations for the lack of phenotype in this dietary model of sAD.

Another explanation could be that there was a difference in how the water was provided between the two Institutes; at Takeda (Cambridge), plastic drip feeders were used whereas at Babraham, water was placed into plastic pouches since mice are normally fed via a centralised system that provides water to all cages eliminating the use of standard drip feeders. One possibility could be that D-Galactose binds to the pouches thereby reducing the effective concentration in solution. This could be assessed via measuring D-Galactose concentration immediately after preparation as well as from undisturbed water bags. It is possible that D-Galactose sedimented in the water bag. This would not be a problem when using drip feeders since the water is released directly below where it is stored so if the D-Galactose did sediment, it would be collected in the water as it passed through to the mouse. However, this would not happen in the water bags since most of the surface is flat against the cage lid providing a larger surface area over which D-Galactose could sediment and water would not pass through this as the mouse drinks from the delivery site. Furthermore, the pouches of water containing D-Galactose or vehicle were replaced every two days to prevent the possibility that D-Galactose would sediment or break down in the water thereby reducing the amount consumed.

To confirm delivery of D-Galactose, there are a number of methods that could have been explored: D-Galactose levels could have been measured from the blood of mice. Blood glucose levels are easily measured with a tiny drop of blood. However, the same is not true for all molecules in blood circulation; D-Galactose and its metabolites are not easily measured in a drop of blood. Since commercially available assays (at the time of the study) to measure D-Galactose and its metabolites required a volume of blood that would have been high risk to take from a live mouse given the small volume of blood the possess (around 1.5 ml), repeated measures were certainly not an option. However, weekly or a single post-mortem sample may have provided useful information on the effectiveness of our delivery method. Actual, rather than predicted, water consumption could have been assessed to ensure mice were really receiving the dose expected and levels of D-Galactose or metabolites in urine could also have been measured. However, obtaining these measures would have required mice to be individually caged in a cage with grid flooring to facilitate accurate measures of D-Galactose consumption and urine production. These are two alterations to normal husbandry that increase stress and decrease well-being of the animal, which contravenes guidelines on minimising trauma to experimental animals. As an alternative, possibly more quantifiable method of administration, D-Galactose could have been added into mashed food which is normally given to mice after surgery or if they have an impairment that would hinder them reaching their normal standard chow. Alternatively, it could be administered *per os* as a compromise to drinking, without injecting into the peritoneum or subcutaneously, meaning that D-Galactose still passes through the digestive system (as would be the case for food and drink consumption) and isn't absorbed or metabolised by other means. However, multiple low doses to mimic food/drink consumption are another cause of stress to mice and would lead to irritation of the oesophagus with repeated *per os* administration over the 8 weeks required. In addition, this would be laborious and expensive to perform.

Since *in vivo* studies are time-consuming, tightly regulated, and expensive to perform, and since there were no positive findings from the aforementioned experiments, the effects of D-Galactose application were then explored using an *in vitro* organotypic hippocampal slice culture system (OHSC). OHSCs were explored for their potential as a faster method to study direct effects of D-Galactose on hippocampal structures and genetic and pharmacological interventions that may enable discovery of links between programmed axon degeneration and sAD.

5.10.2 The *ex vivo* D-Galactose model

The organotypic hippocampal slice cultures (OHSCs) used retain their hippocampal architecture including axonal projections from the dentate gyrus to the hippocampus and synaptic connections between neurones which were formed during development *in vivo*. They contain a mix of endogenous cells found in brain (neurones, microglia, astrocytes and oligodendrocytes). D-Galactose (55 μM) or vehicle (MEM) was applied to two-week old mouse-matched OHSCs for three successive weeks. At the end of each week, media was collected and Aβ40 and Aβ42 were consistently decreased in D-Galactose-treated cultures. At first this decrease seems to contradict the hypothesis that D-Galactose can induce sAD; one would expect increased Aβ42 in a model of AD. However, the decreased secretion could be due to an increase in retention of Aβ in the slice tissue. This theory is difficult to demonstrate empirically due to several factors: Firstly, the expression levels of Aβ in wild-type mice are low, especially in comparison to transgenic models often used, making any measure of Aβ unfavourable. Secondly, there is currently no reliable antibody to detect Aβ or distinguish between different Aβ isoforms. Combined, these first two factors mean it is currently not possible to detect any difference in Aβ accumulation through immunocytochemistry or Western blotting.

There is however, a reliable antibody to the amyloid precursor protein (APP). However, Western blot showed no differences in APP levels or synaptic proteins (presynaptic synaptophysin or postsynaptic PSD95) in OHSC tissue after three weeks of D-Galactose application. In fact, it seemed that all proteins (including housekeepers β-actin, cyclophilin, and β-III tubulin) were consistently downregulated in D-Galactose-treated slices compared to pup-matched controls. This may suggest that D-Galactose was killing the cultures, rather than promoting a sAD phenotype. Whilst no obvious changes were seen in the calbindin immunostaining of the alveolar tract, this is only one plane of view through the cultured tissue and may not represent the situation across the thickness of the tissue. The widespread consistently decreased protein expression, combined with decreased secretion of Aβ into the media after D-Galactose application, leads to the speculation that D-Galactose was killing cells in the cultures in contrast to the hypothesis that D-galactose was causing Aβ to accumulate in the OHSC tissue. Staining for markers of cell death and/or an ELISA to check for changes in Aβ levels or isoforms in the actual slice tissue could have been done. However, ELISA measures would require many cultures due to low levels of Aβ. However, the abundance of negative data in response to D-Galactose meant it was deemed not good use of resources to continue this line of enquiry.

5.10.3 Direction study would have taken if there was an indication of a role of programmed axon degeneration in sAD

Since there were no axonal transport impairments or biochemical alterations in Aβ or Tau levels from the *in vivo* study, there was no indication that D-Galactose induced sAD in these mice or that programmed axon degeneration was initiated in this model. Therefore, there was no scientific justification to look further at proposed links between hyperphosphorylated Tau, PP2A, and NMNAT2 or the role of NMNAT2:HSP90 chaperone activity in AD. The lack of phenotypes also meant there was no deficit to observe whether decreased SARM1 levels or removal could counter potential inflammatory changes observed by Takeda (Cambridge), as indicated in a high fat dietary-induced model of liver disease [507], and no reason to look at whether there were morphological changes in pyramidal neurones of D-Galactose-treated YFP-H mice.

A commonality between models utilising AD risk alleles and those using environmental risk factors is that they either do not lead to disease or they show heterogeneity in results from lab-to-lab. A logical progression beyond risk gene or environmental models is to start combining both genetic and environmental factors in aged mice to model prolonged accumulation of subtle factors over decades in human disease to observe whether this induces AD-like pathologies in newer rodent models, and whether they do this more consistently. In the context of this study, D-Galactose could have been administered to mice double knock-in for *APOE-ε4* and *TREM2* mutants, as well as fluorescently tagged mitochondria or NMNAT2. Alternatively, D-Galactose could have been administered to mice compound heterozygote for a complete *LoF Nmnat2* allele and a 50% efficient allele (creating mice that lack 75% neuronal NMNAT2) to explore susceptibility of brain to biochemical/inflammatory changes seen by Takeda (Cambridge). Therefore, testing whether low NMNAT2 levels confer susceptibility in combination with dietary risks to developing sAD in a similar way to which low NMNAT2 confers age-related sensory and motor deficits *in vivo* as well as sensitivity to physical and neurotoxic injuries *in vitro* [110]. These dietary and genetic risk factors could also be combined with moderate ageing of mice. Furthermore, it would be possible to observe if, *in vivo*, the synaptic changes associated in culture with decreasing NMNAT2 levels[116] or the proposed relationships between NMNAT2 and hyperphosphorylated Tau [118,119] are present in mice with decreasing levels of NMNAT2 and if so, are they more pronounced in a model of sAD? If so, would *Sarm1* hemizygosity in these mice be sufficient to reverse or prevent development of these phenotypes or are the proposed actions of NMNAT2 in regulating hyperphosphorylated Tau levels independent of its role in programmed axon degeneration?

It is clear that many diverse triggers can initiate programmed axon degeneration, such as physical injury, mitochondrial disruption, protein translation inhibition, neurotoxic effects in metabolic disease, and via distinct mechanisms in bortezomib and vincristine chemotherapy-induced peripheral neuropathy. The presence of WLD^S or absence of SARM1 is protective in models of all of the abovementioned triggers [21,37,58,59,63–72,74,75,79,81–83,87,88,91,98–101,239,300,508]. This suggests that targeting programmed axon degeneration presents an opportunity for a potentially widely-applicable therapy involving inhibiting or decreasing SARM1 expression levels or NADase activity, or increasing stability or activity of NMNAT2. Clearly, no conclusions over the role of programmed axon degeneration in sAD can be made from this chapter, but continued refinement of AD models could make this possible in future studies.

Chapter 6: Discussion

6.1.1 Implications of the results presented in this thesis

The results in this thesis demonstrate that:

(i) a genetic decrease in SARM1 levels confers protection against programmed axon degeneration in mice *in vivo* and *in vitro*

(ii) a similar decrease in SARM1 levels can be achieved *in vitro* in wild-type cells by application of *Sarm1* antisense oligonucleotides and this causes a similar delay in programmed axon degeneration as genetically decreasing levels of SARM1

(iii) applying antisense oligonucleotides *in vitro* to cells which already have genetically lowered SARM1 levels further delays programmed axon degeneration

(iv) the D-Galactose model was not reproducible so could not be used to model sAD. Therefore, questions remain over the role of programmed axon degeneration and whether patients with sAD would respond to treatments targeting it.

These findings correspond to the following implications for targeting SARM1 therapeutically:

(i) Haploinsufficiency in humans could confer a partially protective phenotype making axons less susceptible to a diverse range of programmed axon degeneration triggers

(ii) It is possible to decrease SARM1 levels and delay programmed axon degeneration via exogenous application of antisense oligonucleotides (at least *in vitro*) meaning this strategy could be developed into a therapy

(iii) Certain patient populations could be more responsive to anti-SARM1 therapies, if they already express lowered levels of SARM1

(iv) Consideration of which disorders would respond best to anti-SARM1 therapies is needed. This requires further research into the effects of decreasing SARM1 levels in disease models and testing antisense oligonucleotide efficacy, or targeting SARM1 with other therapeutic strategies, to provide information on which disorders may respond best to treatment

Results in this thesis demonstrate in principle that antisense oligonucleotides effectively decrease SARM1 levels and delay programmed axon degeneration, to a similar extent as removing one *Sarm1* allele. Therefore, it can be inferred that similar delay could be seen after sciatic nerve transection if a similar decrease in SARM1 levels is achievable *in vivo* with antisense oligonucleotides. However, this requires optimisation of antisense oligonucleotide targeting to peripheral nerves and *in vivo* confirmation of decreased SARM1 levels.

Since sciatic nerve transection is an extreme injury with limited clinical relevance, the relevance of delayed axon degeneration conferred by decreased SARM1 levels needs to be explored in disease models. Given similarities in phenotypes between the *in vitro* delays in degeneration between the *Sarm1* hemizygous cultures and those treated with antisense oligonucleotides, *Sarm1* hemizygous mice could be used as a way to explore which diseases might respond to anti-SARM1 therapies in parallel to developing improved *in vivo* methods for delivering antisense oligonucleotide therapies or other anti-SARM1 therapeutic strategies.

6.1.2 Which diseases would likely respond to anti-SARM1 therapies?

The *in vitro* results after antisense oligonucleotide application were particularly strong in reversing neurite outgrowth deficits of DRGs lacking NMNAT2, and against axon degeneration induced by protein translation inhibition. These data suggest that targeting SARM1 in diseases caused by depletion or loss of NMNAT2 function, or by inhibition of protein translation could be promising strategies to pursue in the first instance when targeting human patients with anti-SARM1 therapies. This could improve quality of life and outlook in patients in which genes involved in programmed axon degeneration play a causative or contributory role, such as pain present in sisters with polyneuropathy caused by *NMNAT2 LoF* [112].

Preclinically, this theory could be tested in *Nmnat2* compound heterozygous mice to explore whether anti-SARM1 therapies can prevent *in vivo* age-associated axon loss, temperature insensitivity, and motor impairments, as well as vulnerability to physical and neurotoxic stresses *in vitro* [110]. Alternatively, new models containing human mutations thought to cause pain in sisters with biallelic NMNAT2 *LoF* [112] could be developed. Phenotypes in such models could be subtle, but continued optimisation of preclinical models to show strong statistically significant phenotypes does not necessarily address biological relevance, and over-reliance on these models is likely one contributing factor to a lack of therapeutic translation. In humans, phenotypes are more complex and causes of disease multifactorial. However, overcoming the

issues around modelling human disease preclinically is challenging, as described in more detail in the previous chapter.

In terms of protein translation inhibition, models of neurodegenerative protein aggregation disorders which trigger the unfolded protein response and inhibit protein translation could be used. For example, exploring anti-SARM1 therapies in an FTD model of tauopathy where re-activation of protein translation was shown to be protective [347] or in TDP-43^{Q331K} mutant model of ALS-FTD in which removal of *Sarm1* decreases loss of axons and dendritic spines [105].

The modest delay in axon degeneration which results in this thesis demonstrate can be achieved after axotomy-, vincristine- and rotenone-induced degeneration by decreasing SARM1 levels, suggests potential for wider use of anti-SARM1 therapies in more common diseases and conditions. Future studies should explore these possibilities in animal models of peripheral neuropathy. For example, development of painful neuropathies caused by temporary and predictable exposure to neurotoxic chemotherapeutic agents have been shown to activate SARM1 via distinct mechanisms and complete *Sarm1* removal is prevents loss of intraepidermal nerve fibres (IENFs) [79,300,81]. The predictability of axon stress in chemotherapy makes targeting pain associated with axon degeneration and IENF loss a promising strategy to prevent development of neuropathy which could improve lives of cancer patients undergoing or surviving chemotherapy [309]. Anti-SARM1 therapies could also have implications for chronic SARM1-dependent metabolic neuropathy [79], though this disease mechanism would be less predictable and likely require chronic treatment.

Immediate suppression of SARM1 would be needed in circumstances where injury cannot be predicted (such as after traumatic injury), unlike in chronic disease which could have a longer therapeutic window for intervention. Therefore, therapies targeting SARM1 at the level of gene expression may be useful in cases where SARM1 activation is predictable and treatment can commence prior to SARM1 activation (especially given the long half-life of SARM1 and need for degradation of pre-existing proteins if the therapy targets protein levels). Conversely, treatment in response to injury or neurotoxicity would likely require more immediate SARM1 suppression, such as may be more achievable through small molecule inhibition.

There are a few examples of disease models where targeting programmed axon degeneration through overexpression of WLD^{S} or removal of SARM1 are not protective, such as a mouse model of prion disease [350,351] and models of ALS caused by SOD1 mutations [102–104]. This could indicate that if other disease mechanisms occur in parallel to programmed axon degeneration or via cell soma death signals, targeting programmed axon degeneration alone may not be

efficacious. In such instances, anti-SARM1 therapies may need to be considered as part of combined therapies targeting other aspects of disease pathology.

6.1.3 Clarifying the role of programmed axon degeneration in human disease

Current preclinical research in the Coleman lab is working towards clarifying whether *SARM1* variants present in the human population affect axon vulnerability to stress and whether these are protective *LoF* or pro-degenerative *GoF* mutants. How these mutants are related to SARM1 NADase activity and rate of programmed axon degeneration in culture is being explored. Further work in the lab is exploring whether *GoF* variants appear in higher frequency in diseased populations or whether *LoF* variants appear in higher frequency in a control population using data from Project MinE (which aims to explore the genetic basis of ALS). This information can then be used to look at whether these variants appear in disease populations, whether they differ between diseases, and be used to help delineate the extent to which programmed axon degeneration plays a role in human diseases. This could help direct preclinical efforts to appropriate animal models for optimising anti-SARM1 therapies.

Work on understanding the phenotypes associated with *SARM1* variants in the human population could have implications when deciding therapeutic strategies for individual patients. Given that *Sarm1* hemizygosity confers a level of protection, this could indicate that humans with *LoF* mutations could already be at lower risk of disease affecting axon health. However, since in *Sarm1* hemizygous cells degeneration does eventually ensue in most models tested here, this could indicate that even axons with a lower vulnerability can degenerate in disease states. Thus, targeting patients with *SARM1 LoF* mutations with anti-SARM1 therapies could improve outcome in certain patient populations. Preclinically, combining anti-SARM1 therapies with already decreased levels of SARM1 in *Sarm1* hemizygous mice could explore these possibilities. Conversely, patient populations with increased genetic risk for developing chronic disease due to SARM1 *GoF* mutations might benefit from prophylactic treatment with anti-SARM1 therapies to remove this as a risk factor.

Once a role of programmed axon degeneration in human disease-related axon pathology is clarified, the extent to which SARM1 suppression is needed in disease may be clearer. As discussed in depth in Chapter 3, decreasing SARM1 protein levels by 50% confers stronger protection than complete removal of other programmed axon degeneration modifiers (using *in vivo* axotomy as a benchmark for comparison). The work in this thesis demonstrates that it is possible to achieve strong rescue in some circumstances from knockdown, but removal is still needed for prolonged protection after severe injury. If elimination of SARM1 is needed to elicit

a prolonged protective effect in humans, this will raise a number of challenges and may affect the therapeutic strategy that needs to be employed to prevent or counter disease progression.

6.1.4 Optimising anti-SARM1 therapies

Optimising a therapy to eliminate SARM1 completely is limited by accessibility of the nervous system, stability or duration of therapeutic molecules, and bioavailability of the active therapeutic agent. Antisense oligonucleotides have a long half-life in comparison to small molecules, but short in comparison to duration of other gene therapies, such as AAV-mediated delivery used to introduce compound dominant negative SARM1 [80]. Both antisense oligonucleotide therapies and gene therapies require bypassing the blood-brain and blood-nerve barriers in order to be effective, but this could be useful in preventing off target effects of anti-SARM1 therapies administered systemically, such as small molecule compounds. Combining more than one approach to prevent SARM1 activity could also be explored. For example, could *Sarm1* expression levels be decreased followed by inhibition of residual levels by small molecules?

Crucially, eliminating any protein also eliminates its role in all biological processes it is involved in. This could be problematic since there are outstanding questions relating to whether or not SARM1 plays a role outside of axon degeneration. Is basal activity of SARM1 physiologically important? To what extent is SARM1 activity required in response to viral infection and other immune-related events in light of new work highlighting potential roles of passenger mutations in commonly used *Sarm1*$^{-/-}$ mice [133]? *Sarm1*$^{-/-}$ mice appear to live healthy lives [111], but how transferrable are results from a 'clean' animal house to 'everyday' exposure to pathogens, and between mice compared to humans? Could SARM1 activation be protective in some circumstances? For example, a neuronal mechanism evolved to prevent the pathological prion-like spread of proteins or viruses through the nervous system.

One way around the potential problem of complete SARM1 elimination could be design of combination therapies. Multiple subtle modifications to the pathway that do not individually prevent axon degeneration could together have a more profound effect if co-applied. This strategy could also improve selectivity for the programmed axon degeneration pathway, and decrease potential for off-target negative effects if SARM1 has roles in other cell types or responses. Such a therapy could incorporate the recent findings that NMN activates SARM1 [216,302,160]. Decreasing NMN accumulation through NAMPT inhibition, NMNAT2 upregulation/stabilisation, or other methods of NMN sequestration would likely decrease the probability of NMN activating SARM1. By using low doses that alone are ineffective, this could

decrease potential negative effects of NMN depletion in terms of NAD^+ synthesis whilst decreasing NMN levels low enough to favour the inactive formation of SARM1. This, in combination with lowered SARM1 levels or activity could lead to stronger suppression of SARM1 prodegenerative function and prolong protection against axon degeneration in chronic disease.

6.2 NMNAT2-induced neurite outgrowth deficit in predicting the ability of therapies to delay programmed axon degeneration

Finally, this section will note how the neurite outgrowth deficits in DRGs lacking NMNAT2 could be used as a phenotypic screen for identifying novel compounds to inhibit programmed axon degeneration. Manipulations that deplete NMN (overexpression of WLD^S or NMN deamidase) which strongly delay programmed axon degeneration in mature axons [62,177,216], also restore neurite outgrowth deficits in developing axons lacking NMNAT2 [77,216]. FK866 which depletes NMN through NAMPT inhibition and modestly delays axon degeneration [216] also partially restores neurite outgrowth in neurites lacking NMNAT2, though only when administered in the presence of NaAD which allows cells to produce NAD^+ through an alternative synthetic pathway [78]. Finally, *Sarm1*$^{-/-}$ mice exhibit delayed axon degeneration for several weeks *in vivo* [62] and removal of *Sarm1* reverses deficits in neurite outgrowth for the lifespan of mice lacking NMNAT2 [78,111]. In addition, the work in this thesis demonstrates that *Sarm1* hemizygosity confers a modest delay in programmed axon degeneration as well as partially restoring neurite outgrowth. Further, *Sarm1* antisense oligonucleotides reverse neurite outgrowth deficits and prolong protection in DRGs (compared to SCGs) after *in vitro* axon injury. The strength of protection conferred with each of these manipulations in mature axons after *in vitro* axotomy appears to be reflected in the strength of rescue in neurite outgrowth in mice lacking NMNAT2. Long-term prevention of axon degeneration is not achieved by FK866 or *Sarm1* hemizygosity and this is reflected in the partial reversal of neurite outgrowth deficits. Conversely, WLD^S, NMN deamidase, and complete removal of *Sarm1* confer stronger protection after *in vitro* axotomy and show greater capacity for reversing the neurite outgrowth deficit. This could indicate that a phenotypic screen using this system would filter out weaker modifiers of programmed axon degeneration and most likely highlight stronger modifiers. Phenotypic screens also enable the effects of compounds to be tested on full-length endogenous proteins in their cellular environment, which could improve the predictive capacity in contrast to the caveats associated with isolated protein domains and biochemical assays.

6.3 Other outstanding questions in the field

How do SARM1 octamers form? Could SARM1 monomers start interacting as they are synthesised, such as could occur during polyribosome-mediated protein translation? Do non-octameric SARM1 species exist in the axon? Is SARM1 basal activity physiologically important? Do NMNAT2 and SARM1 co-exist in a physically close signalling complex to monitor or regulate axonal nucleotide levels? What happens downstream of SARM1? How do NMN accumulation, SARM1 activation, NAD^+ and ATP depletion, raised Nam and ADPR/cADPR, and the second calcium wave lead to axon fragmentation? Are these events independent, interconnected, sequential, or is there an unidentified molecule connecting them? If there is a downstream effector of SARM1 in mammals, as there appears to be in *Drosophila* [509], could this explain why barely detectable levels of SARM1 can still induced axon fragmentation in the *in vitro* assays used in this work? To what extent can SARM1 be involved in death mechanisms outside of the axon?

6.4 Conclusions

The work in this thesis demonstrates that programmed axon degeneration can be delayed by lowering *Sarm1* expression levels. This can be achieved by removal of one allele or through exogenous application of antisense oligonucleotides. The data suggest that some disorders, like those caused by loss of NMNAT2 or involving defective protein translation, are more likely to respond to SARM1 modifying therapies than others, such as transection injuries. Future studies need to explore the effects of predicted human *SARM1 GoF* and *LoF* mutations and their potential relevance to disease risk. Data presented here suggest that patients with *SARM1 LoF* could respond better to anti-SARM1 therapies than humans with wild-type *SARM1*. Preclinical work is needed to delineate which diseases could respond to anti-SARM1 therapies. Selection of appropriate diseases to target SARM1, as well as identifying the appropriate patient populations will be important in demonstrating clinical efficacy of anti-SARM1 therapies.

List of abbreviations

AAA-ATPase	ATPases Associated with diverse cellular Activities
AAD	Acute axonal degeneration
AAV	Adeno-associated virus
ACH	Amyloid cascade hypothesis
AD	Alzheimer's disease
ADP	Adenosine diphosphate
ADPR	Adenosine-5'-O-diphosphoribose
ADPRP	Adenosine- 5'- O- diphosphoribose phosphate
ALS	Amyotrophic Lateral Sclerosis
APP	Amyloid precursor protein
ARM	Armadillo
ASO	Antisense oligonucleotide
ATP	Adenosine triphosphate
ATP	Adenosine triphosphate
Aβ	Amyloid beta
BAK	BCL-2 homologous antagonist killer
BAX	BCL-2-associated X
BCA	Bicinchoninic acid assay
BCL-2	B-cell lymphoma 2
cADPR	Cyclic adenosine-5'-O-diphosphoribose
cAMP	Cyclic adenosine monophosphate
CCCP	Carbonyl cyanide m-chlorophenyl hydrazone
CD38	Cluster of differentiation 38
CFP	Cyan fluorescent protein
CHX	Cycloheximide
CIPN	Chemotherapy-induced peripheral neuropathy
CMT	Charcot-Marie-Tooth
CNS	Central Nervous System
CRE	cAMP response element
CREB	cAMP response element-binding protein
CRMP2/4	Collapsin response mediator protein 2/4
CSF	Cerebrospinal fluid
DiI	1,1'-Dioctadecyl-3,3,3',3'-Tetramethylindocarbocyanine Perchlorate ('DiI'; $DiIC_{18}(3)$)
DIV	days *in vitro*
DLK	Dual leucine zipper-bearing kinase
DMEM	Dulbecco's Modified Eagle's Medium
DMSO	Dimethyl sulfoxide
DNA	Deoxyribonucleic acid
dNMNAT	Homolog of NMNAT in *Drosophila melanogaster*
DPN	Diabetic peripheral neuropathy

DR6	Death receptor 6
DRG	Dorsal root ganglion
dSARM	Homologue of SARM1 in *Drosophila melanogaster*
EAE	Experimental autoimmune encephalitis
ECL	Enhanced chemiluminescence
EGTA	Ethylene glycol-bis(β-aminoethyl ether)-N,N,N',N'-tetraacetic acid
ENT	Equilibrative nucleoside transporter
EOAD	Early onset Alzheimer's disease
ER	Endoplasmic reticulum
ERK	Extracellular signal-regulated kinase
fAD	Familial Alzheimer's disease
FAD	Flavin adenine dinucleotide
FK866	N-[4-(1-benzoyl-4-piperidinyl)butyl]-3-(3-pyridinyl)-2E-propenamide
FTD	Frontotemporal dementia
GoF	Gain of function
GWAS	Genome-wide association studies
h	hour(s)
H+	Hydrogen ion
HD	Huntington's disease
HRP	Horseradish peroxidase
HSP	Heat shock protein
ISTID	Isoform-specific targeting and interaction domain
JNK	c-Jun N-terminal kinase
LOAD	Late onset Alzheimer's disease
LoF	Loss of function
M	Molar
m	Milli-
MAP2K	Mitogen-activated protein kinase kinase
MAP3K	Mitogen-activated protein kinase kinase kinase
MAP4K	Mitogen-activated protein kinase kinase kinase kinase
MAPK	Mitogen-activated protein kinase
MEKK4	MAPK/ERK kinase kinase 4
mHTT	Mutant huntingtin
MKK7	MAPK/ERK kinase kinase 7
MLK2	Mixed lineage kinase 2,
MLS	Mitochondrial localisation sequence
mPT	Mitochondrial permeability transition
mPTP	Mitochondrial permeability transition pore
MPTP	1-methyl-4-phenyl-1,2,3,6-tetrahydropyridine
MRI	Magnetic resonance imaging
mRNA	messenger ribonucleic acid
MS	Multiple Sclerosis
MTS	Mitochondrial targeting sequence

MW	Molecular weight
MYCBP2	Myc-binding protein 2 (also known as PHR1)
MyD88	Myeloid differentiation primary response 88
NA	Nicotinic acid
NaAD	Nicotinic acid adenine dinucleotide
NAD+	Nicotinamide adenine dinucleotide
NADH	Reduced nicotinamide adenine dinucleotide
NADP	Nicotinamide adenine dinucleotide phosphate
NADPH	Reduced nicotinamide adenine dinucleotide phosphate
NADS	Nicotinamide adenine dinucleotide synthetases
Nam	Nicotinamide
NaMN	Nicotinic acid mononucleotide
NAMPT	Nicotinamide phosphoribosyltransferase
NaPRT	Nicotinic acid phosphoribosyltransferase
NfH	Neurofilament heavy chain
NfL	Neurofilament light chain
NfM	Neurofilament medium chain
NGF	Nerve growth factor
NMN	Nicotinamide mononucleotide
NMNAT (1/2/3)	Nicotinamide mononucleotide adenylyl transferase 1/2/3
NR	Nicotinamide riboside
PARPs	Poly-ADP-ribose polymerases
PBS	Phosphate buffered saline
PCR	Polymerise chain reaction
pCREB	Phosphorylated CREB
PERK	Protein kinase R-like
PET	Positron emission tomography
PHR1	Pam/highwire/rpm-1 protein (also known as MYCBP2)
pmn	Progressive motor neuropathy
PNS	Peripheral Nervous System
PP2A	Protein phosphatase 2
PTX	PBS, 0.5% TritonX-100
RGC	Retinal ganglion cell
ROS	Reactive oxygen species
RT	Room temperature
RyR	Ryanadine receptor
s	Second(s)
sAD	Sporadic Alzheimer's disease
SAM	Sterile α motif
SARM1	Sterile α-motif-, armadillo-motif-, and Toll-interleukin receptor homology domain-containing protein
SCG	Superior cervical ganglion
SCG10	Superior cervical ganglion 10 (also known as Stathmin 2)

SDS	Sodium dodecyl sulphate
SEM	Standard error of the mean
siRNA	Small interfering ribonucleic acids
SIRTs	Sirtuins
SMA	Spinal muscular atrophy
SOD1	Superoxide dismutase 1
STZ	Streptozotocin
TBS	Tris buffered saline
TBST	TBS with 0.05 % Tween 20
TCA	Tricarboxylic acid cycle
TIR	Toll-interleukin receptor homology domain
TLR	Toll-like receptors
TRITC	Tetramethylrhodamine
UBE4B	Ubiquitin ligase E4B
UPS	Ubiquitin proteasome system
UTR	Untranslated region
V	Volts
VCP	Valosin-containing protein
WLDs	Wallerian degeneration slow
Wnd	Wallenda
xg	centrifugal force
YFP	Yellow fluorescent protein
zDHHCs	Zinc Finger DHHC-Type palmitoyltransferases
ZNRF1	Zinc and ring finger protein 1
2'MOE	2'-O-methoxy-ethyl Bases
2'OMe	2'-O-Methylinosine

Bibliography

1. Tahirovic, S. & Bradke, F. Neuronal Polarity. *Cold Spring Harb Perspect Biol* **1**, (2009).
2. Coleman, M. P. & Freeman, M. R. Wallerian Degeneration, Wld S, and Nmnat. *Annual Review of Neuroscience* **33**, 245–267 (2010).
3. Waller, A. Experiments on the Section of the Glosso-Pharyngeal and Hypoglossal Nerves of the Frog, and Observations of the Alterations Produced Thereby in the Structure of Their Primitive Fibres. *Edinb Med Surg J* **76**, 369–376 (1850).
4. Cavanagh, J. B. The 'dying back' process. A common denominator in many naturally occurring and toxic neuropathies. *Arch. Pathol. Lab. Med.* **103**, 659–664 (1979).
5. Conforti, L., Adalbert, R. & Coleman, M. P. Neuronal death: where does the end begin? *Trends Neurosci.* **30**, 159–166 (2007).
6. Hilliard, M. A. Axonal degeneration and regeneration: a mechanistic tug-of-war. *J. Neurochem.* **108**, 23–32 (2009).
7. Adalbert, R. & Coleman, M. P. Review: Axon pathology in age-related neurodegenerative disorders. *Neuropathology and Applied Neurobiology* **39**, 90–108 (2013).
8. Kerschensteiner, M., Schwab, M. E., Lichtman, J. W. & Misgeld, T. In vivo imaging of axonal degeneration and regeneration in the injured spinal cord. *Nat. Med.* **11**, 572–577 (2005).
9. Knöferle, J. *et al.* Mechanisms of acute axonal degeneration in the optic nerve in vivo. *Proc. Natl. Acad. Sci. U.S.A.* **107**, 6064–6069 (2010).
10. Koch, J. C. *et al.* Acute axonal degeneration in vivo is attenuated by inhibition of autophagy in a calcium-dependent manner. *Autophagy* **6**, 658–659 (2010).
11. George, E., Glass, J. & Griffin, J. Axotomy-induced axonal degeneration is mediated by calcium influx through ion-specific channels. *J Neurosci* **15**, 6445–6452 (1995).
12. Wang, J. T., Medress, Z. A. & Barres, B. A. Axon degeneration: Molecular mechanisms of a self-destruction pathway. *J Cell Biol* **196**, 7–18 (2012).

13. Luttges, M. W., Kelly, P. T. & Gerren, R. A. Degenerative changes in mouse sciatic nerves: electrophoretic and electrophysiologic characterizations. *Exp. Neurol.* **50**, 706–733 (1976).
14. Tsao, J. W., Brown, M. C., Carden, M. J., McLean, W. G. & Perry, V. H. Loss of the compound action potential: an electrophysiological, biochemical and morphological study of early events in axonal degeneration in the C57BL/Ola mouse. *Eur. J. Neurosci.* **6**, 516–524 (1994).
15. Smith, R. S. & Bisby, M. A. Persistence of axonal transport in isolated axons of the mouse. *Eur. J. Neurosci.* **5**, 1127–1135 (1993).
16. Lubinska, L. Early course of Wallerian degeneration in myelinated fibres of the rat phrenic nerve. **130**, 47–63 (1977).
17. Beirowski, B. *et al.* Quantitative and qualitative analysis of Wallerian degeneration using restricted axonal labelling in YFP-H mice. *Journal of Neuroscience Methods* **134**, 23–35 (2004).
18. Gilliatt, R. W. & Hjorth, R. Nerve conduction during Wallerian degeneration in the baloon. *Journal of neurology, neurosurgery, and psychiatry* vol. 35 https://pubmed.ncbi.nlm.nih.gov/4624688/ (1972).
19. Chaudhry, V. & Cornblath, D. Wallerian degeneration in human nerves: serial electrophysiological studies - PubMed. (1992).
20. Di Stefano, M. *et al.* A rise in NAD precursor nicotinamide mononucleotide (NMN) after injury promotes axon degeneration. *Cell death and differentiation* **22**, 731–742 (2015).
21. Osterloh, J. M. *et al.* dSarm/Sarm1 is required for activation of an injury-induced axon death pathway. *Science (New York, N.Y.)* **337**, 481–4 (2012).
22. Gilley, J. & Coleman, M. P. Endogenous Nmnat2 Is an Essential Survival Factor for Maintenance of Healthy Axons. *PLoS Biology* **8**, (2010).
23. Buckmaster, E. A., Perry, V. H. & Brown, M. C. The Rate of Wallerian Degeneration in Cultured Neurons from Wild Type and C57BL/WldS Mice Depends on Time in Culture

and may be Extended in the Presence of Elevated K+ Levels. *European Journal of Neuroscience* **7**, 1596–1602 (1995).

24. Zhai, Q. *et al.* Involvement of the Ubiquitin- Proteasome System in the Early Stages of Wallerian Degeneration. *Neuron* **39**, 217–225 (2003).
25. Sievers, C., Platt, N., Perry, V. H., Coleman, M. P. & Conforti, L. Neurites undergoing Wallerian degeneration show an apoptotic-like process with Annexin V positive staining and loss of mitochondrial membrane potential. *Neurosci. Res.* **46**, 161–169 (2003).
26. Tsao, J. W., George, E. B. & Griffin, J. W. Temperature modulation reveals three distinct stages of Wallerian degeneration. *The Journal of neuroscience : the official journal of the Society for Neuroscience* **19**, 4718–26 (1999).
27. Beirowski, B. *et al.* The progressive nature of Wallerian degeneration in wild-type and slow Wallerian degeneration (WldS) nerves. *BMC neuroscience* **6**, 6–6 (2005).
28. Stirling, D. & Stys, P. Mechanisms of axonal injury: internodal nanocomplexes and calcium deregulation. *Trends in molecular medicine* **16**, (2010).
29. Ma, M. *et al.* Calpains mediate axonal cytoskeleton disintegration during Wallerian degeneration. *Neurobiology of Disease* **56**, 34–46 (2013).
30. Beirowski, B., Nógrádi, A., Babetto, E., Garcia-Alias, G. & Coleman, M. P. Mechanisms of axonal spheroid formation in central nervous system Wallerian degeneration. *J. Neuropathol. Exp. Neurol.* **69**, 455–472 (2010).
31. Brück, W. The role of macrophages in Wallerian degeneration. *Brain pathology* **7**, 741–52 (1997).
32. Vargas, M. E. & Barres, B. A. Why Is Wallerian Degeneration in the CNS So Slow? *Annual Review of Neuroscience* **30**, 153–179 (2007).
33. Stoll, G., Trapp, B. D. & Griffin, J. W. Macrophage function during Wallerian degeneration of rat optic nerve: clearance of degenerating myelin and Ia expression. *J. Neurosci.* **9**, 2327–2335 (1989).

34. Gaudet, A., Popovich, P. & Ms, R. Wallerian degeneration: gaining perspective on inflammatory events after peripheral nerve injury. *Journal of neuroinflammation* **8**, (2011).

35. Bisby, M. A. & Chen, S. Delayed wallerian degeneration in sciatic nerves of C57BL/Ola mice is associated with impaired regeneration of sensory axons. *Brain Res.* **530**, 117–120 (1990).

36. Brown, M. C., Perry, V. H., Hunt, S. P. & Lapper, S. R. Further studies on motor and sensory nerve regeneration in mice with delayed Wallerian degeneration. *Eur. J. Neurosci.* **6**, 420–428 (1994).

37. Ramer, M. S., French, G. D. & Bisby, M. A. Wallerian degeneration is required for both neuropathic pain and sympathetic sprouting into the DRG. *Pain* **72**, 71–8 (1997).

38. Collyer, E. *et al.* Sprouting of axonal collaterals after spinal cord injury is prevented by delayed axonal degeneration. *Exp. Neurol.* **261**, 451–461 (2014).

39. Bignami, A. & Ralston, H. J. The cellular reaction to Wallerian degeneration in the central nervous system of the cat. *Brain Res.* **13**, 444–461 (1969).

40. Perry, V. H., Brown, M. C. & Gordon, S. The macrophage response to central and peripheral nerve injury. A possible role for macrophages in regeneration. *J Exp Med* **165**, 1218–1223 (1987).

41. George, R. & Griffin, J. W. Delayed macrophage responses and myelin clearance during Wallerian degeneration in the central nervous system: the dorsal radiculotomy model. *Exp. Neurol.* **129**, 225–236 (1994).

42. Deckwerth, T. L. & Johnson, E. M. Neurites can remain viable after destruction of the neuronal soma by programmed cell death (apoptosis). *Dev. Biol.* **165**, 63–72 (1994).

43. Adalbert, R., Nógrádi, A., Szabó, A. & Coleman, M. P. The slow Wallerian degeneration gene in vivo protects motor axons but not their cell bodies after avulsion and neonatal axotomy. *European Journal of Neuroscience* **24**, 2163–2168 (2006).

44. Schaefer, A. M., Sanes, J. R. & Lichtman, J. W. A compensatory subpopulation of motor neurons in a mouse model of amyotrophic lateral sclerosis. *J. Comp. Neurol.* **490**, 209–219 (2005).

45. Pun, S., Santos, A. F., Saxena, S., Xu, L. & Caroni, P. Selective vulnerability and pruning of phasic motoneuron axons in motoneuron disease alleviated by CNTF. *Nat. Neurosci.* **9**, 408–419 (2006).

46. Beirowski, B., Babetto, E., Coleman, M. P. & Martin, K. R. The WldS gene delays axonal but not somatic degeneration in a rat glaucoma model. *Eur. J. Neurosci.* **28**, 1166–1179 (2008).

47. Fernandes, K. A. *et al.* Role of SARM1 and DR6 in retinal ganglion cell axonal and somal degeneration following axonal injury. *Exp. Eye Res.* **171**, 54–61 (2018).

48. Finn, J. T. *et al.* Evidence that Wallerian degeneration and localized axon degeneration induced by local neurotrophin deprivation do not involve caspases. *J. Neurosci.* **20**, 1333–1341 (2000).

49. Vohra, B. P. S. *et al.* Amyloid precursor protein cleavage-dependent and -independent axonal degeneration programs share a common nicotinamide mononucleotide adenylyltransferase 1-sensitive pathway. *J. Neurosci.* **30**, 13729–13738 (2010).

50. Simon, D. *et al.* A caspase cascade regulating developmental axon degeneration. *The Journal of neuroscience : the official journal of the Society for Neuroscience* **32**, (2012).

51. Burne, J. F., Staple, J. K. & Raff, M. C. Glial cells are increased proportionally in transgenic optic nerves with increased numbers of axons. *J. Neurosci.* **16**, 2064–2073 (1996).

52. Whitmore, A. V., Lindsten, T., Raff, M. C. & Thompson, C. B. The proapoptotic proteins Bax and Bak are not involved in Wallerian degeneration. *Cell Death & Differentiation* **10**, 260–261 (2003).

53. Saraste, A. & Pulkki, K. Morphologic and biochemical hallmarks of apoptosis. *Cardiovasc. Res.* **45**, 528–537 (2000).

54. Ozaki, E. *et al.* SARM1 deficiency promotes rod and cone photoreceptor cell survival in a model of retinal degeneration. *Life Sci Alliance* **3**, (2020).

55. Shin, J. E. *et al.* SCG10 is a JNK target in the axonal degeneration pathway. *Proc Natl Acad Sci U S A* **109**, E3696–E3705 (2012).

56. Ko, K. W., Milbrandt, J. & DiAntonio, A. SARM1 acts downstream of neuroinflammatory and necroptotic signaling to induce axon degeneration. *J. Cell Biol.* **219**, (2020).

57. Gerdts, J., Brace, E. J., Sasaki, Y., DiAntonio, A. & Milbrandt, J. SARM1 activation triggers axon degeneration locally via NAD^+ destruction. *Science* **348**, 453–457 (2015).

58. Gerdts, J., Summers, D. W., Sasaki, Y., DiAntonio, A. & Milbrandt, J. Sarm1-mediated axon degeneration requires both SAM and TIR interactions. *J. Neurosci.* **33**, 13569–13580 (2013).

59. Summers, D. W., DiAntonio, A. & Milbrandt, J. Mitochondrial dysfunction induces Sarm1-dependent cell death in sensory neurons. *J. Neurosci.* **34**, 9338–9350 (2014).

60. Zhu, S. S. *et al.* WldSprotects against peripheral neuropathy and retinopathy in an experimental model of diabetes in mice. *Diabetologia* **54**, 2440 (2011).

61. Conforti, L., Gilley, J. & Coleman, M. P. Wallerian degeneration: an emerging axon death pathway linking injury and disease. *Nature reviews. Neuroscience* **15**, 394–409 (2014).

62. Osterloh, J. M. *et al.* dSarm/Sarm1 is required for activation of an injury-induced axon death pathway. *Science (New York, N.Y.)* **337**, 481–4 (2012).

63. Perry, V. H., Brown, M. C., Lunn, E. R., Tree, P. & Gordon, S. Evidence that Very Slow Wallerian Degeneration in C57BL/Ola Mice is an Intrinsic Property of the Peripheral Nerve. *Eur. J. Neurosci.* **2**, 802–808 (1990).

64. Ludwin, S. K. & Bisby, M. A. Delayed wallerian degeneration in the central nervous system of Ola mice: an ultrastructural study. *J. Neurol. Sci.* **109**, 140–147 (1992).

65. Steward, O. & Trimmer, P. A. Genetic influences on cellular reactions to CNS injury: the reactive response of astrocytes in denervated neuropil regions in mice carrying a mutation (Wld(S)) that causes delayed Wallerian degeneration. *J. Comp. Neurol.* **380**, 70–81 (1997).

66. Sajadi, A., Schneider, B. L. & Aebischer, P. Wlds-mediated protection of dopaminergic fibers in an animal model of Parkinson disease. *Curr. Biol.* **14**, 326–330 (2004).

67. Wang, M. S. *et al.* The Wlds protein protects against axonal degeneration: A model of gene therapy for peripheral neuropathy. *Annals of Neurology* **50**, 773–779 (2001).

68. Wang, M. S., Davis, A. A., Culver, D. G. & Glass, J. D. WldS mice are resistant to paclitaxel (taxol) neuropathy. *Ann. Neurol.* **52**, 442–447 (2002).

69. Ferri, A., Sanes, J. R., Coleman, M. P., Cunningham, J. M. & Kato, A. C. Inhibiting axon degeneration and synapse loss attenuates apoptosis and disease progression in a mouse model of motoneuron disease. *Curr. Biol.* **13**, 669–673 (2003).

70. Samsam, M. *et al.* The Wlds mutation delays robust loss of motor and sensory axons in a genetic model for myelin-related axonopathy. *J. Neurosci.* **23**, 2833–2839 (2003).

71. Mi, W. *et al.* The slow Wallerian degeneration gene, WldS, inhibits axonal spheroid pathology in gracile axonal dystrophy mice. *Brain* **128**, 405–416 (2005).

72. Gamage, K. K. *et al.* Death Receptor 6 Promotes Wallerian Degeneration in Peripheral Axons. *Curr. Biol.* **27**, 890–896 (2017).

73. Babetto, E., Beirowski, B., Russler, E., Milbrandt, J. & DiAntonio, A. The Phr1 ubiquitin ligase promotes injury-induced axon self-destruction. **16**, 387–393 (2013).

74. Press, C. & Milbrandt, J. Nmnat delays axonal degeneration caused by mitochondrial and oxidative stress. *J. Neurosci.* **28**, 4861–4871 (2008).

75. Loreto, A. *et al.* Mitochondrial impairment activates the Wallerian pathway through depletion of NMNAT2 leading to SARM1-dependent axon degeneration. *Neurobiology of Disease* **134**, 104678 (2020).

76. Gilley, J. & Coleman, M. P. Endogenous Nmnat2 Is an Essential Survival Factor for Maintenance of Healthy Axons. *PLoS Biology* **8**, (2010).

77. Gilley, J., Adalbert, R., Yu, G. & Coleman, M. P. Rescue of peripheral and CNS axon defects in mice lacking NMNAT2. *The Journal of neuroscience : the official journal of the Society for Neuroscience* **33**, 13410–13424 (2013).

78. Gilley, J., Orsomando, G., Nascimento-Ferreira, I. & Coleman, M. P. Absence of SARM1 rescues development and survival of NMNAT2-Deficient axons. *Cell Reports* **10**, 1975–1982 (2015).

79. Turkiew, E., Falconer, D., Reed, N. & Höke, A. Deletion of Sarm1 gene is neuroprotective in two models of peripheral neuropathy. *Journal of the Peripheral Nervous System* **22**, 162–171 (2017).

80. Geisler, S. *et al.* Gene therapy targeting SARM1 blocks pathological axon degeneration in mice. *J Exp Med* **216**, 294–303 (2019).

81. Geisler, S. *et al.* Vincristine and bortezomib use distinct upstream mechanisms to activate a common SARM1-dependent axon degeneration program. *JCI Insight* **4**, (2020).

82. Mack, T. G. *et al.* Wallerian degeneration of injured axons and synapses is delayed by a Ube4b/Nmnat chimeric gene. *Nature neuroscience* **4**, 1199–1206 (2001).

83. Watanabe, M., Tsukiyama, T. & Hatakeyama, S. Protection of vincristine-induced neuropathy by WldS expression and the independence of the activity of Nmnat1. *Neurosci. Lett.* **411**, 228–232 (2007).

84. Cohen, M. S., Ghosh, A. K., Kim, H. J., Jeon, N. L. & Jaffrey, S. R. Chemical genetic-mediated spatial regulation of protein expression in neurons reveals an axonal function for wld(s). *Chem. Biol.* **19**, 179–187 (2012).

85. Myers, R., Heckman, H. & Rodriguez, M. Reduced Hyperalgesia in Nerve-Injured WLD Mice : Relationship to Nerve Fiber Phagocytosis , Axonal Degeneration , and Regeneration in Normal Mice. **101**, 94–101 (1996).

86. Ramer, M. S., French, G. D. & Bisby, M. A. Wallerian degeneration is required for both neuropathic pain and sympathetic sprouting into the DRG. *Pain* **72**, 71–8 (1997).

87. Sommer, C. & Schäfers, M. Painful mononeuropathy in C57BL/Wld mice with delayed Wallerian degeneration: Differential effects of cytokine production and nerve regeneration on thermal and mechanical hypersensitivity. *Brain Research* **784**, 154–162 (1998).

88. Meyer zu Horste, G. *et al.* The Wlds transgene reduces axon loss in a Charcot-Marie-Tooth disease 1A rat model and nicotinamide delays post-traumatic axonal degeneration. *Neurobiol. Dis.* **42**, 1–8 (2011).

89. Stum, M. *et al.* An assessment of mechanisms underlying peripheral axonal degeneration caused by aminoacyl-tRNA synthetase mutations. *Mol. Cell. Neurosci.* **46**, 432–443 (2011).

90. Yin, T. C. *et al.* Acute Axonal Degeneration Drives Development of Cognitive, Motor, and Visual Deficits after Blast-Mediated Traumatic Brain Injury in Mice. *eNeuro* **3**, (2016).

91. Henninger, N. *et al.* Attenuated traumatic axonal injury and improved functional outcome after traumatic brain injury in mice lacking Sarm1. *Brain* **139**, 1094–1105 (2016).

92. Gillingwater, T. H., Haley, J. E., Ribchester, R. R. & Horsburgh, K. Neuroprotection after transient global cerebral ischemia in Wld(s) mutant mice. *J. Cereb. Blood Flow Metab.* **24**, 62–66 (2004).

93. Howell, G. R. *et al.* Axons of retinal ganglion cells are insulted in the optic nerve early in DBA/2J glaucoma. *J Cell Biol* **179**, 1523–1537 (2007).

94. Bull, N. D., Chidlow, G., Wood, J. P. M., Martin, K. R. & Casson, R. J. The mechanism of axonal degeneration after perikaryal excitotoxic injury to the retina. *Experimental Neurology* **236**, 34–45 (2012).

95. WANG, C.-H. *et al.* Protective role of Wallerian degeneration slow (Wlds) gene against retinal ganglion cell body damage in a Wallerian degeneration model. *Exp Ther Med* **5**, 621–625 (2013).

96. Zhu, Y., Zhang, L., Sasaki, Y., Milbrandt, J. & Gidday, J. M. Protection of Mouse Retinal Ganglion Cell Axons and Soma from Glaucomatous and Ischemic Injury by Cytoplasmic Overexpression of Nmnat1. *Invest Ophthalmol Vis Sci* **54**, 25–36 (2013).

97. Massoll, C., Mando, W. & Chintala, S. K. Excitotoxicity upregulates SARM1 protein expression and promotes Wallerian-like degeneration of retinal ganglion cells and their axons. *Invest. Ophthalmol. Vis. Sci.* **54**, 2771–2780 (2013).

98. Hasbani, D. M. & O'Malley, K. L. WldS mice are protected against the Parkinsonian mimetic MPTP. *Experimental Neurology* **202**, 93–99 (2006).

99. Cheng, H.-C. & Burke, R. E. The Wld(S) mutation delays anterograde, but not retrograde, axonal degeneration of the dopaminergic nigro-striatal pathway in vivo. *J. Neurochem.* **113**, 683–691 (2010).

100. Antenor-Dorsey, J. A. V. & O'Malley, K. L. WldS but not Nmnat1 protects dopaminergic neurites from MPP+ neurotoxicity. *Mol Neurodegener* **7**, 5 (2012).

101. Sur, M. *et al.* Sarm1 induction and accompanying inflammatory response mediates age-dependent susceptibility to rotenone-induced neurotoxicity. *Cell Death Discov* **4**, (2018).

102. Vande Velde, C., Garcia, M. L., Yin, X., Trapp, B. D. & Cleveland, D. W. The neuroprotective factor Wlds does not attenuate mutant SOD1-mediated motor neuron disease. *NeuroMolecular Medicine* **5**, 193–203 (2004).

103. Fischer, L. R. *et al.* The WldS gene modestly prolongs survival in the SOD1G93A fALS mouse. *Neurobiology of Disease* **19**, 293–300 (2005).

104. Peters, O. M. *et al.* Loss of Sarm1 does not suppress motor neuron degeneration in the SOD1G93A mouse model of amyotrophic lateral sclerosis. *Hum Mol Genet* **27**, 3761–3771 (2018).

105. White, M. A. *et al.* Sarm1 deletion suppresses TDP-43-linked motor neuron degeneration and cortical spine loss. *Acta Neuropathol Commun* **7**, 166 (2019).

106. Kaneko, S. *et al.* Protecting Axonal Degeneration by Increasing Nicotinamide Adenine Dinucleotide Levels in Experimental Autoimmune Encephalomyelitis Models. *J. Neurosci.* **26**, 9794–9804 (2006).

107. Tsunoda, I., Tanaka, T., Terry, E. J. & Fujinami, R. S. Contrasting Roles for Axonal Degeneration in an Autoimmune versus Viral Model of Multiple Sclerosis: When Can Axonal Injury Be Beneficial? *The American Journal of Pathology* **170**, 214–226 (2007).

108. Chitnis, T. *et al.* Elevated Neuronal Expression of CD200 Protects Wlds Mice from Inflammation-Mediated Neurodegeneration. *The American Journal of Pathology* **170**, 1695–1712 (2007).

109. Griffin, J. W., George, E. B. & Chaudhry, V. Wallerian degeneration in peripheral nerve disease. *Baillieres Clin Neurol* **5**, 65–75 (1996).

110. Gilley, J., Mayer, P. R., Yu, G. & Coleman, M. P. Low levels of NMNAT2 compromise axon development and survival. *Hum. Mol. Genet.* **28**, 448–458 (2019).

111. Gilley, J., Ribchester, R. R. & Coleman, M. P. Sarm1 Deletion, but Not WldS, Confers Lifelong Rescue in a Mouse Model of Severe Axonopathy. *Cell Rep* **21**, 10–16 (2017).

112. Huppke, P. *et al.* Homozygous NMNAT2 mutation in sisters with polyneuropathy and erythromelalgia. *Exp. Neurol.* **320**, 112958 (2019).

113. Lukacs, M. *et al.* Severe biallelic loss-of-function mutations in nicotinamide mononucleotide adenylyltransferase 2 (NMNAT2) in two fetuses with fetal akinesia deformation sequence. *Exp. Neurol.* **320**, 112961 (2019).

114. Hicks, A. N. *et al.* Nicotinamide mononucleotide adenylyltransferase 2 (Nmnat2) regulates axon integrity in the mouse embryo. *PLoS ONE* **7**, e47869 (2012).

115. Schulz, A., Wagner, F., Ungelenk, M., Kurth, I. & Redecker, C. Stroke-like onset of brain stem degeneration presents with unique MRI sign and heterozygous NMNAT2 variant: a case report. *Transl Neurodegener* **5**, (2016).

116. Ali, Y. O. *et al.* NMNAT2:HSP90 Complex Mediates Proteostasis in Proteinopathies. *PLOS Biology* **14**, e1002472–e1002472 (2016).

117. Milde, S., Adalbert, R., Elaman, M. H. & Coleman, M. P. Axonal transport declines with age in two distinct phases separated by a period of relative stability. *Neurobiology of Aging* **36**, 971–981 (2015).

118. Cheng, X.-S. *et al.* Nmnat2 attenuates Tau phosphorylation through activation of PP2A. *J. Alzheimers Dis.* **36**, 185–195 (2013).

119. Ljungberg, M. C. *et al.* CREB-activity and nmnat2 transcription are down-regulated prior to neurodegeneration, while NMNAT2 over-expression is neuroprotective, in a mouse model of human tauopathy. *Hum. Mol. Genet.* **21**, 251–267 (2012).

120. Fogh, I. *et al.* A genome-wide association meta-analysis identifies a novel locus at 17q11.2 associated with sporadic amyotrophic lateral sclerosis. *Hum. Mol. Genet.* **23**, 2220–2231 (2014).

121. van Rheenen, W. *et al.* Genome-wide association analyses identify new risk variants and the genetic architecture of amyotrophic lateral sclerosis. *Nat. Genet.* **48**, 1043–1048 (2016).

122. Coleman, M. P. & Höke, A. Programmed axon degeneration: from mouse to mechanism to medicine. *Nat. Rev. Neurosci.* **21**, 183–196 (2020).

123. Klim, J. R. *et al.* ALS-implicated protein TDP-43 sustains levels of STMN2, a mediator of motor neuron growth and repair. *Nat. Neurosci.* **22**, 167–179 (2019).

124. Melamed, Z. *et al.* Premature polyadenylation-mediated loss of stathmin-2 is a hallmark of TDP-43-dependent neurodegeneration. *Nat. Neurosci.* **22**, 180–190 (2019).

125. Shwe, T., Pratchayasakul, W., Chattipakorn, N. & Chattipakorn, S. C. Role of D-galactose-induced brain aging and its potential used for therapeutic interventions. *Exp. Gerontol.* **101**, 13–36 (2018).

126. Mink, M., Fogelgren, B., Olszewski, K., Maroy, P. & Csiszar, K. A novel human gene (SARM) at chromosome 17q11 encodes a protein with a SAM motif and structural similarity to Armadillo/beta-catenin that is conserved in mouse, Drosophila, and Caenorhabditis elegans. *Genomics* **74**, 234–244 (2001).

127. Couillault, C. *et al.* TLR-independent control of innate immunity in Caenorhabditis elegans by the TIR domain adaptor protein TIR-1, an ortholog of human SARM. *Nat. Immunol.* **5**, 488–494 (2004).

128. Carty, M. *et al.* The human adaptor SARM negatively regulates adaptor protein TRIF–dependent Toll-like receptor signaling. *Nat Immunol* **7**, 1074–1081 (2006).

129. Dalod, M. Studies of SARM1 uncover similarities between immune and neuronal responses to danger. *Sci. STKE* **2007**, pe73 (2007).

130. Mukherjee, P., Woods, T. A., Moore, R. A. & Peterson, K. E. Activation of the innate signaling molecule MAVS by bunyavirus infection upregulates the adaptor protein SARM1, leading to neuronal death. *Immunity* **38**, 705–716 (2013).

131. Szretter, K. J. *et al.* The immune adaptor molecule SARM modulates tumor necrosis factor alpha production and microglia activation in the brainstem and restricts West Nile Virus pathogenesis. *J. Virol.* **83**, 9329–9338 (2009).

132. Kim, Y. *et al.* MyD88-5 links mitochondria, microtubules, and JNK3 in neurons and regulates neuronal survival. *J. Exp. Med.* **204**, 2063–2074 (2007).

133. Uccellini, M. B. *et al.* Passenger Mutations Confound Phenotypes of SARM1-Deficient Mice. *Cell Rep* **31**, 107498 (2020).

134. Neupert, W. & Herrmann, J. M. Translocation of Proteins into Mitochondria. *Annu. Rev. Biochem.* **76**, 723–749 (2007).

135. Dolezal, P., Likic, V., Tachezy, J. & Lithgow, T. Evolution of the Molecular Machines for Protein Import into Mitochondria. *Science* **313**, 314–318 (2006).

136. Hurt, E. C., Pesold-Hurt, B. & Schatz, G. The cleavable prepiece of an imported mitochondrial protein is sufficient to direct cytosolic dihydrofolate reductase into the mitochondrial matrix. *FEBS Lett.* **178**, 306–310 (1984).

137. Panneerselvam, P., Singh, L. P., Ho, B., Chen, J. & Ding, J. L. Targeting of pro-apoptotic TLR adaptor SARM to mitochondria: definition of the critical region and residues in the signal sequence. *Biochem J* **442**, 263–271 (2012).

138. Bratkowski, M. *et al.* Structural and Mechanistic Regulation of the Pro-degenerative NAD Hydrolase SARM1. *Cell Reports* **32**, 107999 (2020).

139. Sporny, M. *et al.* The Structural Basis for SARM1 Inhibition, and Activation Under Energetic Stress. *bioRxiv* 2020.08.05.238287 (2020) doi:10.1101/2020.08.05.238287.

140. Knight, M. J., Leettola, C., Gingery, M., Li, H. & Bowie, J. U. A human sterile alpha motif domain polymerizome. *Protein Sci.* **20**, 1697–1706 (2011).

141. Qiao, F. & Bowie, J. U. The many faces of SAM. *Sci. STKE* **2005**, re7 (2005).

142. Sporny, M. *et al.* Structural Evidence for an Octameric Ring Arrangement of SARM1. *J. Mol. Biol.* **431**, 3591–3605 (2019).

143. Horsefield, S. *et al.* NAD+ cleavage activity by animal and plant TIR domains in cell death pathways. *Science* **365**, 793–799 (2019).

144. Ve, T., Williams, S. J. & Kobe, B. Structure and function of Toll/interleukin-1 receptor/resistance protein (TIR) domains. *Apoptosis* **20**, 250–261 (2015).

145. Gay, N. J., Symmons, M. F., Gangloff, M. & Bryant, C. E. Assembly and localization of Toll-like receptor signalling complexes. *Nat. Rev. Immunol.* **14**, 546–558 (2014).

146. Pawson, T. & Nash, P. Assembly of Cell Regulatory Systems Through Protein Interaction Domains. *Science* **300**, 445–452 (2003).

147. Toshchakov, V. Y. & Neuwald, A. F. A survey of TIR domain sequence and structure divergence. *Immunogenetics* **72**, 181–203 (2020).

148. Vajjhala, P. R., Ve, T., Bentham, A., Stacey, K. J. & Kobe, B. The molecular mechanisms of signaling by cooperative assembly formation in innate immunity pathways. *Mol. Immunol.* **86**, 23–37 (2017).

149. Ve, T. *et al.* Structural basis of TIR-domain-assembly formation in MAL- and MyD88-dependent TLR4 signaling. *Nat. Struct. Mol. Biol.* **24**, 743–751 (2017).

150. Latty, S. L. *et al.* Activation of Toll-like receptors nucleates assembly of the MyDDosome signaling hub. *Elife* **7**, (2018).

151. Zhang, X. *et al.* Multiple functional self-association interfaces in plant TIR domains. *Proc. Natl. Acad. Sci. U.S.A.* **114**, E2046–E2052 (2017).

152. Nishimura, M. T. *et al.* TIR-only protein RBA1 recognizes a pathogen effector to regulate cell death in Arabidopsis. *Proc. Natl. Acad. Sci. U.S.A.* **114**, E2053–E2062 (2017).

153. Gerdts, N. A. D., Gerdts, J., Summers, D. W., Milbrandt, J. & Diantonio, A. Review Axon Self-Destruction : New Links. *Neuron* **89**, 449–460 (2016).

154. Chen, C.-Y., Lin, C.-W., Chang, C.-Y., Jiang, S.-T. & Hsueh, Y.-P. Sarm1, a negative regulator of innate immunity, interacts with syndecan-2 and regulates neuronal morphology. *J. Cell Biol.* **193**, 769–784 (2011).

155. Liu, H. Y., Chen, C. Y. & Hsueh, Y. P. Innate immune responses regulate morphogenesis and degeneration: Roles of Toll-like receptors and Sarm1 in neurons. *Neuroscience Bulletin* **30**, 645–654 (2014).

156. Essuman, K. *et al.* TIR Domain Proteins Are an Ancient Family of NAD+-Consuming Enzymes. *Curr. Biol.* **28**, 421-430.e4 (2018).

157. Essuman, K. *et al.* The SARM1 Toll/Interleukin-1 Receptor Domain Possesses Intrinsic NAD+ Cleavage Activity that Promotes Pathological Axonal Degeneration. *Neuron* **93**, 1334-1343.e5 (2017).

158. Sasaki, Y., Nakagawa, T., Mao, X., DiAntonio, A. & Milbrandt, J. NMNAT1 inhibits axon degeneration via blockade of SARM1-mediated NAD+ depletion. *Elife* **5**, (2016).

159. DiStefano, M. *et al.* NMN Deamidase Delays Wallerian Degeneration and Rescues Axonal Defects Caused by NMNAT2 Deficiency In Vivo. *Current Biology* **27**, 784–794 (2017).

160. Zhao, Z. Y. *et al.* A Cell-Permeant Mimetic of NMN Activates SARM1 to Produce Cyclic ADP-Ribose and Induce Non-apoptotic Cell Death. *iScience* **15**, 452–466 (2019).

161. Loreto, A. *et al.* Potent activation of SARM1 by NMN analogue VMN underlies vacor neurotoxicity. *bioRxiv* 2020.09.18.304261 (2020) doi:10.1101/2020.09.18.304261.

162. Murata, H. *et al.* c-Jun N-terminal kinase (JNK)-mediated phosphorylation of SARM1 regulates NAD+ cleavage activity to inhibit mitochondrial respiration. *J. Biol. Chem.* **293**, 18933–18943 (2018).

163. Sasaki, Y. *et al.* cADPR is a gene dosage-sensitive biomarker of SARM1 activity in healthy, compromised, and degenerating axons. *Experimental Neurology* **329**, 113252 (2020).

164. Berger, F., Ramírez-Hernández, M. H. & Ziegler, M. The new life of a centenarian: Signalling functions of NAD(P). *Trends in Biochemical Sciences* **29**, 111–118 (2004).

165. Yan, T. *et al.* Nmnat2 delays axon degeneration in superior cervical ganglia dependent on its NAD synthesis activity. *Neurochemistry International* **56**, 101–106 (2010).

166. Milde, S., Fox, a N., Freeman, M. R. & Coleman, M. P. Deletions within its subcellular targeting domain enhance the axon protective capacity of Nmnat2 in vivo. *Scientific reports* **3**, 2567–2567 (2013).

167. Milde, S. & Coleman, M. P. Identification of Palmitoyltransferase and Thioesterase Enzymes That Control the Subcellular Localization of Axon Survival Factor Nicotinamide Mononucleotide Adenylyltransferase 2 (NMNAT2). *J Biol Chem* **289**, 32858–32870 (2014).

168. Fang, C., Bourdette, D. & Banker, G. Oxidative stress inhibits axonal transport: implications for neurodegenerative diseases. *Molecular neurodegeneration* **7**, 29–29 (2012).

169. Feng, Y. *et al.* Overexpression of Wld(S) or Nmnat2 in mauthner cells by single-cell electroporation delays axon degeneration in live zebrafish. *J. Neurosci. Res.* **88**, 3319–3327 (2010).

170. Avery, M. A., Sheehan, A. E., Kerr, K. S., Wang, J. & Freeman, M. R. Wld S requires Nmnat1 enzymatic activity and N16-VCP interactions to suppress Wallerian degeneration. *J. Cell Biol.* **184**, 501–513 (2009).

171. Milde, S., Gilley, J. & Coleman, M. P. Subcellular localization determines the stability and axon protective capacity of axon survival factor Nmnat2. *PLoS Biol.* **11**, e1001539 (2013).

172. Levy, A. D. *et al.* Subcellular Golgi localization of stathmin family proteins is promoted by a specific set of DHHC palmitoyl transferases. *Mol Biol Cell* **22**, 1930–1942 (2011).

173. Niu, J. *et al.* Coupled Control of Distal Axon Integrity and Somal Responses to Axonal Damage by the Palmitoyl Acyltransferase ZDHHC17. *bioRxiv* 2020.09.01.276287 (2020) doi:10.1101/2020.09.01.276287.

174. Lunn, E. R., Perry, V. H., Brown, M. C., Rosen, H. & Gordon, S. Absence of Wallerian Degeneration does not Hinder Regeneration in Peripheral Nerve. *The European journal of neuroscience* **1**, 27–33 (1989).

175. Mack, T. G. *et al.* Wallerian degeneration of injured axons and synapses is delayed by a Ube4b/Nmnat chimeric gene. *Nature neuroscience* **4**, 1199–1206 (2001).

176. Conforti, L. *et al.* A Ufd2/D4Cole1e chimeric protein and overexpression of Rbp7 in the slow Wallerian degeneration (WldS) mouse. *Proc. Natl. Acad. Sci. U.S.A.* **97**, 11377–11382 (2000).

177. Lunn, E. R., Perry, V. H., Brown, M. C., Rosen, H. & Gordon, S. Absence of Wallerian Degeneration does not Hinder Regeneration in Peripheral Nerve. *The European journal of neuroscience* **1**, 27–33 (1989).

178. Perry, V. H., Brown, M. C. & Lunn, E. R. Very Slow Retrograde and Wallerian Degeneration in the CNS of C57BL/Ola Mice. *Eur. J. Neurosci.* **3**, 102–105 (1991).

179. Crawford, T. O., Hsieh, S. T., Schryer, B. L. & Glass, J. D. Prolonged axonal survival in transected nerves of C57BL/Ola mice is independent of age. *J. Neurocytol.* **24**, 333–340 (1995).

180. Wang, J. *et al.* A local mechanism mediates NAD-dependent protection of axon degeneration. *J Cell Biol* **170**, 349–355 (2005).

181. Conforti, L. *et al.* Wld S protein requires Nmnat activity and a short N-terminal sequence to protect axons in mice. *J. Cell Biol.* **184**, 491–500 (2009).

182. Gillingwater, T. H. *et al.* Age-dependent synapse withdrawal at axotomised neuromuscular junctions in Wlds mutant and Ube4b/Nmnat transgenic mice. *J Physiol* **543**, 739–755 (2002).

183. Gillingwater, T. H., Ingham, C. A., Coleman, M. P. & Ribchester, R. R. Ultrastructural correlates of synapse withdrawal at axotomized neuromuscular junctions in mutant and transgenic mice expressing the Wld gene. *J. Anat.* **203**, 265–276 (2003).

184. Gillingwater, T. H. *et al.* Delayed synaptic degeneration in the CNS of Wlds mice after cortical lesion. *Brain* **129**, 1546–1556 (2006).

185. Ribchester, R. R. *et al.* Persistence of Neuromuscular Junctions after Axotomy in Mice with Slow Wallerian Degeneration (C57BL/Wlds). *European Journal of Neuroscience* **7**, 1641–1650 (1995).

186. Adalbert, R. *et al.* A rat model of slow Wallerian degeneration (WldS) with improved preservation of neuromuscular synapses. *Eur. J. Neurosci.* **21**, 271–277 (2005).

187. Brown, R. *et al.* Activity-dependent degeneration of axotomized neuromuscular synapses in WldS mice. *Neuroscience* **290**, 300–320 (2015).

188. Glass, J. D., Brushart, T. M., George, E. B. & Griffin, J. W. Prolonged survival of transected nerve fibres in C57BL/Ola mice is an intrinsic characteristic of the axon. *J. Neurocytol.* **22**, 311–321 (1993).

189. Vaquié, A. *et al.* Injured Axons Instruct Schwann Cells to Build Constricting Actin Spheres to Accelerate Axonal Disintegration. *Cell Rep* **27**, 3152-3166.e7 (2019).

190. Babetto, E., Wong, K. M. & Beirowski, B. A glycolytic shift in Schwann cells supports injured axons. *Nat. Neurosci.* (2020) doi:10.1038/s41593-020-0689-4.

191. Shen, H., Hyrc, K. L. & Goldberg, M. P. Maintaining energy homeostasis is an essential component of Wld(S)-mediated axon protection. *Neurobiol. Dis.* **59**, 69–79 (2013).

192. Coleman, M. P. & Perry, V. H. Axon pathology in neurological disease: a neglected therapeutic target. *Trends Neurosci.* **25**, 532–537 (2002).

193. Gillingwater, T. H. & Ribchester, R. R. Compartmental neurodegeneration and synaptic plasticity in the Wld(s) mutant mouse. *J. Physiol. (Lond.)* **534**, 627–639 (2001).

194. Araki, T. Increased Nuclear NAD Biosynthesis and SIRT1 Activation Prevent Axonal Degeneration. *Science* **305**, 1010–1013 (2004).

195. Jia, H. *et al.* Identification of a critical site in Wld(s): essential for Nmnat enzyme activity and axon-protective function. *Neurosci. Lett.* **413**, 46–51 (2007).

196. Yahata, N., Yuasa, S. & Araki, T. Nicotinamide mononucleotide adenylyltransferase expression in mitochondrial matrix delays Wallerian degeneration. *J. Neurosci.* **29**, 6276–6284 (2009).

197. Kitay, B. M., McCormack, R., Wang, Y., Tsoulfas, P. & Zhai, R. G. Mislocalization of neuronal mitochondria reveals regulation of Wallerian degeneration and NMNAT/WLD(S)-mediated axon protection independent of axonal mitochondria. *Hum. Mol. Genet.* **22**, 1601–1614 (2013).

198. MacDonald, J. M. *et al.* The Drosophila cell corpse engulfment receptor Draper mediates glial clearance of severed axons. *Neuron* **50**, 869–881 (2006).

199. Martin, S. M., O'Brien, G. S., Portera-Cailliau, C. & Sagasti, A. Wallerian degeneration of zebrafish trigeminal axons in the skin is required for regeneration and developmental pruning. *Development* **137**, 3985–3994 (2010).

200. Fang, C., Bernardes-Silva, M., Coleman, M. P. & Perry, V. H. The cellular distribution of the Wld s chimeric protein and its constituent proteins in the CNS. *Neuroscience* **135**, 1107–1118 (2005).

201. Beirowski, B. *et al.* Non-Nuclear WldS Determines Its Neuroprotective Efficacy for Axons and Synapses In Vivo. *J. Neurosci.* **29**, 653–668 (2009).

202. Sasaki, Y., Vohra, B. P. S., Lund, F. E. & Milbrandt, J. Nicotinamide Mononucleotide Adenylyl Transferase-Mediated Axonal Protection Requires Enzymatic Activity But Not Increased Levels of Neuronal Nicotinamide Adenine Dinucleotide. *J Neurosci* **29**, 5525–5535 (2009).

203. Babetto, E. *et al.* Targeting NMNAT1 to axons and synapses transforms its neuroprotective potency in vivo. *J. Neurosci.* **30**, 13291–13304 (2010).

204. Wang, J. T., Medress, Z. A., Vargas, M. E. & Barres, B. A. Local axonal protection by WldS as revealed by conditional regulation of protein stability. *Proc. Natl. Acad. Sci. U.S.A.* **112**, 10093–10100 (2015).

205. van den Boom, J. & Meyer, H. VCP/p97-Mediated Unfolding as a Principle in Protein Homeostasis and Signaling. *Mol. Cell* **69**, 182–194 (2018).

206. Wang, Q., Song, C. & Li, C.-C. H. Molecular perspectives on p97-VCP: progress in understanding its structure and diverse biological functions. *J. Struct. Biol.* **146**, 44–57 (2004).

207. Stolz, A., Hilt, W., Buchberger, A. & Wolf, D. H. Cdc48: a power machine in protein degradation. *Trends Biochem. Sci.* **36**, 515–523 (2011).

208. Meyer, H., Bug, M. & Bremer, S. Emerging functions of the VCP/p97 AAA-ATPase in the ubiquitin system. *Nat. Cell Biol.* **14**, 117–123 (2012).

209. Bug, M. & Meyer, H. Expanding into new markets--VCP/p97 in endocytosis and autophagy. *J. Struct. Biol.* **179**, 78–82 (2012).

210. Yamanaka, K., Sasagawa, Y. & Ogura, T. Recent advances in p97/VCP/Cdc48 cellular functions. *Biochim. Biophys. Acta* **1823**, 130–137 (2012).

211. Wójcik, C. *et al.* Valosin-containing protein (p97) is a regulator of endoplasmic reticulum stress and of the degradation of N-end rule and ubiquitin-fusion degradation pathway substrates in mammalian cells. *Mol. Biol. Cell* **17**, 4606–4618 (2006).

212. Conforti, L. *et al.* Reducing expression of NAD+ synthesizing enzyme NMNAT1 does not affect the rate of Wallerian degeneration. *FEBS J.* **278**, 2666–2679 (2011).

213. Sasaki, Y. & Milbrandt, J. Axonal degeneration is blocked by nicotinamide mononucleotide adenylyltransferase (Nmnat) protein transduction into transected axons. *J. Biol. Chem.* **285**, 41211–41215 (2010).

214. Grozio, A. *et al.* Slc12a8 is a nicotinamide mononucleotide transporter. *Nat Metab* **1**, 47–57 (2019).

215. Loring, H. S., Icso, J. D., Nemmara, V. V. & Thompson, P. R. Initial Kinetic Characterization of Sterile Alpha and Toll/Interleukin Receptor Motif-Containing Protein 1. *Biochemistry* **59**, 933–942 (2020).

216. Di Stefano, M. *et al.* A rise in NAD precursor nicotinamide mononucleotide (NMN) after injury promotes axon degeneration. *Cell Death Differ.* **22**, 731–742 (2015).

217. Bonkowski, M. S. & Sinclair, D. A. Slowing ageing by design: the rise of NAD + and sirtuin-activating compounds. *Nature Reviews Molecular Cell Biology* **17**, 679–690 (2016).

218. Brown, K. D. *et al.* Activation of SIRT3 by the NAD^+ precursor nicotinamide riboside protects from noise-induced hearing loss. *Cell metabolism* vol. 20 https://pubmed.ncbi.nlm.nih.gov/25470550/ (2014).

219. Gong, B. *et al.* Nicotinamide riboside restores cognition through an upregulation of proliferator-activated receptor-γ coactivator 1α regulated β-secretase 1 degradation and

mitochondrial gene expression in Alzheimer's mouse models. *Neurobiology of Aging* **34**, 1581–1588 (2013).

220. Zhang, H. *et al.* NAD+ repletion improves mitochondrial and stem cell function and enhances life span in mice. *Science* **352**, 1436–1443 (2016).
221. Mills, K. F. *et al.* Long-Term Administration of Nicotinamide Mononucleotide Mitigates Age-Associated Physiological Decline in Mice. *Cell Metab.* **24**, 795–806 (2016).
222. de Picciotto, N. E. *et al.* Nicotinamide mononucleotide supplementation reverses vascular dysfunction and oxidative stress with aging in mice. *Aging Cell* **15**, 522–530 (2016).
223. Park, J. H., Long, A., Owens, K. & Kristian, T. Nicotinamide mononucleotide inhibits post-ischemic NAD+ degradation and dramatically ameliorates brain damage following global cerebral ischemia. *Neurobiology of Disease* **95**, 102–110 (2016).
224. Cargnello, M. & Roux, P. P. Activation and function of the MAPKs and their substrates, the MAPK-activated protein kinases. *Microbiol. Mol. Biol. Rev.* **75**, 50–83 (2011).
225. Nakata, K. *et al.* Regulation of a DLK-1 and p38 MAP kinase pathway by the ubiquitin ligase RPM-1 is required for presynaptic development. *Cell* **120**, 407–420 (2005).
226. Collins, C. A., Wairkar, Y. P., Johnson, S. L. & DiAntonio, A. Highwire restrains synaptic growth by attenuating a MAP kinase signal. *Neuron* **51**, 57–69 (2006).
227. Miller, B. A DLK and JNK Dependent Axon Self-destruction Program Promotes Wallerian Degeneration. *The Journal of cell …* **12**, 387–389 (2011).
228. Karney-Grobe, S., Russo, A., Frey, E., Milbrandt, J. & DiAntonio, A. HSP90 is a chaperone for DLK and is required for axon injury signaling. *Proc. Natl. Acad. Sci. U.S.A.* **115**, E9899–E9908 (2018).
229. Yang, J. *et al.* Pathological axonal death through a Mapk cascade that triggers a local energy deficit. *Cell* **160**, 161–176 (2015).
230. Walker, L. J. *et al.* MAPK signaling promotes axonal degeneration by speeding the turnover of the axonal maintenance factor NMNAT2. *Elife* **6**, (2017).

231. Gong, B., Radulovic, M., Figueiredo-Pereira, M. E. & Cardozo, C. The Ubiquitin-Proteasome System: Potential Therapeutic Targets for Alzheimer's Disease and Spinal Cord Injury. *Front. Mol. Neurosci.* **9**, (2016).

232. Schwartz, A. L. & Ciechanover, A. Targeting proteins for destruction by the ubiquitin system: implications for human pathobiology. *Annu. Rev. Pharmacol. Toxicol.* **49**, 73–96 (2009).

233. Hwu, W.-L. *et al.* Gene Therapy for Aromatic l-Amino Acid Decarboxylase Deficiency. *Science Translational Medicine* **4**, 134ra61-134ra61 (2012).

234. Wakatsuki, S., Saitoh, F. & Araki, T. ZNRF1 promotes Wallerian degeneration by degrading AKT to induce GSK3B-dependent CRMP2 phosphorylation. *Nat. Cell Biol.* **13**, 1415–1423 (2011).

235. MacInnis, B. L. & Campenot, R. B. Regulation of Wallerian degeneration and nerve growth factor withdrawal-induced pruning of axons of sympathetic neurons by the proteasome and the MEK/Erk pathway. *Mol. Cell. Neurosci.* **28**, 430–439 (2005).

236. Hoopfer, E. D. *et al.* Wlds protection distinguishes axon degeneration following injury from naturally occurring developmental pruning. *Neuron* **50**, 883–895 (2006).

237. Barrientos, S. A. *et al.* Axonal degeneration is mediated by the mitochondrial permeability transition pore. *J. Neurosci.* **31**, 966–978 (2011).

238. Xiong, X. *et al.* The Highwire Ubiquitin Ligase Promotes Axonal Degeneration by Tuning Levels of Nmnat Protein. *PLoS Biology* **10**, 1–18 (2012).

239. Babetto, E., Beirowski, B., Russler, E., Milbrandt, J. & DiAntonio, A. The Phr1 ubiquitin ligase promotes injury-induced axon self-destruction. **16**, 387–393 (2013).

240. Desbois, M. *et al.* PAM forms an atypical SCF ubiquitin ligase complex that ubiquitinates and degrades NMNAT2. *J. Biol. Chem.* **293**, 13897–13909 (2018).

241. Xiong, X. *et al.* The Highwire Ubiquitin Ligase Promotes Axonal Degeneration by Tuning Levels of Nmnat Protein. *PLoS Biology* **10**, 1–18 (2012).

242. Schlaepfer, W. W. Structural alterations of peripheral nerve induced by the calcium ionophore A23187. *Brain Res.* **136**, 1–9 (1977).

243. Schlaepfer, W. W. & Hasler, M. B. Characterization of the calcium-induced disruption of neurofilaments in rat peripheral nerve. *Brain Res.* **168**, 299–309 (1979).

244. LoPachin, R. M., LoPachin, V. R. & Saubermann, A. J. Effects of axotomy on distribution and concentration of elements in rat sciatic nerve. *J. Neurochem.* **54**, 320–332 (1990).

245. Gerdts, J., Sasaki, Y., Vohra, B., Marasa, J. & Milbrandt, J. Image-based screening identifies novel roles for IkappaB kinase and glycogen synthase kinase 3 in axonal degeneration. *J. Biol. Chem.* **286**, 28011–28018 (2011).

246. Adalbert, R. *et al.* Intra-axonal calcium changes after axotomy in wild-type and slow Wallerian degeneration axons. *Neuroscience* **225**, 44–54 (2012).

247. Yang, J. *et al.* Regulation of axon degeneration after injury and in development by the endogenous calpain inhibitor calpastatin. *Neuron* **80**, 1175–1189 (2013).

248. Avery, M. A. *et al.* WldS prevents axon degeneration through increased mitochondrial flux and enhanced mitochondrial Ca2+ buffering. *Curr. Biol.* **22**, 596–600 (2012).

249. Glass, J. D., Schryer, B. L. & Griffin, J. W. Calcium-mediated degeneration of the axonal cytoskeleton in the Ola mouse. *J. Neurochem.* **62**, 2472–2475 (1994).

250. Loreto, A., Di Stefano, M., Gering, M. & Conforti, L. Wallerian Degeneration Is Executed by an NMN-SARM1-Dependent Late Ca(2+) Influx but Only Modestly Influenced by Mitochondria. *Cell Rep* **13**, 2539–2552 (2015).

251. Fliegert, R., Gasser, A. & Guse, A. H. Regulation of calcium signalling by adenine-based second messengers. *Biochem. Soc. Trans.* **35**, 109–114 (2007).

252. Glass, J. D., Culver, D. G., Levey, A. I. & Nash, N. R. Very early activation of m-calpain in peripheral nerve during Wallerian degeneration. *J. Neurol. Sci.* **196**, 9–20 (2002).

253. Kamakura, K., Ishiura, S., Sugita, H. & Toyokura, Y. Identification of Ca2+-activated neutral protease in the peripheral nerve and its effects on neurofilament degeneration. *J. Neurochem.* **40**, 908–913 (1983).

254. Kamakura, K., Ishiura, S., Suzuki, K., Sugita, H. & Toyokura, Y. Calcium-activated neutral protease in the peripheral nerve, which requires microM order Ca2+, and its effect on the neurofilament triplet. *J. Neurosci. Res.* **13**, 391–403 (1985).

255. Billger, M., Wallin, M. & Karlsson, J. O. Proteolysis of tubulin and microtubule-associated proteins 1 and 2 by calpain I and II. Difference in sensitivity of assembled and disassembled microtubules. *Cell Calcium* **9**, 33–44 (1988).

256. Johnson, G. V., Litersky, J. M. & Jope, R. S. Degradation of microtubule-associated protein 2 and brain spectrin by calpain: a comparative study. *J. Neurochem.* **56**, 1630–1638 (1991).

257. Zhang, J.-N. *et al.* Calpain-mediated cleavage of collapsin response mediator protein-2 drives acute axonal degeneration. *Sci Rep* **6**, 37050 (2016).

258. Couto, L. A., Narciso, M. S., Hokoç, J. N. & Martinez, A. M. B. Calpain inhibitor 2 prevents axonal degeneration of opossum optic nerve fibers. *Journal of Neuroscience Research* **77**, 410–419 (2004).

259. Girouard, M.-P. *et al.* Collapsin Response Mediator Protein 4 (CRMP4) Facilitates Wallerian Degeneration and Axon Regeneration following Sciatic Nerve Injury. *eNeuro* **7**, (2020).

260. Andrea Loreto, A. *et al.* Wallerian Degeneration Is Executed by an NMN- SARM1-Dependent Late Ca 2+ Influx but Only Modestly Influenced by Mitochondria Influx but Only Modestly Influenced by Mitochondria. *Cell Reports* **13**, 2539–2552 (2015).

261. Ernster, L. & Schatz, G. Mitochondria: a historical review. *J. Cell Biol.* **91**, 227s–255s (1981).

262. Turrens, J. F. Mitochondrial formation of reactive oxygen species. *J. Physiol. (Lond.)* **552**, 335–344 (2003).

263. Öztürk, Z., O'Kane, C. J. & Pérez-Moreno, J. J. Axonal Endoplasmic Reticulum Dynamics and Its Roles in Neurodegeneration. *Front Neurosci* **14**, 48 (2020).

264. Lin, M. T. & Beal, M. F. Mitochondrial dysfunction and oxidative stress in neurodegenerative diseases. *Nature* **443**, 787–795 (2006).

265. Court, F. A. & Coleman, M. P. Mitochondria as a central sensor for axonal degenerative stimuli. *Trends Neurosci.* **35**, 364–372 (2012).

266. Johri, A. & Beal, M. F. Mitochondrial dysfunction in neurodegenerative diseases. *J. Pharmacol. Exp. Ther.* **342**, 619–630 (2012).

267. Ghemrawi, R. & Khair, M. Endoplasmic Reticulum Stress and Unfolded Protein Response in Neurodegenerative Diseases. *Int J Mol Sci* **21**, (2020).

268. Villegas, R. *et al.* Calcium release from intra-axonal endoplasmic reticulum leads to axon degeneration through mitochondrial dysfunction. *J. Neurosci.* **34**, 7179–7189 (2014).

269. Hu, Y. Axon injury induced endoplasmic reticulum stress and neurodegeneration. *Neural Regen Res* **11**, 1557–1559 (2016).

270. O'Donnell, K. C., Vargas, M. E. & Sagasti, A. WldS and PGC-1α regulate mitochondrial transport and oxidation state after axonal injury. *J. Neurosci.* **33**, 14778–14790 (2013).

271. Wang, X. & Schwarz, T. L. The mechanism of Ca2+ -dependent regulation of kinesin-mediated mitochondrial motility. *Cell* **136**, 163–174 (2009).

272. Schwarz, T. L. Mitochondrial trafficking in neurons. *Cold Spring Harb Perspect Biol* **5**, (2013).

273. Marchi, S. & Pinton, P. The mitochondrial calcium uniporter complex: molecular components, structure and physiopathological implications. *J. Physiol. (Lond.)* **592**, 829–839 (2014).

274. Vial, J. D. The early changes in the axoplasm during wallerian degeneration. *J Biophys Biochem Cytol* **4**, 551–555 (1958).

275. Webster, H. D. Transient, focal accumulation of axonal mitochondria during the early stages of wallerian degeneration. *J. Cell Biol.* **12**, 361–383 (1962).

276. Mattson, M. P. *et al.* Calcium signaling in the ER: its role in neuronal plasticity and neurodegenerative disorders. *Trends Neurosci.* **23**, 222–229 (2000).

277. Baumgartner, H. K. *et al.* Calcium elevation in mitochondria is the main Ca2+ requirement for mitochondrial permeability transition pore (mPTP) opening. *J. Biol. Chem.* **284**, 20796–20803 (2009).

278. Bernardi, P. & Di Lisa, F. The mitochondrial permeability transition pore: molecular nature and role as a target in cardioprotection. *J. Mol. Cell. Cardiol.* **78**, 100–106 (2015).

279. Batandier, C., Leverve, X. & Fontaine, E. Opening of the mitochondrial permeability transition pore induces reactive oxygen species production at the level of the respiratory chain complex I. *J. Biol. Chem.* **279**, 17197–17204 (2004).

280. Essuman, K. *et al.* TIR Domain Proteins Are an Ancient Family of NAD+-Consuming Enzymes. *Current Biology* **28**, 421-430.e4 (2018).

281. Mistry, P. *et al.* Inhibition of TLR2 signaling by small molecule inhibitors targeting a pocket within the TLR2 TIR domain. *PNAS* **112**, 5455–5460 (2015).

282. Loring, H. S., Parelkar, S. S., Mondal, S. & Thompson, P. R. Identification of the first noncompetitive SARM1 inhibitors. *Bioorganic & Medicinal Chemistry* **28**, 115644 (2020).

283. Zinzalla, G. & Thurston, D. E. Targeting protein-protein interactions for therapeutic intervention: a challenge for the future. *Future Med Chem* **1**, 65–93 (2009).

284. Keskin, O., Gursoy, A., Ma, B. & Nussinov, R. Principles of protein-protein interactions: what are the preferred ways for proteins to interact? *Chem. Rev.* **108**, 1225–1244 (2008).

285. Schreiber, G., Haran, G. & Zhou, H.-X. Fundamental Aspects of Protein-Protein Association Kinetics. *Chem Rev* **109**, 839–860 (2009).

286. Anguela, X. M. & High, K. A. Entering the Modern Era of Gene Therapy. *Annu. Rev. Med.* **70**, 273–288 (2019).

287. Simonato, M. *et al.* Progress in gene therapy for neurological disorders. *Nat Rev Neurol* **9**, 277–291 (2013).

288. McPhee, S. W. J. *et al.* Immune responses to AAV in a phase I study for Canavan disease. *J Gene Med* **8**, 577–588 (2006).

289. Kaplitt, M. G. *et al.* Safety and tolerability of gene therapy with an adeno-associated virus (AAV) borne GAD gene for Parkinson's disease: an open label, phase I trial. *The Lancet* **369**, 2097–2105 (2007).

290. Worgall, S. *et al.* Treatment of late infantile neuronal ceroid lipofuscinosis by CNS administration of a serotype 2 adeno-associated virus expressing CLN2 cDNA. *Hum. Gene Ther.* **19**, 463–474 (2008).

291. Mendell, J. R. *et al.* Single-Dose Gene-Replacement Therapy for Spinal Muscular Atrophy. *New England Journal of Medicine* **377**, 1713–1722 (2017).

292. Castle, M. J. *et al.* Postmortem Analysis in a Clinical Trial of AAV2-NGF Gene Therapy for Alzheimer's Disease Identifies a Need for Improved Vector Delivery. *Hum. Gene Ther.* **31**, 415–422 (2020).

293. Finkel, R. S. *et al.* Nusinersen versus Sham Control in Infantile-Onset Spinal Muscular Atrophy. *New England Journal of Medicine* **377**, 1723–1732 (2017).

294. Benson, M. D. *et al.* Inotersen Treatment for Patients with Hereditary Transthyretin Amyloidosis. *N. Engl. J. Med.* **379**, 22–31 (2018).

295. Aslesh, T. & Yokota, T. Development of Antisense Oligonucleotide Gapmers for the Treatment of Huntington's Disease. *Methods Mol. Biol.* **2176**, 57–67 (2020).

296. Misgeld, T., Kerschensteiner, M., Bareyre, F. M., Burgess, R. W. & Lichtman, J. W. Imaging axonal transport of mitochondria in vivo. *Nature methods* **4**, 559–561 (2007).

297. Feng, G. *et al.* Imaging Neuronal Subsets in Transgenic Mice Expressing Multiple Spectral Variants of GFP. *Neuron* **28**, 41–51 (2000).

298. Porrero, C., Rubio-Garrido, P., Avendaño, C. & Clascá, F. Mapping of fluorescent protein-expressing neurons and axon pathways in adult and developing Thy1-eYFP-H transgenic mice. *Brain Res.* **1345**, 59–72 (2010).

299. Wang, M.-S., Wu, Y., Culver, D. G. & Glass, J. D. Pathogenesis of Axonal Degeneration: Parallels Between Wallerian Degeneration and Vincristine Neuropathy. *J Neuropathol Exp Neurol* **59**, 599–606 (2000).

300. Geisler, S. *et al.* Prevention of vincristine-induced peripheral neuropathy by genetic deletion of SARM1 in mice. *Brain* **139**, 3092–3108 (2016).

301. Summers, D. W., DiAntonio, A. & Milbrandt, J. Mitochondrial dysfunction induces Sarm1-dependent cell death in sensory neurons. *J. Neurosci.* **34**, 9338–9350 (2014).

302. Di Stefano, M. *et al.* NMN Deamidase Delays Wallerian Degeneration and Rescues Axonal Defects Caused by NMNAT2 Deficiency In Vivo. *Curr. Biol.* **27**, 784–794 (2017).

303. Andrews, S., Gilley, J. & Coleman, M. P. Difference Tracker: ImageJ plugins for fully automated analysis of multiple axonal transport parameters. *Journal of Neuroscience Methods* **193**, 281–287 (2010).

304. Durrant, C. S. Preparation of Organotypic Hippocampal Slice Cultures for the Study of CNS Disease and Damage. *Methods Mol. Biol.* **2143**, 133–144 (2020).

305. Pal, L. R., Yu, C.-H., Mount, S. M. & Moult, J. Insights from GWAS: emerging landscape of mechanisms underlying complex trait disease. *BMC Genomics* **16**, S4 (2015).

306. Karczewski, K. J. *et al.* The mutational constraint spectrum quantified from variation in 141,456 humans. *Nature* **581**, 434–443 (2020).

307. Loring, H. S. & Thompson, P. R. Emergence of SARM1 as a Potential Therapeutic Target for Wallerian-type Diseases. *Cell Chemical Biology* **27**, 1–13 (2020).

308. Carty, M. & Bowie, A. G. SARM: From immune regulator to cell executioner. *Biochemical Pharmacology* **161**, 52–62 (2019).

309. DiAntonio, A. Axon degeneration: mechanistic insights lead to therapeutic opportunities for the prevention and treatment of peripheral neuropathy. *Pain* **160 Suppl 1**, S17–S22 (2019).

310. Simon, D. J. & Watkins, T. A. Therapeutic opportunities and pitfalls in the treatment of axon degeneration. *Current Opinion in Neurology* **31**, 693–701 (2018).

311. Beirowski, B. *et al.* Quantitative and qualitative analysis of Wallerian degeneration using restricted axonal labelling in YFP-H mice. *Journal of Neuroscience Methods* **134**, 23–35 (2004).

312. Burgess, R. W. *et al.* Evidence for a Conserved Function in Synapse Formation Reveals Phr1 as a Candidate Gene for Respiratory Failure in Newborn Mice. *Mol Cell Biol* **24**, 1096–1105 (2004).

313. Lewcock, J. W., Genoud, N., Lettieri, K. & Pfaff, S. L. The ubiquitin ligase Phr1 regulates axon outgrowth through modulation of microtubule dynamics. *Neuron* **56**, 604–620 (2007).

314. Bloom, A. J., Miller, B. R., Sanes, J. R. & DiAntonio, A. The requirement for Phr1 in CNS axon tract formation reveals the corticostriatal boundary as a choice point for cortical axons. *Genes Dev.* **21**, 2593–2606 (2007).

315. Carty, M. *et al.* Cell Survival and Cytokine Release after Inflammasome Activation Is Regulated by the Toll-IL-1R Protein SARM. *Immunity* **50**, 1412-1424.e6 (2019).

316. Gürtler, C. *et al.* SARM regulates CCL5 production in macrophages by promoting the recruitment of transcription factors and RNA polymerase II to the Ccl5 promoter. *J. Immunol.* **192**, 4821–4832 (2014).

317. Tian, W., Czopka, T. & López-Schier, H. Systemic loss of Sarm1 protects Schwann cells from chemotoxicity by delaying axon degeneration. *Commun Biol* **3**, (2020).

318. Owens, J. Determining druggability. *Nature Reviews Drug Discovery* **6**, 187–187 (2007).

319. Abi Hussein, H. *et al.* Global vision of druggability issues: applications and perspectives. *Drug Discov. Today* **22**, 404–415 (2017).

320. Makley, L. N. & Gestwicki, J. E. Expanding the Number of "Druggable" Targets: Non-Enzymes and Protein-Protein Interactions. *Chem Biol Drug Des* **81**, 22–32 (2013).

321. Yang, W. *et al.* The Evolving Druggability and Developability Space: Chemically Modified New Modalities and Emerging Small Molecules. *AAPS J* **22**, 21 (2020).

322. Teplova, M. *et al.* Crystal structure and improved antisense properties of 2'-O-(2-methoxyethyl)-RNA. *Nat. Struct. Biol.* **6**, 535–539 (1999).

323. Peng Ho, S., Livanov, V., Zhang, W., Li, J. & Lesher, T. Modification of phosphorothioate oligonucleotides yields potent analogs with minimal toxicity for antisense experiments in the CNS. *Brain Res. Mol. Brain Res.* **62**, 1–11 (1998).

324. Stephenson, M. L. & Zamecnik, P. C. Inhibition of Rous sarcoma viral RNA translation by a specific oligodeoxyribonucleotide. *Proc. Natl. Acad. Sci. U.S.A.* **75**, 285–288 (1978).

325. Bennett, C. F., Baker, B. F., Pham, N., Swayze, E. & Geary, R. S. Pharmacology of Antisense Drugs. *Annu. Rev. Pharmacol. Toxicol.* **57**, 81–105 (2017).

326. Hyjek, M., Figiel, M. & Nowotny, M. RNases H: Structure and mechanism. *DNA Repair (Amst.)* **84**, 102672 (2019).

327. Wu, H. *et al.* Determination of the Role of the Human RNase H1 in the Pharmacology of DNA-like Antisense Drugs. *Journal of Biological Chemistry* **279**, 17181–17189 (2004).

328. Liang, X.-H., Sun, H., Nichols, J. G. & Crooke, S. T. RNase H1-Dependent Antisense Oligonucleotides Are Robustly Active in Directing RNA Cleavage in Both the Cytoplasm and the Nucleus. *Molecular Therapy* **25**, 2075–2092 (2017).

329. Dias, N. & Stein, C. A. Antisense oligonucleotides: basic concepts and mechanisms. *Mol. Cancer Ther.* **1**, 347–355 (2002).

330. Juliano, R. L., Carver, K., Cao, C. & Ming, X. Receptors, endocytosis, and trafficking: the biological basis of targeted delivery of antisense and siRNA oligonucleotides. *J Drug Target* **21**, 27–43 (2013).

331. El-Sayed, A. & Harashima, H. Endocytosis of Gene Delivery Vectors: From Clathrin-dependent to Lipid Raft-mediated Endocytosis. *Mol Ther* **21**, 1118–1130 (2013).

332. Crooke, S. T., Wang, S., Vickers, T. A., Shen, W. & Liang, X. Cellular uptake and trafficking of antisense oligonucleotides. *Nature Biotechnology* **35**, 230–237 (2017).

333. Koller, E. *et al.* Mechanisms of single-stranded phosphorothioate modified antisense oligonucleotide accumulation in hepatocytes. *Nucleic Acids Res* **39**, 4795–4807 (2011).

334. Tanowitz, M. *et al.* Asialoglycoprotein receptor 1 mediates productive uptake of N-acetylgalactosamine-conjugated and unconjugated phosphorothioate antisense oligonucleotides into liver hepatocytes. *Nucleic Acids Res.* **45**, 12388–12400 (2017).

335. Biessen, E. A., Vietsch, H., Kuiper, J., Bijsterbosch, M. K. & Berkel, T. J. Liver uptake of phosphodiester oligodeoxynucleotides is mediated by scavenger receptors. *Mol. Pharmacol.* **53**, 262–269 (1998).

336. Miller, C. M. *et al.* Stabilin-1 and Stabilin-2 are specific receptors for the cellular internalization of phosphorothioate-modified antisense oligonucleotides (ASOs) in the liver. *Nucleic Acids Res* **44**, 2782–2794 (2016).

337. Ming, X. *et al.* Intracellular delivery of an antisense oligonucleotide via endocytosis of a G protein-coupled receptor. *Nucleic Acids Res* **38**, 6567–6576 (2010).

338. Wada, S. *et al.* Evaluation of the effects of chemically different linkers on hepatic accumulations, cell tropism and gene silencing ability of cholesterol-conjugated antisense oligonucleotides. *J Control Release* **226**, 57–65 (2016).

339. Liang, X., Shen, W., Sun, H., Prakash, T. P. & Crooke, S. T. TCP1 complex proteins interact with phosphorothioate oligonucleotides and can co-localize in oligonucleotide-induced nuclear bodies in mammalian cells. *Nucleic Acids Res.* **42**, 7819–7832 (2014).

340. Shen, W. *et al.* Chemical modification of PS-ASO therapeutics reduces cellular protein-binding and improves the therapeutic index. *Nat. Biotechnol.* **37**, 640–650 (2019).

341. Shen, W., Liang, X. & Crooke, S. T. Phosphorothioate oligonucleotides can displace NEAT1 RNA and form nuclear paraspeckle-like structures. *Nucleic Acids Res.* **42**, 8648–8662 (2014).

342. Liang, X., Sun, H., Shen, W. & Crooke, S. T. Identification and characterization of intracellular proteins that bind oligonucleotides with phosphorothioate linkages. *Nucleic Acids Res* **43**, 2927–2945 (2015).

343. Wang, S., Sun, H., Tanowitz, M., Liang, X. & Crooke, S. T. Annexin A2 facilitates endocytic trafficking of antisense oligonucleotides. *Nucleic Acids Res* **44**, 7314–7330 (2016).

344. Lorenz, P., Misteli, T., Baker, B. F., Bennett, C. F. & Spector, D. L. Nucleocytoplasmic shuttling: a novel in vivo property of antisense phosphorothioate oligodeoxynucleotides. *Nucleic Acids Res.* **28**, 582–592 (2000).

345. Freeman, O. J. & Mallucci, G. R. The UPR and synaptic dysfunction in neurodegeneration. *Brain Res.* **1648**, 530–537 (2016).

346. Knight, J. R. P. *et al.* Control of translation elongation in health and disease. *Dis Model Mech* **13**, (2020).

347. Halliday, M. *et al.* Repurposed drugs targeting eIF2α-P-mediated translational repression prevent neurodegeneration in mice. *Brain* **140**, 1768–1783 (2017).

348. Ali, Y. O., Ruan, K. & Zhai, R. G. NMNAT suppresses tau-induced neurodegeneration by promoting clearance of hyperphosphorylated tau oligomers in a Drosophila model of tauopathy. *Hum. Mol. Genet.* **21**, 237–250 (2012).

349. White, M. A. *et al.* TDP-43 gains function due to perturbed autoregulation in a Tardbp knock-in mouse model of ALS-FTD. *Nat. Neurosci.* **21**, 552–563 (2018).

350. Gültner, S., Laue, M., Riemer, C., Heise, I. & Baier, M. Prion disease development in slow Wallerian degeneration (WldS) mice. *Neuroscience Letters* **456**, 93–98 (2009).

351. Zhu, C., Li, B., Frontzek, K., Liu, Y. & Aguzzi, A. SARM1 deficiency up-regulates XAF1, promotes neuronal apoptosis, and accelerates prion disease. *J. Exp. Med.* **216**, 743–756 (2019).

352. Stebbins, C. C., Petrillo, M. & Stevenson, L. F. Immunogenicity for antisense oligonucleotides: a risk-based assessment. *Bioanalysis* **11**, 1913–1916 (2019).

353. Krauss, R., Bosanac, T., Engber, T., Devraj, R. & Hughes, R. Small Molecule Inhibitors of SARM1 Prevent Axonal Degeneration in vitro and in vivo. (2019).

354. Detzer, A. *et al.* Increased RNAi is related to intracellular release of siRNA via a covalently attached signal peptide. *RNA* **15**, 627–636 (2009).

355. Silva, A. C. *et al.* Antisense oligonucleotide therapeutics in neurodegenerative diseases: the case of polyglutamine disorders. *Brain* **143**, 407–429 (2020).

356. Mittermeyer, G. *et al.* Long-Term Evaluation of a Phase 1 Study of AADC Gene Therapy for Parkinson's Disease. *Hum Gene Ther* **23**, 377–381 (2012).

357. Naso, M. F., Tomkowicz, B., Perry, W. L., III & Strohl, W. R. Adeno-Associated Virus (AAV) as a Vector for Gene Therapy. *Biodrugs* **31**, 317 (2017).

358. Gao, G. *et al.* Biology of AAV serotype vectors in liver-directed gene transfer to nonhuman primates. *Mol. Ther.* **13**, 77–87 (2006).

359. MacLeod, R. Ionis Drug Discovery: From Ideas to Patient. (2020).

360. Nault, J.-C. *et al.* Recurrent AAV2-related insertional mutagenesis in human hepatocellular carcinomas. *Nature Genetics* **47**, 1187–1193 (2015).

361. Chandler, R. J. *et al.* Vector design influences hepatic genotoxicity after adeno-associated virus gene therapy. *J. Clin. Invest.* **125**, 870–880 (2015).

362. Hanlon, K. S. *et al.* High levels of AAV vector integration into CRISPR-induced DNA breaks. *Nat Commun* **10**, 4439 (2019).

363. Nakai, H. *et al.* AAV serotype 2 vectors preferentially integrate into active genes in mice. *Nature Genetics* **34**, 297–302 (2003).

364. Donsante, A. *et al.* Observed incidence of tumorigenesis in long-term rodent studies of rAAV vectors. *Gene Ther.* **8**, 1343–1346 (2001).

365. Enomoto, M., Hirai, T., Kaburagi, H. & Yokota, T. Efficient Gene Suppression in Dorsal Root Ganglia and Spinal Cord Using Adeno-Associated Virus Vectors Encoding Short-Hairpin RNA. in *SiRNA Delivery Methods: Methods and Protocols* (eds. Shum, K. & Rossi, J.) 277–290 (Springer, 2016). doi:10.1007/978-1-4939-3112-5_22.

366. Summers, D. W., Gibson, D. A., DiAntonio, A. & Milbrandt, J. SARM1-specific motifs in the TIR domain enable NAD+ loss and regulate injury-induced SARM1 activation. *Proc. Natl. Acad. Sci. U.S.A.* **113**, E6271–E6280 (2016).

367. Bekris, L. M., Yu, C.-E., Bird, T. D. & Tsuang, D. W. Genetics of Alzheimer Disease. *J Geriatr Psychiatry Neurol* **23**, 213–227 (2010).

368. Walsh, D. M. & Selkoe, D. J. A beta oligomers - a decade of discovery. *J. Neurochem.* **101**, 1172–1184 (2007).

369. Bilousova, T. *et al.* Synaptic Amyloid-β Oligomers Precede p-Tau and Differentiate High Pathology Control Cases. *Am J Pathol* **186**, 185–198 (2016).

370. Onos, K. D., Sukoff Rizzo, S. J., Howell, G. R. & Sasner, M. Toward more predictive genetic mouse models of Alzheimer's disease. *Brain Res. Bull.* **122**, 1–11 (2016).

371. Strittmatter, W. J. *et al.* Apolipoprotein E: high-avidity binding to beta-amyloid and increased frequency of type 4 allele in late-onset familial Alzheimer disease. *Proc. Natl. Acad. Sci. U.S.A.* **90**, 1977–1981 (1993).

372. Deane, R. *et al.* apoE isoform-specific disruption of amyloid beta peptide clearance from mouse brain. *J. Clin. Invest.* **118**, 4002–4013 (2008).

373. Andersen, O. M. *et al.* Neuronal sorting protein-related receptor sorLA/LR11 regulates processing of the amyloid precursor protein. *Proc. Natl. Acad. Sci. U.S.A.* **102**, 13461–13466 (2005).

374. Spoelgen, R. *et al.* Interaction of the cytosolic domains of sorLA/LR11 with the amyloid precursor protein (APP) and beta-secretase beta-site APP-cleaving enzyme. *J. Neurosci.* **26**, 418–428 (2006).

375. Adalbert, R. & Coleman, M. P. Review: Axon pathology in age-related neurodegenerative disorders. *Neuropathology and Applied Neurobiology* **39**, 90–108 (2013).

376. Hirokawa, N. *et al.* Kinesin Associates with Anterogradely Transported Membranous Organelles In Vivo. 711–713 (1991).

377. Hirokawa, N., Sato-Yoshitake, R., Yoshida, T. & Kawashima, T. Brain dynein (MAP1C) localizes on both anterogradely and retrogradely transported membranous organelles in vivo. *Journal of Cell Biology* **111**, 1027–1037 (1990).

378. Muresan, V. & Muresan, Z. Is abnormal axonal transport a cause, a contributing factor or a consequence of the neuronal pathology in Alzheimer's disease? *Future Neurology* **4**, 761–773 (2009).

379. Lazarov, O. *et al.* Axonal transport, amyloid precursor protein, kinesin-1, and the processing apparatus: revisited. *J. Neurosci.* **25**, 2386–2395 (2005).

380. Hung, C. O. Y. & Coleman, M. P. KIF1A mediates axonal transport of BACE1 and identification of independently moving cargoes in living SCG neurons. *Traffic* **17**, 1155–1167 (2016).

381. Weingarten, M. D., Lockwood, A. H., Hwo, S. Y. & Kirschner, M. W. A protein factor essential for microtubule assembly. *Proc. Natl. Acad. Sci. U.S.A.* **72**, 1858–1862 (1975).

382. Witman, G. B., Cleveland, D. W., Weingarten, M. D. & Kirschner, M. W. Tubulin requires tau for growth onto microtubule initiating sites. *Proc. Natl. Acad. Sci. U.S.A.* **73**, 4070–4074 (1976).

383. Binder, L. I., Frankfurter, A. & Rebhun, L. I. The distribution of tau in the mammalian central nervous system. *J. Cell Biol.* **101**, 1371–1378 (1985).

384. Black, M. M., Slaughter, T., Moshiach, S., Obrocka, M. & Fischer, I. Tau is enriched on dynamic microtubules in the distal region of growing axons. *J. Neurosci.* **16**, 3601–3619 (1996).

385. Biernat, J., Gustke, N., Drewes, G., Mandelkow, E. M. & Mandelkow, E. Phosphorylation of Ser262 strongly reduces binding of tau to microtubules: distinction between PHF-like immunoreactivity and microtubule binding. *Neuron* **11**, 153–163 (1993).

386. Sengupta, A. *et al.* Phosphorylation of tau at both Thr 231 and Ser 262 is required for maximal inhibition of its binding to microtubules. *Arch. Biochem. Biophys.* **357**, 299–309 (1998).

387. Schneider, A., Biernat, J., von Bergen, M., Mandelkow, E. & Mandelkow, E. M. Phosphorylation that detaches tau protein from microtubules (Ser262, Ser214) also protects it against aggregation into Alzheimer paired helical filaments. *Biochemistry* **38**, 3549–3558 (1999).

388. Vicario-Orri, E., Opazo, C. M. & Muñoz, F. J. The pathophysiology of axonal transport in Alzheimer's disease. *J. Alzheimers Dis.* **43**, 1097–1113 (2015).

389. Tang, Y. *et al.* Early and selective impairments in axonal transport kinetics of synaptic cargoes induced by soluble amyloid β-protein oligomers. *Traffic* **13**, 681–693 (2012).

390. Calkins, M. J., Manczak, M., Mao, P., Shirendeb, U. & Reddy, P. H. Impaired mitochondrial biogenesis, defective axonal transport of mitochondria, abnormal mitochondrial dynamics and synaptic degeneration in a mouse model of Alzheimer's disease. *Hum. Mol. Genet.* **20**, 4515–4529 (2011).

391. Decker, H., Lo, K. Y., Unger, S. M., Ferreira, S. T. & Silverman, M. A. Amyloid-beta peptide oligomers disrupt axonal transport through an NMDA receptor-dependent mechanism that is mediated by glycogen synthase kinase 3beta in primary cultured hippocampal neurons. *J. Neurosci.* **30**, 9166–9171 (2010).

392. Hiruma, H., Katakura, T., Takahashi, S., Ichikawa, T. & Kawakami, T. Glutamate and Amyloid β-Protein Rapidly Inhibit Fast Axonal Transport in Cultured Rat Hippocampal Neurons by Different Mechanisms. *J Neurosci* **23**, 8967–8977 (2003).

393. Rui, Y., Tiwari, P., Xie, Z. & Zheng, J. Q. Acute impairment of mitochondrial trafficking by beta-amyloid peptides in hippocampal neurons. *J. Neurosci.* **26**, 10480–10487 (2006).

394. Kasa, P. *et al.* Human amyloid-beta1-42 applied in vivo inhibits the fast axonal transport of proteins in the sciatic nerve of rat. *Neurosci. Lett.* **278**, 117–119 (2000).

395. Vossel, K. A. *et al.* Tau reduction prevents Abeta-induced defects in axonal transport. *Science* **330**, 198 (2010).

396. Adalbert, R. *et al.* Severely dystrophic axons at amyloid plaques remain continuous and connected to viable cell bodies. *Brain* **132**, 402–416 (2009).

397. Llorens-Martín, M., López-Doménech, G., Soriano, E. & Avila, J. GSK3β Is Involved in the Relief of Mitochondria Pausing in a Tau-Dependent Manner. *PLoS One* **6**, (2011).

398. Peethumnongsin, E. *et al.* Convergence of presenilin- and tau-mediated pathways on axonal trafficking and neuronal function. *J. Neurosci.* **30**, 13409–13418 (2010).

399. Hardy, J. A. & Higgins, G. A. Alzheimer's disease: the amyloid cascade hypothesis. *Science* **256**, 184–185 (1992).

400. Glenner, G. G. & Wong, C. W. Alzheimer's disease: initial report of the purification and characterization of a novel cerebrovascular amyloid protein. *Biochem. Biophys. Res. Commun.* **120**, 885–890 (1984).

401. Glenner, G. G., Wong, C. W., Quaranta, V. & Eanes, E. D. The amyloid deposits in Alzheimer's disease: their nature and pathogenesis. *Appl Pathol* **2**, 357–369 (1984).

402. Masters, C. L. *et al.* Neuronal origin of a cerebral amyloid: neurofibrillary tangles of Alzheimer's disease contain the same protein as the amyloid of plaque cores and blood vessels. *EMBO J.* **4**, 2757–2763 (1985).

403. Masters, C. L. *et al.* Amyloid plaque core protein in Alzheimer disease and Down syndrome. *Proc. Natl. Acad. Sci. U.S.A.* **82**, 4245–4249 (1985).

404. Goate, A. *et al.* Segregation of a missense mutation in the amyloid precursor protein gene with familial Alzheimer's disease. *Nature* **349**, 704–706 (1991).

405. St George-Hyslop, P. *et al.* Genetic evidence for a novel familial Alzheimer's disease locus on chromosome 14. *Nat. Genet.* **2**, 330–334 (1992).

406. Levy-Lahad, E. *et al.* A familial Alzheimer's disease locus on chromosome 1. *Science* **269**, 970–973 (1995).

407. Rogaev, E. I. *et al.* Familial Alzheimer's disease in kindreds with missense mutations in a gene on chromosome 1 related to the Alzheimer's disease type 3 gene. *Nature* **376**, 775–778 (1995).

408. Herrup, K. The case for rejecting the amyloid cascade hypothesis. *Nat. Neurosci.* **18**, 794–799 (2015).

409. Citron, M. *et al.* Mutation of the beta-amyloid precursor protein in familial Alzheimer's disease increases beta-protein production. *Nature* **360**, 672–674 (1992).

410. Suzuki, N. *et al.* An increased percentage of long amyloid beta protein secreted by familial amyloid beta protein precursor (beta APP717) mutants. *Science* **264**, 1336–1340 (1994).

411. Borchelt, D. R. *et al.* Familial Alzheimer's disease-linked presenilin 1 variants elevate Abeta1-42/1-40 ratio in vitro and in vivo. *Neuron* **17**, 1005–1013 (1996).

412. Scheuner, D. *et al.* Secreted amyloid beta-protein similar to that in the senile plaques of Alzheimer's disease is increased in vivo by the presenilin 1 and 2 and APP mutations linked to familial Alzheimer's disease. *Nat. Med.* **2**, 864–870 (1996).

413. Bentahir, M. *et al.* Presenilin clinical mutations can affect gamma-secretase activity by different mechanisms. *J. Neurochem.* **96**, 732–742 (2006).

414. McCarron, M., McCallion, P., Reilly, E. & Mulryan, N. A prospective 14-year longitudinal follow-up of dementia in persons with Down syndrome. *J Intellect Disabil Res* **58**, 61–70 (2014).

415. McCarron, M. *et al.* A prospective 20-year longitudinal follow-up of dementia in persons with Down syndrome. *J Intellect Disabil Res* **61**, 843–852 (2017).

416. Hithersay, R. *et al.* Association of Dementia With Mortality Among Adults With Down Syndrome Older Than 35 Years. *JAMA Neurol* **76**, 152–160 (2019).

417. Wiseman, F. K. *et al.* A genetic cause of Alzheimer disease: mechanistic insights from Down syndrome. *Nat. Rev. Neurosci.* **16**, 564–574 (2015).

418. Rovelet-Lecrux, A. *et al.* APP locus duplication causes autosomal dominant early-onset Alzheimer disease with cerebral amyloid angiopathy. *Nat. Genet.* **38**, 24–26 (2006).

419. Rovelet-Lecrux, A. *et al.* APP locus duplication in a Finnish family with dementia and intracerebral haemorrhage. *J. Neurol. Neurosurg. Psychiatry* **78**, 1158–1159 (2007).

420. Sleegers, K. *et al.* APP duplication is sufficient to cause early onset Alzheimer's dementia with cerebral amyloid angiopathy. *Brain* **129**, 2977–2983 (2006).

421. Swaminathan, S. *et al.* Analysis of copy number variation in Alzheimer's disease in a cohort of clinically characterized and neuropathologically verified individuals. *PLoS ONE* **7**, e50640 (2012).

422. Thonberg, H. *et al.* Mutation screening of patients with Alzheimer disease identifies APP locus duplication in a Swedish patient. *BMC Res Notes* **4**, 476 (2011).

423. Jonsson, T. *et al.* A mutation in APP protects against Alzheimer's disease and age-related cognitive decline. *Nature* **488**, 96–99 (2012).

424. Kero, M. *et al.* Amyloid precursor protein (APP) A673T mutation in the elderly Finnish population. *Neurobiol. Aging* **34**, 1518.e1–3 (2013).

425. Prasher, V. P. *et al.* Molecular mapping of alzheimer-type dementia in Down's syndrome. *Annals of Neurology* **43**, 380–383 (1998).

426. Tsuda, T. *et al.* Failure to detect missense mutations in the S182 gene in a series of late-onset Alzheimer's disease cases. *Neurosci. Lett.* **201**, 188–190 (1995).

427. Tanimukai, H. *et al.* Presenilin-2 mutation and polymorphism in Japanese Alzheimer disease patients. *Clin. Chim. Acta* **283**, 57–61 (1999).

428. Helisalmi, S. *et al.* Is the presenilin-1 E318G missense mutation a risk factor for Alzheimer's disease? *Neurosci. Lett.* **278**, 65–68 (2000).

429. Nowotny, P. *et al.* Association studies using novel polymorphisms in BACE1 and BACE2. *Neuroreport* **12**, 1799–1802 (2001).

430. Gold, G. *et al.* Specific BACE1 genotypes provide additional risk for late-onset Alzheimer disease in APOE epsilon 4 carriers. *Am. J. Med. Genet. B Neuropsychiatr. Genet.* **119B**, 44–47 (2003).

431. Clarimón, J. *et al.* Association study between Alzheimer's disease and genes involved in Abeta biosynthesis, aggregation and degradation: suggestive results with BACE1. *J. Neurol.* **250**, 956–961 (2003).

432. Combarros, O., Cortina-Borja, M., Smith, A. D. & Lehmann, D. J. Epistasis in sporadic Alzheimer's disease. *Neurobiol. Aging* **30**, 1333–1349 (2009).

433. Sala Frigerio, C. *et al.* On the identification of low allele frequency mosaic mutations in the brains of Alzheimer's disease patients. *Alzheimers Dement* **11**, 1265–1276 (2015).

434. Corder, E. H. *et al.* Gene dose of apolipoprotein E type 4 allele and the risk of Alzheimer's disease in late onset families. *Science* **261**, 921–923 (1993).

435. Scott, W. K. *et al.* No genetic association between the LRP receptor and sporadic or late-onset familial Alzheimer disease. *Neurogenetics* **1**, 179–183 (1998).

436. Bertram, L. *et al.* Candidate genes showing no evidence for association or linkage with Alzheimer's disease using family-based methodologies. *Exp. Gerontol.* **35**, 1353–1361 (2000).

437. Forero, D. A., Arboleda, G., Yunis, J. J., Pardo, R. & Arboleda, H. Association study of polymorphisms in LRP1, tau and 5-HTT genes and Alzheimer's disease in a sample of Colombian patients. *J Neural Transm (Vienna)* **113**, 1253–1262 (2006).

438. Yankner, B. A., Duffy, L. K. & Kirschner, D. A. Neurotrophic and neurotoxic effects of amyloid beta protein: reversal by tachykinin neuropeptides. *Science* **250**, 279–282 (1990).

439. Chapman, P. F. *et al.* Impaired synaptic plasticity and learning in aged amyloid precursor protein transgenic mice. *Nat. Neurosci.* **2**, 271–276 (1999).

440. Oddo, S. *et al.* Triple-transgenic model of Alzheimer's disease with plaques and tangles: intracellular Abeta and synaptic dysfunction. *Neuron* **39**, 409–421 (2003).

441. Billings, L. M., Oddo, S., Green, K. N., McGaugh, J. L. & LaFerla, F. M. Intraneuronal Abeta causes the onset of early Alzheimer's disease-related cognitive deficits in transgenic mice. *Neuron* **45**, 675–688 (2005).

442. Greeve, I. *et al.* Age-dependent neurodegeneration and Alzheimer-amyloid plaque formation in transgenic Drosophila. *J. Neurosci.* **24**, 3899–3906 (2004).

443. Kim, J. *et al.* Normal cognition in transgenic BRI2-Aβ mice. *Molecular Neurodegeneration* **8**, 15 (2013).

444. Games, D. *et al.* Alzheimer-type neuropathology in transgenic mice overexpressing V717F beta-amyloid precursor protein. *Nature* **373**, 523–527 (1995).

445. Irizarry, M. C. *et al.* Abeta deposition is associated with neuropil changes, but not with overt neuronal loss in the human amyloid precursor protein V717F (PDAPP) transgenic mouse. *J. Neurosci.* **17**, 7053–7059 (1997).

446. Herreman, A. *et al.* Presenilin 2 deficiency causes a mild pulmonary phenotype and no changes in amyloid precursor protein processing but enhances the embryonic lethal phenotype of presenilin 1 deficiency. *Proc. Natl. Acad. Sci. U.S.A.* **96**, 11872–11877 (1999).

447. Aizenstein, H. J. *et al.* Frequent Amyloid Deposition Without Significant Cognitive Impairment Among the Elderly. *Arch Neurol* **65**, 1509–1517 (2008).

448. Villemagne, V. L. *et al.* Longitudinal Assessment of Aβ and Cognition in Aging and Alzheimer Disease. *Ann Neurol* **69**, 181–192 (2011).

449. Perez-Nievas, B. G. *et al.* Dissecting phenotypic traits linked to human resilience to Alzheimer's pathology. *Brain* **136**, 2510–2526 (2013).

450. Holmes, C. *et al.* Long-term effects of Abeta42 immunisation in Alzheimer's disease: follow-up of a randomised, placebo-controlled phase I trial. *Lancet* **372**, 216–223 (2008).

451. Doody, R. S. *et al.* Phase 3 Trials of Solanezumab for Mild-to-Moderate Alzheimer's Disease. *New England Journal of Medicine* **370**, 311–321 (2014).

452. Salloway, S. *et al.* Two Phase 3 Trials of Bapineuzumab in Mild-to-Moderate Alzheimer's Disease. *New England Journal of Medicine* **370**, 322–333 (2014).

453. Serrano-Pozo, A. *et al.* Beneficial effect of human anti-amyloid-β active immunization on neurite morphology and tau pathology. *Brain* **133**, 1312–1327 (2010).

454. Duyckaerts, C., Colle, M. A., Dessi, F., Piette, F. & Hauw, J. J. Progression of Alzheimer histopathological changes. *Acta Neurol Belg* **98**, 180–185 (1998).

455. Giannakopoulos, P. *et al.* Tangle and neuron numbers, but not amyloid load, predict cognitive status in Alzheimer's disease. *Neurology* **60**, 1495–1500 (2003).

456. Jackson, R. J. *et al.* Human tau increases amyloid β plaque size but not amyloid β-mediated synapse loss in a novel mouse model of Alzheimer's disease. *Eur J Neurosci* **44**, 3056–3066 (2016).

457. Braak, H., Thal, D. R., Ghebremedhin, E. & Del Tredici, K. Stages of the pathologic process in Alzheimer disease: age categories from 1 to 100 years. *J. Neuropathol. Exp. Neurol.* **70**, 960–969 (2011).

458. Coric, V. *et al.* Safety and tolerability of the γ-secretase inhibitor avagacestat in a phase 2 study of mild to moderate Alzheimer disease. *Arch. Neurol.* **69**, 1430–1440 (2012).

459. Tamayev, R. & D'Adamio, L. Inhibition of γ-secretase worsens memory deficits in a genetically congruous mouse model of Danish dementia. *Mol Neurodegener* **7**, 19 (2012).

460. McGeer, P. L., Schulzer, M. & McGeer, E. G. Arthritis and anti-inflammatory agents as possible protective factors for Alzheimer's disease: A review of 17 epidemiologic studies. *Neurology* **47**, 425–432 (1996).

461. Karran, E. & De Strooper, B. The amyloid cascade hypothesis: are we poised for success or failure? *J. Neurochem.* **139 Suppl 2**, 237–252 (2016).

462. Liu, P.-P., Xie, Y., Meng, X.-Y. & Kang, J.-S. History and progress of hypotheses and clinical trials for Alzheimer's disease. *Signal Transduct Target Ther* **4**, 29 (2019).

463. Newcombe, E. A. *et al.* Inflammation: the link between comorbidities, genetics, and Alzheimer's disease. *Journal of Neuroinflammation* **15**, 276 (2018).

464. Swerdlow, R. H. & Khan, S. M. A 'mitochondrial cascade hypothesis' for sporadic Alzheimer's disease. *Med. Hypotheses* **63**, 8–20 (2004).

465. Ebanks, B., Ingram, T. L. & Chakrabarti, L. ATP synthase and Alzheimer's disease: putting a spin on the mitochondrial hypothesis. *Aging (Albany NY)* **12**, 16647–16662 (2020).

466. Nagy, Z., Esiri, M. M., Cato, A. M. & Smith, A. D. Cell cycle markers in the hippocampus in Alzheimer's disease. *Acta Neuropathol.* **94**, 6–15 (1997).

467. Chow, H. & Herrup, K. Genomic integrity and the ageing brain. *Nat. Rev. Neurosci.* **16**, 672–684 (2015).

468. Fischer, V. W., Siddiqi, A. & Yusufaly, Y. Altered angioarchitecture in selected areas of brains with Alzheimer's disease. *Acta Neuropathol.* **79**, 672–679 (1990).

469. de la Torre, J. C. & Mussivand, T. Can disturbed brain microcirculation cause Alzheimer's disease? *Neurol. Res.* **15**, 146–153 (1993).

470. Iadecola, C. Neurovascular regulation in the normal brain and in Alzheimer's disease. *Nat. Rev. Neurosci.* **5**, 347–360 (2004).

471. Hoyer, S., Oesterreich, K. & Wagner, O. Glucose metabolism as the site of the primary abnormality in early-onset dementia of Alzheimer type? *J. Neurol.* **235**, 143–148 (1988).

472. Hoyer, S. Abnormalities of glucose metabolism in Alzheimer's disease. *Ann. N. Y. Acad. Sci.* **640**, 53–58 (1991).

473. Hoyer, S., Nitsch, R. & Oesterreich, K. Predominant abnormality in cerebral glucose utilization in late-onset dementia of the Alzheimer type: a cross-sectional comparison against advanced late-onset and incipient early-onset cases. *J Neural Transm Park Dis Dement Sect* **3**, 1–14 (1991).

474. Butterfield, D. A. & Halliwell, B. Oxidative stress, dysfunctional glucose metabolism and Alzheimer disease. *Nat. Rev. Neurosci.* **20**, 148–160 (2019).

475. Frost, B., Jacks, R. L. & Diamond, M. I. Propagation of tau misfolding from the outside to the inside of a cell. *J. Biol. Chem.* **284**, 12845–12852 (2009).

476. Small, S. A. & Duff, K. Linking Abeta and tau in late-onset Alzheimer's disease: a dual pathway hypothesis. *Neuron* **60**, 534–542 (2008).

477. Davies, P. & Maloney, A. J. Selective loss of central cholinergic neurons in Alzheimer's disease. *Lancet* **2**, 1403 (1976).

478. Chen, Y., Fu, A. K. Y. & Ip, N. Y. Synaptic dysfunction in Alzheimer's disease: Mechanisms and therapeutic strategies. *Pharmacol. Ther.* **195**, 186–198 (2019).

479. Silverman, J. M. *et al.* The Consortium to Establish a Registry for Alzheimer's Disease (CERAD). Part VI. Family history assessment: a multicenter study of first-degree relatives of Alzheimer's disease probands and nondemented spouse controls. *Neurology* **44**, 1253–1259 (1994).

480. Nigam, S. M. *et al.* Exercise and BDNF reduce Aβ production by enhancing α-secretase processing of APP. *J. Neurochem.* **142**, 286–296 (2017).

481. Whitmer, R. A., Gunderson, E. P., Barrett-Connor, E., Quesenberry, C. P. & Yaffe, K. Obesity in middle age and future risk of dementia: a 27 year longitudinal population based study. *BMJ* **330**, 1360 (2005).

482. Launer, L. J. *et al.* Midlife blood pressure and dementia: the Honolulu-Asia aging study. *Neurobiol. Aging* **21**, 49–55 (2000).

483. McMaster, M. *et al.* Lifestyle Risk Factors and Cognitive Outcomes from the Multidomain Dementia Risk Reduction Randomized Controlled Trial, Body Brain Life for Cognitive Decline (BBL-CD). *Journal of the American Geriatrics Society* https://pubmed.ncbi.nlm.nih.gov/32909259/ (2020) doi:10.1111/jgs.16762.

484. Nagpal, R. *et al.* Gut mycobiome and its interaction with diet, gut bacteria and alzheimer's disease markers in subjects with mild cognitive impairment: A pilot study. *EBioMedicine* vol. 59 https://pubmed.ncbi.nlm.nih.gov/32861197/ (2020).

485. Bush, A. I. *et al.* Rapid induction of Alzheimer A beta amyloid formation by zinc. *Science* **265**, 1464–1467 (1994).

486. Clements, A., Allsop, D., Walsh, D. M. & Williams, C. H. Aggregation and metal-binding properties of mutant forms of the amyloid A beta peptide of Alzheimer's disease. *J. Neurochem.* **66**, 740–747 (1996).

487. Wang, Z. *et al.* Chronic exposure to aluminum and risk of Alzheimer's disease: A meta-analysis. *Neuroscience Letters* **610**, 200–206 (2016).

488. Osorio, R. S. *et al.* Greater risk of Alzheimer's disease in older adults with insomnia. *J Am Geriatr Soc* **59**, 559–562 (2011).

489. Zarrouk, A. *et al.* Lipid Biomarkers in Alzheimer's Disease. *Curr Alzheimer Res* **15**, 303–312 (2018).

490. Mattson, M. P. *et al.* beta-Amyloid peptides destabilize calcium homeostasis and render human cortical neurons vulnerable to excitotoxicity. *J. Neurosci.* **12**, 376–389 (1992).

491. McGeer, P. L. & Rogers, J. Anti-inflammatory agents as a therapeutic approach to Alzheimer's disease. *Neurology* **42**, 447–449 (1992).

492. Martins, R. N. *et al.* Alzheimer's Disease: A Journey from Amyloid Peptides and Oxidative Stress, to Biomarker Technologies and Disease Prevention Strategies-Gains from AIBL and DIAN Cohort Studies. *J. Alzheimers Dis.* **62**, 965–992 (2018).

493. Suzuki, K. & Terry, R. D. Fine structural localization of acid phosphatase in senile plaques in Alzheimer's presenile dementia. *Acta Neuropathol.* **8**, 276–284 (1967).

494. Nixon, R. A. *et al.* Extensive Involvement of Autophagy in Alzheimer Disease: An Immuno-Electron Microscopy Study. *J Neuropathol Exp Neurol* **64**, 113–122 (2005).

495. Ji, Z.-S. *et al.* Reactivity of apolipoprotein E4 and amyloid beta peptide: lysosomal stability and neurodegeneration. *J. Biol. Chem.* **281**, 2683–2692 (2006).

496. Ulrich, J. D. *et al.* Altered microglial response to Aβ plaques in APPPS1-21 mice heterozygous for TREM2. *Mol Neurodegener* **9**, 20 (2014).

497. Jay, T. R. *et al.* TREM2 deficiency eliminates TREM2+ inflammatory macrophages and ameliorates pathology in Alzheimer's disease mouse models. *J. Exp. Med.* **212**, 287–295 (2015).

498. Rivest, S. TREM2 enables amyloid β clearance by microglia. *Cell Res.* **25**, 535–536 (2015).

499. Acosta, P. B. & Gross, K. C. Hidden sources of galactose in the environment. *Eur. J. Pediatr.* **154**, S87-92 (1995).

500. Caputto, R., Leloir, L. F., Cardini, C. E. & Paladini, A. C. The enzymatic transformation of galactose into glucose derivatives. **137**, 497–499 (1948).

501. Stokin, G. B. *et al.* Axonopathy and transport deficits early in the pathogenesis of Alzheimer's disease. *Science* **307**, 1282–1288 (2005).

502. Sontag, J.-M. & Sontag, E. Protein phosphatase 2A dysfunction in Alzheimer's disease. *Front. Mol. Neurosci.* **7**, (2014).

503. Milde, S., Adalbert, R., Elaman, M. H. & Coleman, M. P. Axonal transport declines with age in two distinct phases separated by a period of relative stability. *Neurobiology of Aging* **36**, 971–981 (2015).

504. Shen, Y. *et al.* Glutamine synthetase plays a role in D-galactose-induced astrocyte aging in vitro and in vivo. *Exp. Gerontol.* **58**, 166–173 (2014).

505. Sadigh-Eteghad, S. *et al.* D-galactose-induced brain ageing model: A systematic review and meta-analysis on cognitive outcomes and oxidative stress indices. *PLoS ONE* **12**, e0184122 (2017).

506. Bridge, K. E. *et al.* Late onset distal axonal swelling in YFP-H transgenic mice. *Neurobiology of Aging* **30**, 309–321 (2009).

507. Pan, Z.-G. & An, X.-S. SARM1 deletion restrains NAFLD induced by high fat diet (HFD) through reducing inflammation, oxidative stress and lipid accumulation. *Biochem. Biophys. Res. Commun.* **498**, 416–423 (2018).

508. Myers, R., Heckman, H. & Rodriguez, M. Reduced Hyperalgesia in Nerve-Injured WLD Mice : Relationship to Nerve Fiber Phagocytosis , Axonal Degeneration , and Regeneration in Normal Mice. **101**, 94–101 (1996).

509. Neukomm, L. J. *et al.* Axon Death Pathways Converge on Axundead to Promote Functional and Structural Axon Disassembly. *Neuron* **95**, 78-91.e5 (2017).